TECHNOLOGY TRANSFER/A CASE STUDY: TARGET STRENGTH

Ronald New, et al

Catholic University of America

Prepared for:

Office of Naval Research

March 1974

AD-A012 871

Security Classification

DOCUMENT CONTROL DATA - R & D

(Security classification of title, body of abstract and indexing annotation must be entered when the overall report is classified)

1. ORIGINATING ACTIVITY (Corporate author)	2a. REPORT SECURITY CLASSIFICATION
The Catholic University of America Washington, D.C. 20017	Unclassified 2b. GROUP

3. REPORT TITLE

TECHNOLOGY TRANSFER/A CASE STUDY: TARGET STRENGTH

4. DESCRIPTIVE NOTES (Type of report and inclusive dates)
Technical report, August 1973 - March 1974

5. AUTHOR(S) (First name, middle initial, last name)

Frank A. Andrews, Donald Brill, Thomas J. Eisler, Ronald New, and Herbert M. Überall

6. REPORT DATE	7a. TOTAL NO. OF PAGES	7b. NO. OF REFS
March 1974	254	

8a. CONTRACT OR GRANT NO.	9a. ORIGINATOR'S REPORT NUMBER(S)
N00014-67-A-0377-0016 b. PROJECT NO.	
c.	9b. OTHER REPORT NO(S) (Any other numbers that may be assigned this report)
d.	

10. DISTRIBUTION STATEMENT

Approved for public release; distribution unlimited

11. SUPPLEMENTARY NOTES	12. SPONSORING MILITARY ACTIVITY
	Office of Naval Research Code 431 Naval Analysis Programs Naval Application and Analysis Division

13. ABSTRACT

In this report we have tried to communicate technical subject matter in a way better than it has been done previously — the subject is Acoustic Target Strength. We have collected the components of the subject — analyzed them — synthesized them — and now, herein, we attempt the TECHNOLOGY TRANSFER.

Our case study is limited to scattering from fixed targets in the mid- to high-frequency range. We first analyze the available exact methods, and then establish their limitations. We introduce, and describe in detail, the principal approximate theories and methods; their bounds, limitations, and potential extensions are discussed. We form a SYNTHESIS of the component parts at four levels, including: example problems, comparative formulas, guidelines in analytical terms, and finally "wave intuition". Some examples of the correlation between theory and experiment are shown in order to give some evidence of the current state-of-the-art.

PRICES SUBJECT TO CHANGE

DD FORM 1 NOV 68 1473 (PAGE 1)

S/N 0101-807-6801

Security Classification

14. KEY WORDS	LINK A		LINK B		LINK C	
	ROLE	WT	ROLE	WT	ROLE	WT
ACCUSTICS						
TARGET STRENGTH						
SCATTERING						
DIFFRACTION						
KIRCHHOFF						
KELLER						
GEOMETRICAL ACOUSTICS						

TECHNOLOGY TRANSFER

A CASE STUDY/TARGET STRENGTH

by

R. NEW, PROJECT DIRECTOR

F.A. ANDREWS
D.W. BRILL
T.J. EISLER
H.M. ÜBERALL

School of Engineering and Architecture

The Catholic University of America

Washington, D. C. 20064

TECHNOLOGY TRANSFER

A CASE STUDY/TARGET STRENGTH

by

R. NEW, PROJECT DIRECTOR

F.A. ANDREWS
D.W. BRILL
T.J. EISLER
L.M. ÜBERALL

ONR CONTRACT N00014-67-A-0377-0016

MARCH 1974

THE ACOUSTICS GROUP

THE CATHOLIC UNIVERSITY OF AMERICA

WASHINGTON, D.C. 20017

PREFACE

The purpose of this report is to create a coherent picture of acoustic scattering from obstacles based on the important and current knowledge of the subject. The report is meant to be step one in a two step process. The second step will be the design and construction of a learning package for the rapid and effective communication of the critical knowledge found mainly in this report. The subject, acoustic scattering, was chosen because of its pertinence in undersea warfare, which is a major responsibility of our sponsor, the U.S.Navy.

The assemblage of knowledge into the format of this report, and ultimately into a learning package, was motivated by the thought that the criticisms of Toffler [Future Shock, 1970] and the predictions of Kemeny [Man and the Computer, 1972] are both correct. The first man, a former newspaper writer, credits the intense rate of change now being experienced in society to a knowledge explosion, and suggests that continuing education is an absolute essential for all of humanity. The second man, a mathematics professor and President of Darmouth University, forecasts future continuing education programs in which televised lectures are brought into the home or the office, in which a computer-based, nationwide, automated reference library is available for query from remote home or office terminals, and in which student interaction with home computer terminals takes place for quizzing, for drill, and for the transfer of basic knowledge. Thus, the work reported herein, and its ultimate translation into a learning package, is meant to be a contribution to the huge body of information which will have to be assembled to make Kemeny's vision into a reality.

The Material Command, the Training Command, and certain Tactical Development Commands of the U.S.Navy are all potential users of the learning package which will

be based on this report. For managers, as well as technical workers in these commands, there is an ever pressing need to understand in detail, all facets of underwater sound, as well as many other technical subjects. Yet, the time available to devote to such study becomes less and less. The authors of this report envision therefore, the establishment one day within the buildings of the Naval Material Command, or at the headquarters of certain Tactical Development commands, a Technical Information Center. Subscribers to the Center can sign out — or through query by telephone, by closed net television, or by remote computer terminal receive — the learning package which will be based on the material assembled in this report.

It is our firm belief that learning packages on this and many other topics will have to become a reality, which makes one realize that the notion of a rapid retrieval technical information center can only come to pass where there exists both financial support and the needs of a large audience. However, if knowledge is power, it certainly appears that the rapid and responsible dissemination of technical knowledge within the Navy technical and operational communities is a worthy topic for effort, just as it is within the medical, law, and other professional communities.

The sponsor of the work upon which this report is based is the Director of Naval Analysis Programs, Office of Naval Research, Code 462 (now changed to code 431).

CONTENTS

ABSTRACT

In this report we have tried to communicate technical subject matter in a way better than it has been done previously — the subject is Acoustic Target Strength. We have collected the components of the subject — analyzed them — synthesized them — and now, herein, we attempt the TECHNOLOGY TRANSFER.

Our case study is limited to scattering from fixed targets in the mid- to high-frequency range. We first analyze the available exact methods, and then establish their limitations. We introduce, and describe in detail, the principal approximate theories and methods; their bounds, limitations, and potential extensions are discussed. We form a SYNTHESIS of the component parts at four levels, including: example problems, comparative formulas, guidelines in analytical terms, and finally "wave intuition". Some examples of the correlation between theory and experiment are shown in order to give some evidence of the current state-of-the-art.

ACKNOWLEDGEMENTS

We are grateful to the Office of Naval Research, Naval Applications and Analysis Division for financial support of the project under contract No.N00014-67-A-0377-0016, and to Mr. Robert Miller and Mr. Randy Simpson for their foresight and encouragement. Appreciation is expressed to research associates, Mr. John Pijanowski, Mr. David Kaplan, and Dr. Marilyn Andrulis for aid in the development of the example problems and comparative tables. We are indebted to Mrs. Margaret Patterson and Mrs. Elizabeth Holford for the typing of the manuscript.

The foundations of this work are contained in Appendices A through E. Individual technical contributions were as follows:

Appendix A	-	LINEAR ACOUSTICS	-	Dr. Herbert Überall
Appendix B	-	GEOMETRICAL ACOUSTICS	-	Dr. Ronald New
Appendix C	-	KIRCHHOFF THEORY	-	Dr. Herbert Überall
Appendix D	-	KELLER THEORY	-	Dr. Thomas Eisler
Appendix E	-	COMPARISONS OF CALCULATED AND OBSERVED TARGET STRENGTH (under separate cover)	-	Dr. Donald Brill of the U.S. Naval Academy

SECTION 1

INTRODUCTION

1.1 OBJECTIVES

We live in a world of accelerating complexity and specialization. Highly sophisticated knowledge is developed by theoreticians, but often in a form which makes it inaccessible to potential users. Conversely, the potential users speak a language not understood by theoreticians, and therefore, do not make their needs known. Neither side has been able to bridge the gap. We believe that this transfer of knowledge, which we have termed "technology transfer", is a proper function of the University and one which the University is uniquely qualified to undertake.

By transfer of knowledge from the theoretician to the user we do not imply an attempt to train the user to be a theoretician. Our goal is to make theoretical knowledge accessible to the user in an understandable form. To accomplish this, it is not necessary to teach him the detailed workings of the theory, but it is important to introduce him to its conceptual framework and main results. We wish to provide him with an intuition which can be a reliable resource for assessing what is available to him, and to provide guidelines for acquiring it.

Our study objectives can be stated succinctly:

1) Develop a methodology for critically synthesizing technical information of significant importance to various aspects of Anti-Submarine Warfare.
2) Develop and test means (tools) for effectively communicating the synthesized knowledge to specific technical and management levels in the Navy.
3) Demonstrate an application of the methodology in a case study of acoustic "target strength".

We chose target strength as an appropriate field in which to attempt technology transfer because; (1) it contains a very wide variety of prediction methods, ranging from the very sophisticated to the very crude, (2) there is little agreement or real understanding of the analytical methods and their domains of applicability, and (3) there is little communication between theoreticians and practioners in this field. We also felt that development of a successful method for technology transfer in this field would perform a valuable practical service for the Navy.

1.2 CONTENT AND PROCEDURE

Modern diffraction theory began with Sommerfeld in 1896 and was developed academically until World War II when the need arose for practical methods for calculating target strength of complex bodies. Since then there has been a proliferation of approximate methods for calculating target strength; there are presently more than ten different methods in the mid-to high-frequency domain. We have judged three of these methods to be practical. We have called these the Geometrical Acoustics, the Kirchhoff, and the Keller, methods. All three are presently in use by the Navy. They have overlapping domains of validity, but in fact, they are often used as if they had identical domains of validity. This is partly because the main mathematical tool used in high-frequency scattering analysis, the asymptotic expansion, does not readily allow for rigorous error analysis.

To accomplish our first objective (relating to the development of a methodology) we prepared, refined, and executed the procedural flow diagram in Fig.1-1. Our initial effort was devoted to a careful review of all available books, papers, and reports on the subject of target strength. A filtering process was used to catagorize the literature at three levels — Useful (U), Not Useful (NU), and Possibly Useful (PU). This was (and still is) a continuing process. At some later time a saturation (of the minds of the investigators) takes place and a confidence level

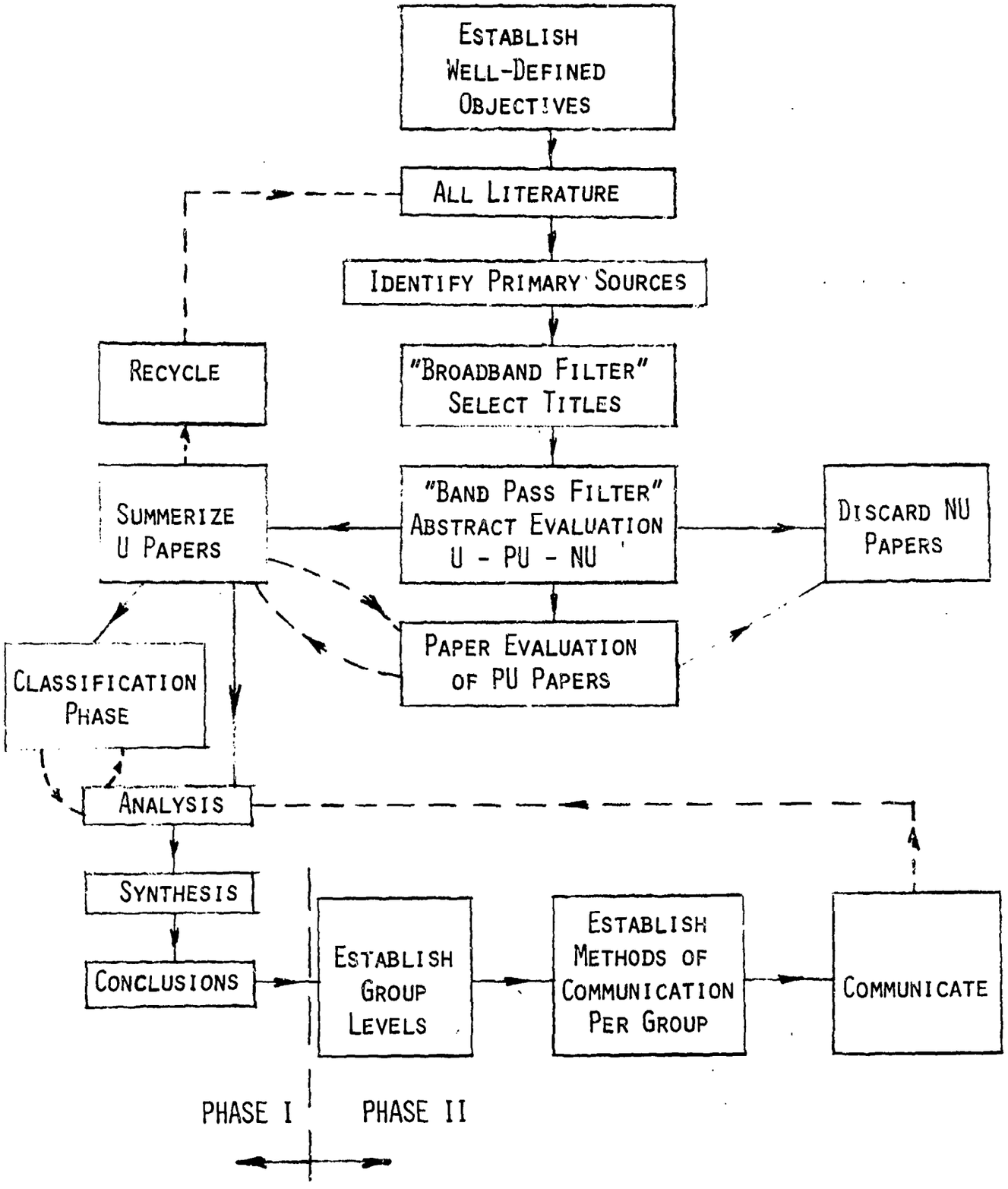

Fig.1-1 A PROCEDURAL FLOW DIAGRAM

is reached enabling the start of the analysis effort. The results of this ANALYSIS are contained in section 2.2 of this report, and in the detailed Appendices A through E. Analysis naturally leads to an attempt to synthesize and draw conclusions; the last, purely technical effort, in phase I. The results of this SYNTHESIS are contained in section 2.3 of this report. Phase II begins the communication effort and involves the creation of a "learning package". We define a learning package as an integrated collection of instructional media, including (1) textual material, (2) motion visualizations (films, video tapes, slides, etc.), and (3) computer programs and instruction. This report is one part of that learning package; the remaining parts are currently under development. The successful conclusion of phase II will satisfy the 2nd and 3rd objectives of our overall effort.

Analyze, synthesize, and communicate — these, we contend, are the vital steps in technology transfer. A complex technical subject like target strength must be thoroughly analyzed and then critically synthesized. To synthesize is to obtain a coherent sum of diverse information; but, what is coherent t some people may be confusing and vague to others. We speak of a critical synthesis because it is critically important to develop the synthesis in a form which will be truly coherent to the intended audience. Our development of the target strength SYNTHESIS has been structured with these points clearly in mind. In theory, it is directly from the SYNTHESIS that the learning package is created. Therefore, it is desirable that we elaborate here on the structure of the SYNTHESIS.

Initially we were faced with a body of considerably diversified knowledge. An ideal synthesis would include (at least) the results of rigorous analytical validation of the various approximate methods; i.e., a precise delineation of their domains of validity through rigorous error bounds. However, the state of the mathematical art is such that this is not presently possible. Keeping in mind

that our ultimate goal is the development of a learning package for the transfer of knowledge, and that this transfer is to take place at more than one level, we decided that it would be appropriate to attempt a synthesis at four different levels of generality. We characterize these levels as follows, in order of increasing generality.

1. Numerical comparison of solutions of specific problems with well-defined norms.
2. Comparison of predictive formulas.
3. General guidelines stated in analytical terms.
4. General guidelines applicable to all scattering problems (development of "wave intuition").

We have limited our case study to the three practical approximate methods mentioned above, together with the exact solutions when available. We chose as a baseline for comparison the "sonar backscattering cross-section" from rigid bodies (though all of the theories can, in principle, be applied to penetrable and absorptive bodies as well).

At the first level, which is the most specific and least general, we made numerical comparisons of the cross-sections of specific bodies, calculated according to the approximate theories with well-defined norms. We defined the norm to be the exact solution when available, and experimental results otherwise. We have called this section EXAMPLE PROBLEMS. The sphere, the prolate spheroid, and the finite cylinder were used as example targets. These shapes were chosen for reasons internal to the theories, i.e., to illustrate all of their important features, and also for their practical importance to the Navy. The comparisons produced a variety of different conclusions. Cases were found in which all methods

were in good agreement with the norm, others in which one method was found to be superior, and still others in which no method was satisfactory. It also became clear that the most sophisticated method is not necessarily the best.

The second level, comparison of formulas, was implemented by preparing tables of cross-section formulas as functions of aspect according to the three approximate theories, together with exact solutions when available, for more than ten different shapes. These tables can serve a number of purposes. They show the relative complexity of different methods and display the interrelationships. Perhaps their most important feature is the blank space — cases for which no formula now exists. Each of these cases is accompanied by an explanation. The explanation may simply be that the method, while applicable, has never been developed. But more important are those cases in which methods fail for various reasons, revealing intrinsic limitations of the approximate methods.

The third level consists of a set of general statements expressed in analytical terms, such as "formula fails within an angle of $(ka)^{-1}$ about a caustic and must be replaced by a uniform asymptotic approximation". At the fourth level, we have formulated general guidelines such as "the Kirchhoff method is most reliable near normal incidence", and "edge diffraction is generally more important than tip diffraction". At the third and fourth levels our main purpose is to develop what we have come to call "wave intuition". The non-specialist usually conceptualizes scattering in terms of rays. This picture can be very misleading in many diffraction problems. Our major objective here is to give the student an adequate feeling for situations in which "ray intuition" is inadequate and in these cases to replace it by an appropriate "wave intuition".

Section 2 follows and begins the case study on target strength. Section 2 consists of three subsections: 2.1 GENERAL, 2.2 ANALYSIS, and 2.3 SYNTHESIS. The rationale for the analysis and synthesis sub-sections have already been given. Sub-section 2.1 GENERAL, provides the "bridge" to introduce the technical subject, define the important terms, and establish the bounds of our problem.

Section 2

A CASE STUDY: TARGET STRENGTH

2.1 GENERAL

As an exercise in technology transfer, we have chosen to analyze, synthesize and communicate the technological subject of "target strength". This report, and this section in particular, contain the analysis and synthesis. The communication, in the form of a "learning package", is currently under development.

2.1.1 TARGET STRENGTH AND THE SONAR EQUATION

The target strength of a body or bodies is a measure of its reflecting or scattering properties, accounting for the shape and compliance of the scatterer, and the spatial variation of the scattered field. The symbol N_{ts} is often used to represent target strength but we shall use the simple abbreviation, TS. In acoustics, we have come to define TS as a logarithmic ratio of intensities [URICK - 1967]

$$TS\ (\theta,\phi) \triangleq 10 \log_{10} \frac{I_{sca}\ (r,\theta,\phi)}{I_{inc}} \qquad (2.1\text{-}1)$$

where the incident intensity I_{inc} is measured at the acoustic center of the target and the scattered intensity I_{sca} is measured at, or referenced to, one yard from the acoustic center along the direction (θ,ϕ). Often, if not always, it is impossible or unrealistic to determine I_{sca} at one yard from the acoustic center. In practice, I_{sca} is measured or calculated at some large distance r from the acoustic center and extrapolated back to r = 1 yard, using a $1/r^2$ spreading law. That is, we use

$$TS\ (\theta,\phi) = 10 \log_{10} \frac{I_{sca}\ (r,\theta,\phi)}{I_{inc}} \Big|_{r\,=\,1} \qquad (2.1\text{-}2)$$

and, if the measurement point is in the far-field, then I_{sca} can be written as

$$I_{sca}\ (\theta,\phi) = f^2_{sca}\ (\theta,\phi).\ 1/r^2 \qquad (2.1\text{-}3)$$

and TS becomes independent of the range of the measurement. Of course, if the measurement or calculation is made at some range within the near-field, then

1) TS will not be independent of range, r;
2) The scattered intensity at r = 1 yard will not be the actual intensity (nor will it be the actual intensity in most other cases);
3) The TS at any other range will not be known, nor can it be determined without knowledge as to the actual spreading law.

Simply stated, the near-field target strength problem is range dependent, whereas the far-field problem is not. We will deal only with the far-field problem. For those who are interested, the complexities of the near-field problem are discussed more fully in MAJOR [1946] and FREEDMAN [1962].

An alternative measure of the far-field scattering properties of a target is the sonar cross section $\sigma(\theta,\phi)$ related by analogy to the radar cross-section of electromagnetics.

$$\sigma\ (\theta,\phi) \triangleq \lim_{r\to\infty} \left\{ 4\pi r^2 \cdot \frac{I_{sca}}{I_{inc}}\ (\theta,\phi) \right\} \qquad (2.1\text{-}4)$$

The far-field TS, and the sonar cross-section σ, are in turn related by

$$TS = 10 \log_{10} \{\sigma/4\pi\} \qquad (2.1\text{-}5)$$

where σ is expressed in square yards.

In our work we will use either form, TS or σ to measure or describe the scattering properties of targets.

The definition of TS, as given by Eq. (2.1-5) and (2.1-4), is a convenient form for use in the active sonar equation [URICK - 1967; p. 2?]. For noise limited conditions the active sonar equation is (in URICK'S [1967] symbols)

$$SL - 2TL + TS - (NL - DI) = DT \qquad (2.1\text{-}6)$$

or, in the older symbols

$$L_s - 2N_w + N_{ts} - (L_n - N_{di}) = N_{rd} \qquad (2.1\text{-}7)$$

where

SL $\triangleq$ source level

TL $\triangleq$ transmission loss

NL $\triangleq$ isotropic noise level

DI $\triangleq$ receiving directivity index

DT $\triangleq$ detection threshold

This equation establishes an equality of the signal power to noise power ratios between the required condition at the receiver (DT) and the actual condition which exists, subject to certain probability criteria. The TS is only one of the system factors, but its role in influencing sonar system performance is clearly shown by Eq. (2.1-6).

2.1.2 ORGANIZATION

During this study it was necessary to assemble, digest, and organize a vast amount of information relating to the TS problem. Our specific objective was to develop a synthesis of the pertinent information in a form which could be easily understood and used by those who are not familiar with the techniques of TS prediction.

In this section (2.1) we introduce and establish the bounds of the problem.

Section 2.2 presents the various means by which TS can be analyzed and predicted. This ANALYSIS section is supported by five detailed appendices, A through E. Appendix A establishes the basics of linear acoustics and is used often for reference. Appendices B, C, and D are detailed discussions of the three principal target strength prediction theories for irregular targets. Appendix E (under separate cover) reports on the correlation which has been achieved between theory and experiment.

Section 2.3 contains the SYNTHESIS of the target strength problem. This synthesis is presented at four levels in ascending order of generality - from specific formulas and example numerical results, to general guidelines.

A bibliography, in alphabetic order, is appended, which includes all cited references.

2.1.3 ASSUMPTIONS AND LIMITATIONS

The general scattering problem to which we address ourselves is illustrated below.

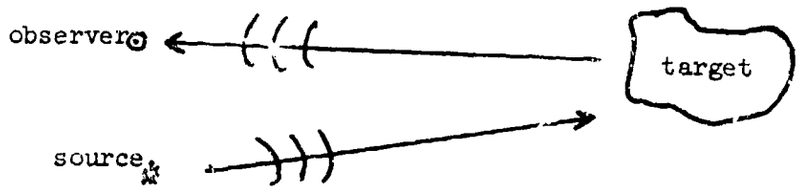

The source of acoustic energy and the observation point are sufficiently far from the scatterer that the incident field at the target and the observed field are plane. The target is an irregularly shaped body which is acoustically penetrable. The medium exterior to the target is an homogeneous, inviscid fluid, and the source is assumed to oscillate harmonically at some angular frequency, ω.

Exact, asymptotic, or approximate methods of analysis are in theory capable of dealing with this problem, but few specific results can be obtained without further specialization or simplification. Consequently, in the material that follows we will often specialize to:

1) coincidence of the source and observer (i.e., monostatic sonar as a special case of bi-static sonar);

2) impenetrable targets (i.e., acoustically "hard" or "soft" bodies);

3) special aspects to take advantage of symmetry.

In addition to these specializations, our consideration of the scattering problem will be limited to cases in which the maximum dimension ℓ of the scatterer is approximately equal to the acoustic wavelength λ (the so-called "resonance" region), or $\ell > \lambda$ (the so-called "optics" region). This limitation is (1) partly due to the relative importance of the mid- to high-frequency scattering problem as opposed to the low-frequency (Rayleigh) scattering problem, but also (2) necessary to allow ourselves to deal with a manageable amount of material within our available resources.

2.2 ANALYSIS

This subsection will present an overview and discussion of the mathematical methods commonly employed for an analysis of the acoustic sonar cross section of penetrable objects - but often specializing to the hard (rigid) or soft (resilient) boundary conditions. This will include a discussion of exact methods and of high-frequency asymptotic expansions (applicable only to special shapes), while the approximate methods (applicable to irregular shapes), such as geometrical acoustics and the theories of Kirchhoff and Keller, will be treated fully in Appendices B, C and D. Examples of the exact and asymptotic theories will be demonstrated in significant detail for the sphere and cylinder geometries. It is felt that such detail is necessary to develop intuition about the exact phenomena, and an appreciation of the severity of the assumptions made in the approximate theories. Appendix E discusses some comparisons between theory and experiment.

On several occasions, we shall use results of linear acoustics that are derived in Appendix A, and shall refer to specific equations of that appendix as needed.

2.2.1 EXACT METHODS OF SONAR CROSS SECTION* ANALYSIS

The basic quantities and concepts of acoustics, as needed in the following, are introduced in Appendix A, as is the development and definition of the sonar cross-section (c. s.). Here, we proceed to an illustration of how to obtain the latter by an exact mathematical calculation for some of the few cases (mainly those where the target is of simple shape) in which the exact method is applicable. [For most cases of practical importance (i.e. irregularly shaped scatterers), the approximate methods discussed in the Appendices must be used]. Following this, we shall also present a discussion of some high-frequency expansion methods for the exact solutions, which either entail useful simplifications of the latter, or which lead to additional physical insight.

2.2.1.1 Exact Solution for the Infinite Right Circular Cylinder.

For bodies of simple shape, such as the one considered here, the sonar c. s. problem may be solved exactly. The solution, besides being useful in its own right, may also be

---

*To be abbreviated by "sonar c. s."

employed for gauging the accuracy of an approximate solution against it.

The problem of scattering from an infinite right circular cylinder is here presented as an example of a two-dimensional scattering problem.

The plane incident wave of Eq. (a-32), i.e.

$$p_{inc} = P \exp\{i(\vec{k}.\vec{r} - \omega t)\} \tag{2.2-1}$$

may be expanded in terms of "cylindrical harmonics" as follows:

$$p_{inc} = P \exp\{-i\omega t\} \sum_{n=-\infty}^{\infty} i^n \exp\{in\phi\} J_n(kr) \tag{2.2-2}$$

$$= P \exp\{-i\omega t\} \sum_{n=0}^{\infty} (2 - \delta_{n0}) i^n J_n(kr) \cos n\phi. \tag{2.2-3}$$

The second form follows from the first by substituting $n' = -n$ for $n < 0$, and using the property [JAHNKE - 1945]

$$J_{-n}(x) = (-1)^n J_n(x) \tag{2.2-4}$$

of the Bessel functions with integer index. Eq. (2.2-2) is proved by Fourier-expanding

$$\exp\{ikx\} = \exp\{ikr\cos\phi\} = \sum_n f_n(r) \exp\{in\phi\}, \tag{2.2-5}$$

multiplying by $\exp\{-im\phi\}$, integrating over $d\phi$ and using the integral representation [JAHNKE - 1945]

$$2\pi i^n J_n(x) = \int_0^{2\pi} \exp\{ix\cos\phi - in\phi\}\, d\phi \tag{2.2-6}$$

of the Bessel function.

If the pressure is written as a function of the cylindrical coordinates: $p = p(r, \phi, t)$, the boundary conditions Eqs. (a-73) and (a-75) become, respectively,

$$p(a,\phi,t) = 0 \qquad \text{(soft)} \tag{2.2-7}$$

and

$$\left.\frac{\partial p(r,\phi,t)}{\partial r}\right|_{r=a} = 0 \qquad \text{(rigid)} \tag{2.2-8}$$

where $r = a$ is the radius of the scattering cylinder.

Using the expression for ∇^2 in cylindrical coordinates (and assuming no z-dependence)

$$\nabla^2\psi = \frac{1}{r}\frac{\partial}{\partial r}\left(r\frac{\partial\psi}{\partial r}\right) + \frac{1}{r^2}\frac{\partial^2\psi}{\partial\phi^2} \tag{2.2-9}$$

[MORSE -1953], the Helmholtz equation for the scattering problem, Eq. (a-83) in source-free space*, becomes

$$\frac{1}{r}\frac{\partial}{\partial r}\left(r\frac{\partial p}{\partial r}\right) + \frac{1}{r^2}\frac{\partial^2 p}{\partial\phi^2} + k^2 p = 0 \tag{2.2-10}$$

The method of solution proceeds via the so-called method of "separation of variables", writing

$$p(r,\phi) = R(r)\,\Phi(\phi), \tag{2.2-11}$$

and inserting in Eq. (2.2-10), one finds

$$\frac{r}{R}\frac{d}{dr}\left(r\frac{dR}{dr}\right) + k^2r^2 = -\frac{1}{\Phi}\frac{d^2\Phi}{d\phi^2} = \nu^2, \tag{2.2-12}$$

---

* The source of a plane incident wave lies at infinity, hence outside the finite region of space in which we want to find the solution.

where both expressions are set equal to a "separation constant" ν^2 since they depend on different variables each. The "ϕ-equation"

$$\frac{d^2\Phi}{d\phi^2} + \nu^2\Phi = 0 \qquad (2.2\text{-}13)$$

has the solution

$$\Phi(\phi) = \exp\{i\nu\phi\}, \qquad (2.2\text{-}14)$$

and the condition for a unique solution,

$$\Phi(\phi + 2\pi) = \Phi(\phi) \qquad (2.2\text{-}15)$$

requires that $\nu = n$, i.e., an integer . The "r-equation"

$$\frac{1}{r}\frac{d}{dr}\left(r\frac{dR}{dr}\right) + \left(k^2 - \frac{n^2}{r^2}\right)R = 0 \qquad (2.2\text{-}16)$$

may, by the substitution $\rho = kr$, be transformed into Bessel's equation [MORSE - 1953], with the solution

$$R(r) = Z_n(kr), \qquad (2.2\text{-}17)$$

Z_n being any cylinder function. One sees that the plane incident wave, Eq. (2.2-2) , is then a solution of Helmholtz's equation. The total pressure field may be written as

$$p_{total} = p_{inc} + p_{sca}\ , \qquad (2.2\text{-}18)$$

where the scattered wave p_{sca} has the same form, but with the Hankel function $H_n^{(1)}(kr)$ replacing $J_n(kr)$ since it must asymptotically ($r\to\infty$) represent an outgoing wave, $\propto \exp\{i(kr-\omega t)\}$. (This is known as the Sommerfeld "radiation condition".) Indeed, the asymptotic form of $H_n^{(1)}$ is given by [JAHNKE - 1945]

$$\lim_{\rho\to\infty} H_n^{(1)}(\rho) = (2/\pi\rho)^{1/2} \exp\{i[\rho - \tfrac{1}{2}\pi(n+\tfrac{1}{2})]\} \tag{2.2- 19}$$

which leads to the desired form. The total pressure field is thus

$$p_{tot} = P\exp\{-i\omega t\} \sum_{n=-\infty}^{\infty} i^n \exp\{in\phi\}\ [J_n(kr) + c_n H_n^{(1)}(kr)]. \tag{2.2- 20}$$

The coefficients c_n may be determined by demanding that p satisfy the boundary conditions of Eqs. (2.2- 7) or (2.2- 8), and one finds

$$p_{total}^{(soft)} = P\exp\{-i\omega t\} \sum_{n=-\infty}^{\infty} i^n \exp\{in\phi\} \{J_n(kr) - [J_n(ka)/H_n^{(1)}(ka)] H_n^{(1)}(kr)\} \tag{2.2- 21}$$

or*

$$p_{total}^{(hard)} = P\exp\{i\omega t\} \sum_{n=-\infty}^{\infty} i^n \exp\{in\phi\}\{J_n(kr) - [J_n'(ka)/H_n^{(1)\prime}(ka)] H_n^{(1)}(kr)\} \tag{2.2- 22}$$

for the soft or hard case respectively. These expressions are known as "normal mode series" or "Rayleigh series".

For obtaining the target strength of the cylinder, we must bring Eqs. (2.2- 21), (2.2- 22) in the form of Eq. (a-66), which is possible by using Eq. (2.2- 19). This leads to

$$f(\hat{r}) = -(2/\pi k)^{1/2} \exp\{-i\pi/4\} \sum_{n=-\infty}^{\infty} \exp\{in\phi\}\ J_n'(ka)/H_n^{(1)\prime}(ka) \tag{2.2-23}$$

---

*here, e.g., $H_n^{(1)\prime}(kr)$ denotes the derivative of the Hankel function with respect to its argument.

(for the hard cylinder; for the soft one , the primes are to be dropped), and one finds for the differential cross section:

$$\frac{d\sigma}{d\Omega} = \frac{2}{\pi k}\left|\sum_{n=-\infty}^{\infty}(-1)^n \frac{J_n'(ka)}{H_n^{(1)\prime}(ka)}\right|^2 , \qquad (2.2\text{-}24)$$

and for the sonar c. s.:

$$\sigma_{cyl} = \frac{4}{k}\left|\sum_{n=-\infty}^{\infty}(-1)^n \frac{J_n'(ka)}{H_n^{(1)\prime}(ka)}\right|^2 , \qquad (2.2\text{-}25)$$

according to Eqs. (a-69) and (a-72).

2.2.1.2 Exact Solution for the Sphere

As an example of a three-dimensional scatterer, the sonar c. s. will be found by the exact method for a sphere of radius a. The calculation proceeds analogous to the preceding one for the cylinder. The plane incident wave, Eq. (2.2- 1), may be expanded in terms of "spherical harmonics" or Legendre polynomials $P_\ell(\cos\theta)$ [WATSON - 1952]:

$$p_{inc} = P\exp\{-i\omega t\}\sum_{\ell=0}^{\infty} i^\ell (2\ell+1)\, j_\ell(kr)\, P_\ell(\cos\theta), \qquad (2.2\text{-}26)$$

where we introduce the "spherical Bessel functions"

$$j_\ell(\rho) = (\pi/2\rho)^{1/2} J_{\rho+\frac{1}{2}}(\rho). \qquad (2.2\text{-}27)$$

Writing $p = p(r,\theta,\phi,t)$, the boundary conditions to be satisfied are

$$p(a,\theta,\phi,t) = 0 \qquad \text{(soft)} \qquad (2.2\text{-}28)$$

or

$$\left.\frac{\partial p(r,\theta,\phi,t)}{\partial r}\right|_{r=a} = 0 \qquad \text{(rigid)} \tag{2.2-29}$$

The Helmholtz equation in spherical coordinates,

$$\frac{1}{r^2}\frac{\partial}{\partial r}\left(r^2\frac{\partial p}{\partial r}\right)+\frac{1}{r^2\sin\theta}\frac{\partial}{\partial\theta}\left(\sin\theta\frac{\partial p}{\partial\theta}\right)+\frac{1}{r^2\sin^2\theta}\frac{\partial^2 p}{\partial\phi^2}+k^2p=0 \tag{2.2-30}$$

is separated by writing $p = R(r)\Theta(\theta)$ (no ϕ dependence appears since the problem is cylindrically symmetric about the z-axis) so that

$$\frac{1}{R}\frac{d}{dr}\left(r^2\frac{dR}{dr}\right)+k^2r^2 = -\frac{1}{\Theta\sin\theta}\frac{d}{d\theta}\left(\sin\theta\frac{d\Theta}{d\theta}\right)=\lambda \tag{2.2-31}$$

The "θ-equation"

$$\frac{d^2\Theta}{d\theta^2}+\cot\theta\frac{d\Theta}{d\theta}+\lambda\Theta=0 \tag{2.2-32}$$

is the Legendre equation, whose only solutions that are finite at $\theta = 0$ and π are obtained for a separation constant equal to $\lambda = \ell(\ell+1)$ with ℓ = integer; these solutions are simply the Legendre polynomials

$$\Theta = P_\ell(\cos\theta) \tag{2.2-33}$$

The "r-equation"

$$\frac{d^2R}{dr^2}+\frac{2}{r}\frac{dR}{dr}+\left[k^2-\frac{\ell(\ell+1)}{r^2}\right]R=0 \tag{2.2-34}$$

has as its solution the spherical Bessel functions:

$$R(r) = z_\ell(kr) \tag{2.2-35}$$

where z_ℓ is related to $z_{\ell+1/2}$ as given by Eq. (2.2-27)
The scattered wave must contain the spherical Hankel function whose asymptotic form is

$$\lim_{\rho\to\infty} h_\ell^{(1)}(\rho) = (1/\rho)\exp\{i[\rho - \tfrac{1}{2}(\ell+1)\pi]\}, \quad (2.2\text{-}36)$$

so that the total pressure field becomes

$$p_{total} = P\exp\{-i\omega t\}\sum_{\ell=0}^{\infty} i^\ell(2\ell+1)[j_\ell(kr) + c_\ell h_\ell^{(1)}(kr)]P_\ell(\cos\theta) \quad (2.2\text{-}37)$$

The boundary conditions, Eqs. (2.2-28) and (2.2-29), again determine the coefficients c_ℓ, leading to:

$$p_{total}^{(soft)} = P\exp\{-i\omega t\}\sum_{\ell=0}^{\infty} i^\ell(2\ell+1)\{j_\ell(kr) - [j_\ell(ka)/h_\ell^{(1)}(ka)]h_\ell^{(1)}(kr)\}P_\ell(\cos\theta) \quad (2.2\text{-}38)$$

and

$$p_{total}^{(hard)} = P\exp\{-i\omega t\}\sum_{\ell=0}^{\infty} i^\ell(2\ell+1)\{j_\ell(kr) - [j_\ell'(ka)/h_\ell^{(1)\prime}(ka)]h_\ell^{(1)}(kr)\}P_\ell(\cos\theta) \quad (2.2\text{-}39)$$

By using Eq. (2.2-36), we bring these expressions into the form of Eq. (a-58) and find

$$f(\hat{r}) = -(1/ik)\sum_{\ell=0}^{\infty}(2\ell+1)[j_\ell'(ka)/h_\ell^{(1)\prime}(ka)]P_\ell(\cos\theta) \quad (2.2\text{-}40)$$

(for the hard case; no primes for the soft case). The differential cross section and the sonar c. s. become from Eqs. (a-62) and (a-65):

$$\frac{d\sigma}{d\Omega} = \frac{1}{k^2}\left|\sum_{\ell=0}^{\infty}(2\ell+1)\frac{j_\ell'(ka)}{h_\ell^{(1)'}(ka)}P_\ell(\cos\theta)\right|^2 \qquad (2.2\text{-}41)$$

and

$$\sigma_{sph} = \frac{4\pi}{k^2}\left|\sum_{\ell=0}^{\infty}(-1)^\ell(2\ell+1)\frac{j_\ell'(ka)}{h_\ell^{(1)'}(ka)}\right|^2 \qquad (2.2\text{-}42)$$

respectively, where the property

$$P_\ell(-1) = (-1)^\ell P_\ell(1) \qquad (2.2\text{-}43)$$

[JAHNKE - 1945] has been used. A plot vs. ka of the exact sonar c. s. of the sphere is shown, e.g., in Figure 2.3-2.

2.2.2 HIGH FREQUENCY APPROXIMATION METHODS OF SONAR C. S. ANALYSIS.

If the scatterer is not simply shaped, so that the method of separation of variables cannot be applied, exact solutions cannot be obtained. It may, however, be possible to find an asymptotic approximation of the solution, valid for high frequencies, i.e. in the form of a power series in inverse powers of $k\ell$ where ℓ is a characteristic dimension of the target. These asymptotic expansions may not be convergent expansions and, in general, are invalid for small $k\ell$, hence, they do not satisfy our definition of an exact solution. Two such methods will be discussed below: the Luneburg-Kline method, and the method based on the Watson transformation. The Luneburg-Kline method consists in an expansion in terms of integer inverse powers of $k\ell$. This is correct for the specularly reflected protion of the scattered field which does contain integer powers only (see below). It misses any components of the field that depend on non-integer powers of $k\ell$;

and as will be seen from the Watson transformation and the Keller theory [Appendix D], there exist in fact components of the scattered field that encircle the target body ("creeping waves"), which contain powers of $(k\ell)^{1/3}$ and "edge" components which contain powers of $(k\ell)^{1/2}$. The Luneburg -Kline method, therefore, only furnishes an incomplete expression of the scattered field inasmuch as it fails to account for certain diffraction phenomena; and it will give correct results only for cases where these diffraction phenomena do not appear, as in the case of an infinite body (such as a paraboloid). However, the method is applicable to targets of non-separable geometry, while the Watson transformation method, which furnishes high-frequency asymptotic expansions of both reflected and creeping waves, still can be applied to bodies of separable geometry only.

2.2.2.1 The Luneburg-Kline Method

A method of solving the problem of scattering from bodies with given boundary conditions (taken here as that of a rigid body) was devised by LUNEBURG [1944] and KLINE [1951] by expanding the fields in integer inverse powers of k. The solution of the source-free Helmholtz equation, Eq. (a-6), is written as

$$P = \sum_{n=0}^{\infty} (2\pi/k)^n P_n e^{i(kS-\omega t)} \qquad (2.2\text{-}44)$$

where $S(\vec{r})$ is taken as the eikonal (phase function) of geometrical optics [GOLDSTEIN - 1950], satisfying

$$|\vec{\nabla} S|^2 = 1 \qquad (2.2\text{-}45)$$

Insertion leads to the successive equations for p_n:

$$\vec{s}\cdot\vec{\nabla}p_n + \tfrac{1}{2}p_n\vec{\nabla}\cdot\vec{s} = (i/4\pi)\nabla^2 p_{n-1} \quad , \tag{2.2-46}$$

where we designated by

$$\vec{s} = \vec{\nabla}S \tag{2.2-47}$$

the normal vector to the surfaces of constant phase, S = constant. The rigid boundary condition now leads to the boundary conditions for the functions p_n on the surface of the scatterer:

$$p_n\Big|_S = \frac{i}{2\pi}\,\frac{\vec{n}\cdot\vec{\nabla}p_{n-1}}{\vec{n}\cdot\vec{s}} \quad , \tag{2.2-48}$$

where $\vec{n}$ is the outward normal to the surface. When Eqs. (2.2-46) and (2.2-48) are solved, the series of Eq. (2.2-44) then constitutes a high-frequency asymptotic series.

The method has been developed more fully by SCHENSTED [1955] for bodies of revolution and axial incidence. For an infinite impenetrable parabolic, he finds e.g.

$$\sigma = \pi R^2 C \tag{2.2-49}$$

where R is the radius of curvature at the vertex of the paraboloid, and where C is the function

$$C = \tfrac{1}{4}\Big\{1 + (kR/2)^2\left[\left(Si(kR) - \pi/2\right)^2 + \left(Ci(kR)\right)^2\right] + kR\left[\left(Si(kR) - \pi/2\right)\cos(kR) - Ci(kR)\sin(kR)\right]\Big\}^{-1} \tag{2.2-50}$$

which varies monotonically from 0.25 at kR = 1 to unity for kR = ∞. Asymptotically, therefore, σ of Eq. (2.2-49) becomes πR^2, which is a special case of the cross section for

impenetrable targets given by geometrical acoustics:

$$\sigma_{GA} = \pi R_1 R_2 \ , \qquad (2.2\text{-}51)$$

R_1 and R_2 bring the principal radii of curvature at the point of specular reflection.

As mentioned above, the Luneburg-Kline result of Eq. (2.2-49) should be correct as the paraboloid represents an infinite body which does not support circumferential waves. For a finite body, the creeping waves are not contained in the Luneburg-Kline solution, but they may be obtained (together with the reflected wave) by an application of the Sommerfeld-Watson transformation.

2.2.2.2 The Sommerfeld-Watson Transformation Method

This method has first been used by WATSON [1919], and was later extended by SOMMERFELD [1949]. It has been intensively applied to the acoustic case by FRANZ [1954], but as mentioned before, the method may only be used if the geometry of the target corresponds to a separable coordinate system. In fact, the method is based on the exact solution for this case, which is known in the form of a Rayleigh series. After the Watson transformation has been applied, the transformed solution may be seen to consist of reflected and creeping waves that provide an especially simple picture of the scattering process in the high-frequency limit.

All this will be illustrated in the following using the example of two-dimensional scattering from an infinite cylinder. The exact solution for this case, Eq. (2.2-22), may be

rewritten using the identity [JAHNKE - 1945]

$$J_\nu(\xi) = \tfrac{1}{2}\left[H_\nu^{(1)}(\xi) + H_\nu^{(2)}(\xi)\right], \tag{2.2-52}$$

in the form

$$p_{total} = P \exp\{i\omega t\} \sum_{n=0}^{\infty} (1 - \tfrac{1}{2}\delta_{n0}) i^n \left\{H_n^{(2)}(\rho) - \right.$$

$$\left. - \left[H_n^{(2)\prime}(x)/H_n^{(1)\prime}(x)\right] H_n^{(1)}(\rho)\right\} \cos n\phi \tag{2.2-53}$$

(for a rigid cylinder; if the cylinder is soft, the primes are absent), where $\rho = kr$, $x = ka$. Note that the incident field p_{inc}, which in Eq. (2.2- 22) was represented by the term with $J_n(\rho)$, is now partly contained in the term with $H_n^{(2)}(\rho)$, and partly in the remainder.

The Watson transformation now consists in a reformulation of the sum in Eq. (2.2-53) in terms of a contour integral in the complex plane of the index n which becomes a complex variable ν. If the contour C is chosen to encircle tightly the positive real axis of the ν-plane in the negative sense, i.e. $+\infty - i\varepsilon \ldots 0 \ldots +\infty + i\varepsilon$ (with the principal value P at the origin, i.e. leaving the origin half inside, half outside C) as shown in Figure 2.2-1, one may express a sum such as contained in Eq. (2.2- 53) as follows:

$$\sum_{n=0}^{\infty} (1 - \tfrac{1}{2}\delta_{n0}) f(n) = -\tfrac{1}{2} i P \oint_C (d\nu/\sin \pi\nu) \exp\{-i\nu\pi\} f(\nu) \tag{2.2-54}$$

The proof of Eq. (2.2- 54) is based on the Cauchy theorem which states that

$$\oint F(\nu)\, d\nu = 2\pi i \sum \text{Res}\, F(\nu_0), \tag{2.2-55}$$

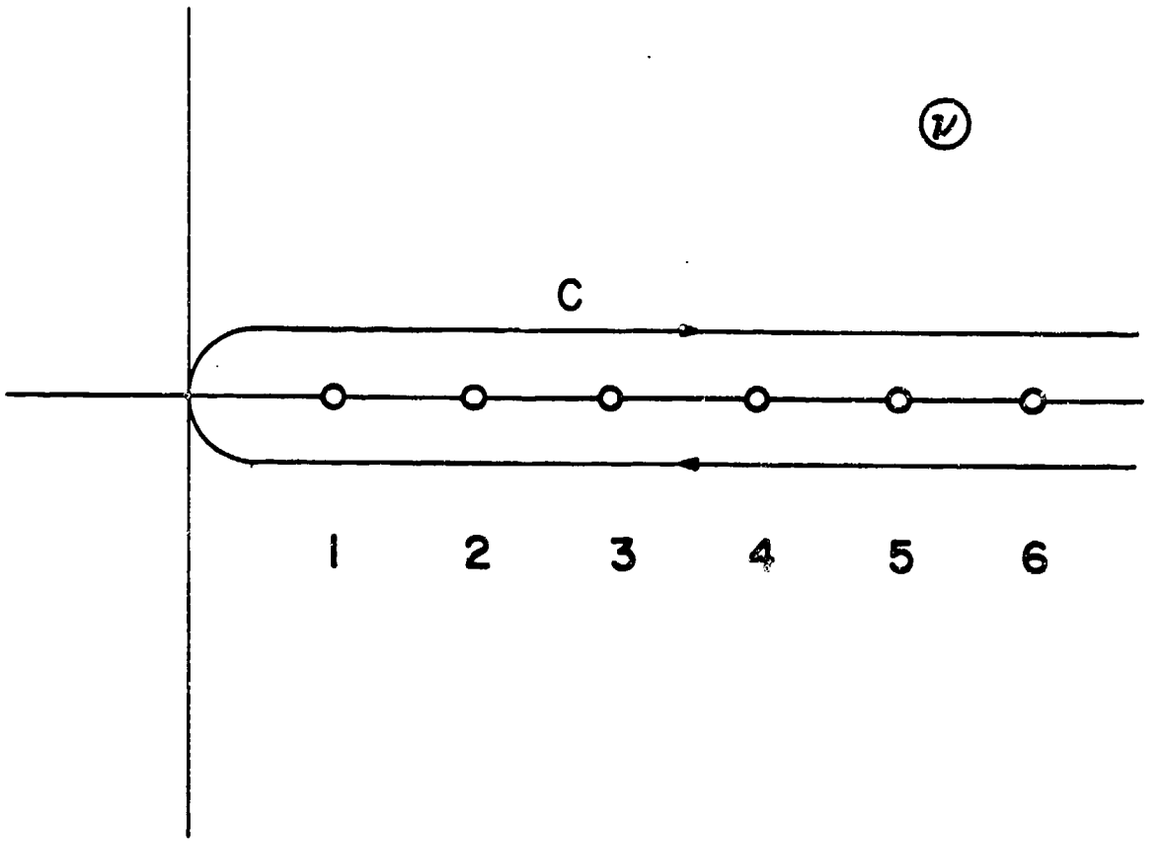

Fig. 2.2-1. Contour for the Watson Transformation in the complex ν-plane.

expressing the integral over a closed contour by the residues of the function F at its poles $\nu = \nu_o$. In Eq. (2.2-54), the poles of the integrand are given by the zeros of sin $\pi\nu$, i.e. the positive integers $\nu_n = n$; the corresponding residue is found as the factor of $1/\zeta$ of the integrand if the latter is expanded about the integers, $\nu = n + \zeta$ ($\zeta << 1$), leading to Eq. (2.2-54). When applied to Eq. (2.2-53), we obtain

$$P_{tot} = P_{exp}\{-i\omega t\} \mathcal{P} \oint_C (d\nu/\sin\pi\nu) \exp\{-i\nu\pi/2\} \cdot \{H_\nu^{(2)}(\rho) - [H_\nu^{(2)\prime}(x)/H_\nu^{(1)\prime}(x)] H_\nu^{(1)}(\rho)\} \cos\nu\phi \quad (2.2\text{-}56)$$

Transforming now the contour C into another one C' that lies immediately above the entire real axis ($-\infty + i\varepsilon \ldots +\infty + i\varepsilon$), by setting $\nu = -\nu'$ on the lower portion of C and using the equations [JAHNKE - 1945]

$$H_{-\nu}^{(1)}(x) = \exp\{\nu\pi i\} H_\nu^{(1)}(x), \quad (2.2\text{-}57)$$

$$H_{-\nu}^{(2)}(x) = \exp\{-\nu\pi i\} H_\nu^{(2)}(x), \quad (2.2\text{-}58)$$

[relations which also hold for the derivatives, $H_\nu^{(i)\prime}(x)$], we find

$$P_{tot} = P_{exp}\{-i\omega t\} \int_{C'} (d\nu/\sin\pi\nu) \exp\{-i\nu\pi/2\} \cdot \{H_\nu^{(2)}(\rho) - [H_\nu^{(2)\prime}(x)/H_\nu^{(1)\prime}(x)] H_\nu^{(1)}(\rho)\} \cos\nu\phi \quad (2.2\text{-}59)$$

Next, we split up the cosine by the identity

$$\cos\nu\phi = \exp\{i\nu\pi\} \cos\nu(\phi-\pi) - i \exp\{i\nu(\pi-\phi)\} \sin\pi\nu, \quad (2.2\text{-}60)$$

which leads to

$$p_{total} = p_{geom} + p_{creep} \tag{2.2-61}$$

with

$$p_{geom} = \tfrac{1}{2} P \exp\{-i\omega t\} \int_{C'} d\nu \exp\{i\nu(\tfrac{1}{2}\pi - \phi)\} \cdot \{H_\nu^{(2)}(\rho) - [H_\nu^{(2)\prime}(z)/H_\nu^{(1)\prime}(x)]\, H_\nu^{(1)}(\rho)\}, \tag{2.2-62}$$

$$p_{creep} = \tfrac{1}{2} i P \exp\{i\omega t\} \int_{C'} (d\nu/\sin\pi\nu) \{[\exp\{i\nu\pi/2\}]/H_\nu^{(1)\prime}(x)\} \cdot D_\nu(x,\rho) \cos\nu(\phi - \pi) \tag{2.2-63}$$

where

$$D_\nu(x,\rho) = \begin{vmatrix} H_\nu^{(1)\prime}(x) & H_\nu^{(1)}(\rho) \\ H_\nu^{(2)\prime}(x) & H_\nu^{(2)}(\rho) \end{vmatrix} . \tag{2.2-64}$$

We now close the contour C' by adding an infinite semicircle C_∞ towards the upper half-plane, noting that the integral over C_∞ gives zero additional contribution. To show this, we need the asymptotic forms of the Hankel functions as functions of their complex index ν. These are given, e.g., by FRANZ [1957]: dividing the ν-plane into four regions, I - IV, separated by the curves $h_{\pm 1}$, $h_{\pm 2}$ defined by

$$\cos\zeta + (\zeta - \tfrac{1}{2}\pi)\sin\zeta = \text{real} \tag{2.2-65}$$

with

$$\sin\zeta = \nu/x \tag{2.2-66}$$

(see Figure 2.2-2), one has for $|\nu| >> x$ the following asymptotic forms in these regions: e.g.,

$$\text{I: } H_\nu^{(2)}(x) \sim i\,(2/\pi\nu)(2\nu/ex)^\nu , \tag{2.2-67}$$

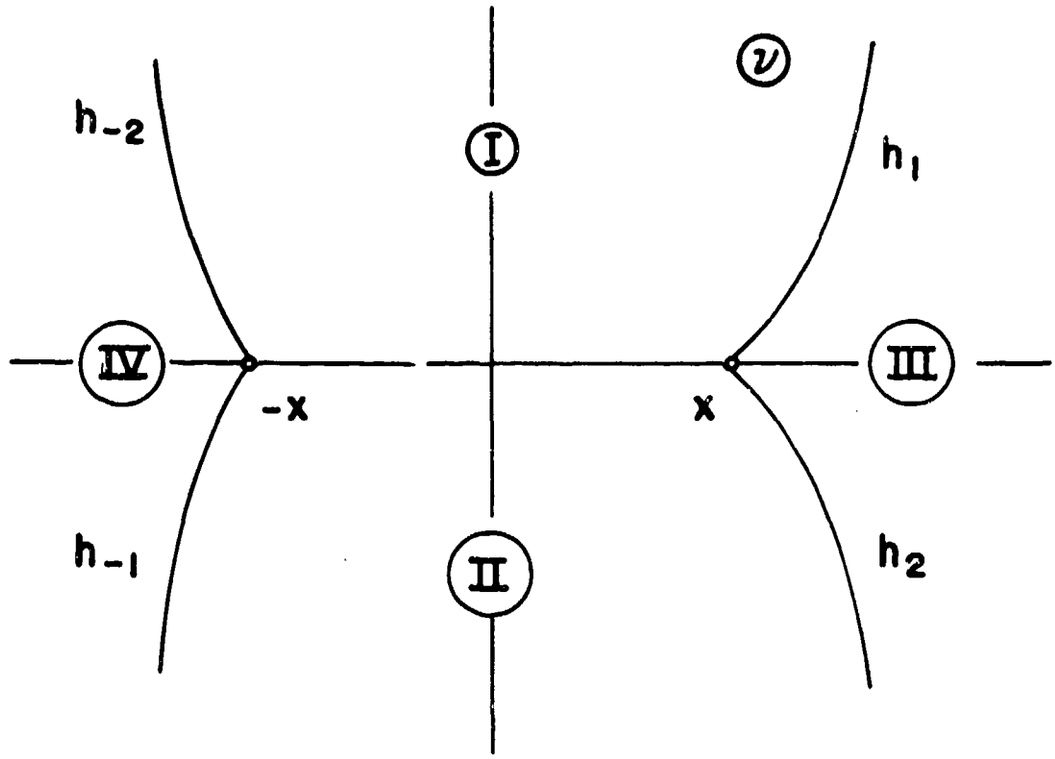

Fig. 2.2-2. "Stokes Lines" separating the asymptotic forms of the cylinder functions in the complex plane of their index.

corresponding to a behavior

$$\left[H_\nu^{(2)}(x)\right]_{asy} \propto (\mathrm{Im}\nu)^{\mathrm{Re}\nu-\frac{1}{2}} \exp\left\{-\tfrac{1}{2}\pi\,\mathrm{Im}\nu\right\}, \tag{2.2-68}$$

so that $H_\nu^{(2)}(x)$ is exponentially small for $\mathrm{Im}\nu \to +\infty$. Furthermore,

$$2J_\nu(x) \sim H_\nu^{(1)}(x) \sim \left[(2i/\pi\nu)/H_\nu^{(2)}(x)\right], \tag{2.2-69}$$

so that $J_\nu(x)$ and $H_\nu^{(1)}(x)$ are exponentially large in region I (and so are the derivatives, e.g. $J_\nu'(x)$, etc.). Similarly, in II, $H_\nu^{(1)}(x)$ is small (and the other functions large); in III, $J_\nu(x)$ is small [which incidentally makes Eq. (2.2-53) converge], and in IV, $J_{-\nu}(x)$ is small.

Now, $D_\nu(x,\rho)$ may be rewritten as

$$D_\nu(x,\rho) = 2\begin{vmatrix} H_\nu^{(1)\prime}(x) & H_\nu^{(1)}(\rho) \\ J_\nu'(x) & J_\nu(\rho) \end{vmatrix} = 2\begin{vmatrix} J_\nu'(x) & J_\nu(\rho) \\ H_\nu^{(2)\prime}(x) & H_\nu^{(2)}(\rho) \end{vmatrix} \tag{2.2-70}$$

where we used Eq. (2.2-52). Further, we may substitute in all forms of D_ν everywhere $\nu \to -\nu$, because of Eqs. (2.2-57), (2.2-58). In each region I - IV, we may thus choose that form of D_ν where each term is a product of a large with a small cylinder function, and one has

$$D_\nu(x,\rho) \sim \pm(2/i\pi\nu)\left[(\rho/x)^\nu - (x/\rho)^\nu\right]. \tag{2.2-71}$$

In this way, it is shown [FRANZ - 1957] that the asymptotic behavior of the integrand of Eq. (2.2-59) is such that one obtains zero when integrating over C_∞. One may thus rewrite

p_{tot} as an integral over C" ≡ C' + C_∞, i.e., the entire upper half-plane. The same holds for p_{geom} and p_{creep}, Eqs. (2.2-62) and (2.2-63), when separated by Eq. (2.2-60).

We shall now consider these latter expressions individually. First, consider p_{creep}:

$$p_{creep} = \tfrac{1}{2} i P \exp\{-i\omega t\} \oint_{C"} (d\nu/\sin\pi\nu)\left[\exp\{i\nu\pi/2\}/H_\nu^{(1)\prime}(x)\right] \cdot \cdot D_\nu(x,\rho)\cos\nu(\phi-\pi). \tag{2.2-72}$$

This expression will be seen to describe "creeping waves" that circumnavigate the cylinder circumferentially. The integral is taken over the closed contour C", and may again be evaluated by the Cauchy theorem, in terms of the residues at the poles of the integrand in the upper half-plane. The only poles here are provided by the zeros of the denominator, $H_\nu^{(1)\prime}(x)$; these lie on the lines $h_{\pm 1}$ of Figure 2.2-2 [FRANZ - 1954]. These are best described in terms of the Schöbe asymptotic forms*,† for $H_\nu^{(1)}(x)$, valid for $x \sim |\nu| >> 1$:

$$H_\nu^{(1)}(x) \sim (2/\pi)\exp\{-i\pi/3\}(6/x)^{1/3} A(q) \tag{2.2-73}$$

where

$$A(q) = \tfrac{1}{2}\int_{-\infty}^{\infty} \exp\{i(qt - t^3)\}\, dt \tag{2.2-74}$$

---

*Note this corresponds to x ≡ ka >> 1, so that at this place we now depart from the exact expression for p_{creep}, and perform a high frequency asymptotic approximation.

†Eq. (2.2-73) also holds for the derivatives of the functions on both sides.

(Airy function), and

$$q = (6/x)^{1/3} \exp\{-i\pi/3\}(\nu - x). \tag{2.2-75}$$

The (real) zeros of A(q) will be denoted by $\bar{q}_\ell$, and those of A'(q) by q_ℓ where $\ell = 1,2,\ldots$; they are listed in Table 2.2-1 together with the corresponding values of $A'(\bar{q}_\ell)$ and $A(q_\ell)$. The zeros of $H_\nu^{(1)\prime}(x)$ are thus given by

$$\nu_\ell = x + (x/6)^{1/3} \exp\{i\pi/3\} q_\ell + \cdots , \tag{2.2-76}$$

$$\bar{\nu}_\ell = x + (x/6)^{1/3} \exp\{i\pi/3\} \bar{q}_\ell + \cdots , \tag{2.2-77}$$

i.e. in the form of an asymptotic expansion in powers of $x^{-2/3}$.

Using the Cauchy theorem, p_{creep} may thus be written as a residue series of the poles along the curve h_1 which is enclosed by the contour C":

$$p_{creep} = -\pi P \exp\{i[\nu_\ell \pi/2 - \omega t]\} \left[D_{\nu_\ell}(\tau,\rho)/(\sin \pi\nu_\ell)\, \dot{H}_{\nu_\ell}^{(1)\prime}(x)\right] \cdot \cos \nu_\ell (\phi - \pi) \tag{2.2-78}$$

where

$$\dot{H}_\nu^{(1)}(x) \equiv (\partial/\partial\nu) H_\nu^{(1)}(x) \tag{2.2-79}$$

One may now expand

$$\frac{1}{\sin \pi\nu_\ell} = -2i \exp\{i\pi\nu_\ell\} \sum_{m=0}^{\infty} \exp\{2im\pi\nu_\ell\} ; \tag{2.2-80}$$

and if we also split the cosine factor:

$$\cos x = \tfrac{1}{2}(\exp\{ix\} + \exp\{-ix\}), \tag{2.2-81}$$

TABLE 2.2-1

ℓ	q_ℓ	$A(q_\ell)$	$\overline{q_\ell}$	$A'(\overline{q_\ell})$
1	1.469	1.1668	3.372	-1.0591
2	4.685	-0.9127	5.896	1.2130
3	6.952	0.8286	7.962	-1.3067
4	8.889	-0.7796	9.788	1.3757
5	10.633	0.7456	11.457	-1.4308

Zeros of the Airy function and its derivative, and corresponding functional values.

it is seen that p_{creep} contains a factor

$$p^{(1)}_{creep} \propto \exp\{i[\nu_\ell(\phi + 2m\pi) - \omega t]\} \tag{2.2-82}$$

[the second term of Eq. (2.2- 81) would lead to $p^{(2)}_{creep}$ as a similar expression with $-\phi$ in place of ϕ]. This represents circumferential (creeping) waves encircling the cylinder in both directions. Since we have a steady-state situation, there appear terms containing m, representing the waves that already have encircled the cylinder m times. The azimuthal propagation constant is given by $\mathrm{Re}\,\nu_\ell$, and the waves are attenuated* as determined by $\mathrm{Im}\,\nu_\ell$. The creeping waves may be written as

$$\exp\{-(\pm\phi + 2m\pi)/\Phi_\ell\} \exp\{i\omega[a(\pm\phi + 2m\pi)/c^*_\ell - t]\} \tag{2.2-83}$$

and in this form depend on the phase velocity

$$c^*_\ell \cong c\{1 + [q_\ell/2.6^{1/3}(ka)^{4/3}]\}^{-1} \tag{2.2-84}$$

and the attenuation angle

$$\Phi_\ell = 2/[3^{1/2}(ka/6)^{1/3} q_\ell]. \tag{2.2-85}$$

Note this involves powers of $(ka)^{1/3}$ characteristic for creeping waves†. There is an infinity of creeping waves labeled by $\ell = 1,2,\ldots$; the first one ($\ell = 1$) is least at-

---

*The attenuation comes about by the fact that the creeping waves radiate off energy tangentially as they propagate.

†Because of this fractional power, creeping waves cannot be included in the Luneburg-Kline solution discussed above.

tenuated, and is thus the most important one. Those with $m \geq 1$ (i.e. corresponding to one or more accomplished circumnavigations) are even more attenuated and hence less important. Note that $q_1 \equiv 1.469$ is much smaller than $\tilde{q}_1 \equiv 3.372$; hence even the first creeping wave on a soft cylinder is quite strongly attenuated, while that on a hard cylinder is only weakly attenuated.

Next we consider p_{geom} of Eq. (2.2-62) :

$$p_{geom} = -\frac{1}{2} P \exp\{-i\omega t\} \oint_{C''} d\nu \exp\{i\nu(\tfrac{1}{2}\pi - \phi)\} [H_\nu^{(2)\prime}(x) / H_\nu^{(1)\prime}(x)] H_\nu^{(1)}(\rho) \qquad (2.2\text{-}86)$$

The contribution of the term with $H_\nu^{(2)}(\rho)$ in the integrand of Eq. (2.2-62) was found to give zero over the closed path C" since it contains no singularities. Incidentally, the separation of p_{total} into p_{geom} and p_{creep} by using Eq. (2.2-60) is dictated by the fact, as shown by FRANZ [1957], that the residue series for p_{creep} in the insonified region* (containing the back scattering direction which we are interested in) is convergent, while a direct evaluation of p_{total} of Eq. (2.2- 59) as a residue series of circumferential waves would not have been. (For an observer in the shadow region, i.e. for forward scattering in the far field, it would have been the other way around).

Let us now go to the far field ($\rho \to \infty$), using the (Hankel) asymptotic form for $H_\nu^{(1)}(\rho)$, Eq. (2.2-19) . For $H_\nu^{(1),(2)}(x)$, we use the Debye asymptotic form [FRANZ - 1957] valid for

---

*This is the region around the cylinder which is directly reached by the incident wave, in contrast to the (geometrical) shadow region behind the cylinder which is not.

$|\nu| \sim x >> 1$:

$$H_\nu^{(1)(2)}(x) \sim (2/\pi k \sin\alpha)^{\frac{1}{2}} \exp\{\pm i x(\sin\alpha - \alpha\cos\alpha) \mp i\pi/4\} \tag{2.2-87}$$

where

$$\nu = x \cos\alpha \,. \tag{2.2-88}$$

One then has

$$H_\nu^{(1),(2)\prime}(x) \sim \pm i(\sin\alpha - \alpha\cos\alpha)\, H_\nu^{(1),(2)}(x) \tag{2.2-89}$$

and

$$H_\nu^{(2)\prime}(x) \Big/ H_\nu^{(1)\prime}(x) \sim -\exp\{-2ik(\sin\alpha - \alpha\cos\alpha) + i\pi/2\} \tag{2.2-90}$$

with neglect of terms $\sim \mathcal{O}(1/x)$. This again means that we perform a high-frequency asymptotic expansion, restricting ourselves to the leading term of p_{geom}.

Using the parameter α as an integration variable in place of ν, we then find

$$p_{geom} \sim -\tfrac{1}{2} P \exp\{-i\omega t\}(2x^2/\pi kr)^{1/2} \exp\{ikr + i\pi/4\} \cdot \int d\alpha \sin\alpha \exp\{G(\alpha)\} \tag{2.2-91}$$

where

$$G(\alpha) = 2ikr(\alpha\cos\alpha - \sin\alpha - \tfrac{1}{2}\phi\cos\alpha) \tag{2.2-92}$$

The integral in Eq. (2.2-91) is now best evaluated using the saddle point method (or the method of steepest descent) [SOMMERFELD - 1949]. A saddle point, or point of stationary phase, is a point in the α-plane where $G'(\alpha)$ vanishes*, and

---

*In the complex domain, $G(\alpha)$ has neither a maximum nor a minimum at such a point, but represents a saddle between two mountains.

the main contribution to the integral comes from its vicinity, since for $x >> 1$ (in line with our high frequency expansion), the phase of the integrand varies so rapidly that the contributions cancel). The saddle point α_s is found to lie at

$$\alpha_s = \tfrac{1}{2}\phi, \tag{2.2-93}$$

and a Taylor expansion of $G(\alpha)$ about α_s reads

$$G(\alpha) \cong -2ix \sin\tfrac{1}{2}\phi \left[1 - \tfrac{1}{2}(\alpha-\alpha_s)^2 + \dots\right] \tag{2.2-94}$$

or, setting

$$\alpha - \alpha_s = v e^{i\gamma}: \tag{2.2-95}$$

$$G(\alpha) \cong -2ix \sin\tfrac{1}{2}\phi \left[1 + \tfrac{1}{2}v^2\cos 2\gamma + \tfrac{1}{2}iv^2 \sin 2\gamma + \dots\right] \tag{2.2-96}$$

The integral will be most accurately evaluated if its path is shifted so that it follows a line of steepest descent over the saddle. This path is determined by Re $G(\alpha)$, and Eq. (2.2-96) shows (taking $\phi > 0$) that the descent of the integrand is steepest if we choose $\gamma = -\pi/4$, v being taken as a new (real) integration variable in place of α. The integral then becomes*

$$\int_{-\infty}^{\infty} \exp\left\{-[x \sin\tfrac{1}{2}\phi]\, v^2\right\} dv = (\pi/x \sin\tfrac{1}{2}\phi)^{1/2}, \tag{2.2-97}$$

and we find for the geometrically reflected wave:

$$P_{geom} \cong P\,(a \sin\tfrac{1}{2}\phi / 2r)^{1/2} \exp\{i(kr-\omega t)\} \exp\{-2ika \sin\tfrac{1}{2}\phi\} \tag{2.2-98}$$

as the leading term of a high-frequency series. Inspection shows that higher terms would be obtained as successive integer

---

*The limits may be extended to $\pm\infty$ with negligible error, due to the rapid descent of the integrand.

powers of ka, and these are also the higher-order contributions that would be obtained by using the Luneburg-Kline method.

That p_{geom} may indeed be interpreted as the geometrically reflected portion of the scattered field, can be seen from Figure 2.2-3. For the wave reflected at the point of specular reflection S, the quantity $\exp\{-2ik \sin(1/2)\phi\}$ is precisely the phase difference compared to that of the plane incident wave that continues straight, which arises at such a reflection.

The preceding referred to scattering from a hard cylinder. For a soft cylinder, the ratio of Eq. (2.2-90) without primes would be needed, which does not have the minus sign. Accordingly, the reflection amplitude for a soft scatterer acquires a phase jump of π over that for a rigid reflector.

The scattering amplitude is determined by taking out the factor

$$(P/r^{\frac{1}{2}}) \exp\{i(kr-\omega t)\} \tag{2.2-99}$$

from p_{geom}, so that [cf. Eq. (a-66)]:

$$f_{geom}(\phi) = \pm(\tfrac{1}{2}a \sin\tfrac{1}{2}\phi)^{1/2} \exp\{-2ika \sin\tfrac{1}{2}\phi\} \tag{2.2-100}$$

for the rigid (+) or soft (-) cylinder. The backscattering amplitude needed by us is

$$f_{geom}(\pi) = \pm (a/2)^{1/2} \exp\{-2ika\} \tag{2.2-101}$$

To this, we have to add coherently the contribution of the creeping wave scattering amplitude, which may be found from Eq. (2.2-78) as

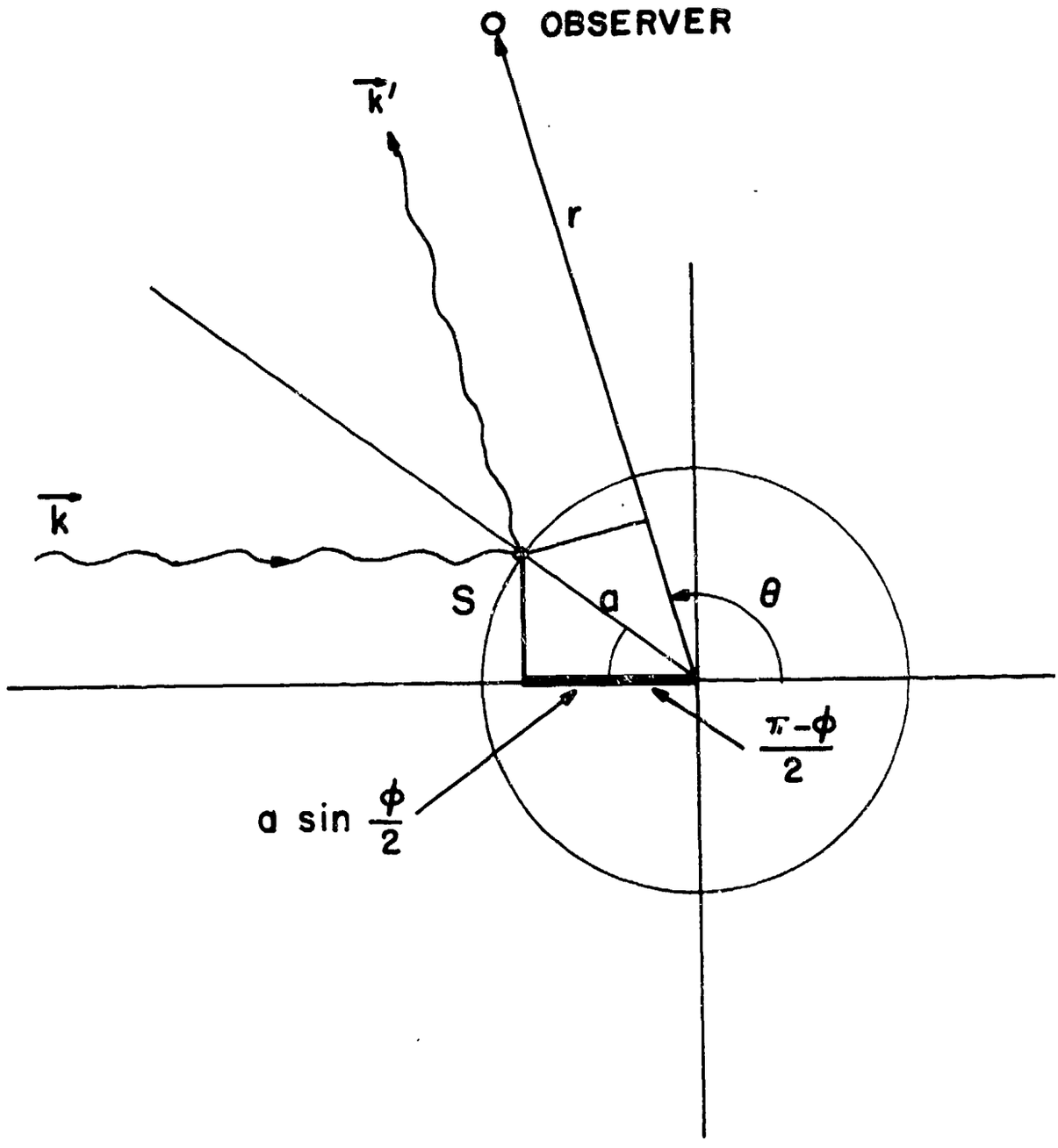

Fig.2.2-3. Geometry of the specularly reflected wave.

$$f_{creep}(\phi) = (2\pi/ik)^{1/2} \sum_{\ell=1}^{\infty} \sum_{m=0}^{\infty} \sum_{\pm} \left[H_{\nu_\ell}^{(2)\prime}(x) / i H_{\nu_\ell}^{(1)\prime}(x) \right] \cdot \exp\{ 2im\pi\nu_\ell + i\nu_\ell \phi_\pm \} \tag{2.2-102}$$

where we introduced

$$\phi_+ = \phi, \quad \phi_- = 2\pi - \phi \tag{2.2-104}$$

which corresponds to the two creeping wave components that are launched on opposite shadow boundaries and encircle the shadow side of the cylinder in opposite directions. For backscattering, one has $\phi_+ = \phi_- = \pi$ and the two waves add with equal strength:

$$f_{creep}(\pi) = 2(2\pi/ik)^{1/2} \sum_{\ell=1}^{\infty} \sum_{m=0}^{\infty} \left[H_{\nu_\ell}^{(2)\prime}(x) / i H_{\nu_\ell}^{(1)\prime}(x) \right] \cdot \exp\{ 2im\pi\nu_\ell + i\nu_\ell \pi \}. \tag{2.2-105}$$

The target strength is given by Eq. (a-72) as

$$\sigma_{cyl} = 2\pi \left| f_{geom}(\pi) + f_{creep}(\pi) \right|^2, \tag{2.2-106}$$

valid in the high-frequency limit.

Figure 2.2-4 shows $\sigma_{cyl}/\pi a$ (for the rigid cylinder) as a function of $\mathcal{K} \equiv ka$ [ÜBERALL - 1966]. While the solid curve represents the exact result of Eq. (2.2- 25) as calculated by HICKLING [1958], with a number of terms contributing importantly to the sum as indicated by encircled numbers in the figure, the dashed curve represents the creeping-wave high-frequency limit result using a single creeping wave ($\ell = 1$, $m = 0$) only. This demonstrates a practically important property of the Watson transformation: it gives results that converge rapidly (with fewer terms) in the high-frequency limit while the exact

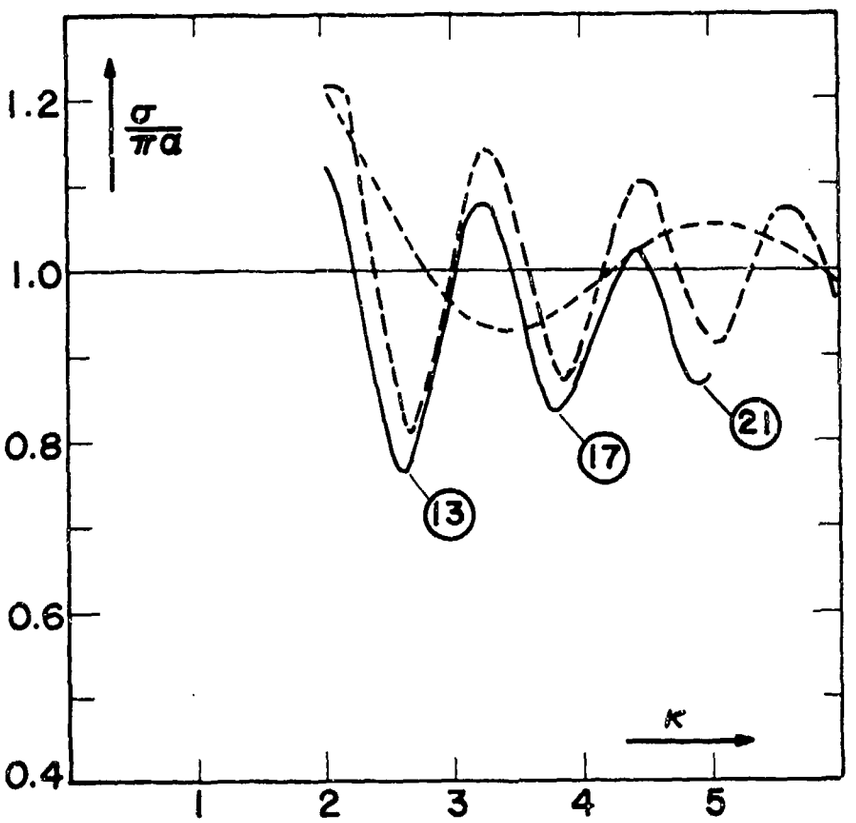

Fig.2.2-4. Normalized sonar c. s. of rigid cylinder plotted vs. k ≡ ka. Solid curve: Exact calculation. Dashed curves: Creeping wave theory (ℓ = 1, m = 0 only). Dotted curve: Kirchhoff approximation. (Figure taken from ÜBERALL [1966].)

(Rayleigh-series) method converges successively more slowly in this limit.

It should be noted that the important interference wiggles in Figure 2.2-4 originate from the interference of the creeping waves with the geometrically reflected wave. The latter contribution above would just give rise, from Eq. (2.2-101), to the horizontal line $\sigma = \pi a$ representing the asymptotic limit for $ka \to \infty$ (at least in its leading term).

The dotted line in Figure 2.2-4 represents the result of the Kirchhoff approximation, to be discussed in Appendix C (together with other approximation methods for sonar c. s. analysis). Its (spurious) oscillations arise from the fact, as will be discussed there, that this method (at least when it is applied blindly) substitutes the creeping wave effects by a spurious reflection from the shadow boundary.

A comparison of formulas or results implies that some measure of comparison has been chosen. The measure which we have chosen is the backscattering cross-section, σ, as discussed in Section 2.1, and defined in detail in Appendix A. In levels (1) and (2), we compute σ for various bodies and methods; in (3) and (4) we discuss the comparative forms of σ.

2.3.2 EXAMPLE PROBLEMS

2.3.2.1 EXAMPLE PROBLEM 1- σ OF A RIGID SPHERE

2.3.2.1.1 PROBLEM DESCRIPTION. We consider here plane wave incidence on a rigid (hard) sphere of radius a.

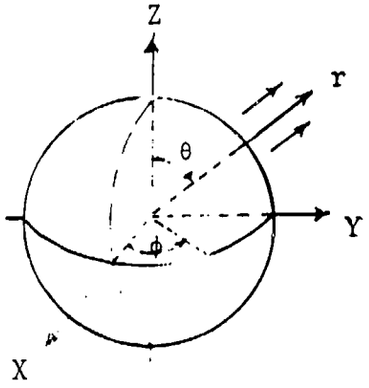

Assume the field is harmonic in time ($\exp\{-i\omega t\}$), and is incident from a direction (θ_o, ϕ_o). The pressure representation is therefore

$$p_{inc} = A \exp\{-i(\omega t + kr[\cos\theta_o\cos\theta + \sin\theta_o\sin\theta\cos(\phi - \phi_o)])\} \qquad (2.3\text{-}1)$$

We desire to obtain the scattered pressure field p_{sca} such that $p_{total} = p_{inc} + p_{sca}$. To obtain σ, the scattered field is required, and is most conveniently expressed in the spherical coordinate system, i.e.

$$p_{sca} = p_{sca}(r, \theta, \phi); \quad r \geq a \qquad (2.3\text{-}2)$$

By inspection, the backscattered field is independent of ϕ_o and σ is independent of the aspect angle θ_o. Hence, we can choose $\theta_o = \phi_o = 0$ in Eq. (2.3-1) for the incident field without loss of generality.

2.3.2.1.2 THE EXACT SOLUTION for σ can be obtained by the method of separation - of - variables and is given in [BOWMAN - 1969] as

$$\sigma_E = \frac{4\pi}{k^2} \left| \sum_{m=0}^{\infty} (-1)^n (2n + 1) a'_n \right|^2 \qquad (2.3\text{-}3)$$

where $a'_n = j'_n(ka)/h'^{(1)}_n(ka)$; j_n and h_n are the spherical Bessel functions defined in ABRAMOWITZ [1964]. $\sigma_E/\pi a^2$ versus ka is plotted in Figure (2.3-1a) where σ_E

has been normalized to the physical cross-section of the sphere.

2.3.2.1.3 THE GEOMETRICAL ACOUSTICS solution for σ is obtained from Eq. (b-30) in the special case of monostatic scattering as $r \to \infty$. As shown in Eq.(b-31) through Eq. (b-32), $\sigma_{G\,A}$ for any hard convex body is

$$\sigma_{GA} = \pi R_1 R_2 \tag{2.3-4}$$

where R_1 and R_2 are the principal radii of curvature at the specular point. For the sphere, both R_1 and R_2 equal the sphere radius, a, for any aspect; therefore, $\sigma_{G\,A}$ for the sphere is simply

$$[\sigma_{GA}]_{sphere} = \pi a^2 \tag{2.3-5}$$

That is, the geometrical acoustics cross-section of the hard sphere is equal to its physical cross-section. Since $\sigma_{G\,A}$ of the sphere is independent of frequency, the plot of $\sigma_{G\,A}$ normalized to πa^2 is a horizontal straight line with ordinate 1.0, as shown in Figure (2.3-1b).

2.3.2.1.4 THE KIRCHHOFF SOLUTION for σ is obtained by use of the procedure in Appendix C. Specifically, the result for σ_{KIR} is from (c-84):

$$\sigma_{KIR} = \pi a^2 \{1 + \sin^2(ka)/(ka)^2 - \sin(2ka)/ka\} \tag{2.3-6}$$

Note that σ_{KIR} adds two correction terms to the $\sigma_{G\,A}$ solution. Both correction terms decay to zero for $ka \to \infty$; hence, σ_{KIR} corrects* $\sigma_{G\,A}$ at low frequencies (or low a for a fixed frequency). σ_{KIR} normalized versus ka is plotted in Figure (2.3-1c).

2.3.2.1.5 THE KELLER SOLUTION for σ for the hard sphere is obtained from one of those special Keller problems known as canonical problems. That is, the hard sphere problem is one for which an exact solution exists, and from which an asymptotic form can be obtained, valid for large ka. Hence for this problem we do not develop an approximate Keller solution, but simply use the existing asymptotic solution. This solution is obtained in LEVY -[1959] by applying a caustic

*This "standard" Kirchhoff result contains spurious contributions (see section C.4.1) and improved estimates are available.

correction (their equation (91) on page 187 to equation (11) on page 201 of the reference). A more accurate form has subsequently been developed by SENIOR - [1965]. A convenient representation of σ_{KEL} is [BOWMAN - 1969]:

$$\sigma_{KEL} = \frac{4\pi}{k^2} \left| S_{refl} + S_{cr.w.} \right|^2 \qquad (2.3\text{-}7)$$

where S_{refl} and $S_{cr.w.}$ are given in Table (2.3-18). Rarely are these expressions used in actual calculations because of their complexity. Instead, approximations accurate to about 2% (as verified by term by term comparisons) are used. The approximations are valid down to ka $\doteq$ 2 [SENIOR - 1965]. Thus

$$S_{refl} = (ka/2)\{1 - 3i/2ka - 5/2\ (ka)^2\} \exp(-2ika) \qquad (2.3\text{-}8)$$

and

$$S_{cr.w.} = -mka \exp\{i\pi/3\} \{1 + [(32\beta_1^3 - 21)\exp(i\pi/3)]/60m^2\beta_1^2\}$$
$$\{1/(\beta_1[Ai(-\beta_1)]^2)\}\exp\ (i\pi ka - \pi m\beta_1 \exp(-i\pi/6) \qquad (2.3\text{-}9)$$
$$-[\pi(\beta_1^3 + 21)\exp(i\pi/6)]/60m\beta_1 + i\pi(\beta_1^6 + 63\beta_1^3 + 343/4)/1400m^3\beta_1^3\}$$

where β_1 = 1.018 792 97...

$Ai(-\beta_1)$ = 0.545 656 66...

are used t calculate σ_{KEL} Figure (2.3-1d) is a plot of the percentage difference (Δ) between σ_{KEL} and σ_E (i.e., $(\sigma_{KEL} - \sigma_E)\ 100/\sigma_E$) for selected values of ka.

2.3.2.1.6 DISCUSSION OF COMPARATIVE RESULTS. The Keller solution is less than 2% in error for ka $\geq$ 4.5, while the geometrical acoustics solution is within 33.3% error for ka $\geq$ 5.5. Even though the Kirchhoff cross-section is within 60% error for ka $\geq$ 5.5, the period of oscillation as well as its inability to distinguish between different spheroidal body shapes via different cross sections (see discussion in 2.3.2.2.6) indicates the theory is not consistent with the underlying physics of the phenomena. All three solutions, however, can be seen to converge to the geometrical acoustics as ka increases without limit, and (relative to other body shapes) all three approximate solutions compare to within 1.0 dB of the exact solution for ka $\geq$ 6.0.

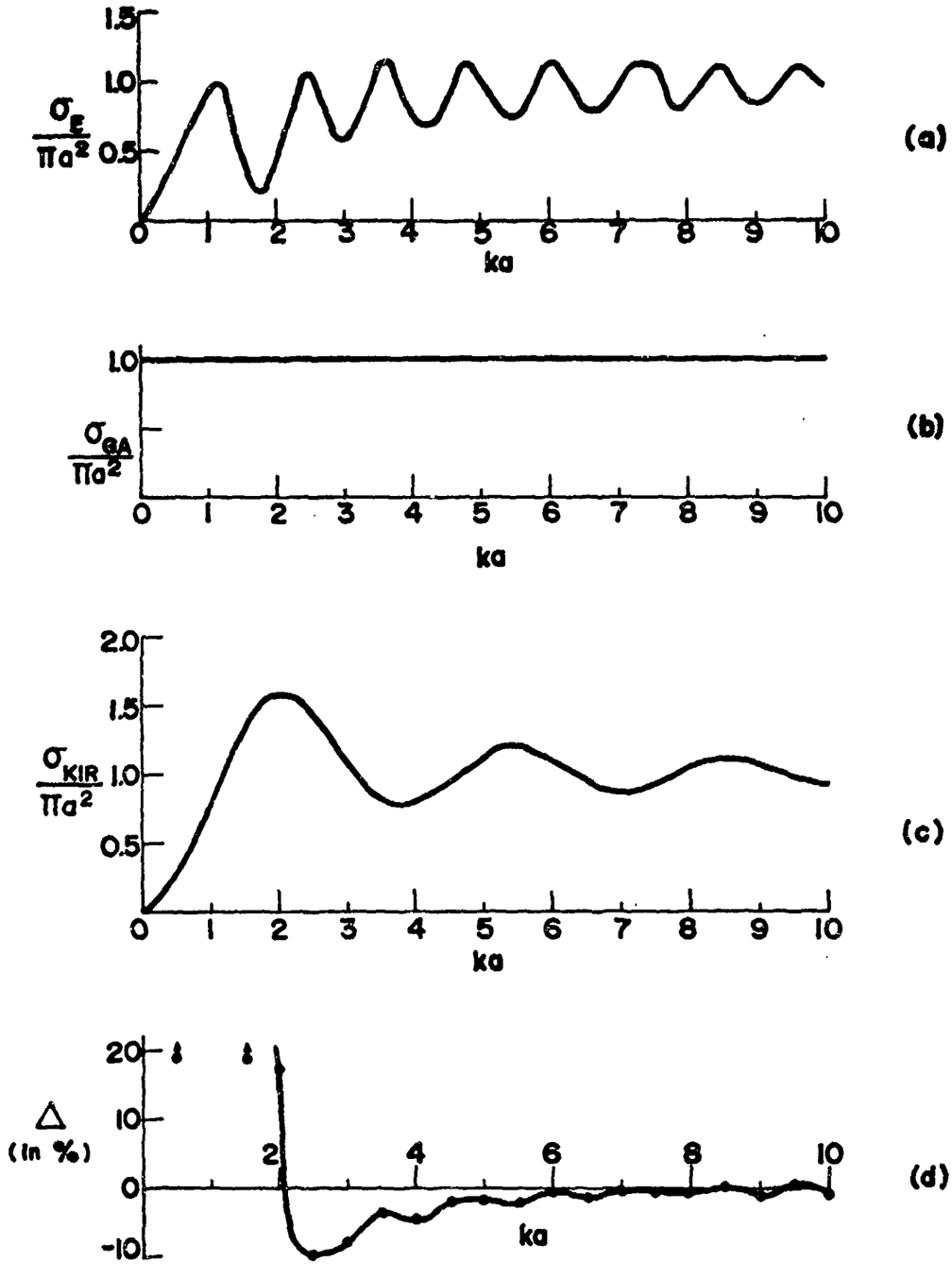

FIGURE 2.3-1

NORMALIZED SONAR CROSS-SECTION VS ka, RIGID SPHERE

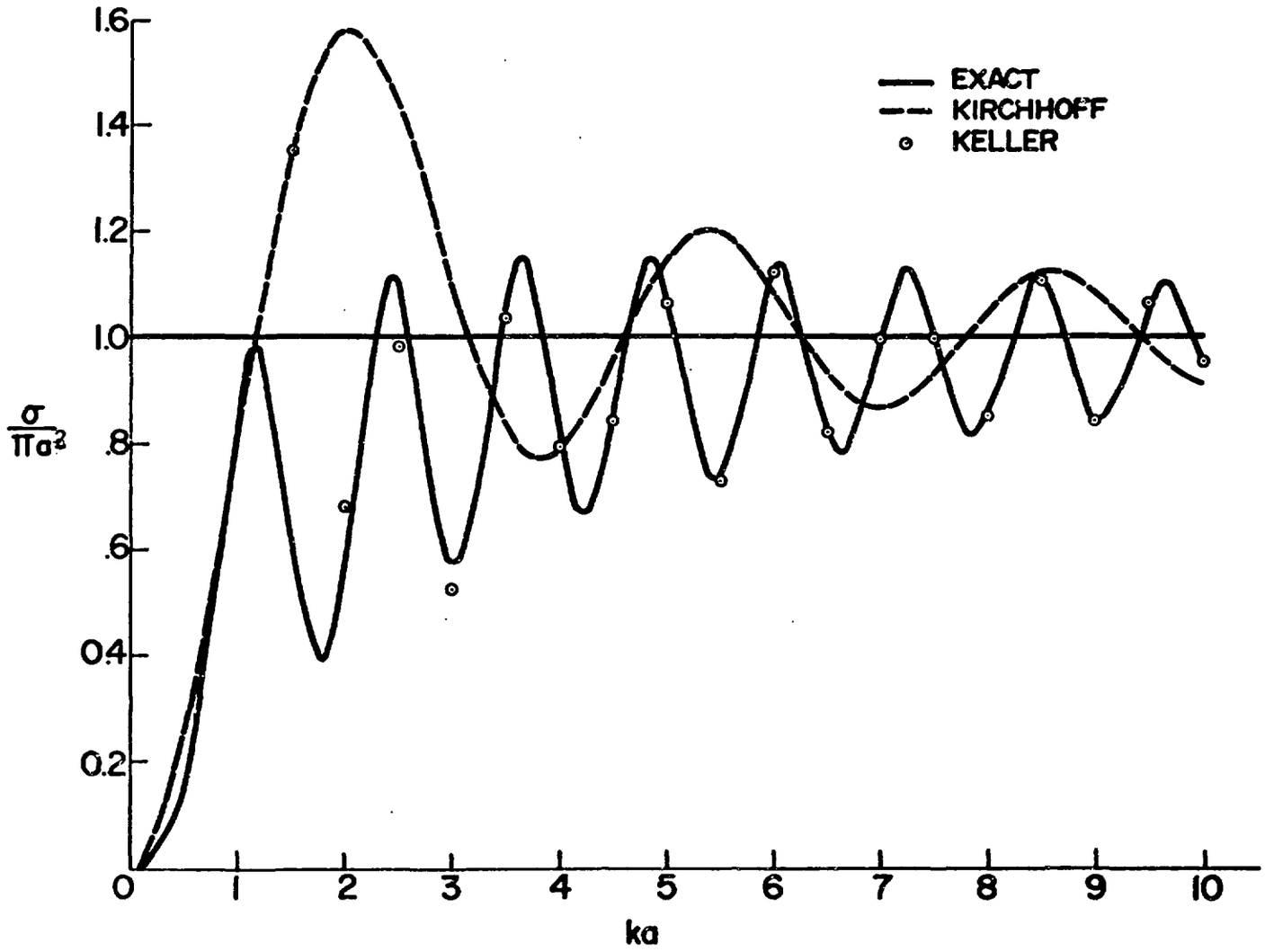

FIGURE 2.3-2

NORMALIZED SONAR CROSS-SECTION VS ka, RIGID SPHERE

2.3.2.2 EXAMPLE PROBLEM 2 - σ OF A RIGID PROLATE SPHEROID

2.3.2.2.1 PROBLEM DESCRIPTION. A plane wave is axially incident on a rigid (hard) prolate spheroid. The ratio of the major-to-minor axes (T = b/a) of the spheroid is 10:1. The incident field is assumed to have the harmonic time dependence exp[-iωt] and be travelling in the -z direction.

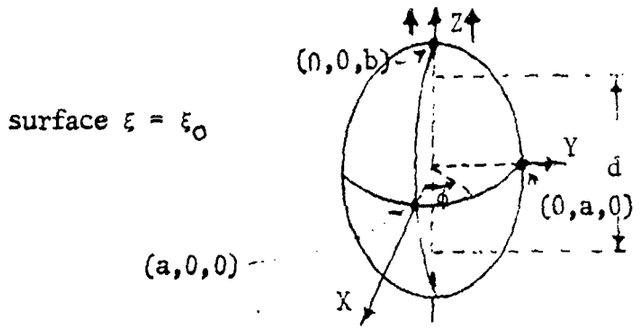

The incident pressure can be represented

$$p_{inc} = A \exp\{-i(kz + \omega t)\} \qquad (2.3\text{-}12)$$

The total pressure field is defined as the incident pressure plus the scattered pressure; i.e.,

$$p_{total} = p_{inc} + p_{sca} \; ; \quad \xi \geq \xi_0 \qquad (2.3\text{-}13)$$

The required scattered pressure can be functionally expressed in the prolate spheroidal coordinate system as

$$p_{sca} = p_{sca}(\eta, \xi, \phi)$$

The transformation equations between prolate spheroidal coordinates (η, ξ, ϕ) and Cartesian coordinates are

$$x = (1/2)d\sqrt{(\xi^2-1)(1-\eta^2)}\cos\phi \qquad (2.3\text{-}14)$$

$$y = (1/2)d\sqrt{(\xi^2-1)(1-\eta^2)}\sin\phi$$

$$z = (1/2)d\,\xi\eta$$

where d is the interfocal distance. Since we are limiting ourselves to monostatic axial backscattering with the incident pressure wave travelling in the -z direction, then the field point is at $\eta = +1$. Due to symmetry, we can choose $\phi = 0$ in the evaluation of the scattered pressure field without loss of generality.

2.3.2.2.2 THE EXACT WAVE HARMONIC SOLUTION for σ for axial incidence on a prolate spheroid with major to minor axes of ratio 10:1 has been evaluated. The complete analytical form of the solution for exp(iωt) dependence can be found in SENIOR [1966; p. 656].

This solution for axial incidence, adjusted to the exp(-iωt) dependence, is

$$\sigma_E = \frac{16\pi}{k^2}\left[\sum_{n=0}^{\infty}(-1)^n \frac{S_n^2(h,1)}{N_n} \frac{R_n'^{(1)}(h,\xi_0)}{R_n'^{(3)}(h,\xi_0)}\right]^2 \qquad (2.3\text{-}15)$$

where FLAMMER [1957] defines

$S_n(h, 1)$ as the prolate spheroidal angular wave function, $S_n(h, \eta)$, evaluated on the +z axis; i.e., at $\eta = +1$;

$R_n'(h, \xi_0)$ as the derivative of the radial wave function evaluated on the spheroidal surface $\xi = \xi_0$, and

N_n as the normalization factor.

Normalizing $[\sigma_E]$ to the geometrical acoustics solution $[\sigma_{GA}]$ from Eq. (2.3-21) results in

$$\left[\frac{\sigma_E}{\sigma_{GA}}\right] = \frac{16}{h^2}\left(\frac{\xi_0}{\xi_c^2 - 1}\right)^2\left[\sum_{n=0}^{\infty}(-1)^n \frac{S_n^2(h,1)}{N_n} \times \frac{R_n'^{(1)}(h,\xi_0)}{R_n'^{(3)}(h,\xi_0)}\right]^2 \qquad (2.3\text{-}16)$$

where ξ_0 is the surface radial coordinate and h is the wave radius; and

$$h = kd/2 . \qquad (2.3\text{-}17)$$

Computer evaluation of this equation was performed for increments of the product $h\xi_0$ of 0.125 up to 50. This product, $h\xi_0$, can be shown to be equal to the wave-number times the semi-major axis; i.e., kb. Subroutines developed at the Naval Research Laboratory, as described by VAN BUREN [1972], were used to evaluate the prolate spheroidal wave functions.

2.3.2.2.3 THE GEOMETRICAL ACOUSTICS SOLUTION for σ is obtained from Eq.(b-31) for the case of monostatic axial backscattering from a hard spheroid ($\mathcal{R} = 1$) as $r \to \infty$. As shown in Appendix B.2, σ_{GA} for any convex hard body is

$$\sigma_{GA} = \pi R_1 R_2 \qquad (2.3\text{-}18)$$

where R_1 and R_2 are the principal radii of curvature at the specular point. For axial incidence on the prolate spheroid, $R_1 = R_2$, and from Eq.(b-41) in Appendix B with $\theta = \varphi = 0$, we obtain (replacing c with b)

$$\sigma_{GA} = \pi a^4/b^2 . \qquad (2.3\text{-}19)$$

As with the sphere, [σ_{GA}] is independent of frequency. The projected cross-sectional area of the spheroid in the (x, y) plane is $A = \pi a^2$ and the ratio of major-to-minor axes is $T = b/a$. In terms of these quantities,

$$\sigma_{GA} = A/T^2 .$$

This means that for a fixed ratio, T, the quantity [σ_{GA}] is directly proportional to the projected area, A, of the spheroid. σ_{GA} can be expressed in the coordinates of the prolate spheroidal system by noting [FLAMMER - 1957; p. 6] that

$$\text{major axis} = 2b = d\xi_0 \qquad (2.3\text{-}20a)$$

and

$$\text{minor axis} = 2a = d(\xi_0^2 - 1)^{1/2} ; \qquad (2.3\text{-}20b)$$

therefore since

$$\sigma_{GA} = \pi a^4/b^2$$

and using Eq. (2.3-20a), we have:

$$\sigma_{GA} = \frac{\pi d^2(\xi_0^2-1)^2}{4\ \xi_0^2} . \qquad (2.3\text{-}21)$$

2.3.2.2.4 THE KIRCHHOFF SOLUTION for σ for axial incidence on a prolate spheroid is from Eq. (c-143)

$$[\sigma_{KIR}] = \frac{\pi a^4}{b^2}\left\{1 + \frac{\sin^2(kb)}{(kb)^2} - \frac{\sin(2kb)}{kb}\right\} . \qquad (2.3\text{-}22)$$

Normalizing to $[\sigma_{GA}]$ we obtain

$$\left[\frac{\sigma_{KIR}}{\sigma_{GA}}\right] = 1 + \frac{\sin^2(kb)}{(kb)^2} - \frac{\sin(2kb)}{kb} . \qquad (2.3\text{-}23)$$

It is interesting to note that for any ratio of the major-to-minor axes of the spheroid, this normalized Kirchhoff result is identical to that of a sphere of radius b*. Figure (2.3-4) displays the numerical results of Eq. (2.3-23) up to $h\xi_0 = kb = 50$.

2.3.2.2.5 THE KELLER SOLUTION for σ of a prolate spheroid is given in a convenient form by BOWMAN [1969; p. 457]. The expression for the normalized backscattering cross-section can be put in the form

$$\left[\frac{\sigma_{KEL}}{\sigma_{GA}}\right] = 1 + (\alpha \exp\{\beta\})^2 \qquad (2.3\text{-}24)$$

where

$$\alpha = \frac{2(0.5A)^{1/3}\ \xi_0^{5/3}}{(\xi_0^2-1)^{2/3}\beta_1\,[Ai(-\beta_1)]^2} \qquad (2.3\text{-}25)$$

---

* A similar phenomena occurs for the geometrical acoustics solution for σ for edge-on incidence on an oblate spheroid (See Table (2.3-12). Here $\sigma_{GA} = \pi a^2$ is not normalized, but is independent of the ratio of the major-to-minor axes of the spheroid.

and

$$\beta = \left(\frac{\pi}{3}\right)^{i} + 2h\xi_o i + 2hi\int_0^1 \sqrt{\frac{\xi_o^2 - \eta^2}{1-\eta^2}}\, d\eta + \gamma \exp\left\{\frac{i5\pi}{6}\right\} \tag{2.3-26}$$

with

$$\gamma = h^{1/3}\beta_1 \left(2\xi_o\sqrt{\xi_o^2 - 1}\right)^{2/3} \int_0^1 \frac{d\eta}{\sqrt{(\xi_o^2 - \eta^2)(1-\eta^2)}} \tag{2.3-27}$$

$$\beta_1 = 1.01879\ldots; \quad Ai(\beta_1) = 0.53565\ldots$$

The backscattered field which is used to calculate σ_{KEL} was originally obtained by LEVY [1960].

2.3.2.2.6 NUMERICAL RESULTS AND DISCUSSION. For a fixed ratio of major-to-minor axes of 10:1, Figure(2.3-3)displays the exact solution for σ as expressed by Eq. (2.3-16). From the curve it can be seen that oscillations are very pronounced even at $h\xi_o = 50$. The curve does not even seem to be approaching the geometrical acoustic solution. Figure (2.3-4) displays the Kirchhoff solution as a function of $h\xi_o$. This normalized Kirchhoff solution for the prolate spheroid is equivalent to that of a sphere of radius b with $kb = h\xi_o$, and as noted previously, is independent of the magnitude of the minor axis. Figure (2.3-5) displays the normalized Keller solution, and the scale of the ordinate σ/σ_{GA} is not in error. For comparison of the results displayed in Figures (2.3-3)through (2.3-5), target strength for the three normalized solutions of σ can be calculated using the definition [see Eq. (2.1-5)]: $TS = 10 \log (\sigma) - 10 \log 4\pi$. The quantity $10 \log (\sigma/\sigma_{GA})$ is plotted in Figure (2.3-6) for the three normalized solutions.

As can be seen in comparing the three figures, the differences among them are very striking. Tremendous errors are obtained in applications of this Keller solution to thin spheroids in this range of $h\xi_o$. It has been established by CRISPIN [1963] that the Keller solution will be within 20% of the geometrical acoustics

solution for the 10:1 spheroid when $h\xi_0 \geq 575$. This is far above the highest value of $h\xi_0$ displayed here. Crispin's analogous condition for the 2:1 spheroid occurs when $h\xi_0 \geq 33$. This has been verified as can be seen in Figure (2.3-7).

The Kirchhoff solution for the prolate spheroid reflects none of the deep minima present in the exact solution wherein the strong periodicity is due to creeping waves over the spheroid [SENIOR - 1966]. Although the magnitude of the Keller solution is very much in error, it should be noted that the periodicity of this solution is in close agreement with the exact solution. This agreement means that (in some sense) the Keller assumptions have accounted for the creeping wave phenomenon.

Generally it can be concluded that the geometrical acoustics, Kirchhoff, and Keller methods of determining σ for thin prolate spheroids, whose dimensions approximate those of a submarine, come nowhere near representing the exact solution below the optics region. It should be noted, however, that what we call in this paper the geometrical acoustics, Kirchhoff, and Keller solutions, are in fact only first order approximations. The Luneburg-Kline method [KLINE - 1951] extends geometrical acoustics; the Physical Theory of Diffraction [UFIMTSEV - 1962] extends the Kirchhoff method, and the complete Keller theory includes higher order correction terms [VOLTMER - 1970] which have not been included in Eq. (2.3-24). Certainly these extensions or additions of higher order correction terms will add complexity to the numerical evaluations—but as is plain to see, unless they are used, no reasonable approximation to the exact solutions will be obtained. The numerical comparisons made in this example problem merely highlight the inadequacy of the first order theories for the thin spheroid.

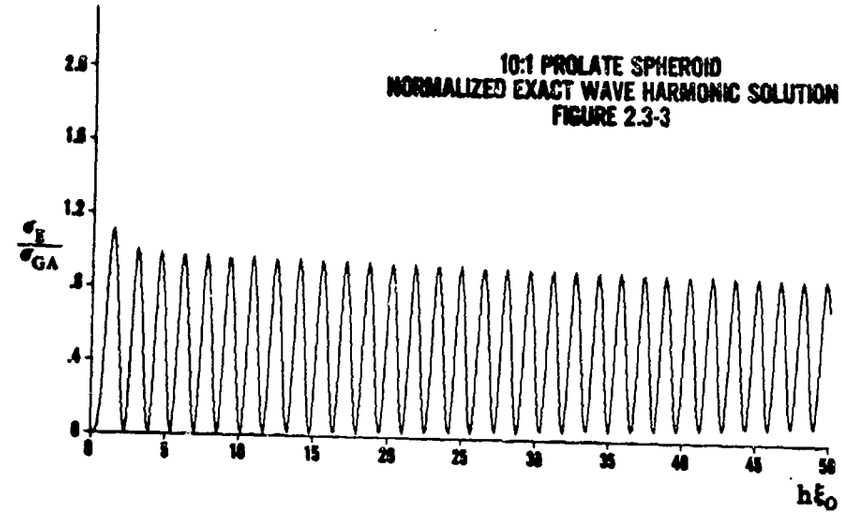

10:1 PROLATE SPHEROID
NORMALIZED EXACT WAVE HARMONIC SOLUTION
FIGURE 2.3-3

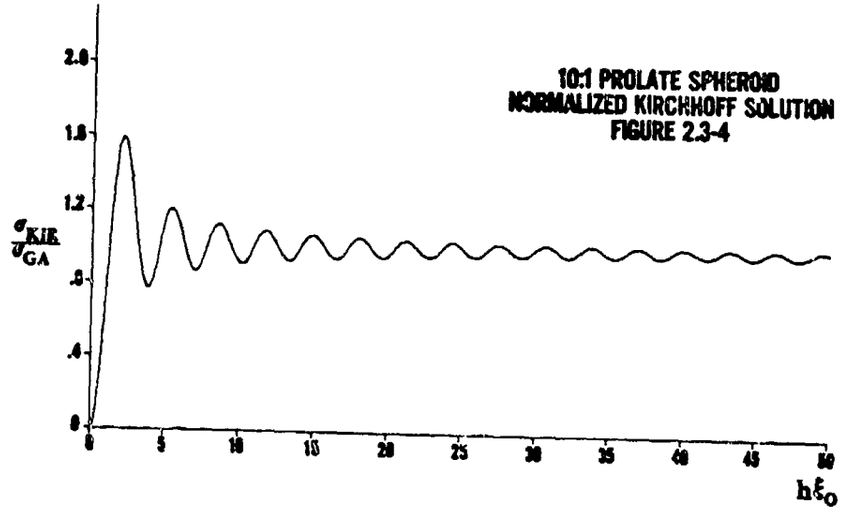

10:1 PROLATE SPHEROID
NORMALIZED KIRCHHOFF SOLUTION
FIGURE 2.3-4

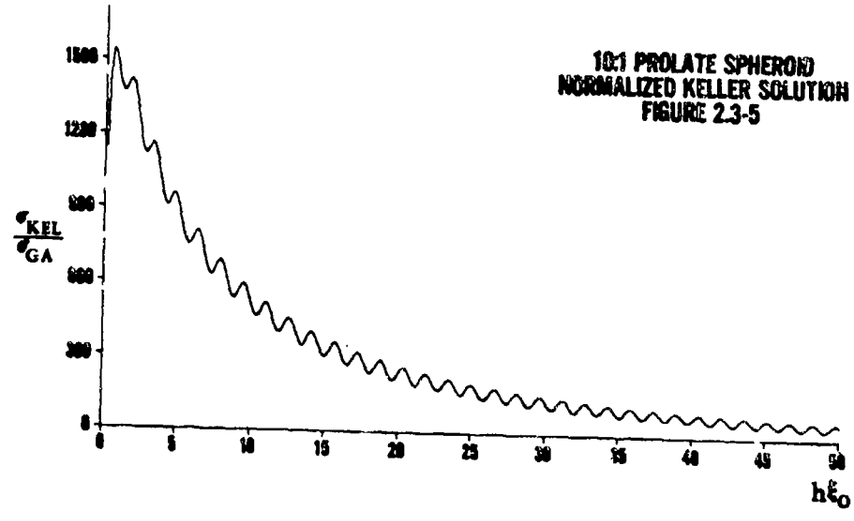

10:1 PROLATE SPHEROID
NORMALIZED KELLER SOLUTION
FIGURE 2.3-5

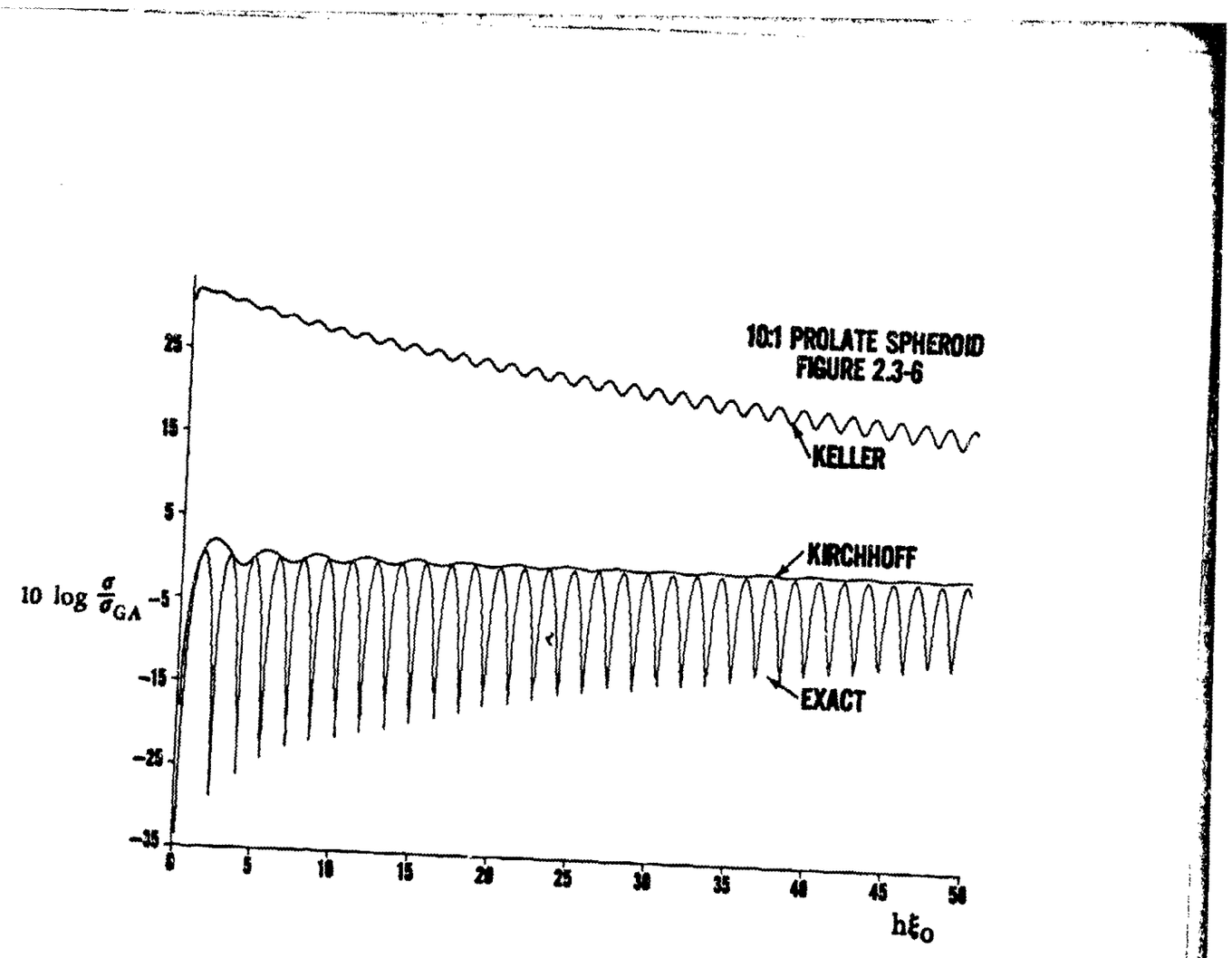
10:1 PROLATE SPHEROID
FIGURE 2.3-6
KELLER
KIRCHHOFF
EXACT
10 log $\frac{\sigma}{\sigma_{GA}}$
25
15
5
−5
−15
−25
−35
0
5
10
15
20
25
30
35
40
45
50
$h\xi_o$

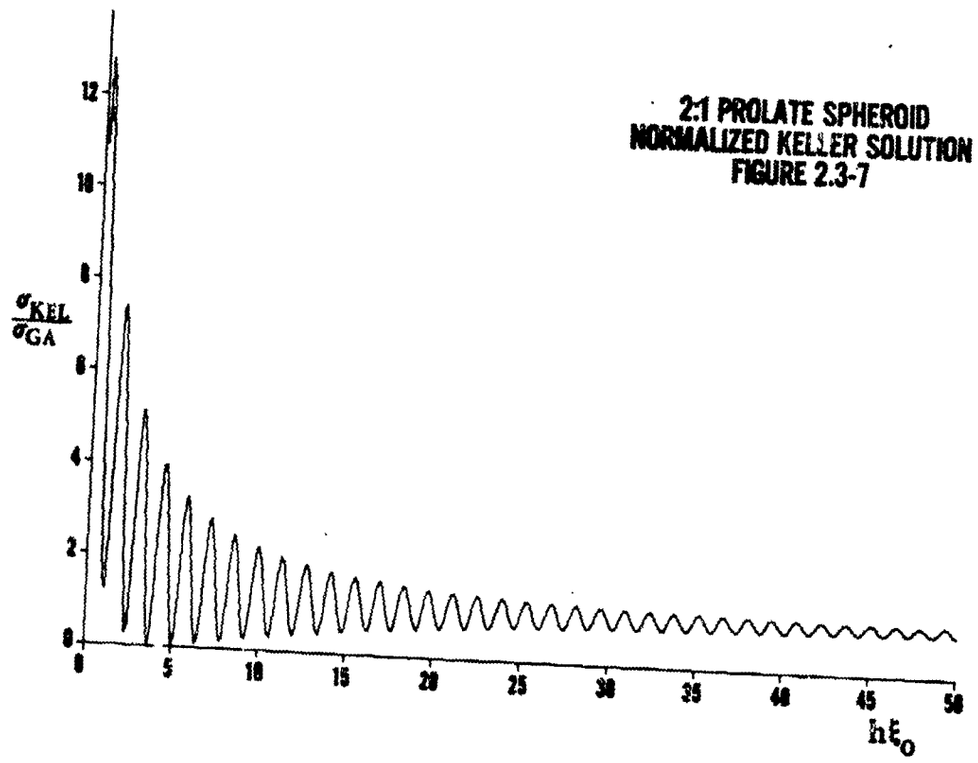
2:1 PROLATE SPHEROID
NORMALIZED KELLER SOLUTION
FIGURE 2.3-7
$\frac{\sigma_{KEL}}{\sigma_{GA}}$
12
10
8
6
4
2
0
0
5
10
15
20
25
30
35
40
45
50
$h\xi_o$

2.3.2.3 EXAMPLE PROBLEM 3 - σ OF A RIGID FINITE CYLINDER

2.3.2.3.1 PROBLEM DESCRIPTION

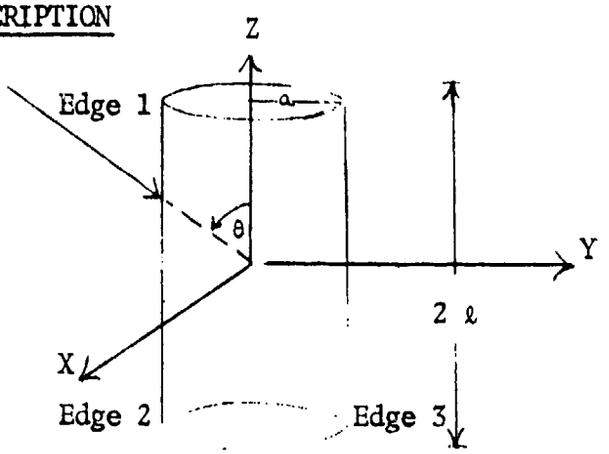

As an example in which edge diffraction dominates, we now consider the backscattering of a plane wave from a finite rigid cylinder. For the cylindrical geometry above, and for a field incident at arbitrary aspect θ, with harmonic time dependence ($\exp\{-i\omega t\}$), there is φ symmetry. Hence, no φ dependence exists. The incident pressure can be represented as

$$p_{inc} = A \exp\{-i(\omega t + \vec{k}\cdot\vec{r})\}.$$

Since no exact solution is known for this problem, and because the geometrical acoustics solution for it is either trivial (zero) or meaningless (infinite at beam and axial aspects), we are interested only in the Kirchhoff and Keller solutions.

2.3.2.3.2 THE KIRCHHOFF SOLUTION

for σ computed from Eq. (c-118) is

$$\sigma_{KIR} = 4\pi (ka)^2 |S|^2 \qquad (2.3\text{-}28)$$

$$S = \frac{a}{2}\cos\theta \exp\{-2ik\ell\cos\theta\} \frac{J_1(2ka\sin\theta)}{ka\sin\theta} + \frac{2}{\pi}\ell\sin\theta\, J_0(2k\ell\cos\theta) \left(\frac{\pi}{4ka\sin\theta}\right)^{1/2} J(2ka\sin\theta)$$

where J_1 is a cylindrical Bessel function

J_0 is a spherical Bessel function

$$J(\xi) \equiv \left(\frac{\xi}{2\pi}\right)^{1/2} \int_0^{\pi/2} \cos\theta \exp\{-i\xi\cos\theta\}\, d\theta.$$

The first term of S above is due to scattering from the ensonified end cap (disc) while the second term is due to the cylindrical surface. The evaluation of $J(\xi)$ using the "stationary phase method", coupled with a high frequency expansion (see Appendix C-5.2) results in

$$J(\xi) \simeq \exp\{i(\pi/4 - \xi)\} \left[1 - \frac{3i}{8\xi} + \cdots\right].$$

2.3.2.3.3 THE KELLER SOLUTION for σ computed from Eq. (d-28) is

$$\sigma_{KEL} = \frac{\pi a^2}{3\pi ka \sin\theta} \left| \sum_{i=1}^{3} E_i D_i \right|^2 \qquad (2.3\text{-}29)$$

where

$$E_1 = \exp\left\{2ik(-a\sin\theta + \ell\cos\theta) + \frac{i\pi}{4}\right\} \qquad (2.3\text{-}30)$$

$$E_2 = \exp\left\{2ik(-a\sin\theta - \ell\cos\theta) + \frac{i\pi}{4}\right\}$$

$$E_3 = \exp\left\{2ik(a\sin\theta - \ell\cos\theta) - \frac{i\pi}{4}\right\}$$

$$D_1 = -\tfrac{2}{3} + \left[-\tfrac{1}{2} - \cos\tfrac{4}{3}\theta\right]^{-1}$$

$$D_2 = -\tfrac{2}{3} + \left[-\tfrac{1}{2} - \cos\tfrac{2}{3}(\pi + 2\theta)\right]^{-1}$$

$$D_3 = -\tfrac{2}{3} + \left[-\tfrac{1}{2} - \cos\tfrac{4}{3}(\pi + \theta)\right]^{-1}.$$

Each of the contributions (i = 1, 2, 3) in Eq. (2.3-29) is due to scattering from one of three edges ensonified by the incident plane wave. The three contributions are added in phase to obtain the total field.

2.3.2.3.4 DISCUSSION OF RESULTS. Since no exact solution is known for this problem, we will use experimental results as our norm. The only such results available are those of DUNSINGER [1970] who performed the experiment for two different length to radius ratios (ℓ/a).

Figure (2.3-8) shows the Kirchhoff and Keller backscattering cross-sections computed from Eq. (2.3-28) and Eq. (2.3-29) for ka = 10 and $\ell/a = 1$ (there are no experimental results for these values). We note that the two results agree near axial and broadside incidence, but there are large discrepancies in mid-aspect range (near $\theta = 45°$), where the peak-to-peak difference is about 20 dB and the peak-to-trough difference about 40 dB.

It is difficult to compare these curves because of their highly oscillatory character. However, the comparison of these two methods can be simplified as follows. Terms in both the Kirchhoff and Keller solutions can be identified with the three ensonified edges of the cylinder. We can define a cross-section for each edge. The backscattering cross-section is then a weighted sum of the edge cross-sections and its jagged character is a result of the oscillatory exponential weighting functions. Plots of the edge cross-sections are smooth curves. These quantities can be determined experimentally by means of a pulse technique [DUNSINGER-1970].

In Figure (2.3-9) we plot functions $g_i = \sqrt{\pi\sigma_i}/k$ associated with the cross-sections σ_i of the three ensonified edges. The Kirchhoff formulas for these functions are given by DUNSINGER [1970]. The Keller formulas are obtained from

$$\sigma_i = |D_i|^2/3\pi ka\sin\theta \qquad i = 1, 2, 3$$

where D_i is given by Eq. (2.3-30). The results, which are shown together with Dunsinger's experimental points, are for ka = 253, $\ell/a = 3.04$, and are given relative to a standard target (a 2 cm. diameter solid aluminum sphere).

The Keller and Kirchhoff curves differ most significantly from corners 1 and 3 in mid-aspect range. Comparison with the experimental points is indecisive and our strongest conclusion is the need for further experimental work, preferably at lower frequencies, with special attention to aspects at which the Keller and Kirchhoff results differ significantly. A similar comparison has been made with Dunsiger's other set of experimental data with the same conclusion.

In Figure (2.3-10) we plot - $\sigma_{KEL} / \sigma_{KIR}$ vs. ka for axial incidence using Eq. (d-40) for σ_{KEL}, which includes the effect of double diffraction. We see that the two methods differ significantly only at very low ka. This is reasonable. The Kirchhoff method neglects multiple scattering, which should be least important at normal incidence and most important near grazing incidence.

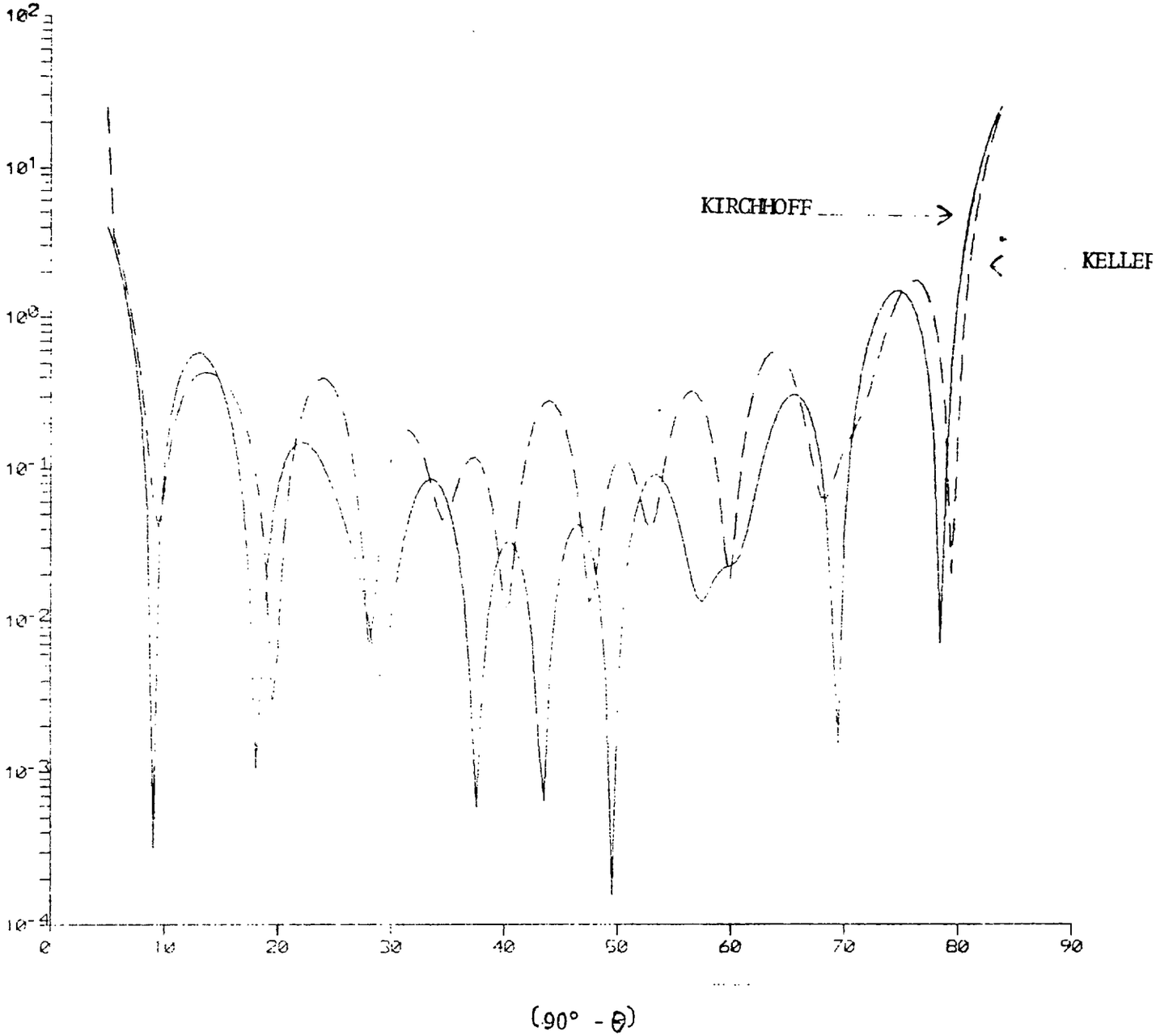

FIGURE 2.3-8 SONAR CROSS-SECTION VS ASPECT; FINITE CYLINDER, ka = 10, ℓ/a = 1

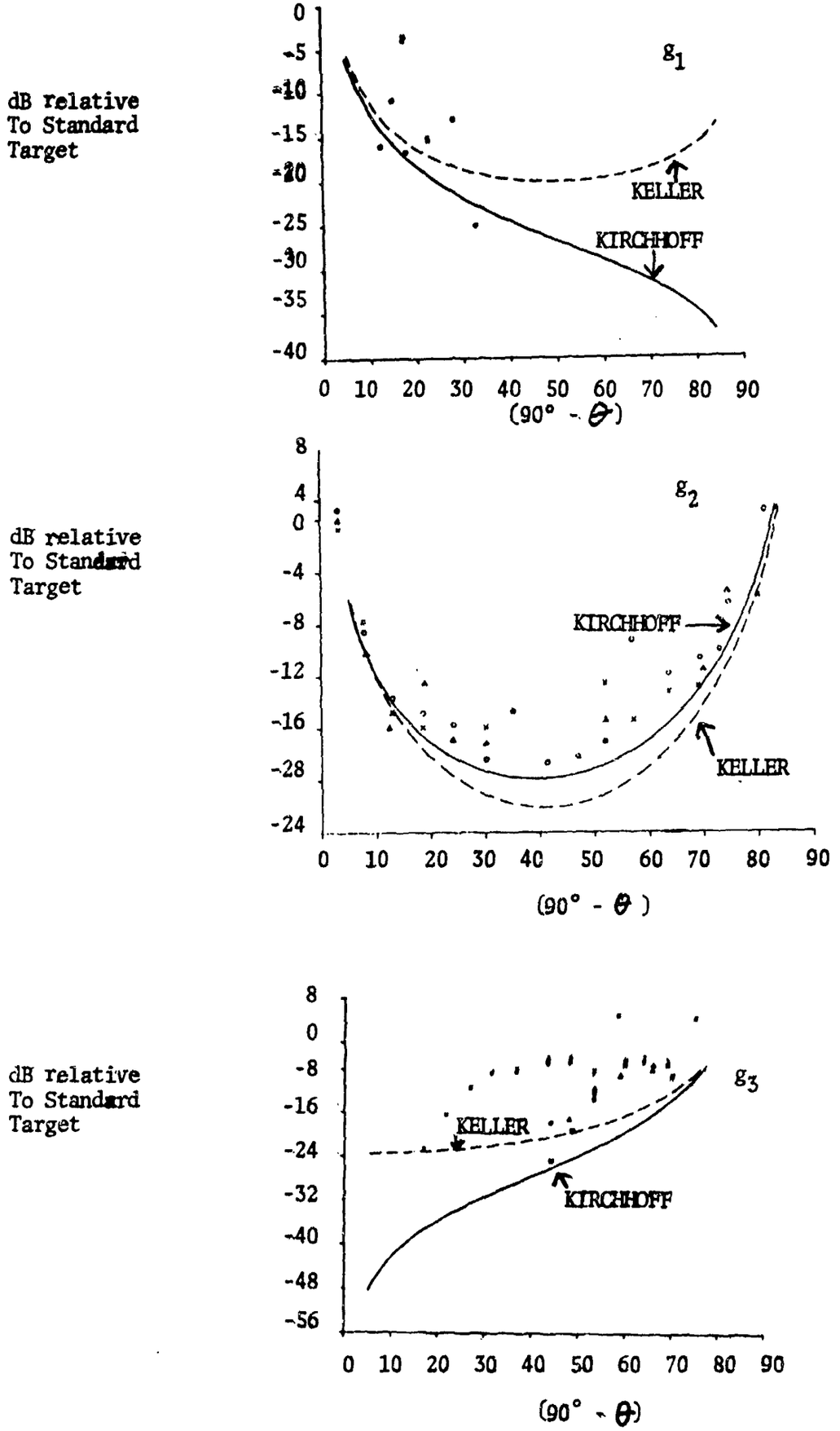

Figure 2.3-9 g_i VS (90° - θ); FINITE CYLINDER

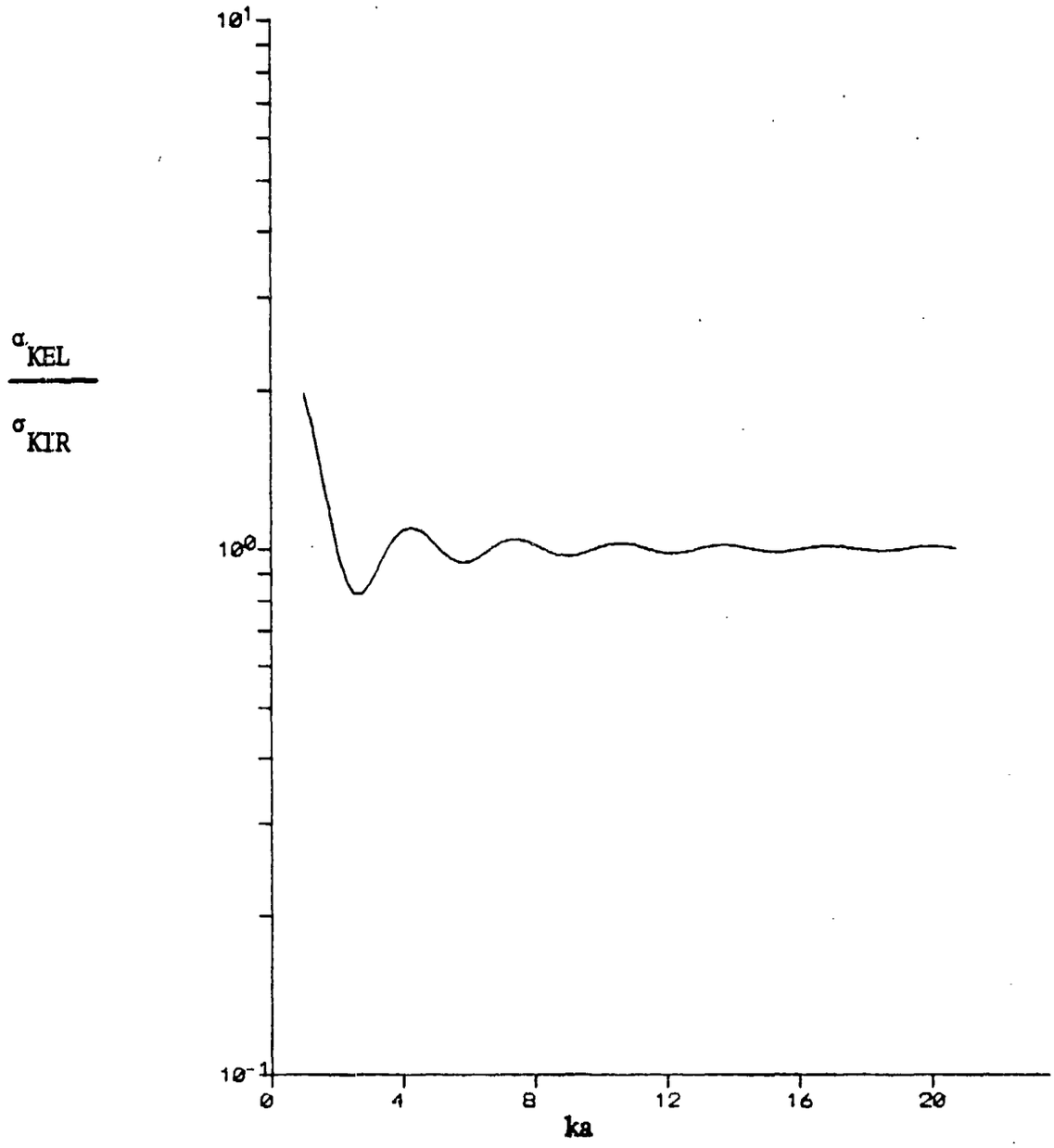

Figure 2.3-10

COMPARATIVE SONAR CROSS-SECTION. VS ka; AXIAL INCIDENCE, FINITE, RIGID CYLINDER

2.3.3 TABLES OF COMPARATIVE FORMULAS. Tables (2.3-1) through (2.3-18) represent an extensive compilation of comparative analytic solutions for the three-dimensional, back-scattering cross-section for acoustically hard simple shapes. The identifier "simple" is meaningful in two senses: in the geometric sense, the shapes are characterized by rather simple geometry; in the field analytic sense, many of the shapes conform to surfaces for which the wave equation is separable. These tables constitute the second level of our synthesis and offer the reader the opportunity to make detailed comparisons between the predictions of the various theories. Example comparisons for the sphere, spheroid, and finite cylinder, presented previously, are illustrative of the use to which these tables can be put.

Backscattering cross-section, as defined in Eq. (a-57) is proportional to the ratio of scattered to incident energy where source and receiver are coincident and located in the far field. It is implicit, therefore, that all of the formulas in these tables are applicable only for dimensions, frequencies, and ranges satisfying the conditions $kr>>1$ and $r>\ell^2/\lambda$ where k is the wave number, r is the distance between the sonar and the target, and ℓ is the maximum dimension of the target.

Where possible, the scattering formulas have been recorded for arbitrary angles of incidence. By arbitrary incidence is meant a wave impingent upon a scattering surface from any direction (θ,ϕ). In many cases, formulas have not yet been developed for arbitrary angles of incidence, but do exist for specific angles.

Three methods which approximate the exact solution of scattering from simple shapes have been selected for study and comparision; specifically, geometrical acoustics (G A), Kirchhoff theory, and Keller theory. These methods are discussed in depth in Appendices B, C, and D, respectively. The method of geometrical acoustics is a frequency-independent first-order approximation to the exact solution, whereas both the Kirchhoff and Keller methods have frequency dependent correction terms. All three methods afford high frequency approximate solutions to the wave equation which require that $ka>>1$ where "a" is a characteristic dimension of the

scatterer. In general, the ka constraint on geometrical acoustics is greater than on Kirchhoff or Keller; that is,

$$(ka)_{G\,A} > (ka)_{KIR\,,KEL} > 1$$

In an effort to facilitate comparison where possible, the formulas have been normalized to the geometrical acoustics cross-section, $\sigma_{G.A}$ Exact analytical solutions are shown in each table whenever they exist. If they do not, then experimental results are referenced (if available).

These tables are similar, in some respects, to those in URICK [1967], MAJOR [1946] and FESSENDEN [1972]. However, we have sought to present comparative results and to emphasize the uncertainty which exists. Blank entries in the tables are very informative since they indicate that results are not now available, or that the method fails (as noted under comments). Furthermore, one should not assume that relative complexity implies a more accurate prediction, since in certain situations (e.g., see section 2.3.2.2) this is not so. The tables are ordered alphabetically by body type and included are:

TABLE 2.3-1 . . . . Finite circular cone, axial incidence
-2 . . . . Semi-infinite circular cone, axial incidence
-3 . . . . Finite circular cylinder, arbitrary incidence
-4 . . . . " " " , axial incidence
-5 . . . . " " " , beam incidence
-6 . . . . Ellipsoid, arbitrary incidence
-7 . . . . Circular ogive, arbitrary incidence
-8 . . . . " " , axial incidence
-9 . . . . Circular flat plate, arbitrary incidence
-10 . . . . " " " , axial incidence
-11 . . . . Rectangular flat plate, arbitrary incidence
-12 . . . . Oblate spheroid, arbitrary incidence
-13 . . . . Oblate spheroid, axial incidence
-14 . . . . " " , edge-on incidence
-15 . . . . Prolate spheroid, arbitrary incidence
-16 . . . . " " , axial incidence
-17 . . . . " " , beam incidence
-18 . . . . Sphere, arbitrary incidence

Table 2.3-1. Backscattering Cross-Section

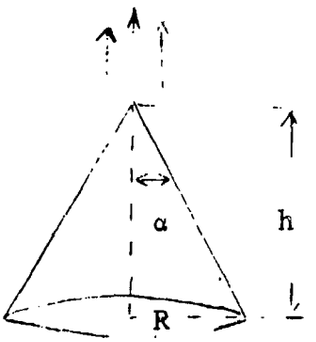

METHOD	BACKSCATTERING CROSS-SECTION, σ
Geometrical Acoustics	$\sigma = 0$
Kirchhoff	$\sigma = \frac{\lambda^2}{\pi} \left\| \frac{1}{4} \tan^2\alpha \, [1 + (2ikh - 1)\exp(2ikh)] \right\|^2$
Keller	$\sigma = \sigma_1 \left\| 1 + Ae^{iB} \right\|^2$ where $\sigma_1 = \{\pi^3 R^2/[3\pi/2 + \alpha]^2\} \csc^2[4\pi^2/(3\pi + 2\alpha)]$ and $A = \frac{\sin^2(\pi/n)\sin(2\pi/n)}{2n(\pi kR)^{1/2}\sin^2(5\pi/4n)\sin^2(\pi/4n)}$ $B = 2kR - \pi/4; \quad n = 3/2 + \alpha/\pi$
Exact	

Of A Finite Circular Cone

Nose-On Axial Incidence

REFER TO	COMMENTS
Appendix B.3	
[RUCK - 1970; Vol. 1, p. 397]	First term is tip contribution; second is edge singularity contribution.
[CRISPIN - 1968; p. 100]	
	No exact solution exists for flat-based cone problem; however, a numerical solution to the capped cone problem has been developed [PUCK - 1970; Vol. 1, p. 391].

Table 2.3-2. Backscattering Cross-Section Of A

METHOD	BACKSCATTERING CROSS-SECTION, σ
Geometrical Acoustics	$\sigma = 0$
Kirchhoff	$\sigma = \frac{\lambda^2}{16\pi} \tan^4 \alpha$
Keller	
Exact	Restricted cone angles $\alpha \approx \pi/2 \qquad \sigma_{WIDE} \approx \frac{\lambda^2}{16\pi(\alpha - \frac{\pi}{2})^4}$ $\alpha \approx 0 \qquad \sigma_{THIN} \approx \frac{\lambda^2 \alpha^4}{16\pi}$

Semi-Infinite Circular Cone

Nose-On Incidence, $\alpha < 90°$

REFER TO	COMMENTS
Appendix B.3	
Appendix C-4.5	
Appendix D.2	Same as Exact Solution. This is a "canonical problem" in the Keller method.
[FELSEN - 1955; p. 145] [SIEGEL et al. - 1955; p. 312] [BOWMAN - 1969; p. 658]	These are first order approximations obtained from an exact solution. There is first order agreement with the Kirchhoff result for wide angle cones but there is a discrepancy of a factor of four for thin angle cones. There are some confusing misprints in the literature. In Felsen's eq. 2.28, $64\pi^2$ should be replaced by 16π. In Bowman's eq. 18.124, $(\pi - \theta_1)^2$ should be replaced by $(\pi - \theta_1)^4$.

Table 2.3-3. Backscattering Cross-Section of

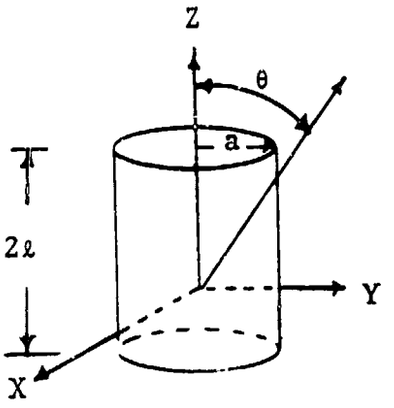

METHOD	BACKSCATTERING CROSS-SECTION, σ
Geometrical Acoustics	$\sigma = 0$
Kirchhoff	$\sigma = 4\pi(ka)^2 \lvert S \rvert^2$ $S = \frac{a \cos\theta}{2} \frac{J_1(2ka \sin\theta)}{ka \sin\theta} \exp(-2ik\ell\cos\theta)$ $+ \ell\sqrt{\frac{\sin\theta}{\pi ka}}\, j_0(2k\ell\cos\theta)\, J(2ka \sin\theta)$ where $J(x) \equiv \sqrt{\frac{x}{2\pi}} \int_0^{\pi/2} \cos\theta \exp(-ix\cos\theta)\, d\theta \tilde{=} [1 - \frac{3i}{8x} + \ldots] \cdot \exp\{-ix-\pi/4)$
Keller	$\sigma = \frac{a}{3k \sin\theta} \left\lvert \sum_{i=1}^{3} E_i D_i \right\rvert^2$, where $E_1 = \exp\{2ik(-a \sin\theta+\ell\cos\theta)+\pi i/4\}$ $D_1 = -2/3 + [-1/2 - \cos$ $E_2 = \exp\{2ik(-a \sin -\ell\cos\theta)+\pi i/4\}$ $D_2 = -2/3 + [-1/2 - \cos$ $E_3 = \exp\{2ik(a \sin -\ell\cos\theta)-\pi i/4\}$ $D_3 = -2/3 + [-1/2 - \cos$
Exact	

A Finite Circular Cylinder

Arbitrary Incidence, $0 < \theta < 90°$ and $0 < \Theta < 180°$

	REFER TO	COMMENTS
	Appendix B.3	
	Appendix C-4.4, 4.5	Takes into account the phase contributions of the ends of the cylinder and for $\theta \rightarrow \pi/2$ reduces to Eq. 22 in [CRISPIN - 1968; p. 186].
		$J(2ka\sin\theta)$ evaluated using method of stationary phase and asymptotic series (see Appendix C-5.2).
	Appendix D.3	Single diffraction accounted for only.
$2/3(2\theta)]^{-1}$		
$2/3(\pi+2\theta)]^{-1}$		
$4/3(\pi/2-\theta)]^{-1}$		
		Not presently known.

Table 2.3-4. Backscattering Cross-Section

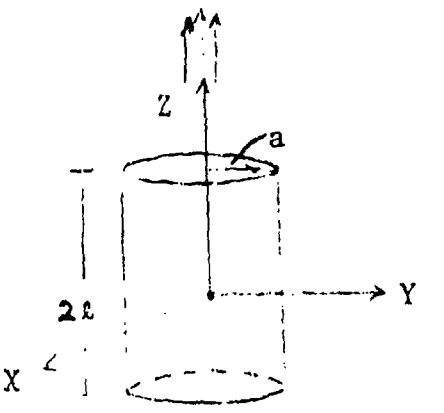

METHOD	BACKSCATTERING CROSS-SECTION, σ
Geometrical Acoustics	
Kirchhoff	$\sigma = \frac{k^2}{\pi} A^2 \qquad A = \pi a^2$
Keller	$\sigma = \pi a^2 (ka)^2 \left\lvert 1 + \frac{4}{3\sqrt{\pi}} \frac{\exp\{2ika - 3\pi i/4\}}{(ka)^{3/2}} \right\rvert^2$
Exact	

Of A Finite Cylinder

Axial Incidence

	REFER TO	COMMENTS
	Appendix B.3	Method fails.
	Appendix C-4.2	Appears as a disc.
	Appendix D.3	Double diffraction accounted for.
		Not presently known.

Table 2.3-5. Backscattering Cross-Section

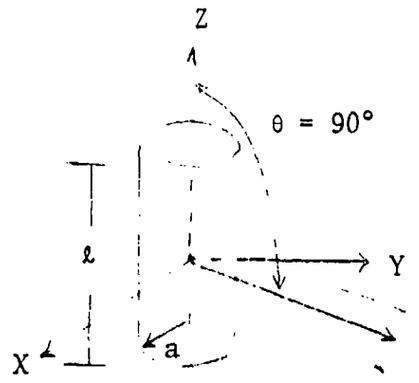

METHOD	BACKSCATTERING CROSS-SECTION, σ
Geometrical Acoustics	
Kirchhoff	$\sigma = \frac{2\pi \ell^2 a}{\lambda}$
Keller	$\sigma = \frac{2\pi \ell^2 a}{\lambda}$
Exact	

Of A Circular Cylinder

Beam Incidence

	REFER TO	COMMENTS
	Appendix B.3	Method fails.
	Appendix C.4-4	
	Appendix D.3	Result based on singly diffracted rays only.
		Not presently known.

Table 2.3-6. Backscattering Cross-Section

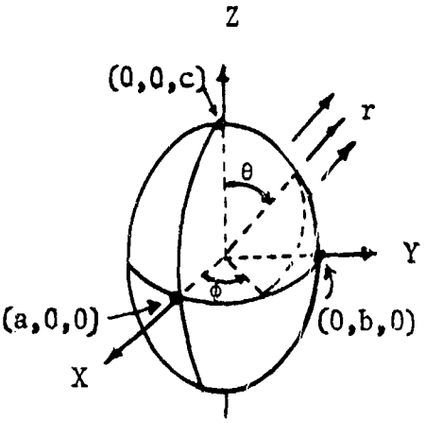

METHOD	BACKSCATTERING CROSS-SECTION, σ
Geometrical Acoustics	$\sigma = \dfrac{\pi a^2 b^2 c^2}{(a^2\sin^2\theta\cos^2\phi + b^2\sin^2\theta\sin^2\phi + c^2\cos^2\theta)^2}$
Kirchhoff	$\sigma = \dfrac{\pi a^2 b^2}{c^2}\left(1 - \dfrac{\sin(2kc)}{kc} + \dfrac{\sin^2(kc)}{(kc)^2}\right)$ (note; $\theta = 0, 180°$ only)
Keller	
Exact	

Of An Ellipsoid

Arbitrary Incidence

Spherical Coordinate System:

$X = r \sin\theta \cos\phi$

$Y = r \sin\theta \sin\phi$

$Z = r \cos\theta$

	REFER TO	COMMENTS
	Appendix B.3	
	[RUDGERS - 1965; p. 10]	Method applicable but has not yet been developed for other than $\theta = 0°, 180°$.
		Method applicable but has not yet been developed [except for the prolate spheroid at axial incidence; see Table 2.3-16].
		Separation of variables method applicable but has not yet been developed [RUCK - 1970; Vol. 1, p. 341].

Table 2.3-7 Backscattering Cross-Section

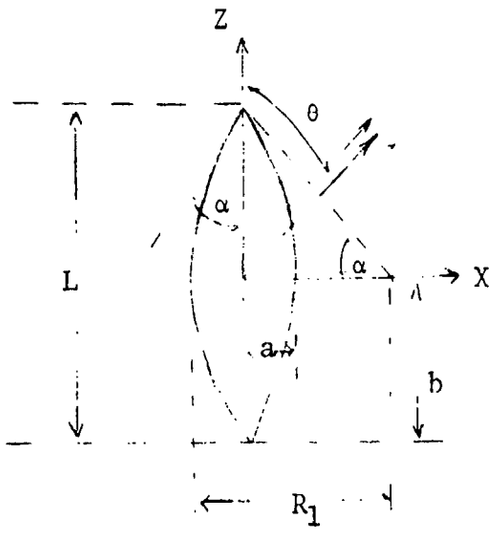

METHOD	BACKSCATTERING CROSS-SECTION, σ
Geometrical Acoustics	$\sigma(\theta) = 0; \quad 0 \le \theta < 90° - \alpha$ $\sigma(90° - \alpha) = \frac{R_1^2 \sin^2\alpha}{4\pi} = \frac{a^2}{4\pi \tan^2(\frac{a}{2})}$; $\theta = 90° - \alpha$ only. $\sigma(\theta) = \pi R_1^2 (1 - \frac{R_1 - a}{R_1 \sin\theta})$; $(90° - \alpha) < \theta \le 90°$
Kirchhoff	$\sigma(\theta) = \frac{\lambda^2 \tan^4\alpha}{16\pi \cos^6\theta (1 - \tan^2\alpha \tan^2\theta)^3}$ with $(\frac{\lambda}{4\pi R_1})^{1/2} < \alpha < \frac{\pi}{2} - (\frac{\lambda}{4\pi R_1})^{1/2}$, and $0° \le \theta < (90° - \alpha)$
Keller	
Exact	

Of A Circular Ogive

Arbitrary Incidence, $0 \leq \theta \leq 90°$

Relationships:

$$\cos \alpha = 1 - \frac{a}{R_1}$$

$$L/2 = [R_1^2 - (R_1 - a)^2]^{1/2}$$

Using cylindrical coordinates (W, θ, Z), the equation of the surface is

$$(W + R_1 - a)^2 + Z^2 = R_1^2 \quad \text{where} \quad |Z| \leq L/2, \; 0 \leq W \leq a$$

R_1 = the radius of curvature in the X-Z plane

$L = 2b$

	REFER TO	COMMENTS
	Appendix B.2 [CRISPIN - 1968; p. 93]	The required tangent plane does not exist for $0 \leq \theta < 90° - \alpha$.
	[CRISPIN - 1968; p. 93]	Excellent agreement with experiment [CRISPIN - 1968; p. 95].
	[CRISPIN - 1968; p. 93]	Stationary phase solution: for quantitative results on tip scattering as a function of aspect and α see [CRISPIN - 1968; pp. 97-98].
		Method applicable but has not been developed.
		Solution not presently known.

Table 2.3-8 Backscattering Cross-Section

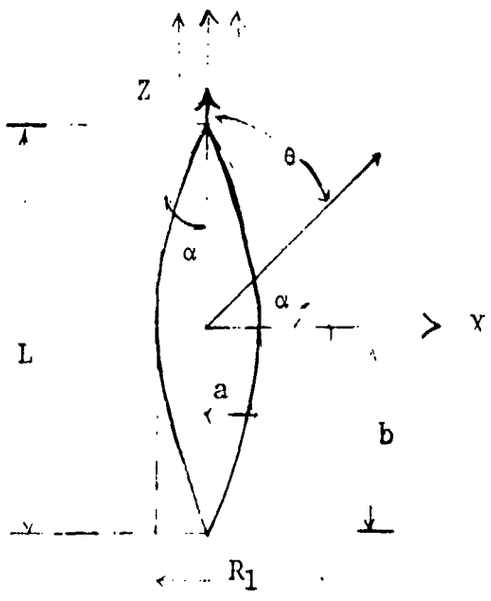

METHOD	BACKSCATTERING CROSS-SECTION, σ
Geometrical Acoustics	$\sigma = 0$
Kirchhoff	$\sigma(0°) = \frac{\lambda^2 \tan^4\alpha}{16\pi} \left[1 + \frac{2\cos^2\alpha\cos 2kb}{1+\cos\alpha} + \frac{\cos^4\alpha}{(1+\cos\alpha)^2}\right]$ $\sigma(0°) = \frac{\pi\lambda^2(2\alpha)^{4.3}}{2 \times 10^{10}} \left\{1 + \sin\left[2\pi\left(\frac{4kb\alpha}{\pi\sin 2\alpha} - 1.25\right)\right]\right\}$ Fat Ogive $\sigma(0°) < \pi R_1^2 \left[\left(\frac{\lambda}{4\pi R_1}\right)^{1/2} \cot\left(\frac{\lambda}{4\pi R_1}\right)^{1/2}\right]^4$ Thin Ogive $\sigma(\theta) = \frac{2[f(\theta)]^4}{[-1 + \mathrm{Cin}(2kb)]^2} \frac{\lambda^2}{4\pi}$ where $f(\theta) = \left[\frac{\sin\theta}{(1-\cos\theta)}\right] \sin[kb]$ • about θ near 0° and where Cin(x) = modified cosine integral of argument x.
Keller	
Exact	

Of A Circular Ogive

Axial Incidence, $\theta = 0°$

Relationships:

$$\cos \alpha = 1 - \frac{a}{R_1}$$

$$L/2 = [R_1^2 - (R_1 - a)^2]^{1/2}$$

Using cylindrical coordinates (W, θ, Z), the equation of the surface is

$(W + R_1 - a)^2 + Z^2 = R_1^2$ where $|Z| \leq L/2$, $0 \leq W \leq a$

R_1 = the radius of curvature in the X-Z plane

$L = 2b$

	REFER TO	COMMENTS
	Appendix B.3	
	[RUCK - 1970; p. 370]	Exact solution of Kirchhoff integral.
	[RUCK - 1970; p. 373]	Empirical solution based on $\alpha = 20°$, $37.5°$, $60°$.
	[CRISPIN - 1968; p. 94]	$\sigma_{max} = \pi R_1^2$; as $\alpha \to 90°$, body takes on shape of sphere.
$(1 - \cos\theta)$	[CRISPIN - 1968; p. 94]	Quantitative results (theoretical) [CRISPIN - 1968; p. 95].
		To first order Keller solution is the same as exact solution for nose-on incidence on infinite cone with cone angle 2α.
	Appendix D.2	Not presently known.

Table 2.3-9. Backscattering Of A

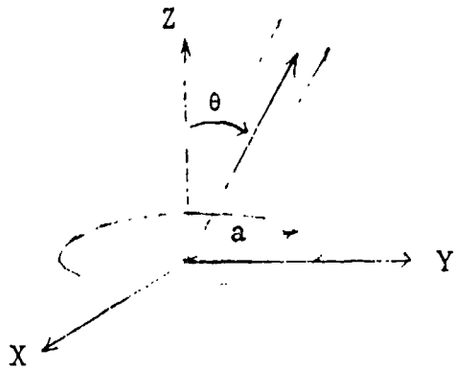

METHOD	BACKSCATTERING CROSS SECTION, σ
Geometrical Acoustics	$\sigma = 0$
Kirchhoff	$\sigma = \frac{\pi a^2}{\tan^2\theta}\left[J_1(2ka\sin\theta)\right]^2$
Keller	$\sigma = \frac{2a^2\{1-\cos^2(2ka\sin\theta-\pi/4)\cos^2\theta\}}{ka\sin^3\theta}$
Exact	$\sigma = \frac{4\pi}{k^2}\mid S \mid^2$ where $S = 2i \sum_{n=0}^{\infty} \frac{1}{\tilde{N}_{on}} \frac{R_{on}^{(1)\prime}(-ika,i0)}{R_{on}^{(3)\prime}(-ika,i0)} S_{on}(-ika,-\cos(\theta)) \cdot S_{on}(-ika,\cos\theta)$ $R_{mn}^{(1)}$, $R_{mn}^{(3)}$, S_{mn} are spheroidal wave functions, $\tilde{N}_{mn}$ is the normalization constant for the spheroidal functions, $\epsilon_o = 1$, $\epsilon_m = 2$ for $m \neq 0$ [ABRAMOWITZ - 1964].

Circular Flat Plate (Disc)

	REFER TO	COMMENTS
	Appendix B.3	
	Appendix C-4.4	
	[KELLER - 1960]	Result based on singly diffracted rays only. Adapted from Eq. 19 by setting wedge angle equal to zero (n = 2).
	[BOWMAN - 1969; p. 545]	Special case of oblate spheroid with surface $\xi_1 = 0$.

Table 2.3-10. Backscattering Of A

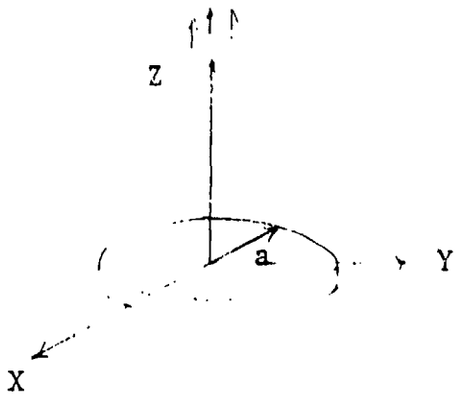

METHOD	BACKSCATTERING CROSS-SECTION, σ
Geometrical Acoustics	
Kirchhoff	$\sigma = 4\pi \frac{A^2}{\lambda^2}, \quad A = \pi a^2$
Keller	$\sigma = \pi a^2 (ka)^2 \left\| 1 - \frac{2}{\sqrt{\pi}(ka)^{3/2}} \exp(2ika + i\pi/4) \right\|^2$
Exact	$\sigma = \frac{4\pi}{k^2} \left\| S \right\|^2$ where $S = 2i \sum_{n=0}^{\infty} \frac{1}{\tilde{N}_{on}} \frac{R_{on}^{(1)'}(-ika, 0)}{R_{on}^{(3)'}(-ika, 0)} S_{on}(-ika,-1)\, S_{on}(-ika,1)$

$R_{mn}^{(1)}$, $R_{mn}^{(3)}$, S_{mn} are spheroidal wave functions, $\tilde{N}_{mn}$ is the normalization constant for the spheroidal functions $\varepsilon_0 = 1$, $\varepsilon_m = 2$ for $m \neq 0$ [ABRAMOWITZ - 1964].

Axial Incidence

Circular Flat Plate (Disc)

	REFER TO	COMMENTS
	Appendix B.3	Method fails.
	[CRISPIN - 1968; p. 121]	Result similar to return from two independent scatterers with the magnitude of each given by $a\lambda/8\pi\sin\theta\tan^2\theta$ [CRISPIN - 1968; p. 122].
	[KELLER - 1960]	Result based on singly and doubly diffracted rays. Adapted from Eqs. 14 and 27 by setting wedge angle equal to zero ($n = 2$) from [KELLER - 1960].
	[BOWMAN - 1969; p. 546]	Special case of oblate spheroid, i.e., $\xi_1 = 0$.

Table 2.3-11. Backscattering Of A

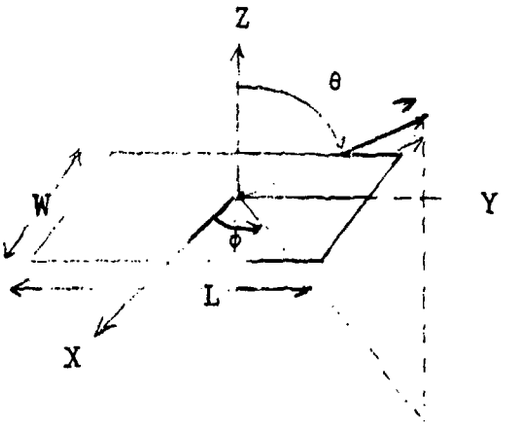

METHOD	BACKSCATTERING CROSS-SECTION, σ
Geometrical Acoustics	$\sigma = 0; \quad 0 < \theta \leq 90°$ ϕ arbitrary
Kirchhoff	$\sigma = \frac{4\pi W^2 L^2}{\lambda^2} \cos^2\theta \frac{\sin^2(kL \sin\theta\sin\phi)\sin^2(kW\sin\theta\cos\phi)}{(kL\sin\theta\sin\phi)^2(kW\sin\theta\cos\phi)2}$
Keller	
Exact	

Rectangular flat plate

	REFER TO	COMMENTS
	Appendix B.3	Method fails at $\theta = 0$.
	Appendix C-4.3	Return is specular return at broadside; contributions from the ends added in a $\frac{\sin x}{x}$ manner.
	Appendix D.2	Keller method applicable in principle but has not been rigorously applied to this problem because the canonical problems corresponding to the corners have not been solved. A solution has been obtained by Ross [1966: p. 329] through the introduction of an ad hoc assumption which is not a part of the Keller method. Nevertheless, this solution seems to yield good agreement with experiment.
		Not presently known.

Table 2.3-12. Backscattering Cross-Section

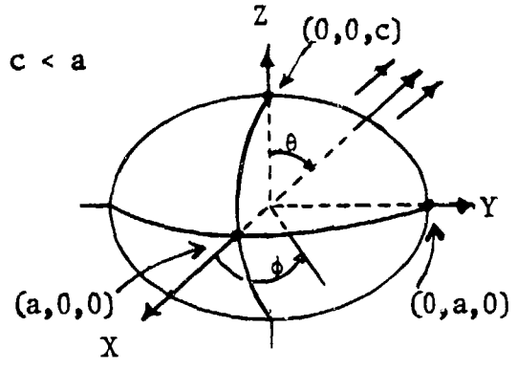

METHOD	BACKSCATTERING CROSS-SECTION, σ
Geometrical Acoustics	$\sigma = \dfrac{\pi a^4 c^2}{(a^2\sin^2\theta + c^2\cos^2\theta)^2}$; θ, ϕ arbitrary
Kirchhoff	
Keller	
Exact	$\sigma = \dfrac{4\pi}{k^2} \mid S \mid^2$ where $S = 2i \sum_{n=0}^{\infty} \dfrac{1}{\tilde{N}_{on}} \dfrac{R_{on}^{(1)\prime}(-ih, i\xi_1)}{R_{on}^{(3)\prime}(-ih, i\xi_1)} S_{on}(-ih, \cos\theta) S_{on}(-ih, -\cos\theta)$ $R_{mn}^{(1)}$, $R_{mn}^{(3)}$, S_{mn} are spheroidal wave functions, $\tilde{N}_{mn}$ is the normalization constant for the spheroidal functions, $\epsilon_o = 1$, $\epsilon_m = 2$ for $m \neq 0$ [ABRAMOWITZ - 1964],

Arbitrary Incidence

Of An Oblate Spheroid

Oblate Spheroidal Coordinates :

$$X = \frac{1}{2} d \sqrt{(\xi^2+1)(1-\eta^2)}\cos\phi$$

$$Y = \frac{1}{2} d \sqrt{(\xi^2+1)(1-\eta^2)}\sin\phi$$

$$Z = \frac{1}{2} d\xi\eta$$

where $0 \leq \xi < \infty$, $-1 \leq \eta \leq 1$, $0 \leq \phi < 2\pi$

Relationships: $2c = d\xi_1$, $2a = d\sqrt{\xi_1^2+1}$, $c/a = \dfrac{\xi_1}{\sqrt{\xi^2+1}}$, $h = (1/2)kd$

	REFER TO	COMMENTS
	Appendix B.3	Obtained from geometrical acoustics formula for ellipsoid by setting $a \equiv b$.
		Method applicable but has not yet been developed.
		Method applicable but has not yet been developed.
	[BOWMAN - 1969; p. 514]	

Table 2.3-13. Backscattering Cross-Section

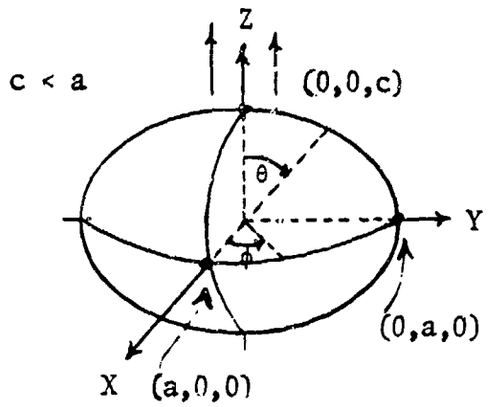

METHOD	BACKSCATTERING CROSS-SECTION, σ
Geometrical Acoustics	$\sigma = \pi \frac{a^4}{c^2}$
Kirchhoff	$\sigma = \pi \frac{a^4}{c^2} \left(1 - \frac{\sin(2kc)}{kc} + \frac{\sin^2(kc)}{(kc)^2}\right)$
Keller	
Exact	$\sigma = \frac{4\pi}{k^2} \lvert S \rvert^2$ $S = 2i \sum_{n=0}^{\infty} \frac{1}{\tilde{N}_{on}} \frac{R_{on}^{(1)'}(-ih, i\xi_1)}{R_{on}^{(3)'}(-ih, i\xi_1)} S_{on}(-ih, -1) S_{on}(-ih, 1)$ $R_{mn}^{(1)}$, $R_{mn}^{(3)}$, S_{mn} are spheroidal wave functions, $\tilde{N}_{mn}$ is the normalization constant for the spheroidal functions, $\epsilon_o = 1$, $\epsilon_m = 2$ for $m \neq 0$ [ABRAMOWITZ - 1964].

Oblate Spheroidal Coordinates: $X = \frac{1}{2} d \sqrt{(\xi^2+1)(1-\eta^2)}\cos\phi$

$$Y = \frac{1}{2} d \sqrt{(\xi^2+1)(1-\eta^2)}\sin\phi$$

$$Z = \frac{1}{2} d\xi\eta$$

where $0 \leq \xi < \infty$, $-1 \leq \eta \leq 1$, $0 \leq \phi < 2\pi$

Relationships: $2c = d\xi_1$, $2a = d\sqrt{\xi_1^2 + 1}$, $c/a = \xi_1/\sqrt{\xi_1^2 + 1}$, $h = (1/2)kd$

	REFER TO	COMMENTS
	Appendix B.3	Obtained from G.A. formula for ellipsoid by setting $\theta = 0$, $\phi = 0$; $b = a$.
	[RUDGERS - 1965; p. 10]	Experimental and theoretical comparisons [CRISPIN and SIEGEL - 1968; p. 88].
		Method applicable but has not been developed.
	[BOWMAN - 1969; p. 514]	

Table 2.3-14. Backscattering Cross-Section

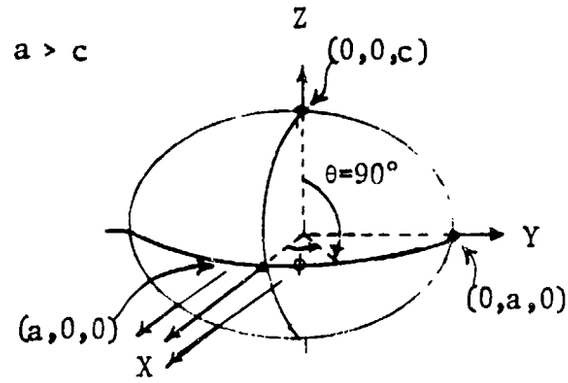

METHOD	BACKSCATTERING CROSS-SECTION, σ
Geometrical Acoustics	$\sigma = \pi c^2$
Kirchhoff	$\sigma = \pi c^2 \left(1 - \frac{\sin(2ka)}{ka} + \frac{\sin^2(ka)}{(ka)^2}\right)$
Keller	
Exact	$\sigma = \frac{4\pi}{k^2} \lvert S \rvert^2$ where $S = 2i \sum_{n=0}^{\infty} \frac{1}{\tilde{N}_{on}} \frac{R_{on}^{(1)'}(-ih, i\xi_1)}{R_{on}^{(3)'}(-ih, i\xi_1)} S_{on}(-ih, -1) S_{on}(-ih, 1)$ $R_{mn}^{(1)}$, $R_{mn}^{(3)}$, S_{mn} are spheroidal wave functions, $\tilde{N}_{mn}$ is the normalization constant for the spheroidal functions, $\varepsilon_o = 1$, $\varepsilon_m = 2$ for $m \neq 0$ [ABRAMOWITZ - 1964].

Edge-On Incidence, $\theta = 90°$

Of An Oblate Spheroid

Oblate Spheroidal Coordinates: $X = \frac{1}{2} d \sqrt{(\xi^2+1)(1-\eta^2)}\cos\phi$

$$Y = \frac{1}{2} d \sqrt{(\xi^2+1)(1-\eta^2)}\sin\phi$$

$$Z = \frac{1}{2} d\xi\eta$$

where $0 \leq \xi < \infty$, $-1 \leq \eta \leq 1$, $0 \leq \phi < 2\pi$

Relationships: $2c = d\xi_1$, $2a = d\sqrt{\xi_1^2 + 1}$, $c/a = \frac{\xi_1}{\sqrt{\xi_1^2+1}}$, $h = (1/2)kd$

	REFER TO	COMMENTS
	Appendix B.3	Obtained from geometrical acoustics formula for ellipsoid by setting $\theta = \pi/2$; $b = a$.
	[RUDGERS - 1965; p. 10]	
		Method applicable but has not yet been developed.
	[BOWMAN - 1969; p. 514]	Numerical results [BRUNDRIT - 1965].

Table 2.3-15. Backscattering Cross-Section

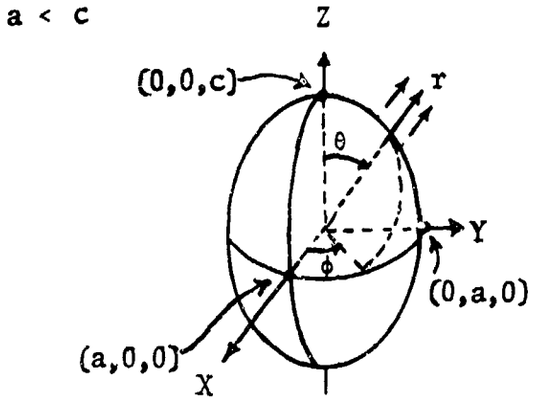

METHOD	BACKSCATTERING CROSS SECTION, σ
Geometrical Acoustics	$\sigma = \dfrac{\pi a^4 c^2}{(a^2\sin^2\theta + c^2\cos^2\theta)^2}$
Kirchhoff	
Keller	
Exact	$\sigma(\theta) = \dfrac{4\pi}{k^2} \mid S \mid^2$ where $S = 2i \sum_{n=0}^{\infty} \dfrac{1}{\tilde{N}_{on}} \dfrac{R_{on}^{(1)'}(h, \xi_1)}{R_{on}^{(3)'}(h, \xi_1)} S_{on}(h, \cos\theta) S_{on}(h, -\cos\theta)$ $R_{mn}^{(1)}$, $R_{mn}^{(1)}$, S_{mn} are spheroidal wave functions, $\tilde{N}_{mn}$ is the normalization constant for the spheroidal functions, $\epsilon_o = 1$, $\epsilon_m = 2$ for $m \neq 0$ [ABRAMOWITZ - 1964].

Arbitrary Incidence

Of A Prolate Spheroid

Spheroidal Coordinate System: $X = \frac{1}{2} d \sqrt{(\xi^2-1)(1-\eta^2)} \cos \phi$

$Y = \frac{1}{2} d \sqrt{(\xi^2-1)(1-\eta^2)} \sin \phi$

$Z = \frac{1}{2} d\xi\eta$

where d = semifocal distance, $1 \leq \xi < \infty$, $-1 \leq \eta \leq 1$, $0 \leq \phi < 2\pi$

Relationship: $2c = d\,\xi_1$ $\qquad h \equiv \frac{1}{2} kd$

$2a = d\,\sqrt{\xi_1^2-1}$ $\qquad h\xi_1 = kc$

REFER TO	COMMENTS
[CRISPIN - 1968; p. 86]	Obtained from geometrical acoustics formula for ellipsoid by setting b ≡ a.
	Method applicable but has not yet been developed
	Method applicable but has not yet been developed.
[BOWMAN - 1969; p. 441]	

Table 2.3-16. Backscattering Cross-Section

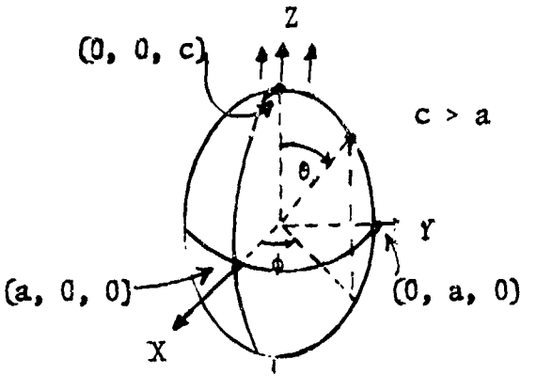

METHOD	BACKSCATTERING CROSS SECTION, σ
Geometrical Acoustics	$\sigma = \frac{\pi a^4}{c^2}$
Kirchhoff	$\sigma = \frac{\pi a^4}{c^2}\left(1 - \frac{\sin(2kc)}{kc} + \frac{\sin^2(kc)}{(kc)^2}\right)$
Keller	$\sigma = 4\pi/k^2 \mid S \mid^2$ where $S = \left\lvert \frac{h(\xi_1^2-1)}{2\xi_1} \exp(-2ih\xi_1)\{1 - \frac{2(h/2)^{1/3}\xi_1^{5/3}}{(\xi_1^2-1)^{2/3}\beta_1[Ai(-\beta_1)]^2} \exp[\frac{\pi i}{3}+2ih\xi_1 \right.$ ($\leftarrow S_{G.A.} \rightarrow$) $\left. + (\exp\{\frac{5}{6}i\pi\}h^{1/3}\beta_1\{2\xi_1\sqrt{\xi_1^2-1}\}^{2/3}\cdot\int_0^1 \frac{d\eta}{\sqrt{\{(\xi_1^2-\eta^2)(1-\eta^2)\}}}\right]\}$ where $\beta_1 = 1.01879\ldots$; $Ai(-\beta_1) = 0.53565$
Exact	$\sigma = \frac{4\pi}{k^2} \mid S \mid^2$ where $S = 2i \sum_{n=0}^{\infty} \frac{1}{\tilde{N}_{on}} \frac{R_{on}^{(1)'}(h, \xi_1)}{R_{on}^{(3)'}(h, \xi_1)} S_{on}(h, -1) S_{on}(h, 1)$ $R_{mn}^{(1)}$, $R_{mn}^{(3)}$, S_{mn} are spheroidal wave functions, $\tilde{N}_{mn}$ is the normalization constant for the spheroidal functions, $\epsilon_0 = 1$, $\epsilon_m = 2$ for $m \neq 0$ [ABRAMOWITZ - 1964].

Axial Incidence, $\theta = 0°$

Of A Prolate Spheroid

Spheroidal Coordinate System:

$$X = \frac{1}{2} d \sqrt{(\xi^2-1)(1-\eta^2)} \cos\phi$$

$$Y = \frac{1}{2} d \sqrt{(\xi^2-1)(1-\eta^2)} \sin\phi$$

$$Z = \frac{1}{2} d\xi\eta$$

Relationships: $2c = d\xi_1$

$$2a = d\sqrt{\xi_1^2-1}$$

$$h \equiv \frac{1}{2}kd$$

$$h\xi_1 = kc$$

where d = semifocal distance, $1 \le \xi < \infty$, $-1 \le \eta \le 1$, $0 \le \phi < 2\pi$

	REFER TO	COMMENTS
	Appendix B.3	Obtained from geometrical acoustic formula for ellipsoid by setting $a \equiv b$, and $\theta = 0°$.
	[RUDGERS - 1965; p. 10]	
$+2ih \int_0^1 \frac{\sqrt{\xi_1^2-\eta^2}}{1-\eta^2} d\eta$	[BOWMAN - 1969; p. 457]	Criterion for σ_{Keller} to be within 20% of $\sigma_{G.A.}$.

c/a	10:1	8:1	5:1	2:1	4:1
$kc \ge$	575	375	160	33	14
$\frac{ka^2}{c} \ge$	5.75	5.86	6.4	8.25	10.0

$$\xi_1 = \frac{c}{\sqrt{c^2 - a^2}}$$

	[BOWMAN - 1969; p. 441]

Table 2.3-17. Backscattering Cross-Section

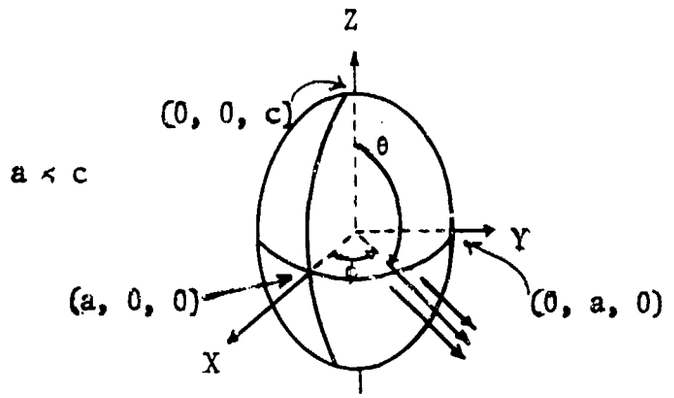

METHOD	BACKSCATTERING CROSS-SECTION, σ
Geometrical Acoustics	$\sigma = \pi c^2$
Kirchhoff	$\sigma = \pi c^2 \left(1 - \frac{\sin(2ka)}{ka} + \frac{\sin^2(ka)}{(ka)^2}\right)$
Keller	
Exact	$\sigma = \frac{4\pi}{k^2} \mid S \mid^2$ where $S = 2i \sum_{n=0}^{\infty} \frac{1}{\tilde{N}_{on}} \frac{P_{on}^{(1)\prime}(h,\xi_1)}{R_{on}^{(3)\prime}(h,\xi_1)} S_{on}(h,-1) S_{on}(h,0)$ $R_{mn}^{(1)}$, $R_{mn}^{(3)}$, S_{mn} are spheroidal wave functions, $\tilde{N}_{mn}$ is the normalization constant for the spheroidal functions, $\epsilon_0 = 1$, $\epsilon_m = 2$ for $m \neq 0$ [ABRAMOWITZ - 1964].

Beam Aspect, $\theta = 90°$

of A Prolate Spheroid

Spheroidal Coordinate System:

$$X = \frac{1}{2} d \sqrt{(\xi^2-1)(1-\eta^2)} \cos \phi$$

$$Y = \frac{1}{2} d \sqrt{(\xi^2-1)(1-\eta^2)} \sin \phi$$

$$Z = \frac{1}{2} d\xi\eta$$

Relationships: $2c = d\xi_1$

$$2a = d\sqrt{\xi_1^2-1}$$

$$h \equiv \frac{1}{2} kd$$

$$h\xi_1 = kc$$

where d = semifocal distance, $1 \leq \xi < \infty$, $-1 \leq \eta \leq 1$, $0 \leq \phi < 2\pi$

	REFER TO	COMMENTS
	Appendix B.3	Obtained from geometrical acoustics formula for ellipsoid by setting $a \equiv b$, and $\theta = \pi/2$.
	[RUDGERS - 1965; p. 10]	
		Method applicable but has not yet been developed.
	[BOWMAN - 1969; p. 441]	

Table 2.3-18. Backscattering Cross-Section

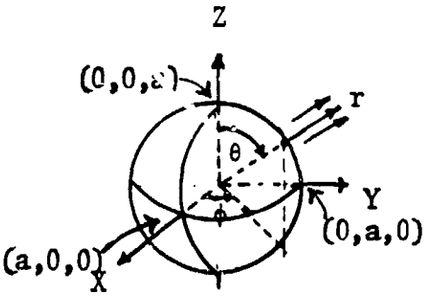

METHOD	BACKSCATTERING CROSS-SECTION, σ
Geometrical Acoustics	$\sigma = \pi a^2$
Kirchhoff	$\sigma = \pi a^2\left(1 - \frac{\sin(2ka)}{ka}\right) + \frac{\sin^2(ka)}{(ka)^2}$
Keller	$\sigma = \frac{4\pi}{k^2} \left\| S_{refl} + S_{cr.w.} \right\|^2$ where $S_{refl} = \left\| \frac{1}{2} ka\exp(-2ika)\{1 \right.$ $\left. - \frac{3i}{2ka} - \frac{5}{2(ka)^2} \right\| + \frac{25i}{4(ka)^3} + \frac{22}{(ka)^4} +$ $\leftarrow S_{g.a.} \rightarrow$ $\leftarrow$ obtained also from the Luneburg-Kline expansion $\rightarrow$ and $S_{cr.w.} = -(\exp(\frac{\pi i}{3}))mka \sum_{\ell=0}^{\infty}(-1)^{\ell} \sum_{n=1}^{\infty}\{1+\frac{\exp(\pi i/3)}{60m^2\beta_n^2}(32\beta_n^3-21) - \frac{\exp(-\frac{\pi i}{3})}{m^4\beta_n^4}$ $(\frac{4}{175}\beta_n^6 + \frac{147}{800}) + 0(m^{-6})\}(\beta_n[Ai(-\beta_n)]^2)^{-1}\exp[i(2\ell+1)\pi$ $\{ka+m\beta_n\exp(i\pi/3) - \frac{(\beta_n^3+21)\exp(-\frac{\pi i}{3})}{60m\beta_n} + (1400m^3\beta_n)^{-1}$ where β_n are zeros of the derivative of the Airy function; i.e. $Ai'(-\beta_n)=0$
Exact	$\sigma = \frac{4\pi}{k^2} \left\| \sum_{n=0}^{\infty}(-1)^n(2n+1)\, a'_n \right\|^2$ where $a'_n = j'_n(ka)/h_n^{(1)\prime}(ka)$ where j_n, h_n are spherical Bessel functions [ABRAMOWITZ - 1964].

Of A Sphere

Spherical Coordinate System: $X = r \sin\theta \cos\phi$

$Y = r \sin\theta \sin\phi$

$Z = r \cos\theta$

	REFER TO	COMMENTS
	Appendix B.3	Obtained from geometrical acoustics formula for ellipsoid by setting $a \equiv b \equiv c$.
	Appendix C.4	
		Refinement of Keller solution provided by [SENIOR - 1965]
$O[(ka)^{-5}]\}$	[BOWMAN - 1969; p. 378]	First three terms in $S_{refl.}$ previously derived by [KELLER - 1956] using Luneburg-Kline expansion technique. $S_{refl.}$ accurate for $ka > 10$; fairly accurate for $ka \simeq 5$.
$(\beta_n^6 + 63\beta_n^3 + \frac{343}{4}) + O(m^{-5})\}]\}$ and, $m = (1/2\ ka)^{1/3}$	[BOWMAN - 1969; p. 379]	$S_{cr.w.}$ accurately approximated by single creeping wave [SENIOR - 1965]. Order of Magnitude guideline for $\sigma_{cr.w.}$ $\sigma_{cr.w.} \simeq \pi a^2 (1.03 (ka)^{-5/2})$. Estimated by [CRISPIN - 1968; p. 128] from exact backscattering curve by assuming that $\sigma_{max.} \simeq \sigma_{g.a.} + \sigma_{cr.w.}$ and $\sigma_{min.} \simeq \sigma_{g.a.} - \sigma_{cr.w.}$ Expression $\sigma_{cr.w.}$ valid for $1 < ka < 15$; provides good estimate for a relatively long, slender body having diameter 2a.
	[BOWMAN - 1969; p. 374]	

2.3.4 COMPARATIVE ANALYSES

The preceding example problems and comparative formulas provide explicit evidence of the differences which obtain from application of the various theories and methods. Now that we see what the differences are, we can and should ask, why? Appendices B, C, and D provide the factual basis for a comparison of the methods themselves - not just the results of the methods. Since few criteria can be given to guide in the selection of one method over another, it is essential that one understands the relative advantages, disadvantages, and limitations of the methods.

Geometrical acoustics is obtained from the wave equation in the limit of infinite frequency. It is, therefore, natural in high frequency problems to think in terms of rays. This picture, however, can be very misleading in many diffraction problems. In fact, geometrical acoustics really describes particle-like behavior rather than wave-like behavior. Cast into the form of the Hamilton-Jacobi equations, the basic equations of classical mechanics are identical with the basic equations of geometrical acoustics (a fact which led Schrödinger to the discovery of wave mechanics). Thus, the geometrical acoustics description of scattering really describes how a stream of particles would be scattered. Indeed, at high frequencies, waves do have many particle-like properties, but there are many subtleties associated with the passage to this limit, particularly in target strength problems.

Since target strength is a far field quantity, in high frequency problems we are concerned with two limits, viz. $r \to \infty$, $k \to \infty$. It is well to keep in mind that these limits are not always interchangeable and that when they are not we should take the limit $r \to \infty$ first. The range at which the far field begins is, in general, a function of aspect. As an example, consider a convex body which has a flat disc-like portion, whose maximum diameter is 2a. Consider a

plane wave normally incident on the disc. The scattered rays are shown in (a) below.

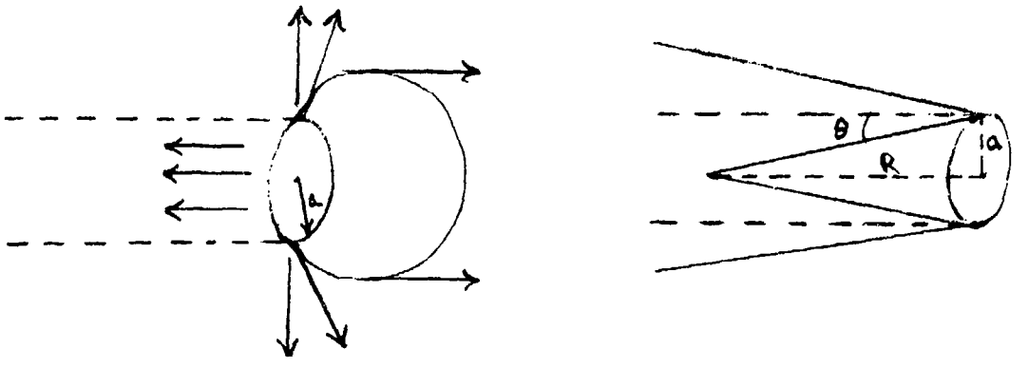

(a) (b)

We see that in the backscattering direction there is a cylinder of rays. According to geometrical acoustics we have a reflected plane wave within the cylinder and the field becomes discontinuously zero outside the cylinder. Here we should be guided by the centuries-old principle natura non facit saltus (nature does not make jumps). This type of discontinuous behavior is unphysical and we would expect to find a thin transition region surrounding the cylinder. A plane section of the transition region, as shown in (b) above, is a sector of half angle θ (the size of θ is greatly exaggerated in the figure). Even though θ is very small, for sufficiently large range, $r > R$, the transition regions will overlap and geometrical acoustics ceases to have any validity. In this situation geometrical acoustics is a valid description of only the near field. The far field begins at range R. Since the large parameter governing this phenomenon is ka, we would expect to have $\theta \sim (ka)^{-m}$ where m is a positive quantity. Then the range at which the far field begins is given by

$$R = a(ka)^{m} \quad \text{(const.)}$$

However, if we consider an aspect other than normal, no such transition phenomenon affects the backscattering. In this situation the far field is approximately equal to the geometrical acoustics field and the first order correction is due to diffraction by the edge of the disc. The ordinary criterion of geometrical acoustics (Appendix B) is applicable in this region giving

$$R >> \sqrt{R_1 R_2}$$

where R_1, R_2 are the principal radii of curvature at the point of specular backscattering. In general then, the far field begins at a point considerably closer to the body for non-normal aspect than it does at normal aspect.

This type of transition phenomenon should be expected whenever approximate methods produce discontinuous behavior. It is for this reason that the Keller method fails for finite straight edges and at shadow boundaries. For example, for a plane wave normally incident on a finite straight edge the method predicts a cylindrical wave within the two planes perpendicular to the edge at its end points. The cylindrical wave vanishes discontinuously across these planes. Thus, the Keller method gives a good description of the near field but fails in the far field in which the scattered wave must be spherical. The method is, therefore, not suitable without modification for a target strength calculation in this case.

We have assumed the width of the transition layer to be given by the relation $\theta \sim (ka)^{-m}$. The value of m, according to Kirchhoff theory (Appendix C), is unity. More detailed guidance as to the value of m under various conditions could be provided by a careful study of the asymptotic properties of solutions for simple bodies, but present treatments are generally not sufficiently thorough for this purpose.

Transition layer phenomena of the type we have been discussing are characteristic of asymptotic formulas. Most high frequency formulas are of this type. By this we mean that they are obtained from a divergent asymptotic expansion by truncation. There is an optimum number of terms for retention but even with the optimum number, the calculation can not be improved beyond a certain minimum residual error (in contrast, the error made by truncating a convergent expansion can always be made as small as we like by retaining a sufficient number of terms). There are, unfortunately, no general theorems which determine the optimum number of terms to retain in an asymptotic expansion. Thus, the inclusion of higher order terms does not necessarily improve the calculation, it may make matters worse!

Some guidance can be obtained by examining the physical meaning of the terms in the expansion. (This was done in Appendix C.4.1 where one term in the expansion of the sphere solution was discarded on the basis of physical reasoning). In general, the terms in the asymptotic expansion can be identified with the following physical phenomena, given in decreasing order of importance:

(1) Specular reflection contributes integer or half-integer powers of k to the expansion of the scattered field. If the aspect is normal to two infinite principal radii of surface curvature (e.g., normal incidence on a flat plate) the expansion begins with the first power of k. If aspect is normal to one principal radius of curvature (e.g. broadside incidence on a finite cylinder) the expansion begins with $k^{1/2}$. In these two cases geometrical acoustics is not suitable for calculating the sonar cross section since, as we have seen, it fails to account for three dimensional spreading in the far field. Instead the Kirchhoff or Keller method can be used. Experience has shown that these two methods can be expected to agree to first order, though there is no theoretical argument which proves they must.

If neither principal radius of curvature is infinite and there is specular backscattering the expansion begins with the constant term. This leading term is determined solely by the shape of the body and can be calculated using formulas from differential geometry (see Appendix B.3). The same first order result should be obtained from the Keller and Kirchhoff methods and is identical with the geometrical acoustics result. Furthermore, the geometrical acoustics result is the leading term in the Luneburg-Kline expansion.

(2) Diffraction by a finite straight edge should be considered as a separate case. The Keller method fails because it predicts outgoing cylindrical waves from the edge but fails to account for their three dimensional spreading in the far field. Therefore, we have to be guided by the Kirchhoff theory. The edge should not be considered in isolation from the rest of the body since the field will depend on the way the edge is terminated. However, we can generalize somewhat from the cross section for a rectangular plate (see Table 2.3-4). For incidence normal to an edge but away from broadside aspect (to exclude specular reflection) the scattered field is proportional to a highly oscillating function of the type sin (kL). Assuming that this function does not happen to vanish for the particular wavelength used, it follows that the cross section is of the same order as for a sphere of diameter equal to the width of the plate (see Table 2.3-18). Therefore, diffraction from a finite straight edge is potentially as important as specular reflection from a convex surface. However, for incidence other than normal the highly oscillating function is multiplied by a damping factor.

(3) A curved edge will contribute to the far scattered field in inverse powers of k beginning with $k^{-1/2}$. The Keller and Kirchhoff solutions will, in general, not agree in the leading term of this series (e.g., the finite cylinder). There is still insufficient experimental data in acoustics, but electromagnetic experience indicates a preference for Keller's method.

(4) A tip (such as the tip of a cone) will contribute to the far scattered field in terms in inverse powers of k beginning with k^{-1}. The Keller method is impractical because of insufficient knowledge of the relevant canonical problems except for certain special cone angles or aspects.

(5) A ray tangentially incident on a convex body launches a surface wave, called a creeping wave or circumferential wave, which propagates along a surface geodesic with exponential damping due to continuous re-radiation to the outside field. Thus, this type of phenomenon contributes exponentially damped terms to the asymptotic expansion of the scattered field. The Kirchhoff method does not account for this type of phenomenon at all and the Keller method should be used with caution. From Example Problem 2 (the spheriod) we have seen that even for moderately thin bodies very large values of ka may be needed for the Keller method to produce good results.

Each of the target strength prediction methods makes assumptions about the problems to facilitate a solution. We would immediately point out that the word assumption is, in most cases, a misnomer because we really mean approximation. Even that which we call an exact solution - because it satisfies the differential equation and its boundary conditions exactly - is really an approximate solution since the simple linear wave equation itself is an approximation. But the geometrical acoustics, Kirchhoff, and Keller theories go beyond this approximation and make additional assumptions (approximations).

The "essence" of the relative differences between the three approximate methods can be brought out in the following example.

Consider a plane wave axially incident on one-half of a rigid prolate spheroid.

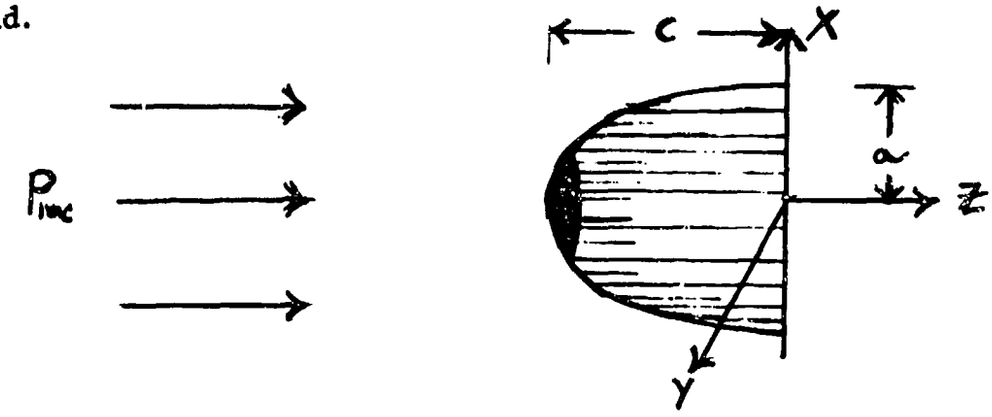

Since the body is convex, the geometrical acoustics method only concerns itself with the specular (blackened) region and, further, assumes the reflection coefficient at the point (o,o,-c) to be equal to that of an infinite flat plate. The Kirchhoff method makes use of the entire ensonified portion of the body but gives largest "weight" to the specular region and lesser and lesser weight to the regions away from the specular point, as illustrated by the density of the hatched lines. The Kirchhoff method also makes the flat-plate approximation as regards the reflection coefficient. Both the geometrical acoustics and Kirchhoff methods completely ignore the shape of the body in the shadow region and, hence, their solutions would not differ if, instead of the above termination, we had a full prolate spheroid, a pointed cone, an infinite cylinder, or any other shape. In contrast, the Keller method is more phenomenological; it identifies the specular region and the truncated portion (edge) as the principal scatterers and ignores the intermediate region. The geometrical acoustics solution at the specular point forms part of the Keller solution but added to it is the 90° circular wedge solution which accounts for the shape of the body in the shadow region, including any multiple diffraction effects. Which of the approximate methods will yield the more accurate prediction for the back-scattering cross-section? we don't know for sure! However, prior experience indicates that at some suffic-

iently high frequency and beyond, the geometrical acoustics prediction will differ negligibly from the exact result (whatever that is) and, at lower frequencies down to $ka^2/c \tilde{=} 2$, the Keller result would be most accurate. It is characteristic of this entire field that little more can be said about the validity of these methods for this and similar problems.

Each of the approximate methods have certain practical advantages, and disadvantages that should be noted. The geometrical acoustics method is exceedingly simple to apply and, with some very definite exceptions, will yield very accurate predictions at sufficiently high frequencies. At these exceptions, or in a region approaching them, the geometrical acoustics method is not only exceedingly simple, but also, exceedingly wrong! The exceptions which preclude the use of geometrical acoustics can usually be handled by the Kirchhoff method which leads to an integral to be evaluated. In many problems involving bodies of revolution this "Kirchhoff integral" can be (and has been) performed exactly with relative ease. In other cases asymptotic (saddle-point or stationary-phase) solutions may be obtained. These solutions are valid approximations to the integral (but we can not give error bounds) when the acoustical size of the body (ka) is sufficiently large. Typically, the Kirchhoff integral will yield the geometrical acoustics solution (if one exists) plus higher order correction terms. Interestingly, the asymptotic evaluation of the Kirchhoff integral sometimes yields more accurate predictions than that which would obtain from an exact evaluation of the integral. This apparent contradiction is suggestive of how delicate is the art. It is also fair to say that one of the advantages of the Kirchhoff method, in contrast to the Keller method, is its age. In addition to the many Kirchhoff solutions (problems) which have been studied over the years, many of the subtleties have also been studied and are relatively well understood. In contrast, the Keller method is new and has not been explored to

the same extent. The Keller postulates are intuitively simple and appealing, but detailed application of the method is often not straightforward. In contrast to the simple "cookbook" type procedure for formulation of the Kirchhoff integral, in the Keller formulation one must identify the highlights, define the canonical sub-problems, and then synthesize the parts. Often the sub-division of the given problem into canonical parts cannot be performed, or is very difficult. The rigid, flat, rectangular plate is a good example. The basic difficulty here is the lack of sufficient types and numbers of canonical problems. This deficiency exists for both "hard" and "soft" acoustic bodies (shapes) as well as for the elastic and visco-elastic bodies. In fact, so few canonical solutions exist for elastic body problems, that the deficiency is really an absence. It is reasonable, therefore, to speculate that the progress of the Keller method in acoustics will largely depend on the progress of the canonical problems.

2.3.5 GENERAL GUIDANCE

The classical theory of diffraction was founded in the mid-nineteenth century by Kirchhoff. Although based on an assumption which has never been made rigorous, it has amazingly endured to the present as a practical method in diffraction theory. Modern diffraction theory can be dated from 1896 when Sommerfeld published perhaps the most famous solution to a boundary value problem in mathematical physics, an exact solution to the problem of diffraction by a semi-infinite half-plane. In Sommerfeld's "Method of Images on Riemann Sheets" the solution was obtained in the form of a contour integral in the complex plane. This was the first exact solution to a diffraction problem not based on the separation of variables method. Unlike the latter type of solution, which is an eigenfunction expansion that is slowly convergent at high frequencies, the Sommerfeld solution is well suited for high frequency problems and it immediate-

ly became a standard for comparison.

Subsequently, other exact methods were discovered, notably the Wiener-Hopf method. However, like the Sommerfeld method these are applicable only to infinite or semi-infinite bodies. The only known exact solution for a three dimensional body is the solution for the spheroid and its limiting cases (sphere, disc) as an eigenfunction expansion.

Eigenfunction expansions converge slowly at high frequencies. As a rule of thumb the number of terms required in a practical calculation is on the order of two times the value of ka. The practical use of these expansions is considerably extended by the use of modern computers. We have been able to perform spheroid calculations up to ka = 50 at moderate cost. Except for very thin spheroids it is feasible to perform numerical calculations up to the geometrical acoustics limit.

An alternative method of utilizing slowly convergent expansions was discovered by Watson in 1919. This method, now generally known as the Watson-Sommerfeld transformation, is a technique for transforming a slowly convergent expansion, requiring perhaps thousands of terms, into a rapidly convergent expansion requiring only one or two terms. In other words, it is a method for transforming an exact solution into a form convenient for high frequency calculations. The transformed expansion reveals a new physical phenomenon typical of high frequency scattering, the creeping wave or circumferential wave. This is a surface wave launched by an incident ray tangent to the body at the shadow boundary. It is the mechanism by which a smooth transition is made from the insonified region to the shadow within a narrow "penumbra" about the shadow boundary. The creeping wave propagates along the surface of the body and may encircle it many times. However, it is exponentially damped as it propagates, and for this reason its amplitude becomes negligible a short distance from the shadow boundary.

Because of the exponential damping, re-radiation from the creeping wave to the external field is the weakest of all scattering mechanisms. For example, the shadow behind a sphere is much deeper than the shadow behind a disc because the edge of the disc scatters much more energy into the shadow region than that which would arrive there via the creeping wave on the sphere.

Thus, by studying simple bodies (including the infinite ones) we can identify different scattering mechanisms and compare their relative strengths. Our intuition tells us that when the wavelength is very short compared with the topographical features of a body these features should behave more or less like separate bodies in isolation from each other. These component parts of the body can then be identified with the various scattering mechanisms. We have seen elsewhere in this report what these mechanisms are. We briefly re-state them here in decreasing order of backscattering effectiveness: (1) specular reflection from flat surface, (2) specular reflection from cylindrical surface, (3) specular reflection from convex surface or normal incidence on straight edge, (4) normal incidence on curved edge, (5) scattering from tip or oblique incidence on straight edge, (6) creeping wave arising from shadow boundary on a smooth convex surface.

Thus, by examining the surface geometry of the target we can identify scattering centers and estimate their relative importance. For example, if there is no specular reflection, then to first order the target strength is determined by the edges with other features such as tips or shadow boundaries contributing higher order corrections. If a pulse is incident on the target, echo returns will be received from the scattering centers at different times. Their relative amplitudes will also correspond to the above rank ordering of scattering mechanisms.

The assumption that a target can be treated as a sum of composite parts is basic to the Keller theory. It is alien to the Kirchhoff approach although

backscattering is interpreted in this way in Freedman's formulation. However, creeping wave phenomena are not incorporated in the Kirchhoff theory as they are in the Keller theory. Instead there is a spurious shadow boundary contribution (Appendix C).

In this report we have concentrated on three approximate methods on the basis of practical importance. However, these methods can also be considered basic in the sense that other approximate methods are modifications or refinements thereof. Such extensions can be valuable but their application is more art than science. Of the three methods, geometrical acoustics is strictly a high frequency method. The Keller and Kirchhoff methods are useful at lower frequencies with the Keller method having potentially the widest range of application in both frequency and aspect because it can incorporate multiple diffraction (interactions between the targets component parts). However, since exact solutions are available only for a very limited class of bodies final judgement must be made on the basis of experimental evidence. At present the amount of experimental evidence in acoustic scattering is far from adequate.

APPENDIX A - LINEAR ACOUSTICS

In this Appendix, we shall review the basic quantities and equations of acoustics, as well as the definitions of the scattering cross section and target strength.

The acoustic field in a fluid medium is essentially described by a small fluctuating pressure field, p, superimposed on the large, constant hydrostatic pressure p_o, adding up to a total pressure

$$p_{tot} = p_o + \bar{p} \tag{a-1}$$

Similarly, the total density of the medium

$$\rho_{tot} = \rho_o + \rho \tag{a-2}$$

is composed of a constant part (ρ_o) and a small fluctuating part (ρ); and the total particle velocity

$$\vec{v}_{tot} = \vec{v}_o + \vec{v} \tag{a-3}$$

consists of acoustic velocity fluctuations $\vec{v}$, while the average (convective) particle velocity $\vec{v}_o$ will be assumed zero appropriate for a medium at rest.

A-1 Equation of State

The basic equations of Acoustics will be derived here, and will be linearized by assuming the fluctuating fields p, ρ, and $\vec{v}$ to be small (while p_o and ρ_o are large). The equation of state of a fluid constitutes a relation between its pressure and density,

$$p_{tot} = f(\rho_{tot}) \qquad (a-4)$$

which for $|\rho| << \rho_o$ may be expanded in a Taylor series:

$$p_o + p \cong f(\rho) + \rho(df/d\rho)_{\rho_o} + \ldots \qquad (a-5)$$

Since $p_o = f(\rho_o)$, we have

$$p = \rho(df/d\rho)_{\rho_o} + \ldots \qquad (a-6)$$

Defining the (constant) sound velocity c by

$$c = [(df/d\rho)_{\rho_o}]^{1/2} \qquad (a-7)$$

we obtain

$$p = \rho c^2 \qquad (a-8)$$

as the linearized equation of state.

A-2 Euler's Equation

This equation is just Newton's force equation applied to a volume element d^3x of the fluid. The net x-component of force (in the positive x-direction) is given by

$$[p(x) - p(x+dx)]\, dy\, dz \cong -(\partial p/\partial x)\, d^3x \qquad (a-9)$$

(since the hydrostatic parts p_o cancel). This equals mass times acceleration, i.e.

$$(\rho_{tot}\, d^3x)(dv_x/dt). \qquad (a\text{-}10)$$

Since $\vec{v} = \vec{v}(\vec{r}(t), t)$, the chain rule of differentiation

$$dv_x/dt = \partial v_x/\partial t + (\vec{\nabla} v_x)\cdot(d\vec{r}/dt) \qquad (a\text{-}11)$$

introduces the "convectional derivative", and one has

$$(\rho_{tot}\, d^3x)[\partial v_x/\partial t + \vec{v}(\vec{\nabla} v_x)], \qquad (a\text{-}12)$$

which has to equal Eq. (a-9). Combining all three Cartesian components, one has

$$-\vec{\nabla} p = \rho_{tot}(\partial\vec{v}/\partial t + \vec{v}\vec{\nabla}\vec{v}). \qquad (a\text{-}13)$$

Linearizing allows to set $\rho_{tot} \cong \rho_o$, and to drop the second term in parenthesis as being of higher order, leading to the linearized Euler equation

$$-\vec{\nabla} p = \rho_o(\partial\vec{v}/\partial t). \qquad (a\text{-}14)$$

A-3 Equation of Continuity

This equation expresses the conservation of mass in the fluid medium. The amount of matter, flowing during the time dt into the volume element d^3x along the positive x-direction as a consequence of the acoustic fluctuations, amounts to

$$\rho_{tot}(x)\; v_x(x)\; dt\; dy\; dz, \qquad (a\text{-}15)$$

while the outflow is

$$\rho_{tot}(x+dx)\; v_x(x+dx)\; dt\; dy\; dz, \qquad (a\text{-}16)$$

leading to a net influx of

$$-\frac{\partial(\rho_{tot} v_x)}{\partial x}\; d^3x\; dt\,. \qquad (a\text{-}17)$$

The total influx through all three faces is then

$$-\vec{\nabla}\cdot(\rho_{tot}\vec{v})\ d^3x\ dt. \qquad (a-18)$$

Furthermore, there may be a source in d^3x generating the additional amount of fluid volume $q\ d^3x\ dt$, or the additional mass $q\ \rho_{tot}\ d^3x\ dt$. Thus, there occurs a total increase in mass which is given by

$$d\rho_{tot}\ d^3x = -\vec{\nabla}\cdot(\rho_{tot}\vec{v})\ d^3x\ dt + \rho_{tot} q\ d^3x\ dt. \qquad (a-19)$$

Differentiating with respect to t at a given point $\vec{r}$ leads to

$$-\vec{\nabla}\cdot(\rho_{tot}\vec{v}) = -\frac{\partial\rho_{tot}}{\partial t} - q\ \rho_{tot}\ . \qquad (a-20)$$

Linearization gives

$$-\rho_o\vec{\nabla}\cdot\vec{v} = -\partial\rho/\partial t - q\rho_o \qquad (a-21)$$

and use of Eq. (a-8) leads to

$$\vec{\nabla}\cdot\vec{v} = -\frac{1}{\rho_o c}\frac{\partial p}{\partial t} + q, \qquad (a-22)$$

the linearized equation of continuity.

A-4 Wave Equation

The preceeding allows the derivation of the scalar wave equation of Acoustics. Taking the divergence of Eq. (a-14), and the partial time derivative of Eq. (a-22), one immediately finds by elimination of $\vec{v}$:

$$\nabla^2 p - \frac{1}{c^2}\frac{\partial^2 p}{\partial t^2} = -\rho_o\frac{\partial q}{\partial t}\ . \qquad (a-23)$$

This is the linearized scalar wave equation, in which the inhomogeneous term on the right-hand side constitutes a source term.

A-5 Velocity Potential

The particle motions in Acoustics may be assumed to be irrotational, i.e. not to give rise to vortices. In this case, a velocity potential $\Phi(\vec{r})$ may be introduced by writing

$$\vec{v} = -\vec{\nabla}\,\Phi, \tag{a-24}$$

since then, $\vec{\nabla} \times \vec{v} \equiv 0$. From Eq. (a-14), one has then (by integration)

$$p = \rho_o \frac{\partial \Phi}{\partial t}, \tag{a-25}$$

adjusting Φ such that the integration constant vanishes. From this and from Eq. (a-23), one again finds

$$\nabla^2 \Phi - \frac{1}{c^2} \frac{\partial^2 \Phi}{\partial t^2} = -q, \tag{a-26}$$

i.e. a wave equation for the *velocity* potential in which -q constitutes a source term.

Differentiating Eq. (a-24) and using Eq. (a-25), we find

$$\frac{\partial \vec{v}}{\partial t} = -\frac{1}{\rho_o} \vec{\nabla} p, \tag{a-27}$$

or an integral relation between velocity and pressure,

$$\vec{v} = -\frac{1}{\rho_o} \vec{\nabla} \int p \, dt \tag{a-28}$$

For periodic motion with frequency ω, where

$$\Phi \propto \exp\{-i\omega t\}, \tag{a-29}$$

Eq. (a-25) gives

$$p = -i\omega\rho_o \Phi; \tag{a-30}$$

and, inserting in Eq. (a-24), one finds the useful relation between velocity and pressure

$$\vec{v} = (1/i\omega\rho_o)\, \vec{\nabla} p \tag{a-31}$$

valid for time-harmonic motion.

A-6 Plane Waves

We shall now consider the important case where the acoustic field consists of a progressive plane wave of amplitude P,

$$p = P \exp\{i(\vec{k}\cdot\vec{r} - \omega t)\}, \qquad (a-32)$$

$\vec{k}$ denoting its propagation vector (of magnitude k and direction $\hat{k} = \vec{k}/k$); we shall always designate unit vectors by a caret ^). The phase velocity of the wave is given by

$$c = \omega/k. \qquad (a-33)$$

Inserting Eq. (a-32) into Eq. (a-31) gives

$$\vec{v} = v\hat{k}, \qquad v = p/\rho_o c \qquad (a-34)$$

The ratio p/v, *i.e.*

$$p/v = \rho_o c \qquad (a-35)$$

is known as the characteristic acoustic impedance of the fluid medium in which the wave propagates. We may write in analogy to Eq. (a-32):

$$\vec{v} = \vec{V} \exp\{i(\vec{k}\cdot\vec{r} - \omega t)\}, \qquad (a-36)$$

where

$$\vec{V} = V\hat{k}, \qquad V = P/\rho_o c\ . \qquad (a-37)$$

A-7 Intensity

The intensity I of a propagating acoustic field is defined as the power* flowing through a unit area oriented normal to the power flux. Since** power = force (ds/dt), and the force per

---

* power = energy expended per unit time

** ds = element of length

unit area equals acoustic pressure, we have

$$I = pv \tag{a-38}$$

as the (instantaneous) intensity. The directed intensity $\vec{I}$, also called the energy flux density, flows parallel to the particle velocity so that

$$\vec{I} = p\vec{v}. \tag{a-39}$$

For a plane wave, one has from Eq. (a-34) the various expressions

$$I = pv = \frac{p^2}{\rho_o c} = \rho_o c v^2 \tag{a-40}$$

for the instantaneous field intensity.

A-8 Time Averaged Intensity

It should be noted that when we use complex notation for the fields, such as for the plane wave of Eq. (a-32), the physically measured quantities (e.g., the measured pressure, p_m) are always thought to be given by the real part of the corresponding complex field (e.g., $p_m = \text{Re } p$). For the plane wave of Eq. (a-32), one has *e.g.*,

$$p_m = P \cos (\vec{k}\cdot\vec{r} - \omega t) \tag{a-41}$$

General oscillating fields may be denoted by

$$p = \bar{p} \exp \{i(\omega t + \psi_p)\} \tag{a-42}$$

$$v = \bar{v} \exp \{i(\omega t + \psi_v)\} \tag{a-43}$$

with certain time-independent amplitudes, $\bar{p}$, $\bar{v}$, and phases ψ_p, ψ_v. The measured field intensity I_m is given by

$$I_m = p_m v_m \tag{a-44}$$

$$= \frac{p + p^*}{2} \cdot \frac{v + v^*}{2} \tag{a-45}$$

$$= \frac{1}{4}[(pv + p^*v^*) + (pv^* + p^*v)] \tag{a-46}$$

$$= \frac{1}{2}[\mathrm{Re}(pv) + \mathrm{Re}(p^*v)] \tag{a-47}$$

$$= \frac{1}{2}\,\mathrm{Re}\{\bar{p}\bar{v}\exp[i(2\omega t + \psi_p + \psi_v)]\} + \frac{1}{2}\,\mathrm{Re}\{\bar{p}\bar{v}\exp[i(\psi_v - \psi_p)]\} \tag{a-48}$$

For rapidly oscillating fields, it is often difficult to measure instaneous intensities, I_m, and only the time average $\langle I_m \rangle$ of the intensity, i.e.

$$\langle I_m \rangle = \frac{1}{\tau}\int_0^\tau I_m\, dt \tag{a-49}$$

where the period τ is given by

$$\tau = 2\pi/\omega\ , \tag{a-50}$$

may be determined. In Eq. (a-48), the first term then integrates to zero, and we have*

$$\langle I \rangle = \frac{1}{2}\,\mathrm{Re}\,\bar{p}\bar{v}\exp[i(\psi_v - \psi_p)] \tag{a-51}$$

$$= \frac{1}{2}\,\mathrm{Re}\{\bar{p}\exp[-i(\omega t+\psi_p)]\bar{v}\exp[i(\omega t+\psi_v)]\} \tag{a-52}$$

From Eq. (a-42) and Eq. (a-43), this gives finally

$$\langle I \rangle = \frac{1}{2}\,\mathrm{Re}(p^*v)\,, \tag{a-53}$$

which is the general form of a measured time-averaged physical quantity that is bilinear in two complex fields (in this case, p and v).

*we denote the measured time-averaged intensity by $\langle I \rangle$ rather than $\langle I_m \rangle$.

Specializing this to a plane wave again, we have from Eqs. (a-39), (a-32) and (a-36):

$$\langle \vec{I} \rangle = \frac{1}{2} \mathrm{Re}\, p^* \vec{v} \qquad \text{(a-54)}$$

$$= \frac{1}{2} p \vec{V} \qquad \text{(a-55)}$$

Alternately, Eq. (a-35) leads to

$$\langle I \rangle = \frac{|p|^2}{2\rho_0 c} \,, \qquad \text{(a-56)}$$

which is the well-known expression for the time-averaged measured intensity of a plane wave described by the complex pressure field p.

A-9 Scattering Cross Section and Sonar Cross Section

A convenient measure for the amount of acoustic back-scattering from a given target is the quantity known as "sonar cross section". * It is related to the so-called "differential scattering cross section" (or "bistatic cross section") $d\sigma$, which is defined as follows:

$$d\sigma = \frac{\text{energy flux scattered into } d\Omega}{\text{incident energy flux density}} \quad [\text{dimension cm}^2] \qquad \text{(a-57)}$$

where the energy flux (i.e., the power) of scattered acoustic energy (= flux density × area) into the three-dimensional solid angle $d\Omega$ is considered.

The geometrical meaning of the differential cross section defined in this way is the following: assuming a uniform distribution of energy in the transverse dimensions of the

* To be abbreviated by "sonar c. s."

incident beam, $d\sigma$ represents the geometrical cross-sectional area in the incident beam that is traversed by an energy flux equal to the one scattered into $d\Omega$. Equivalently, the fraction of the incident flux traversing $d\sigma$ is the flux scattered into $d\Omega$ (while the remaining incident flux does not undergo any scattering into $d\Omega$). The total area $\int d\sigma$ may thus be considered to represent some sort of "cross section" of the scattering object, since the fraction of the incident flux that hits it gets scattered (into $\int d\Omega \equiv 4\pi$), and the remainder of the incident flux that does not hit it, continues straight on.

For a steady-state scattering problem, the acoustic pressure field p may be expressed asymptotically in the far field (for distances r large compared to the dimensions of the scattering object) in the form

$$p \sim P\left\{e^{i(\vec{k}\cdot\vec{r}-\omega t)} + \frac{1}{r} f(\hat{r})\, e^{i(kr-\omega t)}\right\}. \qquad \text{(a-58)}$$

The propagation vector of the scattered wave $\vec{k}'$ is asymptotically $\vec{k}' = k\hat{r}$. The first term of Eq. (a-58) represents the incident plane wave p_{inc}, the second term asymptotically the scattered wave p_{sca}. Using Eq. (a-58), one obtains for the incident energy flux density

$$\langle I_{inc}\rangle \equiv \frac{|p_{inc}|^2}{2\rho_o c} = \frac{P^2}{2\rho_o c}. \qquad \text{(a-59)}$$

For the asymptotic scattered energy flux, one has

$$\lim_{r\to\infty} \langle I_{sca}\rangle r^2\, d\Omega = \lim_{r\to\infty} \frac{|p_{sca}|^2}{2\rho_o c} r^2\, d\Omega \qquad \text{(a-60)}$$

so that insertion into Eq. (a-58) gives

$$\frac{d\sigma}{d\Omega} = \lim_{r\to\infty} r^2 \frac{|p_{scat}|^2}{|p_{inc}|^2} , \tag{a-61}$$

or finally

$$\frac{d\sigma}{d\Omega} = |f(\hat{r})|^2 \tag{a-62}$$

If now the direction of scattering is confined to observations of the echo at a scattering angle $\theta = 180°$, i.e. back-scattering, one arrives at the definition of sonar c. s. σ, which is variously:

$$\sigma = 4\pi \left(\frac{d\sigma}{d\Omega}\right)_{\theta=\pi} , \tag{a-63}$$

$$\sigma = 4\pi \lim_{r\to\infty} r^2 \left(\frac{|p_{scat}|^2}{|p_{inc}|^2}\right)_{\theta=\pi} , \tag{a-64}$$

$$\sigma = 4\pi |f(\pi)|^2 . \tag{a-65}$$

These considerations refer to the case of three-dimensional geometry. They may be repeated here for the two-dimensional case, where the asymptotic distance r of the observation point from the target is large compared to the target dimensions in the x and y directions (x being the direction of incidence), but small compared to the target dimensions in the z direction. (This geometry is important for the case of torpedo sonar devices). In analogy to Eq. (2.2-58), the asymptotic field is here written using cylindrical spreading:

$$p \sim P\left\{e^{i(\vec{k}\cdot\vec{r}-\omega t)} + \frac{1}{r} f(\hat{r})\, e^{i(kr-\omega t)}\right\} \tag{a-66}$$

and one defines a bistatic cross section per unit length of the target as

$$d\sigma = \frac{\text{energy flux scattered into } d\phi}{\text{Incident energy flux density}} \quad [\text{dimension cm}] \tag{a-67}$$

For the scattered energy flux, one has

$$\lim_{r\to\infty} \langle I_{sca} \rangle \, r \, d\phi = \lim_{r\to\infty} \frac{|p_{sca}|^2}{2\rho_0 c} \, r \, d\phi \,, \tag{a-68}$$

leading to a bistatic cross section

$$\frac{d\sigma}{d\phi} = \lim_{r\to\infty} r \frac{|p_{sca}|^2}{|p_{inc}|^2} = |f(\hat{r})|^2 \,. \tag{a-69}$$

The two-dimensional sonar c. s. is here defined as

$$\sigma = 2\pi \left(\frac{d\sigma}{d\varphi}\right)_{\phi=\pi} \tag{a-70}$$

which leads to the expressions

$$\sigma = 2\pi \lim_{r\to\infty} r \left(\frac{|p_{sca}|^2}{|p_{inc}|^2}\right)_{\varphi=\pi} \tag{a-71}$$

or

$$\sigma = 2\pi \, |f(\pi)|^2 \,. \tag{a-72}$$

A-10 Boundary Conditions

On the surface of scattering objects, boundary conditions have to be imposed on the total acoustic field. For impenetrable bodies that admit no sound field into their interior, two special cases arise, namely that of a soft (or resilient) body where the acoustic pressure p vanishes on the surface:

$$p(\vec{r})\,|_S = 0 \tag{a-73}$$

with a subscript S indicating that values of $\vec{r}$ on the surface S have to be taken. This is also known as "Dirichlet boundary condition".

The other case is that of a hard (or rigid) body where the normal component of the acoustic particle velocity $\vec{v}$ vanishes on the surface:

$$\vec{n}\cdot\vec{v}|_S = 0 \quad , \tag{a-74}$$

$\vec{n}$ being a unit vector normal to the surface and pointing to the exterior of the body. We now use the connection between $\vec{v}$ and p as given by the linearized Euler equation, Eq. (a-14), which for the periodic motion ($p,\vec{v} \propto \exp\{-i\omega t\}$) that we consider here, becomes Eq. (a-31). Accordingly, the rigid boundary condition may be rewritten in terms of the normal pressure gradient on the surface:

$$\vec{n}\cdot\vec{\nabla}p|_S = 0 \tag{a-75}$$

This is also known as "Neumann boundary condition".

A-11 The Helmholtz Equation; Steady State and Pulsed Solutions.

The time-dependent wave equation, Eq. (a-23), may be written as

$$\nabla^2 p - \frac{1}{c^2}\frac{\partial^2 p}{\partial t^2} = s(\vec{r},t) \tag{a-76}$$

where we have designated the source as

$$-\rho_o \frac{\partial q}{\partial t} = S(\vec{r},t) \tag{a-77}$$

The scattering problem consists in finding the solution $p(\vec{r},t)$

of Eq. (a-76) for a given source distribution, and with the solution satisfying certain prescribed boundary conditions on the surface of the scattering objects at a given location.

With respect to the time dependence of p, one may Fourier-develop:

$$p(\vec{r},t) = \int_{-\infty}^{\infty} p(\vec{r},\omega) \exp\{-i\omega t\}\, d\omega \,, \qquad \text{(a-78)}$$

$$p(\vec{r},\omega) = \int_{-\infty}^{\infty} p(\vec{r},t) \exp\{i\omega\}\, dt/2\pi \,. \qquad \text{(a-79)}$$

The same may be done for the source $s(\vec{r},t)$. One says $p(\vec{r},t)$ has harmonic time dependence (with frequency ω) if

$$p(\vec{r},\omega') = p(\vec{r})\, \delta(\omega'-\omega) \qquad \text{(a-80)}$$

because then, insertion in Eq. (a-78) gives

$$p(\vec{r},t) = p(\vec{r}) \exp\{-i\omega t\} \qquad \text{(a-81)}$$

Similarly, a harmonic source is given by

$$s(\vec{r},t) = s(\vec{r}) \exp\{-i\omega t\} \qquad \text{(a-82)}$$

A harmonic source s leads to a harmonic solution p, since insertion of Eqs. (a-81) and (a-82) in Eq. (a-76) shows that the time exponential drops out, so that $p(\vec{r})$ satisfies

$$(\nabla^2 + k^2)\, p(\vec{r}) = s(\vec{r}) \,, \qquad \text{(a-83)}$$

where we have designated

$$k = \omega/c \tag{a-84}$$

[for the plane wave of Eq. (a-32), this quantity k is identical to the propagation vector]. Eq. (a-83) is known as the "Helmholtz equation" ("inhomogeneous" for $S \neq 0$, "homogeneous" for $S \equiv 0$), i.e. the form of the wave equation that applies to time-harmonic motion. The plane wave of Eq. (a-32) is a particular solution, as are the asymptotic scattered waves of Eqs. (a-58) or (a-66) in the limit $r \to \infty$.

If the source is "pulsed", i.e. does not depend harmonically on the time, we may insert Eq. (a-78) and its analogue for $S(\vec{r},t)$ into the wave equation, Eq. (a-76), and find

$$\int [\nabla^2 p(\vec{r},\omega')] \exp\{-i\omega' t\}\, d\omega' + \int k^2(\omega') p(\vec{r},\omega') \times \exp\{-i\omega' t\}\, d\omega' = \int S(\vec{r},\omega') \exp\{-i\omega' t\}\, d\omega', \tag{a-85}$$

where we have kept $k(\omega')$ inside the integral since it may depend on the frequency (this fact is called "dispersion"). Multiplying by $\exp\{i\omega t\}/2\pi$, integrating over dt and using the formula

$$\int_{-\infty}^{\infty} \exp\{i(\omega-\omega')\}\, dt/2\pi = \delta(\omega-\omega') \tag{a-86}$$

leads to the Helmholtz equation for the Fourier transform of p:

$$\nabla^2 p(\vec{r},\omega) + k^2 p(\vec{r},\omega) = S(\vec{r},\omega), \tag{a-87}$$

reducing the pulse problem to the previous one of harmonic time dependence. After Eq. (a-87) has been solved for $p(\vec{r},\omega)$, the solution of the pulse problem is then simply obtained from Eq.(a-78). Note that ω appears as a parameter in $s(\vec{r},\omega)$.

APPENDIX B - GEOMETRICAL ACOUSTICS (GA)

This appendix is devoted to an exposition of the theory and applicability of what we have called the Geometrical Acoustics method, as applied to the target scattering problem. We first provide a qualitative description of the method, and then discuss its theoretical foundation. Next, applications of the method are illustrated for various acoustically "hard" bodies. The theoretical and applications sections help to establish the limitations of the method, or what we have called "conditions of applicability". Finally, we consider possible extensions of the method.

B.1 GENERAL DESCRIPTION

The term "Geometrical Acoustics", coined in analogy with the more familiar term "Geometrical Optics", indicates a ray description of acoustical wave motion. The geometrical or ray description of wave phenomena has had three distinct mathematical incarnations, all originally developed for application to electromagnetic waves. The first approach is based on a variational principle (Fermat's principle). It reached its culmination in the work of Hamilton where the now familiar apparatus of rays, caustics, wave fronts, etc., was first given definitive form and made rigorous. The second approach, whose mathematical development was suggested by Sommerfeld [1911], is based on the idea that the geometrical description is a high frequency limit. Since this coincides with the viewpoint of this report it is the approach we will follow in developing geometrical acoustics from the leading term of a high frequency asymptotic expansion. The third approach is based on the discovery by R. K. Luneburg that geometrical optics solutions are exact solutions of Maxwell's equations of a special class, viz., discon-

tinuous solutions. In acoustics this approach was developed by J.B. Keller [1954], who called the discontinuous solutions weak shock waves. This approach is well suited to problems of pulse scattering [FRIEDLANDER - 1958].

The solutions of the geometrical optics (or acoustics) differential equations lead one to the concept that energy travels within "tubes" bounded by "rays". A fundamental result of this theory is that the energy contained within a ray tube remains constant, while the energy density varies, depending upon the convergence or divergence (spreading) of the rays. In homogeneous media (i.e. where the sound speed, c = constant) the rays are straight lines —— in inhomogeneous media [$c=c(\vec{r})$], the rays are curved. These very principles of the propagation of sound energy can be applied to the problem of the scattering of sound from arbitrarily shaped targets. The energy scattered by a target body can be calculated in this geometrical acoustics method by making certain high-frequency approximations relative to the characteristic dimensions of the scatterer.

In some cases, it can be shown that the GA predictions are completely unreasonable and must therefore be rejected. In other cases the GA predictions are quite accurate and useful. The question of the validity, and in particular the limits of validity, of the geometrical optics (acoustics) theory has been studied now for the last two or three centuries, and no completely satisfactory results have been obtained. Nevertheless, we shall undoubtedly continue to use and explore this theory because it is so simple!

B. 2 THEORETICAL BASIS

Recasting Sommerfeld's development from optics into acoustics, we can start with the homogeneous linearized wave equation

$$\nabla^2 p = \frac{1}{c^2} \frac{\partial^2 p}{\partial t^2} \qquad \text{(b-1)}$$

where p is a function of position and time $p(\vec{r}, t)$ and c may be a function of

position, $c(\vec{r})$.

We make the harmonic time assumption

$$p(\vec{r},t) = p(\vec{r}) \exp\{i\omega t\} \tag{b-2}$$

to arrive at the reduced wave equation

$$\nabla^2 p + k^2 p = 0 \; ; \quad k = \omega/c(\vec{r}) \tag{b-3}$$

If one postulates solutions to Eq. (b-3) of the form

$$p(\vec{r}) = A(\vec{r}) \exp\{i k_o S(\vec{r})\} \tag{b-4}$$

(which encompasses <u>almost</u> all propagating wave solutions of interest) and substitutes Eq. (b-4) into Eq. (b-3), one can obtain

$$\frac{\nabla^2 A}{k_o^2 A} - \left[|\nabla S|^2 - \left(\frac{k}{k_o}\right)^2\right] = 0 \tag{b-5}$$

where k_o is some reference wave number, initially chosen to approximate the mean of the range of values of k which are of interest. Eq.(b-5) is certainly no less complex than Eq.(b-3), but it is reasonable to assert that the so-called diffraction term $\nabla^2 A/(k_o^2 A)$ can be neglected in the limit as $\lambda_o = 2\pi/k_o$ approaches zero. The consequence of this approximation to Eq.(b-5) is the eikonal equation

$$|\nabla^2 S|^2 = \left(\frac{k}{k_o}\right)^2 = \left(\frac{\lambda_o}{\lambda}\right)^2 = \left(\frac{c_o}{c(\vec{r})}\right)^2 \triangleq n^2(\vec{r}) \tag{b-6}$$

The solutions to Eq.(b-6) yield the surfaces of constant phase ($S(\vec{r})$ = constant), and the rays of GA which are always perpendicular to these surfaces. In fact, most of the laws of GA can be derived from Eq.(b-6). However, instead of pursuing this development, we shall trace through a recent and more illuminating development due to LUNEBURG [1944] and KLINE [1951]. This development is patterned

from the lecture notes of KOUYOUMJIAN [1972].

Since GA is known to yield results which are correct in the limit of vanishing wavelength, but invalid for large wavelengths, we assume an asymptotic solution of the form

$$p(\vec{r}) \sim \exp\{ik_0 S(\vec{r})\} \sum_{m=0}^{\infty} U_m(\vec{r})/(i\omega)^m \qquad \text{(b-7)}$$

Note, when m = 0 only, we have the first term

$$p(\vec{r}) \sim U_0(\vec{r}) \exp\{ik_0 S(\vec{r})\} \qquad \text{(b-8)}$$

which is identical to the assumed form in Eq.(b-4).

This new form, Eq.(b-7), can be expected to lead to a solution containing frequency dependent correction terms to GA when the index m > 0, but is known to exclude certain diffraction effects - particularly those due to scattering from edges and creeping waves. As before, if we substitute Eq.(b-7) into the reduced wave equation, it is found that

$$k_0^2 \{n^2 - |\nabla S|^2\} p + ik_0 \exp\{ik_0 S\} \cdot \sum_{m=0}^{\infty} \frac{2\nabla S \cdot \nabla U_m + U_m \nabla^2 S + \nabla^2 (U_m/ik_0)}{(i\omega)^m} = 0 \qquad \text{(b-9)}$$

This equation can be satisfied by setting the coefficient of the p term, and all coefficients of each power of $(i\omega)$ equal to zero. Since $k_0 = \omega/c_0$,

$$|\nabla S|^2 = n^2 \qquad \text{(b-10)}$$

and

$$2\nabla S \cdot \nabla U_m + U_m \nabla^2 S + c_0 \nabla^2 U_{m-1} = 0 \qquad \text{(b-11)}$$

where the index m = 0, 1, 2,..., and $U_{-1} \triangleq 0$. The first of these equations, Eq.(b-10), is recognized as the eikonal equation from which one can infer

$$\nabla S = n(\vec{r})\hat{\ell} \tag{b-12}$$

where the unit normal $\hat{\ell}$ is always perpendicular to the surface of constant phase S and is, in fact, the unit tangent vector along the ray at any point $\vec{r}$. Equation (b-12) is a first order partial differential equation which can be solved for $S(\vec{r})$, given $n(\vec{r})$ and an initial value, $S(\vec{r}_o)$. Once $S(\vec{r})$ is determined, Eq. (b-11) can be solved for the coefficients U_m. That is, using Eq. (b-12) in Eq. (b-11), and noting that

$$\nabla S \cdot \nabla U_m = n\hat{\ell} \cdot \nabla U_m = n \frac{dU_m}{d\ell} \tag{b-13}$$

we can write Eq. (b-11) as

$$2n \frac{dU_m}{d\ell} + (\nabla^2 S) U_m = - C_o \nabla^2 U_{m-1} \; ; \; m = 0,1,2,\ldots \tag{b-14}$$

This is a recursive system of equations for finding U_m once U_{m-1} is known; hence, a solution for U_o is required initially. Setting m = 0 and noting that $U_{-1} \triangleq 0$, Eq. (b-14) reduces to the homogeneous form

$$\frac{dU_o}{d\ell} + (\nabla^2 S/2n) U_o = 0 \tag{b-15}$$

which in general form is

$$y'(x) + P(x) y(x) = 0 \tag{b-16}$$

This ordinary differential equation has the solution [BOAS - 1966]

$$y(x) = y(x_0)\exp\left\{-\int_{x_0}^{x} P(x')dx'\right\} \tag{b-17}$$

Hence, the solution to Eq. (b-15) is

$$U_0(l) = U_0(l_0)\exp\left\{-1/2\int_{l_0}^{l}(\nabla^2 S/n)dl'\right\} \tag{b-18}$$

where S and n must be expressed, parametrically, in terms of l', the distance along the ray. To express $S(l)$ we use the fundamental definition of divergence

$$\nabla^2 S = \nabla\cdot\nabla S \triangleq \lim_{\Delta V\to 0}\frac{1}{\Delta V}\oint \nabla S\cdot\hat{a}\,dA \tag{b-19}$$

where $\hat{a}$ is the unit "outward" normal to the closed surface, A. Consider the volume element as shown below.

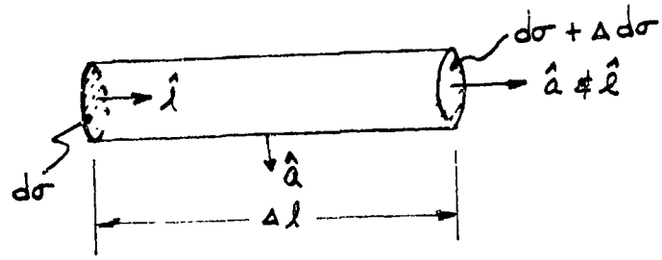

Now if we take the limit as $\Delta l \to 0$, then $\Delta V \to 0$ and since $\nabla S = n\hat{l}$

$$\nabla\cdot\nabla S = \lim_{\Delta l\to 0}\frac{1}{\Delta V}\oint n\hat{l}\cdot\hat{a}\,dA$$

$$= \lim_{\Delta l\to 0}\frac{1}{d\sigma\Delta l}\int_{\text{end caps}} n\,dA$$

or

$$\nabla\cdot\nabla S = \frac{1}{d\sigma}\lim_{\Delta l\to 0}\frac{1}{\Delta l}\left[(n+\Delta n)\cdot(d\sigma+\Delta d\sigma) - n\,d\sigma\right]$$

$$\nabla \cdot \nabla S = \frac{1}{d\sigma} \lim_{\Delta \ell \to 0} \frac{\Delta (n d\sigma)}{\Delta \ell}$$

or, finally

$$\nabla \cdot \nabla S = \frac{1}{d\sigma} \frac{d (n d\sigma)}{d \ell} \tag{b-20}$$

Using this result in Eq. (b-18) yields

$$U_0(\ell) = U_0(\ell_0) \exp \left\{ -1/2 \int_{\ell_0}^{\ell} \frac{1}{n d\sigma} \frac{d (n d\sigma)}{d \ell'} d\ell' \right\}$$

and this integrates simply to

$$U_0(\ell) = U_0(\ell_0) \exp \left\{ -1/2 \ln (n d\sigma) \Big|_{\ell_0}^{\ell} \right\}$$

or finally, inserting the limits and simplifying

$$U_0(\ell) = U_0(\ell_0) \sqrt{\frac{n(\ell_0) d\sigma_0(\ell_0)}{n(\ell) d\sigma(\ell)}} \tag{b-21}$$

This expression gives us the first term in the assumed solution of Eq.(b-7), and from it we could calculate, recursively, the higher order terms. This first term is what we call the geometrical acoustics solution, the higher order terms represent corrections to geometrical acoustics; but, as mentioned previously, do not include diffraction effects. We are primarily concerned here with Eq. (b-21) itself, since it is the derived form of what is usually referred to as the principal "law" of GA: that is, Eq. (b-21) establishes that the amplitude of the GA field varies inversely as the square root of the index $n(\ell)$ and the differential cross-sectional area of the tube of rays predicted by the theory. In fact, for the case of a homogeneous medium where $n(\ell) = n(\ell_0)$, a constant, this same dependence on cross-sectional area remains.

Consequently, one can infer that the energy or intensity of the GA field in an homogeneous medium varies inversely with the spreading of the ray tube. It is this law which allows us to proceed and develop GA formulas for target strength and/or back-scattering cross-section.

The complete first term representation of the GA field, which includes the phase as well as the amplitude variation is, from Eq.(b-7)

$$p(\ell) = U_0(\ell_0)\sqrt{\frac{n(\ell_0)\,d\sigma_0(\ell_0)}{n(\ell)\,d\sigma(\ell)}}\cdot \exp\{ik_0 S(\ell)\} \tag{b-22}$$

Now $\exp\{ik_0 S(\ell)\}$ can be written in the form

$$\exp\{ik_0 S(\ell)\} = \exp\{ik_0 S(\ell_0)\}\cdot \exp\{ik_0[S(\ell) - S(\ell_0)]\}$$

and since

$$S(\ell) - S(\ell_0) = \int_{S(\ell_0)}^{S(\ell)} dS(\ell') = \int_{\ell_0}^{\ell} \frac{dS(\ell')}{d\ell'}\,d\ell' = \int_{\ell_0}^{\ell} n(\ell')\,d\ell'$$

we can write Eq. (b-22) in the form

$$p(\ell) = U_0(\ell_0)\exp\{ik_0 S(\ell_0)\}\cdot\sqrt{\frac{n(\ell_0)\,d\sigma_0(\ell_0)}{n(\ell)\,d\sigma(\ell)}}\cdot \exp\left\{ik_0\int_{\ell_0}^{\ell} n(\ell')\,d\ell'\right\} \tag{b-23}$$

The first two terms in Eq.(b-23) establish a reference or initial amplitude and phase, and the second pair of terms establishes the amplitude and phase dependence along the ray. It is worthwhile to consider further the geometrical spreading term for the case of a homogeneous medium. In this case $n(\ell) = n(\ell_0)$, and therefore Eq.(b-23) becomes

$$p(\ell) = U_0(\ell_0)\exp\{ik_0 S(\ell_0)\}\sqrt{\frac{d\sigma_0(\ell_0)}{d\sigma(\ell)}}\cdot \exp\{ik_0 n(\ell_0)[\ell - \ell_0]\} \tag{b-24}$$

and the ratio of the scattered field at ℓ to the incident field at ℓ_o is simply

$$P(\ell)/P(\ell_o) = \sqrt{\frac{d\sigma_o(\ell_o)}{d\sigma(\ell)}} \cdot \exp\left\{ i k_o n(\ell_o)[\ell - \ell_o] \right\} \quad \text{(b-25)}$$

We wish to study the significance of the factor $\sqrt{d\sigma_o/d\sigma}$. Let us consider a tube of rays as shown below. It can be shown that the most general infinitesimal bundle of rays perpendicular to a given surface (wave front) must be of this general form.

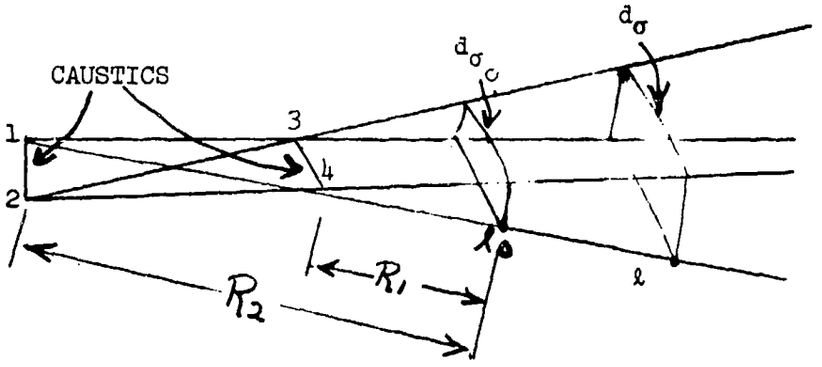

The line segments 1-2 and 3-4 are loci of the intersections of the individual rays which make up the ray tube. These are segments of the so-called caustic surfaces. The distances R_1 and R_2 of a wave front from the caustics are the principal radii of curvature of the wave front. (The principal radii of curvature of a surface at a point are the maximum and minimum radii of curvature among curves formed by the intersection of the surface with all normal planes at the point. The directions of the principal curvatures are at right angles, as are the caustics.) As special cases we may have the caustics coincide in a point (called a focus), we may have one caustic at infinity (cylindrical wave), or both caustics at infinity (plane wave).

The differential areas $d\sigma_0$ and $d\sigma$ can be expressed in terms of their respective principal radii of curvature, R_1 and R_2; that is

$$\frac{d\sigma_0}{d\sigma} = \frac{(R_1 d\theta)(R_2 d\phi)}{(\{R_1+[\ell-\ell_0]\}d\theta)(\{R_2+[\ell-\ell_0]\}d\phi)} = \frac{R_1 R_2}{(R_1+[\ell-\ell_0])(R_2+[\ell-\ell_0])} \quad (b\text{-}25')$$

Or, from Eq. (b-21), with $\ell_0 = 0$

$$U_0(\ell) = U_0(0)\sqrt{\frac{R_1 R_2}{(R_1+\ell)(R_2+\ell)}} \quad (b\text{-}26)$$

The field $U_0(\ell)$ at any point along the ray path, as given by Eq.(b-26) is well behaved except at the caustics where either $\ell = -R_1$, or $\ell = -R_2$. Hence GA

(or for that matter, the higher order Luneburg-Kline theory) is not valid at caustics, but these theories are valid on either side of the caustics. The effect of the passage of a ray through a caustic is a discontinuous jump in the phase of the solution by $-\pi/2$ for an ordinary caustic, and by $-\pi$ for a focus.

Thus far we have discussed GA theory as it applies to propagation within a homogeneous or inhomogeneous fluid medium. We wish now to extend the discussion to encompass the scattering problem, but restricted to a homogeneous medium.

Consider the geometry in Figure (b-1) below:

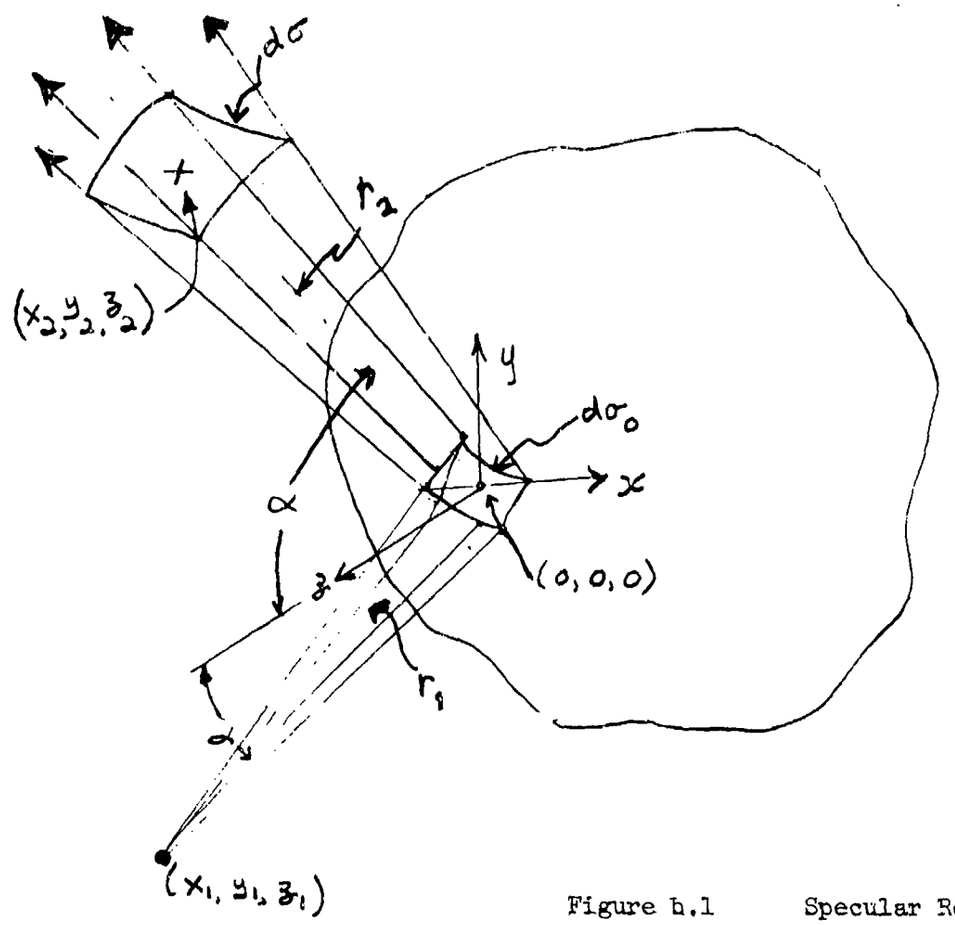

Figure b.1 Specular Reflection

A point source at (x_1, y_1, z_1) ensonifies a doubly-curved target, which in turn scatters energy to an observation point (x_2, y_2, z_2). The center of the coordinate system is chosen to lie at the specular point with the z-axis normal to the tangent surface. We seek the GA approximation of the pressure at (x_2, y_2, z_2) in terms of the pressure at some reference point. We choose the reference point to be the specular point (the origin) since we can determine the incident field at this point with relative ease.

A small differential tube of rays surrounds the central ray from (x_1, y_1, z_1) to (0, 0, 0) and intersects the scatterer, defining a differential area $d\sigma_o$ on the scattering surface. A portion of the incident energy may be refracted into, or absorbed by, the scatterer itself, giving rise to a reflection coefficient, $\mathcal{R}$. The remaining energy scatters back into the fluid medium such that each reflected ray leaves the scatterer tangent plane at an angle equal to the angle of incidence α, measured with respect to the normal at the specular point along the positive z-axis. We are using here the familiar law of specular reflection. The divergence (or convergence) of the ray tube at the observation point is a measure of the acoustic field in the GA approximation. Neglecting phase, we use Eq. (b-23) to write

$$\left| P(x_2, y_2, z_2) \right| = U_o(0,0,0) \sqrt{\frac{d\sigma_o(0,0,0)}{d\sigma(x_2, y_2, z_2)}} \cdot \left| \mathcal{R}(0,0,0) \right| \qquad \text{(b-27)}$$

Assuming that $\mathcal{R}$ can be determined from flat plate theory [BREKHOVSKIKH - 1965] and in general is a function of the angle of incidence, further progress depends on the development of the ratio $d\sigma_o/d\sigma$. But from calculus [WIDDER - 1965], $d\sigma_o/d\sigma$ is recognized as the Jacobian of the transformation which maps (in a one-to-one fashion) the surface at z = 0 to the surface at $z = z_2$, or

$$\frac{d\sigma_o}{d\sigma} \triangleq \left[\frac{\partial(x_2', y_2')}{\partial(x, y)} \right]^{-1} = \left(\frac{\partial x_2'}{\partial x} \cdot \frac{\partial y_2'}{\partial y} - \frac{\partial x_2'}{\partial y} \cdot \frac{\partial y_2'}{\partial x} \right)^{-1}$$

where x_2' and y_2' denote variables on the plane $z = z_2$. Using the law of reflection, and writing the equation of the scattering surface in form

$$z = ax^2 + by^2 + \ldots; \qquad \text{with no } xy \text{ term} \tag{b-28}$$

PRIMAKOFF [1947] has shown that $d\sigma_o/d\sigma$ can be written as

$$\frac{d\sigma_o}{d\sigma} = \left\{1 + 2r_2\left[1/r_1 - 2G_m\cos\alpha - G_i \sin\alpha \tan\alpha\right] + r_2^2\left[1/r_1^2 - 4G_m\cos\alpha/r_1 + 4G_g - 2G_i \sin\alpha \tan\alpha/r_1\right]\right\}^{-1} \tag{b-29}$$

where the G's represent various curvatures at the specular point and G is related to the radius of curvature R by

$$|G| = 1/R$$

G is a signed quantity and is negative if the center of curvature is on the side of the surface opposite that toward which the normal points (which adjusts PRIMAKOFF [1947] for an opposite assumption as to the direction of the surface normal).

$G_m \triangleq (G_1 + G_2)/2$, the mean curvature; R_1 and R_2 are the principal radii of curvature at the specular point corresponding to the principal curvatures, G_1 and G_2.

$G_g \triangleq G_1G_2$, the Gaussian curvature.

G_i = the curvature of the surface in the plane of incidence at the specular point.

$\vec{r}_1 \triangleq$ the source location, $\vec{r}_1\ (x_1, y_1, z_1)$

$\vec{r}_2 \triangleq$ the observer location, $\vec{r}_2(x_2, y_2, z_2)$.

Equation (b-29) in conjunction with Eq. (b-24) will predict the GA scattered field in a homogeneous medium for any location of the source and observation points. However, our primary interest is monostatic back-scattering and for these conditions $\alpha = 0$ and $r_1 = r_2$. Eq. (b-29) therefore becomes

$$\frac{d\sigma_o}{d\sigma} = \frac{1}{4\left\{1 - 2r_1 G_m + r_1^2 G_g\right\}} \qquad \text{(b-30)}$$

To obtain σ_{GA}, the backscattering cross-section, we use Eq. (a-64) and obtain

$$\sigma_{GA} = 4\pi \lim_{r_1 \to \infty} r_1^2 \left(\frac{|P(\ell)|^2}{|P(\ell_o)|^2}\right) \cdot |R|^2 \Big|_{\alpha = 0}$$

or, using Eqs. (b-25), (b-27), and the above,

$$\sigma_{GA} = 4\pi \lim_{r_1 \to \infty} \left\{ r_1^2 \left| \frac{1}{4\left[1 - 2r_1 G_m + r_1^2 G_g\right]} \right| \right\} \cdot |R|^2 \qquad \text{(b-31)}$$

If G_m and G_g are bounded and non-zero, this limit as $r_1 \to \infty$ is

$$\sigma_{GA} = \pi |R|^2 / |G_g| = \pi R_1 R_2 |R|^2 \qquad \text{(b-32)}$$

a useful and widely used result. If $|G_m|$ approaches ∞ then $|G_g|$ also $\to \infty$, as would occur at an edge or vertex, the limit in Eq. (b-31) then exists, but this limit is zero. The GA method therefore predicts zero σ for bodies with physical edges or corners if these bodies have no other backscattering specular points. In the case of G_g equal to zero, the limit in Eq. (b-31) does not exist, and the method fails. Such is the case for bodies which are flat in either one or two dimensions, such as the cylinder, cone, various flat plates, and others. This failure of the method for the case of G_g equal to zero does not mean that GA itself fails, but only that the GA method will fail to predict the three-dimensional infinite range expression σ_{GA}. A GA field does exist if either r_1 or r_2 (or both) are finite.

We see then that we can apply Eq. (b-32) at the specular point on any doubly-curved surface as long as the principal radii of curvature are finite. For strictly convex surfaces (see definition in section B.3.5) only one specular point will exist for back-scattering. However, for non-convex surfaces, two or more specular points may exist and the situation is further complicated by multiple scattering phenomena. This relatively complex situation is discussed more fully in section B.3.6.

To apply Eq. (b-32) to any single specular point, one must know the principal radii of curvature R_1 and R_2, in addition to the reflection coefficient R. R is available [BREKHOVSKIKH - 1965] for most homogeneous fluids or elastic solids. The principal radii, R_1 and R_2, can be determined easily for many simple surfaces using the two-dimensional expression for curvature, G, from calculus [HART - 1957]. That is, since radius of curvature, R, is the reciprocal of |G|,

$$R = \frac{1}{|G|} = \frac{(1+f_x^2)^{3/2}}{|f_{xx}|}; \text{ where } f_x = \frac{2f(x,y)}{2x} \qquad \text{(b-33)}$$

However, if the surface is not simple and/or the principal normal planes are not obvious by inspection, then one must resort to the methods of differential geometry [EISENHART - 1964] to calculate the principal radii. If the equation of the surface in the neighborhood of the specular point is written in the form $z = f(x, y)$, then the product of the principal radii is

$$R_1 R_2 = \frac{1}{G_g} = \frac{(1+f_x^2+f_y^2)^2}{|f_{xx} f_{yy} - f_{xy}^2|} \qquad \text{(b-34)}$$

Other prescriptions from differential geometry may be used to calculate R_1R_2 if the equation of the surface is given in other forms; e.g., $F(x,y,z) = 0$ or parametrically as $x = x(u, v)$, $y = (u, v)$ $z = z(u, v)$; see CRISPIN [1968]. In Eq. (b-34) above, R_1R_2 is evaluated at the specular point, $z_o = f(x_o, y_o)$, or in the geometry of Figure (b-1) at the point (0, 0, 0).

B.3 APPLICATIONS

In this section a number of examples of the application of the GA method will be shown. We shall calculate the sonar c.s. of various acoustically "hard" bodies when ensonified by a plane harmonic wave. Only finite bodies will be considered.

B.3.1 THE ELLIPSOID AND ITS DEGENERATE FORMS

The incoming plane wave is incident from a direction (θ, ϕ) and the ellipsoid is oriented in an x-y-z coordinate system as shown below

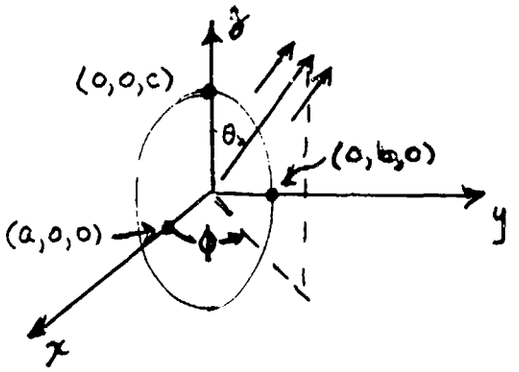

The sonar c.s. is from Eq. (b-32) equal to πR_1R_2 where R_1 and R_2 must be evaluated at the specular point, along the direction (θ,ϕ) on the ellipsoidal surface. The product R_1R_2 can be obtained from Eq. (b-34) if the equation of the ellipsoidal surface is expressed in the form $z = f(x, y)$. In rectangular coordinates the equation of the ellipsoid is

$$\frac{x'^2}{a^2} + \frac{y'^2}{b^2} + \frac{z'^2}{c^2} = 1 \qquad \text{(b-35)}$$

Therefore

$$z' = \pm c\sqrt{1-\left(\frac{x'}{a}\right)^2-\left(\frac{y'}{b}\right)^2} \qquad \text{(b-36)}$$

Using (b-34) we obtain

$$R_1 R_2 = a^2 b^2 c^2 \left(\frac{x'^2}{a^4}+\frac{y'^2}{b^4}+\frac{z'^2}{c^4}\right)^2$$

Now transforming from rectangular to spherical coordinates,

$$R_1 R_2 = a^2 b^2 c^2 \left\{\frac{\frac{\sin^2\theta'\cos^2\phi'}{a^4}+\frac{\sin^2\theta'\sin^2\phi'}{b^4}+\frac{\cos^2\theta'}{c^4}}{\frac{\sin^2\theta'\cos^2\phi'}{a^2}+\frac{\sin^2\theta'\sin^2\phi'}{b^2}+\frac{\cos^2\theta'}{c^2}}\right\} \qquad \text{(b-37)}$$

But this equation expresses the product R_1R_2 in terms of the surface coordinates of the radius vector, $\vec{r}'$, as measured from the origin in two dimensions (see Figure (b-2), below)

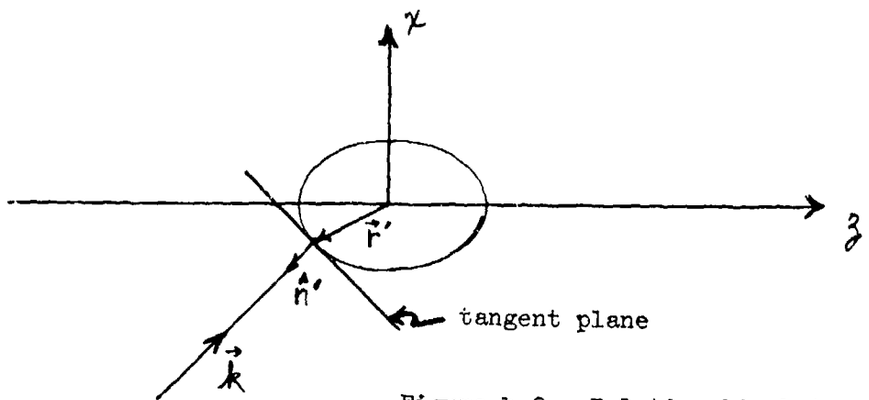

Figure b-2. Relationship between the Wave Vector and Surface Coordinates

It is seen that the angular coordinates (unprimed) of the wave vector $\vec{k}$ do not correspond to these surface coordinates and a transformation between the two is required. If one observes that, at any specular point, the wave vector $\vec{k}$ and the surface normal $\hat{n}'$ are anti-parallel, then

$$\hat{k}\cdot\hat{n}' = -1, \qquad \text{or} \qquad \hat{k} = -\hat{n}' \qquad \text{(b-38)}$$

The solution to the above will yield the wave vector coordinates (unprimed) at the specular point in terms of the surface (primed) coordinates. Thus, by expressing $\hat{k}$ and $\hat{n}'$ in spherical coordinates, unprimed and primed respectively, and using Eq. (b-38) we can obtain (after much algebra)

$$\tan\phi' = \left(\frac{b}{a}\right)^2 \tan\phi \tag{b-39a}$$

and

$$\tan\theta' = \left(\frac{a}{c}\right)^2 \cos\varphi \left\{1 + \left(\frac{b}{a}\right)^4 \tan^2\varphi\right\} \tan\theta \tag{b-39b}$$

Substitution of Eq. (b-39) into Eq. (b-37) will yield the product R_1R_2 or (b-40)

$$\sigma = \pi R_1 R_2 = \pi a^2 b^2 c^2 / \left\{a^2 \sin^2\theta \cos^2\phi + b^2 \sin^2\theta \sin^2\phi + c^2 \cos^2\theta\right\}^2$$

For the prolate spheroid, a = b and c>a. Eq. (b-40) reduces to

$$\sigma = \pi a^4 c^2 / \left\{a^2 \sin^2\theta + c^2 \cos^2\theta\right\}^2 \tag{b-41}$$

For the special case of axial incidence, $\theta = 0$

$$\sigma = \pi a^4/c^2 \quad ; c > a$$

For beam incidence, $\theta = \pi/2$ (b-42)

$$\sigma = \pi c^2$$

and σ suprisingly becomes independent of a. (b-43)

For the oblate spheroid, a = b, Eq.(b-40) reduces again to (b-41) but here c < a.

For axial incidence, $\theta = 0$

$$\sigma = \pi \frac{a^4}{c^2} \quad ; \quad c < a \tag{b-44}$$

For "edge-on" incidence, $\Theta = \pi/2$

$$\sigma = \pi c^2 \tag{b-45}$$

and again σ is independent of a.

B.3.2 THE CYLINDER

For a finite right circular cylinder of length 2ℓ and radius a (below),

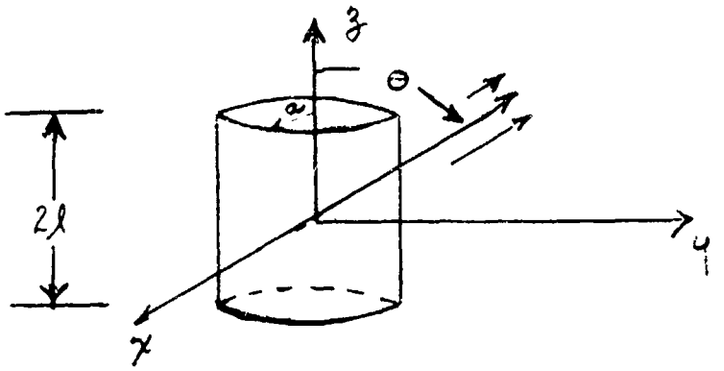

the backscattered GA field is zero for θ in the open intervals $0<\theta<90°$ and $90° <\theta< 180°$; hence, $\sigma = 0$. This result obtains because the direction of the specular reflection is never in the back direction for θ in these intervals. For the special angles of incidence $\theta = 0$ and 180° as well as 90°, there does exist a back-scattered field, but one or both principal radii of curvature are infinite. This situation has been previously discussed in connection with the development of the limiting form of the three-dimensional back-scattering cross-section σ in Eq. (b-31). The conclusion was that $\sigma \to \infty$ (which is not physically reasonable) and hence the method fails.

B.3.3 THE CONE

The curvature at every point on the surface of a right circular finite cone in Figure (b-3) is either zero or infinite.

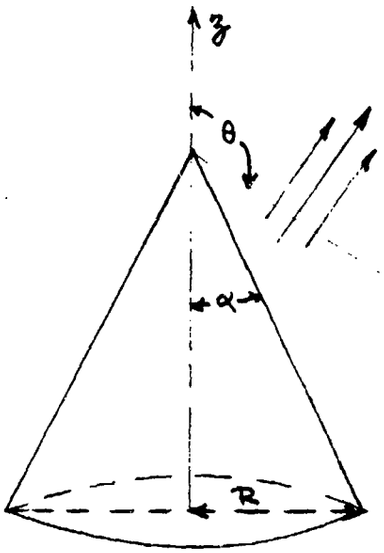

Figure b-3. Geometry of the Right Circular Finite Cone

A specular point(s) exists at $\theta = \pi/2 - \alpha$ and at $\theta = \pi$. At these aspects, however, one or both of the radii of curvature are infinite, hence the method fails. At all other aspects no specular point exists and the GA prediction of σ must be zero. Therefore, like the finite cylinder, GA can provide no useful information concerning σ for this body.

B.3.4 THE FLAT PLATE

Like the cylinder and cone, the curvature at every point on the flat plate of any boundary shape, is either zero or infinite. GA can provide no useful information concerning σ for this body.

B.3.5 ANY CONVEX BODY

A convex, three-dimensional body is one for which the line joining any two surface points will not exit the body. If the body is strictly convex, only

the endpoints of the line joining the two surface points will be coincident with the boundary surface. Illustrations of convex, strictly convex, and non-convex bodies are shown below.

strictly convex

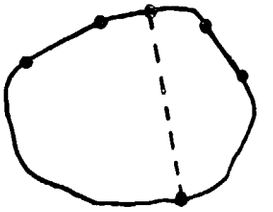

convex

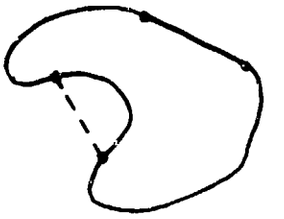

non-convex

A strictly convex body will have one and only one specular point independent of the direction of the incoming plane wave. The specular point is coincident with that tangent plane which is perpendicular to the direction of the incoming wave on the ensonified side of the body.

The sonar c.s. of a strictly convex body exists for all directions of the incoming plane wave and is equal to $\pi R_1 R_2$. The product $R_1 R_2$ can be evaluated at the specular point using an approximate description (equation) of the surface at that point. In rectangular coordinates, one can write this equation as

$$z = ax^2 + by^2 + cxy + \cdots \{\text{higher order terms}\} \qquad \text{(b-46)}$$

In the vicinity of the specular point (recall, the specular point is by definition at the origin) we can neglect the higher order terms. Further simplication of Eq. (b-46) is possible to eliminate the cross-term, cxy. A transformation of the coordinate axes to effect a rotation of the x and y axes about the z axis by an angle ϕ satisfying

$$\tan(2\phi) = \frac{b}{a-c} \qquad \text{(b-47)}$$

will eliminate the cross-term [WILSON - 1949]. The resulting equation of the surface in the new (primed) coordinate system will be of the form

$$z' \doteq a'x'^2 + b'y'^2 \qquad (b\text{-}48)$$

Now it is a simple matter to obtain the product R_1R_2 from Eq. (b-34). It is

$$R_1R_2 = \frac{1 + 4(a'x')^2 + 4(b'y')^2}{|4a'b'|} \qquad (b\text{-}49)$$

The specular point is at the origin ($x' = y' = 0$); therefore

$$\sigma = \pi R_1R_2\Big|_{(0,0,0)} = \frac{\pi}{|4a'b'|} \qquad (b\text{-}50)$$

If the body has "flattened" sub-surfaces and is, therefore, only convex, then one or both principal radii of curvature will be infinite on these sub-surfaces. In such cases, examples of which have already been discussed (the finite cylinder, cone, and flat plate), the prediction of the three-dimensional σ, using the GA method, fails.

B.3.6 NON-CONVEX BODIES

The calculation of σ_{GA} for bodies which are neither convex nor strictly convex is relatively complex. This complexity results from two causes, (1) multiple specular points, and (2) multiple reflections (scatterings) as illustrated below in Figure (b.4)

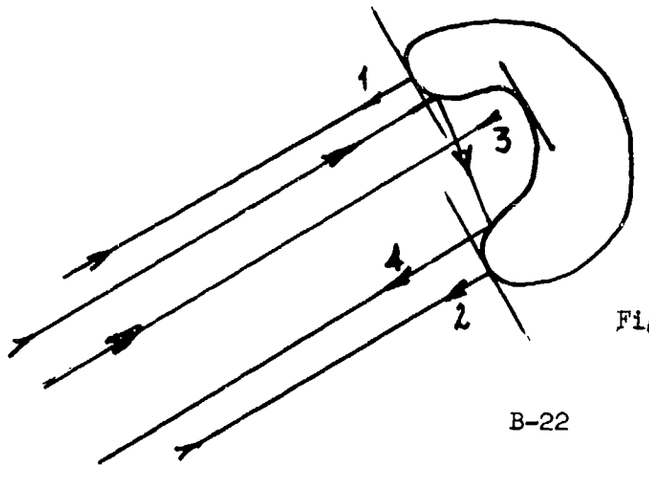

Figure b-4. Multiple Reflections From Non-Convex Bodies

The returns 1 and 2 are single specular scatterings from convex subsurfaces. Return 3 is a single specular scattering from a concave subsurface. Return 4 is one of the many double scatterings which can occur and there are, in addition, higher order multiple scatterings. If we ignore, for the moment, the multiple scatterings then the three single specular returns can be combined to yield the single-scattering cross section σ_{ss} by accounting for the relative phase differences between the highlights, or

$$\sigma_{ss} = \left| \sigma_1^{1/2} e^{i\phi_1} + \sigma_2^{1/2} e^{i\phi_2} + \sigma_3 e^{i\phi_3} \right|^2 \tag{b-51}$$

or, for N specular points by

$$\sigma_{ss} = \left| \sum_{j=1}^{N} \sigma_j^{1/2} \; e^{i\phi_j} \right|^2 \tag{b-52}$$

Since only the relative phase is important, ϕ_1 may be set equal to zero. In Eq. (b-52) above, ϕ_j is given by

$$\phi_j = 2\left(\frac{2\pi d_j}{\lambda}\right) \tag{b-53}$$

where d_j is the distance from the reference highlight to the $j^{\underline{th}}$ highlight measured along the direction of the incident wave (ray). It is important to note that (for the first time) a frequency dependence has "crept in" to a geometrical acoustics formula for σ by virtue of the λ dependence in Eq. (b-53).

If the body is very irregular and exhibits a large number of specular points which are randomly distributed, then a good estimate of the single scattering cross-section σ_{ss} can be obtained by averaging. That is, if we let

$$\alpha = \sum_{j=1}^{N} \sigma_j^{1/2} \exp\{i\phi_j\} \tag{b-54}$$

then

$$|\alpha|^2 = \sum_{j=1}^{N} \sigma_j + \sum_{\substack{i=1 \\ (i \neq j)}}^{N} \sum_{j=1}^{N} (\sigma_i \sigma_j)^{1/2} \exp\{i(\phi_i - \phi_j)\} \quad \text{(b-55)}$$

If the phases, ϕ_i or ϕ_j, are randomly distributed with a uniform probability density, then each term in the second series set above has a mean or expected value of zero. Therefore, the expected value of $|\alpha|^2$ is

$$\bar{\sigma}_{ss} = E\left[|\alpha|^2\right] = \sum_{j=1}^{N} \sigma_j \quad \text{(b-56)}$$

Generally, Eq. (b-56) will suffice for most predictions where the variability of σ_{ss} is not important — otherwise Eq. (b-52) must be used.

Thus far, we have dealt with one of the complexities associated with non-convex bodies — multiple specular points; but we have yet to consider the effect of multiple scatterings. Return 4 in Figure (b-4) contributes to the back-scattering cross-section after having scattered twice from the target body. In general, one or more double scatterings will occur depending upon the geometry of the scatterer. It is probable that the double and higher order scatterings will be weaker than single scatterings as a result of the additi l spreading that occurs at each specular point. However, the strength of each multiple scattering also depends upon the curvatures at each scattering point along the path and in some cases (a flat section) there may be no spreading, and in others (a concave section) the rays will converge. In Figure (b-5) one can see that one of the conditions for the existence of a monostatic double scattering in two dimensions is

$$\theta_1 + \theta_2 = \pi - \theta_3 - \theta_4 \quad \text{(b-57)}$$

For each surface point in the ensonified region, a reflected ray along $\hat{k}'$ due to an incident ray along $\hat{k}_I$ determines $\phi_1 + \phi_2$ by the law of reflection. The second intersection of $\hat{k}'$ with the surface (but it may not intersect) similiarly determines $\theta_3 + \theta_4$.

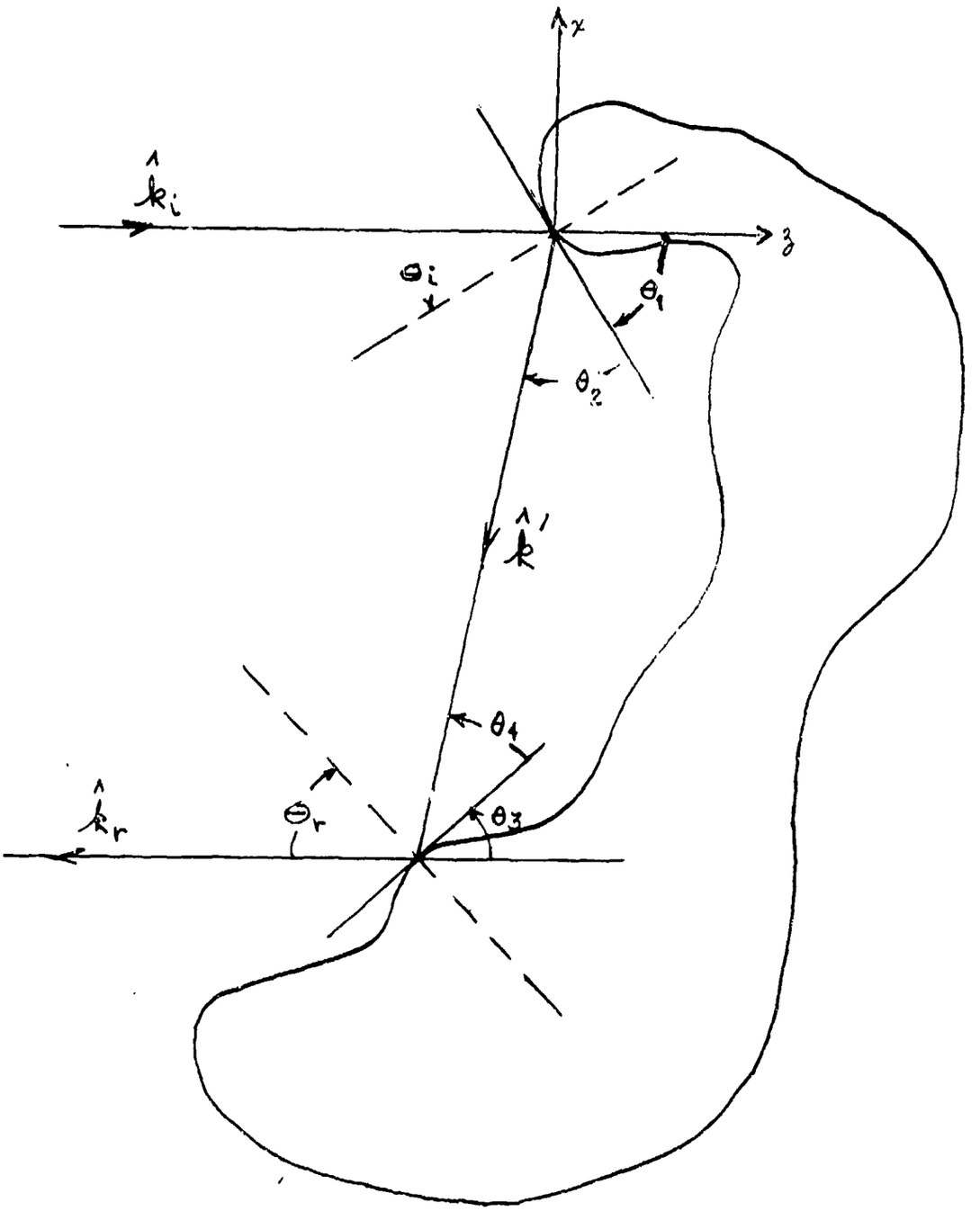

Figure b-5. The Geometry for a Monostatic Double Scattering

Then, if Eq. (b-57) is satisfied, a double scattering will occur. The existence of higher order scatterings can be determined by extending this process. In three dimensions, the condition analogous to Eq. (b-57), for a monostatic, double scattering, is

$$(\hat{z}, \hat{k}') + (\hat{k}', -\hat{z}) = \pi \qquad \text{(b-58)}$$

where $\hat{z}$ is the unit vector in the positive z (incident) direction.

Once it has been determined that double or higher order scatterings can exist, then the amplitude and phase of the multiple scattering can be determined by repeated applications of Eq. (b-24). After the multiple scattering cross-sections are found for each possible path, they can be added to the single scattering cross-sections to yield σ. That is, in analogy to Eq. (b-52)

$$\sigma = \left| \underbrace{\sum_{j=1}^{N} \sigma_j^{1/2} \exp\{i\phi_j\}}_{\text{single scatterings}} + \underbrace{\sum_{m=1}^{M} \sigma_m^{1/2} \exp\{i\phi_m\}}_{\text{multiple scatterings}} \right|^2$$

or, in analogy to Eq. (b-56)

$$\sigma = \sum_{j=1}^{N} \sigma_j + \sum_{m=1}^{M} \sigma_m$$

This process of accounting for multiple scatterings can be very laborious and few specific results exist. The example of two spheres of equal radii has been worked out by CRISPIN [1968; pg. 259].

B.4 CONDITIONS OF APPLICABILITY

Of extreme importance to practitioners is the question - when, and under what conditions, will the GA prediction yield an accurate result? We have seen from Section B.2 that the complete Luneburg-Kline series is an exact, but asymptotic, result when the scattering body is smoothly curved and infinite in extent; even here, however, the prediction breaks down at caustics. In addition, all targets of practical interest are finite, exhibiting shadow boundaries and perhaps physical edges and tips. These boundaries of the target will give rise to diffraction phenomena which are in no way accounted for by GA theory. Hence, even when the frequency is sufficiently high to warrant the use of the Luneburg-Kline asymptotic series, GA will be in error, due to (1) exclusion of the higher order terms of the series and (2) neglect of the diffraction effects. It is generally not possible to make broad sweeping statements regarding the conditions under which these corrections can be neglected. However, some guidance can be offered.

The GA solution to a scattering problem makes use of the first term in the Luneburg-Kline series, and this series is valid in the limit as $\lambda \to 0$ or $\omega \to \infty$. To justify the neglect of the second and higher order terms in this series (Eq. (b-7)) it is sufficient that

$$\left| \frac{U_m(\vec{r})}{U_0(\vec{r})\,(i\omega)^m} \right| \ll 1; \quad m = 1, 2, \ldots \tag{b-59}$$

For m = 1, and since U_1 and U_0 are independent of frequency, it is clear that the criteria in Eq. (b-59) above can be satisfied for sufficiently large ω independent of the particular values of U_1 and U_0. These criteria can also be satisfied if $|U_1|$ is sufficiently small relative to $|U_0|$; however, no generally useful results have been obtained [BOWMAN - 1969; p. 26]. Results specific to particular body shapes have been derived (for example, KELLER [1956] and

SCHENSTED [1955]) but these results, although interesting, are not sufficient to establish general criteria for the validity of (b-59).

More explicit criteria for the validity of GA can be obtained from a consideration of the flat plate (or tangent plane) assumption discussed on page B-12. Such an assumption can be justified only if (1) the minimum radius of curvature at the specular point satisfies

$$kR_{min} \gg 1 \quad \text{or} \quad R_{min} \gg \lambda \tag{b-60}$$

and (2) the minimum dimension (say D) of the body in the vicinity of the specular point satisfies

$$kD \gg 1 \quad \text{or} \quad D \gg \lambda \tag{b-61}$$

Hence, GA would fail for vertices and edges, and scattering from these centers must be calculated by methods of diffraction theory. However, these diffracted fields are inversely proportional to some (possibly fractional) power of k and are therefore dominated by a non-zero GA field. For example, let us compare scattering by a hemisphere and by a cylinder (Figure b-6)

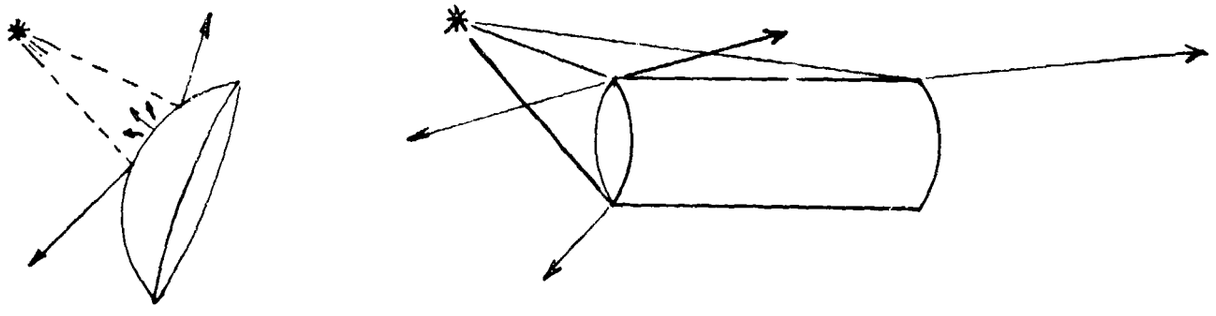

Figure b-6. Zero and Non-Zero GA Fields for a Hemisphere and Finite Cylinder The GA field vanishes except in the specular direction. Hence, according to GA there is back-scattering from the hemisphere but not from the cylinder.

For the hemisphere, edge diffraction gives a higher order correction to the GA cross-section πa^2, whereas for the cylinder the cross-section is entirely due to diffraction.

GA also fails for insufficient target dimensions. For example, consider the GA prediction for σ for the hard sphere and prolate spheroid (axial incidence). For the sphere (see Fig.2.3-2).

$$k R_{min} = ka$$

and

$$k D = 2ka$$

For ka = 1.0 the error in the normalized cross-section prediction is approximately 50% when compared to the exact solution. At ka = 10 or beyond the error is less than 10%. For the 10:1 prolate spheroid (see Fig.2.3-6)

$$k R_{min} = ka^2/b = kb/100$$

and

$$k D = 2ka = kb/5$$

To satisfy the criteria Eq. (b-60) and Eq. (b-61), kb must be >>100; hence, it is not surprising to see such poor correlation between the GA and exact results for the range of kb($\leq$ hξo) plotted.

Regions in which a zero GA field is predicted simply exclude the specular directions and this prediction results from the neglect of diffractic and higher order terms in the Luneburg-Kline series. In the cylinder example, the back-scattered direction falls in one of these zero field regions; hence, the prediction of σ_{GA} is zero. A similar situation would occur, for example, for flat plates, finite cones, polygons, and others. It is difficult in general

to estimate the inaccuracy of this zero-field prediction, and no general guidelines can be given. Nevertheless, a thorough study of the flat circular plate problem (for which an exact solution exists) would be very revealing.

Finally, we discuss the conditions for applicability of the GA method with regard to the far-field approximation. Actually, the GA prediction equation [(b-27), using (b-30)], is valid both in the near-and far-fields of the scattering body. The only far-field approximation made was that associated with the development of σ_{GA} in Eq. (b-31) and specifically that

$$\left| r_1^2 G_q \right| \gg \left| 2 r_1 G_m \right| \text{ and } 1$$

Using the curvature definitions following Eq.(b-29), these far-field criteria become

$$r_1 \gg + \sqrt{R_1 R_2} \tag{b-62}$$

and

$$r_1 \gg R_1 + R_2 \tag{b-63}$$

Since R_1 and R_2 must be finite for the three-dimensional σ_{GA} to exist, the relations Eq. (b-62) and Eq. (b-63) can be replaced by

$$r_1 \gg \max \{R_1, R_2\} \tag{b-64}$$

If R_1 or R_2 are very large, then r_1 must be very far away from the target body (perhaps this explains why GA fails when R_1 or $R_2 \to \infty$!). Note also that Eq. (b-64) is frequency independent, but that an a priori criterion for the validity of GA was that $R_{min} \gg \lambda$.

B.5 EXTENSIONS OF THE GEOMETRICAL ACOUSTICS METHOD

It is somewhat presumptuous to attempt to introduce new improvements or

extensions of the GA method since a large part of the literature on scattering theory for the past two centuries has been devoted to this topic. The Keller and Kirchhoff theories are already viewed by most as extensions of GA - but these theories seek to account for diffraction phenomena! It is perhaps desirable then to consider only those extensions which exclude diffraction, since otherwise we would have to consider practically every related development in scattering theory since the seventeenth century. If we exclude theories which account in some way for diffraction, we are led immediately to the Luneburg-Kline theory. This theory and the resulting asymptotic series solution has been rigorously shown by the authors to be a valid representation of the scattered field from smoothly curved bodies which cast no shadow; i.e., a restricted class of infinite or semi-infinite bodies. For large, but finite, bodies, it is conceivable that the higher-order Luneburg-Kline terms could add a significant correction to the first (GA) term, and at the same time, dominate any contribution due to diffraction. It is conjectured, however, that this situation would be rare. It is much more likely that the higher order Luneburg-Kline terms would be significant when diffraction effects are also significant. Such is the case, for example, in the work of SENIOR [1965] on the sphere. Suffice it to say that the Luneburg-Kline theory is always available if needed, and it does not seem likely that any better non-diffractive theory will emerge. An exposition of this method with many examples is given by KELLER, LEWIS and SECKLER [1956].

APPENDIX C - KIRCHHOFF THEORY

In this appendix, we shall discuss an approximate method for sonar cross-section (c.s.) calculations based on Kirchhoff's approximation in the theory of optical diffraction [SCHOCH - 1950, and BOUWKAMP - 1954]. With some modifications, the theory has been extensively used in calculations of radar cross sections [RICK - 1970], and in this connection, it became known as the method of "Physical Optics". By analogy, it could have been named "Physical Acoustics" in the present context, but this term has already been preempted by another subfield of Acoustics. We shall thus use the designation "Kirchhoff Approximation" even for the modified version of the original Kirchhoff theory.

C.1 GENERAL DESCRIPTION

Kirchhoff's theory has originally been formulated for the diffraction of (scalar) light by an opening in a screen [JACKSON - 1962]. It proceeds by expressing, with the help of Green's theorem, the field at the point of observation in terms of a surface integral containing the values of the field and of its derivative on a boundary (in this case, the area of the opening in the screen). If this surface field were known, the solution at the observation point would likewise be known. Since the former is not the case, the Kirchhoff assumption is made that in the surface integral, the values of the field and of its derivative may be taken as those given by the plane incident wave. This approach, in an intuitive way, may be considered the first step in an iteration method, but there

exists very little justification for this procedure to yield convergent results. Nevertheless, in many cases and when applied judiciously, the Kirchhoff method does lead to surprisingly good results when compared with known, more exact solutions; but it may also, in other situations, give grossly wrong answers, especially if used blindly.

When applied to the sonar c. s. problem, the original Kirchhoff method must be modified due to the fact that we deal with a scattering body rather than an opening in a screen, and due to the curvature of its surface. Accordingly, in analogy to "Physical Optics", the following modifications are introduced:

(1) Tangent plane assumption: Each element of surface area is treated as a part of a plane tangent to the surface element.

(2) Modified Kirchhoff assumption: The total surface fields $p(\vec{r})|_S$ and $\vec{\nabla}p(\vec{r})|_S$ are taken as those of the incident plus the reflected wave above the (infinite) tangent plane at each surface element. In addition, the fields on the shadow side of the scatterer are set equal to zero.

These assumptions, again, are only intuitively justified. (The tangent plane assumption may only vaguely be considered to be correct for the case of wavelengths small as compared to the radii of curvature at all points of the ensonified surface). Accordingly, there is no rigorous way of gauging the accuracy of the Kirchhoff approximation. Nevertheless, it has found widespread application because of its simplicity and because, as mentioned, of its sometimes surprisingly (albeit unpredictably) good results. Its main failures seem to come from the regions of shadow boundaries in the surface integral, especially where our as-

sumption of zero field in the shadow introduces discontinuous changes of surface fields on the shadow boundaries, as will be illustrated below. Integrations up to such shadow boundaries will therefore have to be eschewed, which point we alluded to before by "judicious application" of the method.

C.2 THEORETICAL BASIS

In the following, we shall go through the mathematical steps of the Kirchhoff method in some detail.

C.2.1 FREE-SPACE GREEN'S FUNCTION; KIRCHHOFF'S IDENTITY

The Green's function $G(\vec{r},\vec{r}')$ of free space (i.e. in the absence of any boundaries) is defined to satisfy the Helmholtz equation with a unit point source located at $\vec{r}'$:

$$(\nabla^2 + k^2)\ G(\vec{r},\vec{r}') = \delta(\vec{r}-\vec{r}') \qquad \text{(C.2.1-1)}$$

The point-source δ-function is defined by

$$\delta(\vec{r}-\vec{r}') = 0 \qquad \vec{r} \neq \vec{r}';$$
$$\int f(\vec{r})\ \delta(\vec{r}-\vec{r}')\,d^3r = f(\vec{r}'). \qquad \text{(C.2.1-2)}$$

Calling

$$\vec{\rho} = \vec{r}-\vec{r}' \qquad \text{(C.2.1-3)}$$

we have the well-known expressions [MORSE - 1953] for the free-space Green's function in three dimensions:

$$G(\vec{r},\vec{r}') = \frac{-1}{4\pi\rho}\ \exp\{ik\rho\} \qquad \text{(C.2.1-4)}$$

and in two dimensions:

$$G(\vec{r},\vec{r}') = \frac{1}{4i} H_o^{(1)}(kp). \qquad \text{(C.2.1-5)}$$

In order to derive Kirchhoff's identity, we multiply Eq. (C.2.1-1) by $p(\vec{r})$; further, we multiply the free Helmholtz equation

$$(\nabla^2 + k^2)\, p(\vec{r}) = 0 \qquad \text{(C.2.1-6)}$$

by $G(\vec{r},\vec{r}')$ and subtract from the previous result, yielding

$$p(\vec{r})\nabla^2 G(\vec{r},\vec{r}') - G(\vec{r},\vec{r}')\nabla^2 p(\vec{r}) = p(\vec{r})\,\delta(\vec{r}-\vec{r}') \qquad \text{(C.2.1-7)}$$

We now integrate, $\int d^3r$, over a volume V which does not contain any sources [or else, Eq. (C.2.1-6) would not hold]. This leads to

$$\int_V [p(\vec{r})\nabla^2 G(\vec{r},\vec{r}') - G(\vec{r},\vec{r}')\nabla^2 p(\vec{r})]\, d^3r = p(\vec{r}') \qquad \text{(C.2.1-8)}$$

We use now "Green's Theorem" [JACKSON - 1962]:

$$\int_V (\phi\nabla^2\psi - \psi\nabla^2\phi)\, d^3r = \oint_S (\phi\vec{\nabla}\psi - \psi\vec{\nabla}\phi)\cdot d\vec{\Lambda} \qquad \text{(C.2.1-9)}$$

where **S** is the closed surface bounding the volume V, and

$$d\vec{\Lambda} = \hat{n}\, d\Lambda, \qquad \text{(C.2.1-10)}$$

$\hat{n}$ being the outward unit normal to S. Exchanging now the notation $\vec{r} \longleftrightarrow \vec{r}'$, and using the symmetry of $G(\vec{r},\vec{r}')$ under this operation, we get

$$p(\vec{r}) = \oint_S [p(\vec{r}')\vec{\nabla}' G(\vec{r},\vec{r}') - G(\vec{r},\vec{r}')\vec{\nabla}' p(\vec{r}')]\cdot d\vec{\Lambda}'. \qquad \text{(C.2.1-11)}$$

This equation is sometimes calles "Kirchhoff's Identity". Note it is only true if the point $\vec{r}$ lies inside S; if it were outside,

the left-hand side would be zero instead of $p(\vec{r})$ since the singularity of the δ-function is then outside of the integration volume.

Eq. (C.2.1-11) is an integral equation since the unknown pressure $p(\vec{r})$ occurs not only outside the integral, but also inside it where the values of $p(\vec{r})\big|_S$ and of $\hat{n}.\vec{\nabla}p(\vec{r})\big|_S$ have to be known. It is not possible to make this a known integral, by specifying both $p(\vec{r})$ and $\hat{n}.\vec{\nabla}p$ on the given surface S (in the sense of a boundary value problem): see, e.g., [JACKSON - 1962] who shows that for a solution of the wave (or Helmholtz) equation, specifying both p and $\hat{n}.\vec{\nabla}p$ overdetermines the problem.

C.2.2 KIRCHHOFF-RAYLEIGH INTEGRALS

We now consider a surface S on which the conditions of a soft boundary [Eq. (a-73), or Dirichlet boundary condition],

$$p(\vec{r})\big|_S = 0 \qquad \text{(C.2.2-12)}$$

or of a rigid boundary [Eq. (a-75), or Neumann boundary condition],

$$\hat{n}.\vec{\nabla}p\big|_S = 0 \qquad \text{(C.2.2-13)}$$

hold*. Both cases are recognized to give an impenetrable boundary. Inserting in Eq. (C.2.1-11), we then find the two simplified expressions

*Scattering objects of practical interest, such as submerged steel vessels, behave approximately as rigid bodies and will be treated as such. This condition is not completely satisfied, however; only for a metal object in air, e.g., would it be substantially true.

$$p(\vec{r}) = \oint_S p(\vec{r}')\vec{\nabla}'G(\vec{r},\vec{r}').\hat{n}dA', \qquad \text{rigid S} \qquad \text{(C.2.2-14)}$$

$$p(\vec{r}) = -\oint_S G(\vec{r},\vec{r}')\vec{\nabla}'p(\vec{r}').\hat{n}dA', \qquad \text{soft S} \qquad \text{(C.2.2-15)}$$

Both are still integral equations, since one of p, $\hat{n}.\vec{\nabla}p$ was prescribed on S so the other cannot be known.

Now, we specialize to an incident signal in the form of a plane wave, Eq. (C.2.2-1), i.e. the solution of the wave equation whose source is infinitely far away. Then, we may choose S as the sum of S_s, the surface of the scatterer, and of S_∞, the surface of a sphere of radius $R \to \infty$ (so that the source of the incident plane wave always remains outside S_∞). The integration volume V is hence the volume of all space <u>outside</u> the scatterer. For the surface portion S_∞, we cannot use Eqs. (C.2.2-14), (C.2.2-15) since we cannot assume S_∞ as impenetrable; hence* (for a rigid scatterer):

$$p(\vec{r}) = \int_{S_\infty} [G(\vec{r},\vec{r}')\vec{\nabla}'p(\vec{r}') - p(\vec{r}')\vec{\nabla}'G(\vec{r},\vec{r}')].\hat{n}dA' - \int_{S_s} p(\vec{r}')\vec{\nabla}'G(\vec{r},\vec{r}').\hat{n}dA'. \qquad \text{(C.2.2-16)}$$

We can decompose

$$p(\vec{r}) = p_{inc}(\vec{r}) + p_{sca}(\vec{r}) \qquad \text{(C.2.2-17)}$$

with

$$p_{inc}(\vec{r}) = P \exp\{i\vec{k}.\vec{r}\} \qquad \text{(C.2.2-18)}$$

(where the harmonic time factor exp {-iωt} is always understood).

---

*In the following we take $\hat{n}$ as the <u>outward</u> normal to S_s (and the inward normal to S_∞.)

From Eq. (a-66), one has asymptotically*:

$$p_{sca} \sim (P/r) f(\hat{r}) \exp\{ikr\} \qquad \text{(C.2.2-19)}$$

It follows from the linearity of the wave equation that Eq. (C.2.2-16) holds for p_{inc} and p_{sca} separately ("principle of linear superposition").

On S_∞, we have $\vec{r}' \to \infty$ (while the observation point $\vec{r}$ is in the finite domain), and thus need the corresponding asymptotic forms of $G(\vec{r},\vec{r}')$ and of

$$\begin{aligned} \vec{\nabla}'G(\vec{r},\vec{r}') &\equiv -(\vec{\nabla}'\rho)(d/d\rho)[\exp\{ik\rho\}/(4\pi\rho)] \\ &= (\hat{\rho}/4\pi)[(ik/\rho)-(1/\rho^2)] \exp\{ik\rho\} \end{aligned} \qquad \text{(C.2.2-20)}$$

(where $\hat{\rho} = \vec{\rho}/\rho$) in this limit. Here, $\vec{\rho} \to -\vec{r}$, $\hat{\rho} \to -\hat{r}' \equiv \hat{n}$; but the limit of ρ must be obtained in second order since ρ appears in the rapidly varying exponent:

$$\begin{aligned} \rho &= (r^2 - 2\vec{r}.\vec{r}' + r'^2)^{1/2} \\ &\to r'[1 - 2(\vec{r}.\hat{r}')/r']^{1/2} \\ &\cong r' - \vec{r}.\hat{r}' \quad . \end{aligned} \qquad \text{(C.2.2-21)}$$

We then have, asymptotically,

$$G(\vec{r},\vec{r}') \sim -(1/4\pi r') \exp\{ik(r' - \vec{r}.\hat{r}')\} \qquad \text{(C.2.2-22)}$$

and

$$\vec{\nabla}'G(\vec{r},\vec{r}') \sim (ik\hat{n}/4\pi r') \exp\{ik(r' - \vec{r}.\hat{r}')\}. \qquad \text{(C.2.2-23)}$$

First, we shall evaluate the contribution to the S_∞ integral

---

*We shall only treat the case of three dimensions here; the calculations in the two-dimensional case are quite similar.

of the p_{inc} part of p:

$$\oint_{S_\infty}^{(inc)} = \oint_{S_\infty} [G(\vec{r},\vec{r}')i\vec{k}P \exp\{i\vec{k}.\vec{r}'\} - P \exp\{i\vec{k}\ \vec{r}'\}\vec{\nabla}'G(\vec{r},\vec{r}')].\hat{n}dA' \qquad (C.2.2\text{-}24)$$

This integral being taken at $\vec{r}' \to \infty$, one may use Eqs. (C.2.2-22) and (C.2.2-23), and find by carrying out the integration in this limit:

$$\oint_{S_\infty}^{(inc)} \to P \exp\{i\vec{k}.\vec{r}\} = p_{inc}(\vec{r}), \qquad (C.2.2\text{-}25)$$

i.e. the incident wave again, which thus cancels against the $p_{inc}(\vec{r})$ part contained in $p(\vec{r})$ on the left-hand side of Eq. (C.2.2-16), leaving there only the $p_{sca}(\vec{r})$ contribution. Similarly, when calculating the contribution of p_{sca} to the S_∞ integral in Eq. (C.2.2-16), we find

$$\oint_{S_\infty}^{(sca)} = 0 \qquad (C.2.2\text{-}26)$$

so that finally, for rigid or soft bodies:

$$p_{sca}(\vec{r}) = -\oint_{S_s} p(\vec{r}')\vec{\nabla}'G(\vec{r},\vec{r}').\hat{n}dA', \quad \text{rigid } S_s \qquad (C.2.2\text{-}27)$$

$$p_{sca}(\vec{r}) = \oint_{S_s} G(\vec{r},\vec{r}')\vec{\nabla}'p\ (\vec{r}').\hat{n}dA', \quad \text{soft } S_s \qquad (C.2.2\text{-}28)$$

These equations are known as the Rayleigh-Kirchhoff formulas for the scattered pressure; they hold in exactly the same form also for two-dimensional scattering, which we state here without proof. Note that in the integrals enters the total, rather than the incident, field on the surface of the scatterer. Eqs. (C.2.2-27) and (C.2.2-28) may be considered the mathematical expression of Huygens' principle in which the Green's function $G(\vec{r},\vec{r}'$ describes

the propagation of elementary wavelets from source points on S_s to the observer located at $\vec{r}$. The equations are (exact) integral equations, no approximation having been made yet.

C.2.3 ASYMPTOTIC SCATTERED FIELD

For an observer located at $\vec{r} \to \infty$, we want to obtain the scattered field in the form

$$p_{sca} \sim (P/r) f(\hat{r}) \exp\{ikr\}, \qquad \text{3 dimensions} \qquad \text{(C.2.3-29)}$$

or

$$p_{sca} \sim (P/r^{1/2}) f(\hat{r}) \exp\{ikr\}, \qquad \text{2 dimensions} \qquad \text{(C.2.3-30)}$$

In this limit now, $\vec{r} \to \infty$ and $\vec{r}'$ remains finite. From the symmetry of $G(\vec{r},\vec{r}')$, Eqs. (C.2.2-22) and (C.2.2-23) give us the needed asymptotic forms for the three-dimensional case:

$$G(\vec{r},\vec{r}') \sim -(1/4\pi r) \exp\{ik(r - \vec{r}'.\hat{r})\} \qquad \text{(C.2.3-31)}$$

and

$$\vec{\nabla}' G(\vec{r},\vec{r}') \sim (ik\hat{r}/4\pi r) \exp\{ik(r - \vec{r}'.\hat{r})\} \qquad \text{(C.2.3-32)}$$

For cylindrical geometry, G is given by Eq. (C.2.1-5) and we may use the asymptotic limit of Eq. (2.2-19) to give us

$$G(\vec{r},\vec{r}') \sim (1/4i)(2/\pi kr)^{1/2} \exp\{i(kr - \vec{k}'.\vec{r}' - \pi/4)\}, \qquad \text{(C.2.3-33)}$$

where we also introduced $\hat{r} = \hat{k}'$, the direction of the scattered wave vector (note that $|\vec{k}'| = |\vec{k}|$). Further, we find in both two and three dimensions in the limit of $r \to \infty$:

$$\vec{\nabla}'G(\vec{r},\vec{r}') \sim -i\vec{k}'G(\vec{r},\vec{r}'). \qquad \text{(C.2.3-34)}$$

These asymptotic Green's functions may now be inserted in Eqs. (C.2.2-27) or (C.2.2-28), and by comparison with Eqs. (C.2.3-29) and (C.2.3-30), we find the scattering amplitudes (Dimensions being indicated by an index 2 or 3) for a rigid S_s:

$$f_3(\hat{r}) = -(ik/4\pi P)\oint_{S_s} \exp\{-i\vec{k}'.\vec{r}'\}(\hat{n}.\hat{k}')p(\vec{r}')dA' \qquad \text{(C.2.3-35)}$$

$$f_2(\hat{r}) = (1/P)(k/8\pi i)^{1/2}\oint_{S_s} \exp\{-i\vec{k}'.\vec{r}'\}(\hat{n}.\hat{k}')p(\vec{r}')dA' \qquad \text{(C.2.3-36)}$$

or for a soft S_s

$$f_3(\hat{r}) = -(1/4\pi P)\oint_{S_s} \exp\{-i\vec{k}'.\vec{r}'\}\hat{n}.\vec{\nabla}'p(\vec{r}')dA' \qquad \text{(C.2.3-37)}$$

$$f_2(\hat{r}) = (1/iP)(1/8\pi ik)^{1/2}\oint_{S_s} \exp\{-i\vec{k}'.\vec{r}'\}\hat{n}.\vec{\nabla}'p(\vec{r}')dA' \qquad \text{(C.2.3-38)}$$

Again, these equations for the scattering amplitudes are exact if the correct total surface field is inserted in the integrals.

If the surface S_s is neither rigid nor soft, both p and $\hat{n}.\vec{\nabla}p$ terms appear, and we have

$$f_3(\hat{r}) = (k/4\pi iP)\oint_{S_s} \exp\{-i\vec{k}'.\vec{r}'\}[\hat{k}'p(\vec{r}') - (i/k)\vec{\nabla}'p(\vec{r}')].\hat{n}dA' \qquad \text{(C.2.3-39)}$$

$$f_2(\hat{r}) = (1/P)(k/8\pi i)^{1/2}\oint_{S_s} \exp\{-i\vec{k}'.\vec{r}'\}[\hat{k}'p(\vec{r}') - (i/r)\vec{\nabla}'p(\vec{r}')].\hat{n}dA' \qquad \text{(C.2.3-40)}$$

and as before, these amplitudes are exact in the far-zone limit. Using Eqs. (a-62) or (a-69), one has the differential ("bistatic")

cross-sections

$$d\sigma/d\Omega = |f_3(\hat{r})|^2 \qquad \text{(C.2.3-41)}$$

$$d\sigma/d\phi = |f_2(\hat{r})|^2, \qquad \text{(C.2.3-42)}$$

and Eqs. (a-65), (a-72), give the expressions for the sonar c. s.'s (note that for backscattering, $\hat{k}' = -\hat{k}$):

$$\sigma = 4\pi|\{f_3(\hat{r})\}_{\hat{k}' = -\hat{k}}|^2 = 4\pi|f_3(\pi)|^2 \qquad \text{(C.2.3-43)}$$

$$\sigma = 2\pi|\{f_2(\hat{r})\}_{\hat{k}' = -\hat{k}}|^2 = 2\pi|f_2(\pi)|^2 \qquad \text{(C.2.3-44)}$$

The Kirchhoff method as will be discussed in the following, permits an evaluation of Eqs. (C.2.3-35) to (C.2.3-40) and of the sonar c. s. in an approximate fashion.

C.2.4 THE KIRCHHOFF APPROXIMATION

The assumptions on which the Kirchhoff approximation is based, have been stated in subsection C.1. The first of these, the "tangent plane assumption", considers each surface element as part of an infinite plane, and the second one (the modified Kirchhoff assumption), takes the total surface fields which are to be used in Eqs. (C.2.3-35) to (C.2.3-39) as those on the surface of this tangent plane with the appropriate boundary condition.

In order to determine the surface fields, we consider the situation shown in Fig. C.1, with $\hat{n}$ the outward normal to an infinite half-space with a plane boundary given by

$$\hat{n}.\vec{r} = 0 \qquad \text{(C.2.4-45)}$$

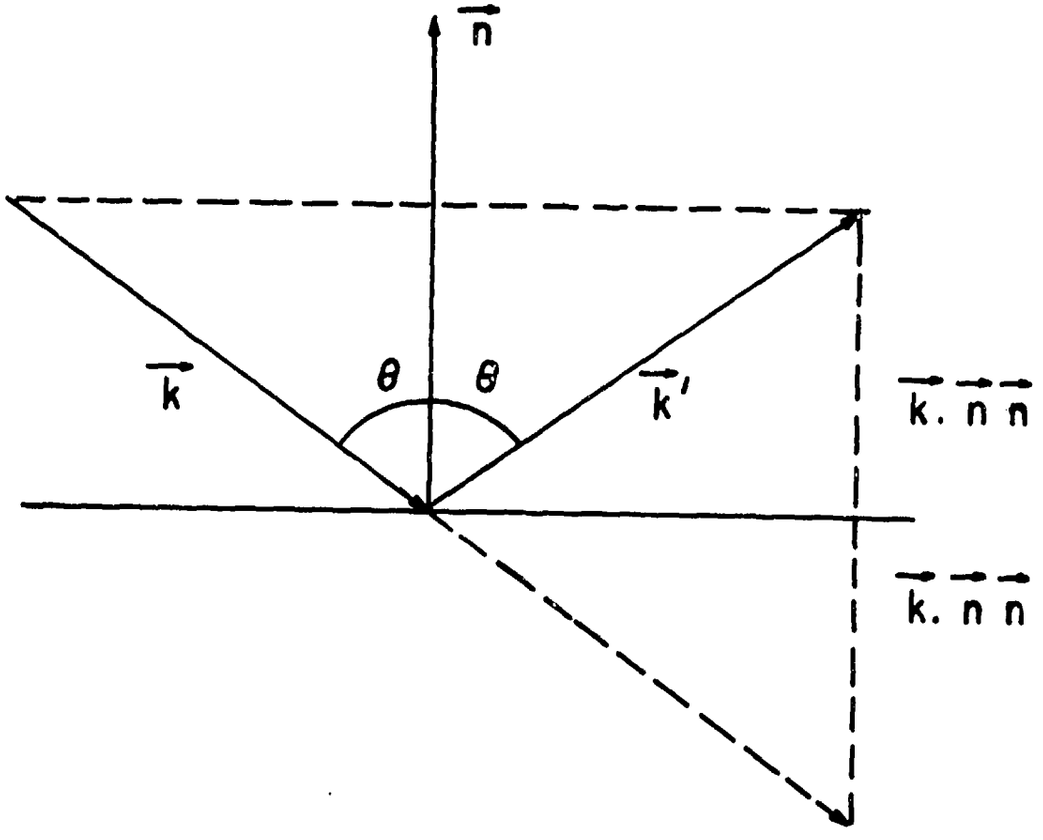

Fig. C.1

Geometry of incident and reflected wave vectors on infinite flat half space.

Above the surface, we have a plane wave

$$p_{inc} = P \exp\{i\vec{k}.\vec{r}\} \qquad \text{(C.2.4-46)}$$

incident along $\vec{k}$ at an angle θ with respect to the normal, and a reflected (scattered) wave

$$p_{ref} = \alpha P \exp\{i\vec{k}'.\vec{r}\} \qquad \text{(C.2.4-47)}$$

reflected at the same angle θ so that

$$\vec{k}' = \vec{k} - 2(\vec{k}.\hat{n})\hat{n} \qquad \text{(C.2.4-48)}$$

(with the magnitudes $k' = k$, since the frequency does not change by reflection), having a reflection coefficient α which, in general, is a function of θ. The total field

$$p_{total} = P(\exp\{i\vec{k}.\vec{r}\} + \alpha \exp\{i\vec{k}'.\vec{r}\})$$

is then, using (C.2.4-48):

$$p_{total} = P \exp\{i\vec{k}.\vec{r}\}(1 + \alpha \exp\{-2i(\vec{k}.\hat{n})\hat{n}.\vec{r}\}); \qquad \text{(C.2.4-49)}$$

it satisfies the boundary conditions of Eqs. (C.2.2-12) or (C.2.2-13). Inserting, we find that the rigid or soft surface corresponds to

$$\alpha = 1 \qquad \text{rigid S} \qquad \text{(C.2.4-50)}$$

$$\alpha = -1 \qquad \text{soft S} \qquad \text{(C.2.4-51)}$$

respectively, and the surface fields are given by

$$\text{rigid S,} \qquad p|_S = 2P \exp\{i\vec{k}.\vec{r}'\}, \quad \hat{n}.\vec{\nabla}p_{|S} = 0 \tag{C.2.4-52}$$

$$\text{soft S,} \qquad p|_S = 0, \quad \hat{n}.\vec{\nabla}p_{|S} = 2i\vec{k}.\hat{n}P \exp\{i\vec{k}.\vec{r}'\} \tag{C.2.4-53}$$

for the impenetrable plane half-space. If the surface is neither rigid nor soft, the surface fields are

$$p|_{S'} = P(1 + \alpha)\exp\{i\vec{k}.\vec{r}'\},$$

$$\hat{n}.\vec{\nabla}p_{|S'} = i\vec{k}.\hat{n}P(1 - \alpha)\exp\{i\vec{k}.\vec{r}'\} \tag{C.2.4-54}$$

where α is the appropriate reflection coefficient.

According to our assumptions, these surface fields are now used in the integrals of our expressions for the scattering amplitudes f, Eqs. (C.2.3-35) to (C.2.3-40); and furthermore, the integration is extended over the insonified surface S_{enson} of the scatterer only since we take $p \equiv 0$ on the shadow side of the scatterer. Insertion gives

$$f_3(\hat{r}) = (k/2\pi i)\int_{S_{enson}} \alpha(\vec{r}')\hat{k}'.\hat{n} \exp\{i(\vec{k}-\vec{k}').\vec{r}'\}dA' \tag{C.2.4-55}$$

$$f_2(\hat{r}) = (k/2\pi i)^{1/2}\int_{S_{enson}} \alpha(\vec{r}')\hat{k}'.\hat{n} \exp\{i(\vec{k}-\vec{k}').\vec{r}'\}dA' \tag{C.2.4-56}$$

Of special interest in our calculation of sonar c. s. is the case of backscattering, $\vec{k}' = -\vec{k}$ $(\theta=\pi)$, which leads to

$$f_3(\pi) = -(k/2\pi i)\int_{S_{enson}} \alpha(\vec{r}')\hat{k}.\hat{n} \exp\{2i\vec{k}.\vec{r}'\}dA' \tag{C.2.4-57}$$

$$f_2(\pi) = -(k/2\pi i)^{1/2}\int_{S_{enson}} \alpha(\vec{r}')\hat{k}.\hat{n} \exp\{2i\vec{k}.\vec{r}'\}dA' \tag{C.2.4-58}$$

The Kirchhoff expression of the sonar c. s. is now obtained by inserting Eqs. (C.2.4-57), (C.2.4-58) in Eqs. (C.2.3-43), (C.2.3-44) respectively.

In the following we shall discuss some conditions of applicability of the Kirchhoff method, and shall apply the latter to the calculation of the sonar c. s. of some selected bodies as an example. At this point, we shall still add some comments on geometrical interpretations of the Kirchhoff formulas.

If we take $\vec{k} \parallel z$, the integral in Eq. (C.2.4-57), for the case $\alpha = \pm 1$, may be written as

$$\int_{A_z} \exp\{2ikz\} dA_z \qquad \text{(C.2.4-59)}$$

and may be called the "equivalent flat-plate area" of the scatterer. It is obtained by taking the projection dA_z of the element dA on a plane normal to the direction of incidence, then multiplying by a phase factor $\exp\{2ikz\}$ which assigns each area element the correct phase depending on its relative distance from the source, and integrating over the entire projected area A_z.

If the equation of the surface is $z = z(x,y)$, the integral may be rewritten as

$$\int_0^L (dA_z/dz) \exp\{2ikz\} dz, \qquad \text{(C.2.4-60)}$$

which makes it the Fourier transform of dA_z/dz. This form is useful if we know the equation of the surface of the scatterer, since we may then determine A_z and dA_z/dz as functions of z. Here, L is the maximum length of the scatterer in the z-direction, and $A_z = 0$ $(z > L)$, $A_z = A_{z\,max}$ $(z < 0)$.

C.3 CONDITIONS OF APPLICABILITY

We shall here discuss the conditions of applicability of the far-zone limit $\vec{r} \to \infty$, as well as of the Kirchhoff approximation itself.

C.3.1 FAR-ZONE APPROXIMATION

The far-zone limit $\vec{r} \to \infty$ entailed certain simplifications in the form of $G(\vec{r},\vec{r}')$ and $\vec{\nabla}'G$ leading to Eqs. (C.2.3-31), (C.2.3-32). The gradient in the latter equation originally led to an expression ($\vec{\rho} = \vec{r} - \vec{r}'$):

$$(ik/\rho) + (1/\rho^2) \qquad \text{(C.3.1-61)}$$

which we approximated by the leading term, ik/ρ. This implies the inequality

$$kr >> 1 \quad \text{or} \quad r >> \lambda \qquad \text{(C.3.1-62)}$$

indicating that the far zone begins at a distance of many wavelengths.

In addition, in the exponential of G, the quantity

$$\rho = (r^2 - 2\vec{r}.\vec{r}' + r'^2)^{1/2} \qquad \text{(C.3.1-63)}$$

was approximated by $r - \hat{r}.\vec{r}'$ to obtain Eq. (C.2.3-31), while inclusion of the next-higher term would have led to

$$\exp\{ik\rho\} \cong \exp\{ik(r - \hat{r}.\vec{r}')\} \exp\{ikr'^2/2r\}, \qquad \text{(C.3.1-64)}$$

This seems to entail the condition

$$kr'^2/r << 1 \qquad \text{(C.3.1-65)}$$

Here $\vec{r}'$ is the surface coordinate vector on S_s, thus typically

some distance D of the transverse dimensions of the scatterer, implying

$$r/k >> D \qquad \text{or} \qquad r >> D^2/\lambda \tag{C.3.1-66}$$

This condition, which may be relaxed as shown below, is too stringent and would lead to the follwoing difficulties:

(a) In the "Fraunhofer Region" defined by

$$r >> D \tag{C.3.1-67}$$

(which is the far-zone limit in which our sonar c. s. is obtained), Eq. (C.3.1-66) could be satisfied for $D \lesssim \lambda$, but not for $D >> \lambda$ or $kD >> 1$, i.e., no high-frequency (or short-wavelength) approximation were possible (unless $r >>> D$). As will be seen below, the Kirchhoff approximation is intrinsically a high-frequency approximation, however.

(b) In the "Fresnel Region" defined by

$$r \gtrsim D \tag{C.3.1-68}$$

(which would be the case e.g. for the two-dimensional situation of an infinite cylinder), Eq. (C.3.1-66) could be satisfied only for $D << \lambda$ or $kD << 1$, i.e. only in the low-frequency (or long wavelength) approximation.

Fortunately, Eq. (C.3.1-65), (C.3.1-66) are not true restrictions, as seen using the concept of "Fresnel zones". The rightmost exponential in Eq. (C.3.1-61), neglected in our far-field Green's functions, alternates in phase for

$$kr'^2/2r = 0, \pi, 2\pi \ldots, \tag{C.3.1-69}$$

i.e. for

$$r' = (n\lambda r)^{1/2} \qquad \text{(C.3.1-70)}$$

which is called the nth Fresnel zone on the surface of the scatterer. The sign changes of this phase factor make the $n \geq 1$ contributions to the Kirchhoff integral effectively cancel out, so that most of the contribution comes solely from the first Fresnel zone. Thus, the effective distance parameter in Eq. (C.3.1-66) is not D but $D' = (\lambda r)^{1/2}$, and insertion of D' makes Eq. (C.3.1-66) essentially an identity, so that it no longer constitutes a restrictive condition, and Eq. (C.3.1-62) remains solely to be satisfied.

C.3.2 CONDITIONS FOR THE KIRCHHOFF APPROXIMATION

As stated in Subsection C.1, there exist no clearcut conditions of applicability of the Kirchhoff method. As for the tangent plane assumption, it seems intuitively clear that for it to hold it is necessary (although perhaps not sufficient) that at each insonified surface point, we have

$$kR_i >> 1 \qquad \text{(C.3.2-71)}$$

where R_i are the radii of curvature of the surface at that point; i.e., the curvature should be gentle, and be considerable over a distance of many wavelengths only; otherwise, the surface fields will not resemble those over a flat plane. Since R_i are quantities comparable to the scatterer's dimensions [at least the transverse dimensions D, in consideration of Eq. (C.2.4-59)], we also have

$$\lambda << D \quad \text{or} \quad kD >> 1 \qquad \text{(C.3.2-72)}$$

This shows that intrinsically, the Kirchhoff method is a high-frequency approximation. Note that Eq. (C.3.2-71) does not allow, in principle, that the scatterer have sharp edges, corners, or tips; it must be a smooth, gently curved object. The body may also not have any abrupt terminations (such as the edges of a plate of finite dimensions): the surface field close to these will simply not resemble that on an infinite surface.

An abrupt change of the assumed surface field also occurs at the shadow boundary

$$\vec{k}.\vec{n} = 0 \qquad \text{(C.3.2-73)}$$

of the body, since the field is taken as nonvanishing on the ensonified surface, and as identically zero in the shadow. In fact, however, the transition is steady over a penumbra region; and since the width of the latter decreases with decreasing wavelength, we are intuitively led back to the condition of Eq. (C.3.2-72). Quantitatively, the decay of the surface field in the penumbra region is caused by the creeping waves discussed in subsection 2.2.2.2, with an azimuthal decay region given by Φ_ℓ of Eq. (2.2-85), i.e. essentially by $(kD)^{-1/3}$. Thus, our assumption of an abrupt field change to zero into the shadow is only warrented if

$$(kD)^{1/3} >> 1 \qquad \text{or} \qquad \lambda^{1/3} >> D^{1/3} \qquad \text{(C.3.2-74)}$$

This is more stringent than Eq. (C.3.2-72), since it implies

$$kD >>> 1 \qquad \text{or} \qquad \lambda <<< D \qquad \text{(C.3.2-75)}$$

Thus, if the situation is such that a shadow boundary contribution enters in the Kirchhoff integral in an essential way, the latter

is a valid approximation only in the extreme high-frequency limit (in which the Kirchhoff result essentially gives us no more than the geometric-acoustic result). The only other contribution to the Kirchhoff integral as discussed above, is essentially that from the first Fresnel zone, i.e. from the point of specular reflection (cf. Figure 2.2-3). From what was said above, it stands to reason that if the Kirchhoff approximation is used only for a calculation of the specular return* (not including the reflections from the shadow boundary), the corresponding results may have some validity also in the usual high-frequency limit, i.e., comprising several terms in an expression in inverse powers of kD, without obliging us to adopt the extreme high frequency limit in which all these terms except the lowest (geometric-acoustic) one have to be discarded.

C.4 APPLICATIONS AND COMPARISONS WITH EXACT RESULTS

In this subsection, we shall consider various examples of the application of Kirchhoff's approximation, and shall obtain the sonar c. s.'s for a number of selected scatterers using this method of calculation.

C.4.1 KIRCHHOFF CROSS SECTION OF THE SPHERE

The three-dimensional backscattering amplitude of a rigid or soft body is obtained from Eq. (C.2.4-57) as

$$f(\pi) = \pm(ik/2\pi)\int_{\text{Senson}} \hat{k}.\hat{n}\, \exp\{2i\vec{k}.\vec{r}'\}dA', \qquad \text{(C.4.1-76)}$$

the upper sign corresponding to a rigid, the lower to a soft boun-

*This point will be illustrated later on in Appendix C.

dary. We shall take the plane wave to be incident along the z' axis from $-\infty$, i.e. $\vec{k} || \hat{z}'$. With a polar angle θ and an azimuth ϕ, one has for a sphere of radius a (Fig. C.2)

$$\vec{k}.\vec{r}' = ka\cos\theta \qquad \text{(C.4.1-77)}$$

$$d\Lambda' = a^2 \sin\theta \, d\theta \, d\phi \qquad \text{(C.4.1-78)}$$

$$\hat{k}.\hat{n} = \cos\theta \qquad \text{(C.4.1-79)}$$

With $\cos\theta = \mu$, this gives

$$f(\pi) = \pm ika^2 \int_{-1}^{0} \mu \exp\{2ika\mu\} d\mu \qquad \text{(C.4.1-80)}$$

where $\mu = 0$ corresponds to the shadow boundary (equator), and $\mu = -1$ to the vertex (south pole) that gives the specular reflection. The integral can be obtained analytically, so that

$$f(\pi) = f_{sp.r}(\pi) + f_{sh.b}(\pi) \qquad \text{(C.4.1-81)}$$

separating the part corresponding to specialr reflection (sp. r., $\mu = -1$) from the one corresponding to reflection by the shadow boundary (sh. b., $\mu = 0$). These are, respectively,

$$f_{sp.r.}(\pi) = \pm(1/4ik)(1+2ika)\exp\{-2ika\}$$
$$= \pm(a/2)\{\cos\beta - (\sin\beta/\beta) - i[\sin\beta + (\cos\beta/\beta)]\} \qquad \text{(C.4.1-82)}$$

where we called $\beta = 2ka$, and

$$f_{sh.b.}(\pi) = \pm(a/2)(i/\beta). \qquad \text{(C.4.1-83)}$$

The sonar c.s. $\sigma = 4\pi|f(\pi)|^2$ is then

$$\sigma = \pi a^2\{[1 + (1/\beta^2)] - 2[(\sin\beta/\beta) + (\cos\beta/\beta^2)] + (1/\beta^2)\} \qquad \text{(C.4.1-84)}$$

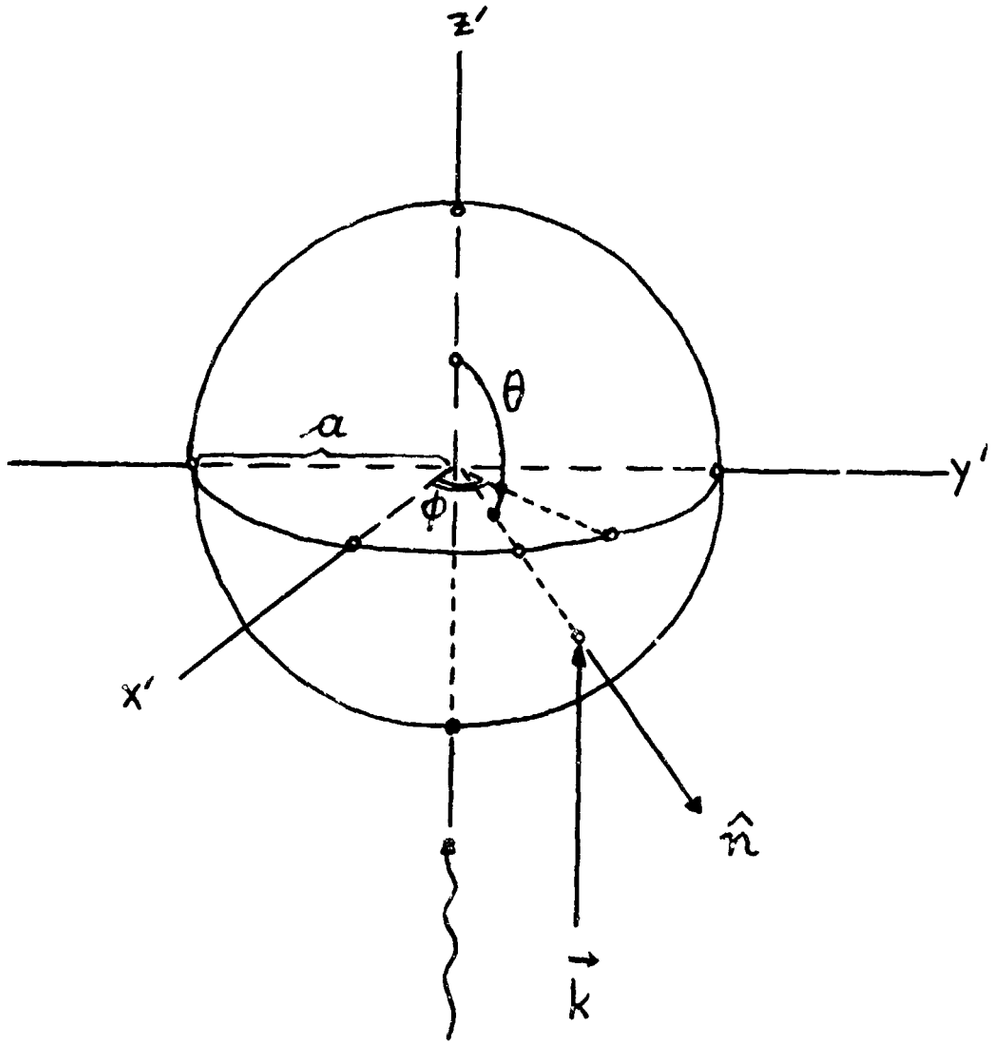

Fig. C.2

Geometry of sound scattering from a sphere.

where the first two terms correspond to the specular reflection (squared), the third term to the specular and shadow boundary interference, and the last term to the shadow boundary reflection. The geometrical-acoustics cross section being

$$\sigma_{GA} = \pi a^2 \qquad \text{(C.4.1-85)}$$

one has for the Kirchhoff sonar c. s. of both the rigid and soft sphere:

$$\sigma_{KIR}/\sigma_{GA} = 1 + 1/[2(ka)^2] - (\sin 2ka)/ka - (\cos 2ka)/[2(ka)^2], \qquad \text{(C.4.1-36)}$$

as obtained by a straight forward application of the Kirchhoff approximation.

In Fig. C.3, we compare the Kirchhoff result of Eq. (C.4.1-86) for both the rigid and soft sphere, plotted as a dot-dashed curve [NEUBAUER - 1963], with the sonar c. s. for a soft and for a rigid sphere [BOWMAN - 1969]; these differ greatly from each other and from the Kirchhoff result. The reason for this is the following: as shown in Section 2.2.2.2 for the cylinder (and similar for the sphere), the sonar c. s. consists of the coherent superposition of a geometrically reflected contribution and of the contribution of creeping waves that encircle the body and re-emerge again, interfering with the reflected wave. As mentioned there, the creeping wave strength is considerable for rigid bodies, giving rise to a strong interference pattern as seen in Figure C.3. For soft bodies, the creeping waves are highly attenuated and thus weak as they re-emerge, giving rise only to small wiggles in the exact curve. The Kirchhoff approximation, however, consists of an interference be-

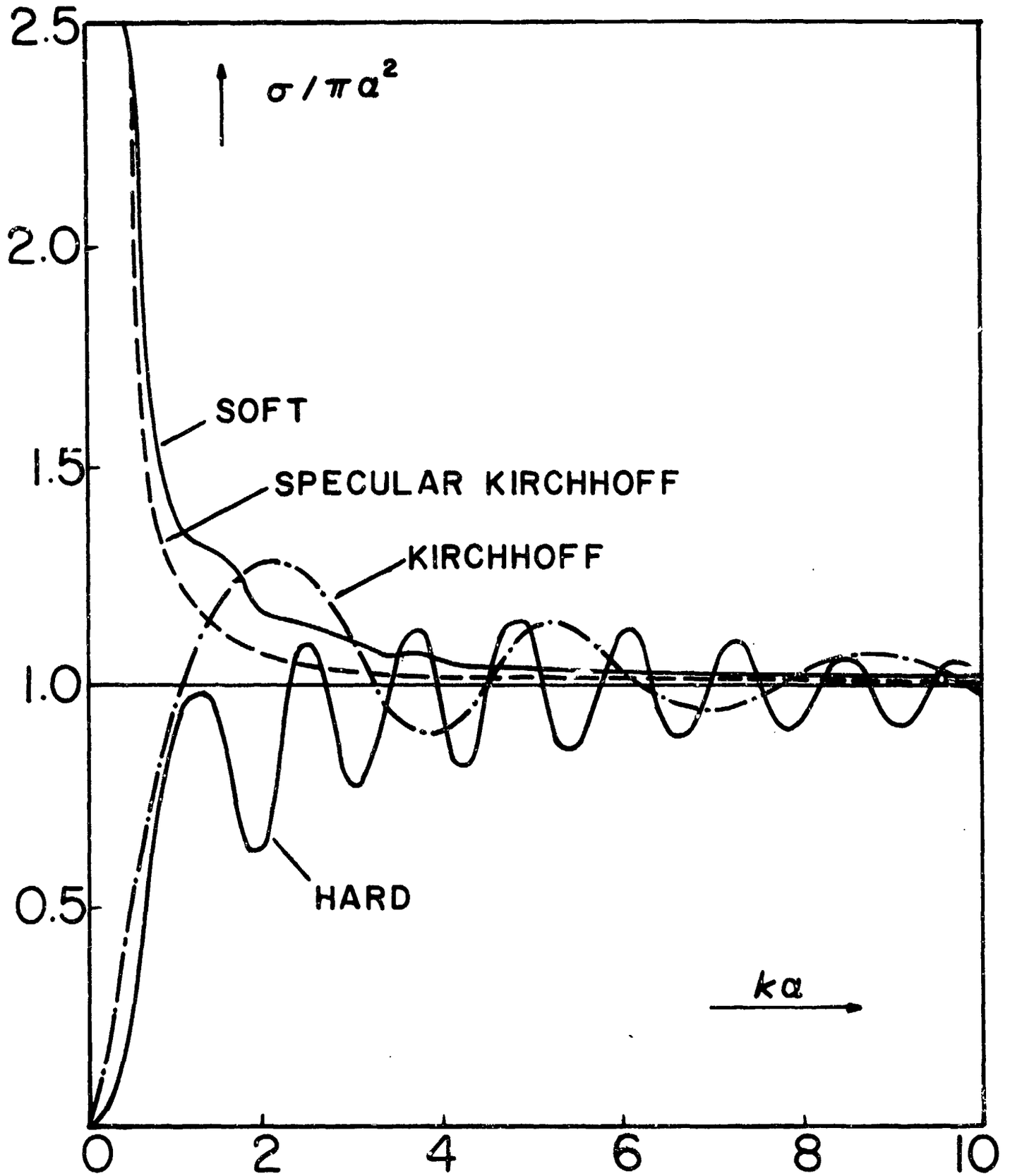

Fig. C.3 Sonar cross section for hard and soft sphere, and the Kirchhoff result, plotted vs. ka.

tween the geometrical-reflected wave and a reflection contribution from the shadow boundary, causing an interference pattern completely different from the actual situation.

This suggests that this reflection from the shadow boundary is a completely spurious effect that renders the straightforward Kirchhoff result invalid. In fact, as mentioned earlier, the sharp shadow boundary assumption in this approximation is incorrect except in the limit where there are no creeping waves, $(ka)^{1/3} >> 1$. Therefore, the terms in Eq. (C.4.1-86) that involve shadow boundary contributions,

$$\sigma_{KIR}^{sh.b}/\pi a^2 = 1/[4(ka)^2] - (\sin 2ka)/ka - \cos 2ka/[2(ka)^2] \qquad (C.4.1\text{-}87)$$

are correct only in the limit $ka >>> 1$, in which $\sigma_{KIR}^{sh.b} \to 0$; i.e., if it's nonvanishing, it's wrong. Note, however, that no such condition is violated in the specular reflection contribution,

$$\sigma_{KIR}^{sp.r}/\pi a^2 = 1 + 1/[4(ka)]^2 \qquad (C.4.1\text{-}88)$$

since no abrupt field change occurs at the specualr point. Thus, Eq. (C.4.1-83) is expected to be correct, including the term with $(ka)^{-2}$. In fact, when plotted in Figure C.3 (dashed curve), the specular-Kirchhoff sonar c. s. resembles that of the soft sphere, which latter is mainly specular with small creeping-wave contributions only. It is suggestive, therefore, that the Kirchhoff method be modified so as to disregard any shadow boundary contributions, and to retain the specular-reflection contributions only in order to furnish more reliable results. This point will be considered again later on in this subsection.

C.4.2 KIRCHHOFF CROSS SECTION OF THE INFINITE CIRCULAR CYLINDER

The two-dimensional backscattering amplitude of a rigid (upper sign) or soft body (lower sign) is obtained from Eq. (C.2.4-58) as

$$f(\pi) = \mp(k/2\pi i)^{1/2}\int_{S_{enson}} \hat{k}.\hat{n}\, \exp\{2i\vec{k}.\vec{r}'\}d\Lambda' \qquad (C.4.2\text{-}89)$$

The plane wave shall be incident along the -x' axis coming from $+\infty$ ($\vec{k}||-x'$). With an azimuth θ, one has (see Fig. C.4)

$$\vec{k}.\vec{r}' = -ka\cos\theta \qquad (C.4.2\text{-}90)$$

$$d\Lambda' = a\, d\theta \text{ (per unit length } ||z') \qquad (C.4.2\text{-}91)$$

$$\hat{k}.\hat{n} = -\cos\theta \qquad (C.4.2\text{-}92)$$

This gives

$$f(\pi) = \pm(a/2i)^{1/2}\, J(2ka) \qquad (C.4.2\text{-}93)$$

where

$$J(z) = (2z/\pi)^{1/2}\int_0^{\pi/2}\cos\theta\, \exp\{-zi\,\cos\theta\}d\theta \qquad (C.4.2\text{-}94)$$

Here, $\theta = 0$ is the specular point and $\theta = \pi/2$ the shadow boundary. The sonar c. s. $\sigma = 2\pi|f(\pi)|^2$ is then simply

$$\sigma_{KIR}/\sigma_{GA} = |J(2ka)|^2, \qquad (C.4.2\text{-}95)$$

using the sonar c. s. of geometrical acoustics,

$$\sigma_{GA} = \pi a. \qquad (C.4.2\text{-}96)$$

Using the mehtods introduced later on (C.5.2), it can be shown that

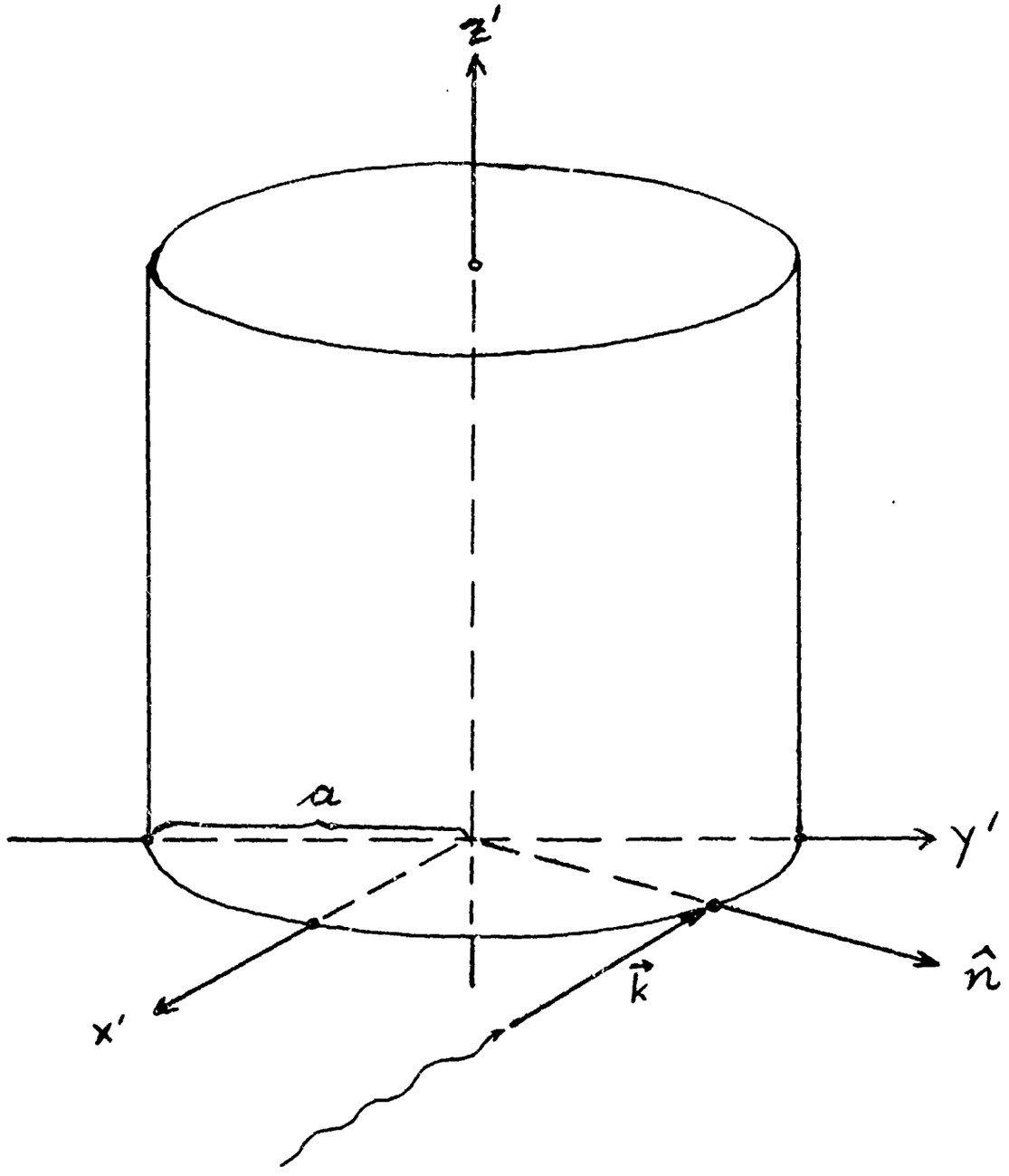

Fig. C.4

Geometry of two-dimensional sound scattering from an infinite cylinder.

$$\lim_{z\to\infty} |J(z)| = 1 \qquad \text{(C.4.2-97)}$$

so that this limit

$$\lim_{ka\to\infty} \sigma_{KIR} = \sigma_{GA} \qquad \text{(C.4.2-98)}$$

i.e. for high frequencies, the Kirchhoff result tends toward the geometrical-acoustics sonar c. s. As a function of ka, σ_{KIR} is plotted in Fig. 2.2.4 and is compared there with the exact result for the rigid cylinder. The same remarks that were made for the sphere apply to this comparison also.

C.4.3 KIRCHHOFF CROSS SECTION OF A FINITE RECTANGULAR FLAT PLATE

Consider a rectangular flat plate in the xy plane, centered at the origin, and of dimensions 2a||x and 2b||y. The incident wave vector is taken to point toward the origin along the straight line of direction (θ,ϕ). One then has Eq. (C.4.1-76) for the backscattering amplitude, with (see Fig. C.5)

$$\vec{k}.\vec{r}' = -k(x' \sin\theta \cos\phi + y' \sin\theta \sin\phi) + z'\cos\theta \qquad \text{(C.4.3-99)}$$

$$dA' = dx'\, dy' \qquad \text{(C.4.3-100)}$$

$$\hat{k}.\hat{n} = -\cos\theta \qquad \text{(C.4.3-101)}$$

The integration is elementary, and if one uses the definition of the spherical Bessel function of zero order,

$$j_0(z) = (\sin z)/z \qquad \text{(C.4.3-102)}$$

one finds for the backscattering amplitude:

$$f(\pi) = \mp(2kiab \cos\theta/\pi)\, j_0(2ka \sin\theta \cos\phi) \times j_0(2kb \sin\theta \sin\phi) \qquad \text{(C.4.3-103)}$$

The geometrical area is σ_{geo} (note, this is not σ_{GA})

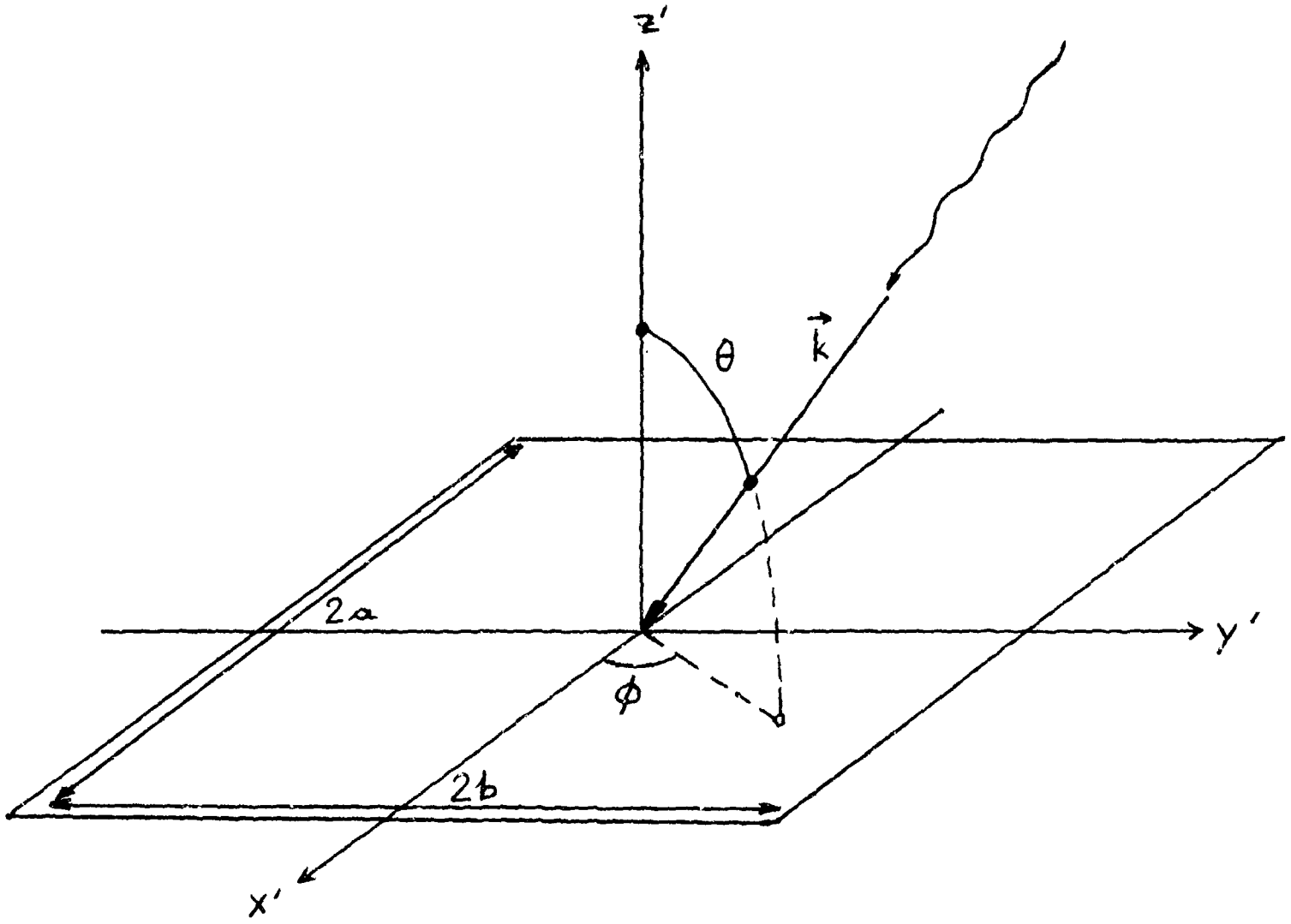

Fig. C.5

Geometry of sound scattering from a flat rectangular plate.

$$\sigma_{geo} = 4ab \qquad \text{(C.4.3-104)}$$

leading to the Kirchhoff cross section

$$\sigma_{KIR}/\sigma_{geo} = (4ab/\pi)[k \cos\theta \; j_0(2ka \sin\theta \cos\phi) \times j_0(2kb \sin\theta \sin\phi)]^2 \qquad \text{(C.4.3-105)}$$

It is seen from the integration that this result consists entirely of edge contributions. Indeed, there is no specular backscattering contribution except at normal incidence. Since at a sharp edge, our condition of applicability of the Kirchhoff approximation, Eq. (C.3.2-71), is never satisfied, the value of Eq. (C.4.3-105) is not a priori clear. It may be seen, however, that here as well as in other cases where there is no geometric-acoustics contribution to the sonar cross section (for example for the cone), the Kirchhoff result, coming entirely from edges or tips, nevertheless leads to surprisingly good results, although its conditions of applicability seem to be violated here. This is shown in Fig. C.6 where we plot the sonar cross section normalized to the area (in the db scale) for a square plate of dimensions $2a = 2b = 20\lambda$ versus the aspect angle θ (setting $\phi = 0$). The Kirchhoff approximation result (dashed curve) is seen to agree quite well up to angles $\theta \lesssim 45°$ with the exact result (solid curve) which was obtained by a numerical solution of the Kirchhoff-Rayleigh integral equation, Eq. (C.2.2-27), as well as with the results (points) of Keller's geometrical theory of diffraction, to be discussed in Appendix D [ROSS - 1966]. The agreement is almost perfect for small angles of incidence, $\theta \leq 27°$. An explanation for the good quality of the Kirchhoff result lies in the fact that if the scattering amplitude is obtained from an integration over the

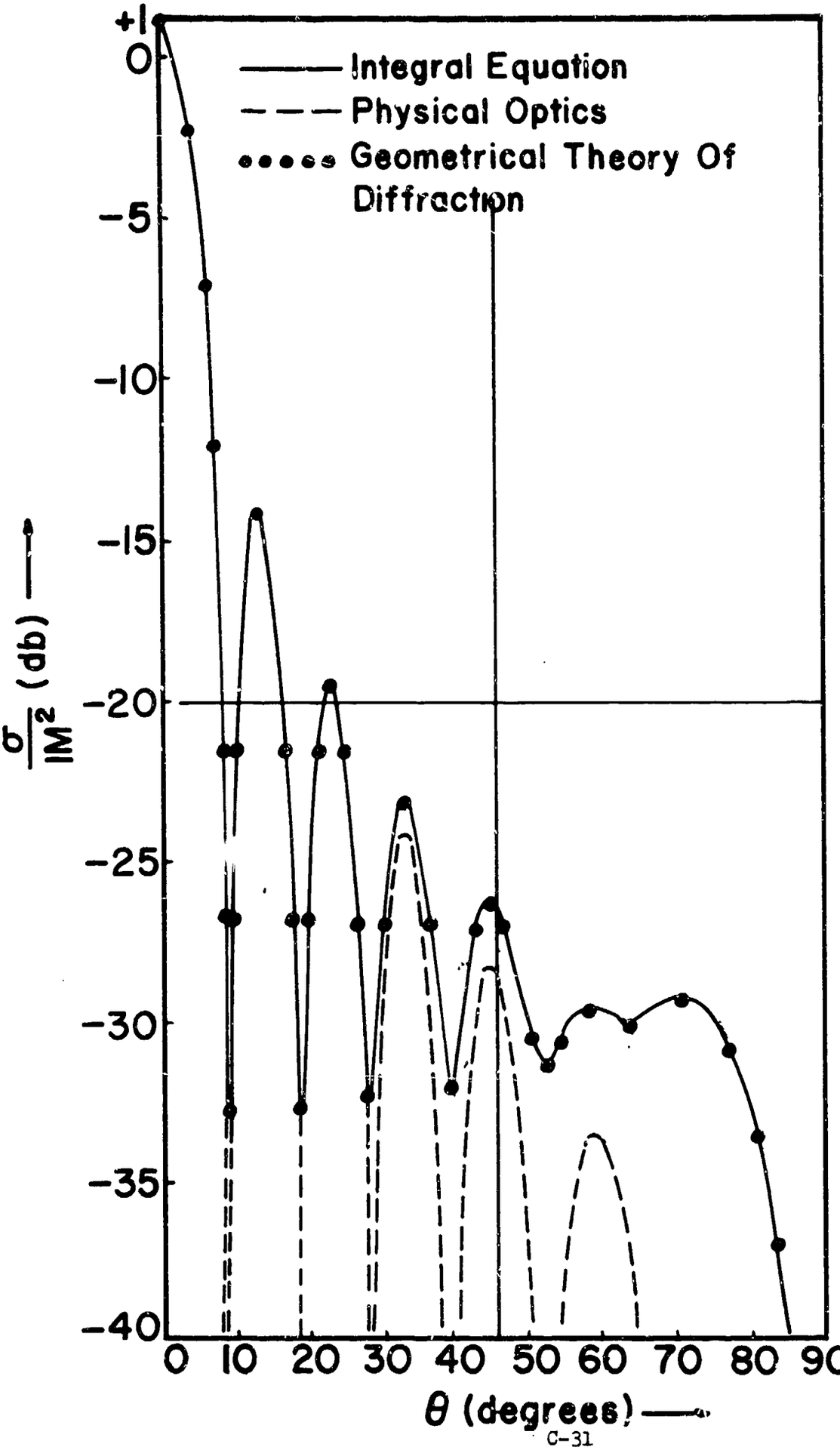

Fig. C.6

Normalized sonar cross section for a rigid square flat plate of dimension 20λ, given by exact theory (solid curve) and Keller's theory (points), plotted versus aspect angle θ.

surface pressure such as in Eq. (C.2.3-35), then, although $p(\vec{r}')$ deviates from the expression Eq. (C.2.4-52) used in the Kirchhoff approximation in the vicinity of the edges, the near-edge pressure does not furnish an important contribution to the total integral. This remark also points out a way for improving the Kirchhoff result wherever it goes wrong: in this case, this would consist in employing the exact surface pressure $p(\vec{r}')$ as found e.g. from Sommerfeld's exact edge solution, in the near-edge region of the Kirchhoff integral. Such an approach has been used by [UFINTSEV - 1962] for improving the Kirchhoff solution. Another approach, for the case that specular reflection contributions are present, will be pointed out later on in this Appendix.

C.4.4 KIRCHHOFF CROSS SECTION FOR A FINITE CYLINDER

We consider a finite circular cylinder of length 2ℓ and radius a, oriented with its axis $||$ z'. The incident wave vector $\vec{k}$ is taken as pointing towards the origin along a straight line in the x'z' plane, which makes an angle θ with the z' axis (for discussion's sake, we consider $\theta < \pi/2$). The contribution to the (three-dimensional) Kirchhoff amplitude, Eq. (C.4.1-76), then has two parts, coming from the circular top end, and from the illuminated portion of the side of the cylinder. We shall consider them one at a time.

(a) Top contribution. With an azimuthal variable φ, we have here (see Fig. C.7)

$$\vec{k}.\vec{r}' = -k(r\sin\theta\cos\varphi + \ell\cos\theta) \qquad \text{(C.4.4-106)}$$

$$d\Lambda' = r\,dr\,d\varphi \qquad \text{(C.4.4-107)}$$

$$\hat{k}.\hat{n} = -\cos\theta \qquad \text{(C.4.4-108)}$$

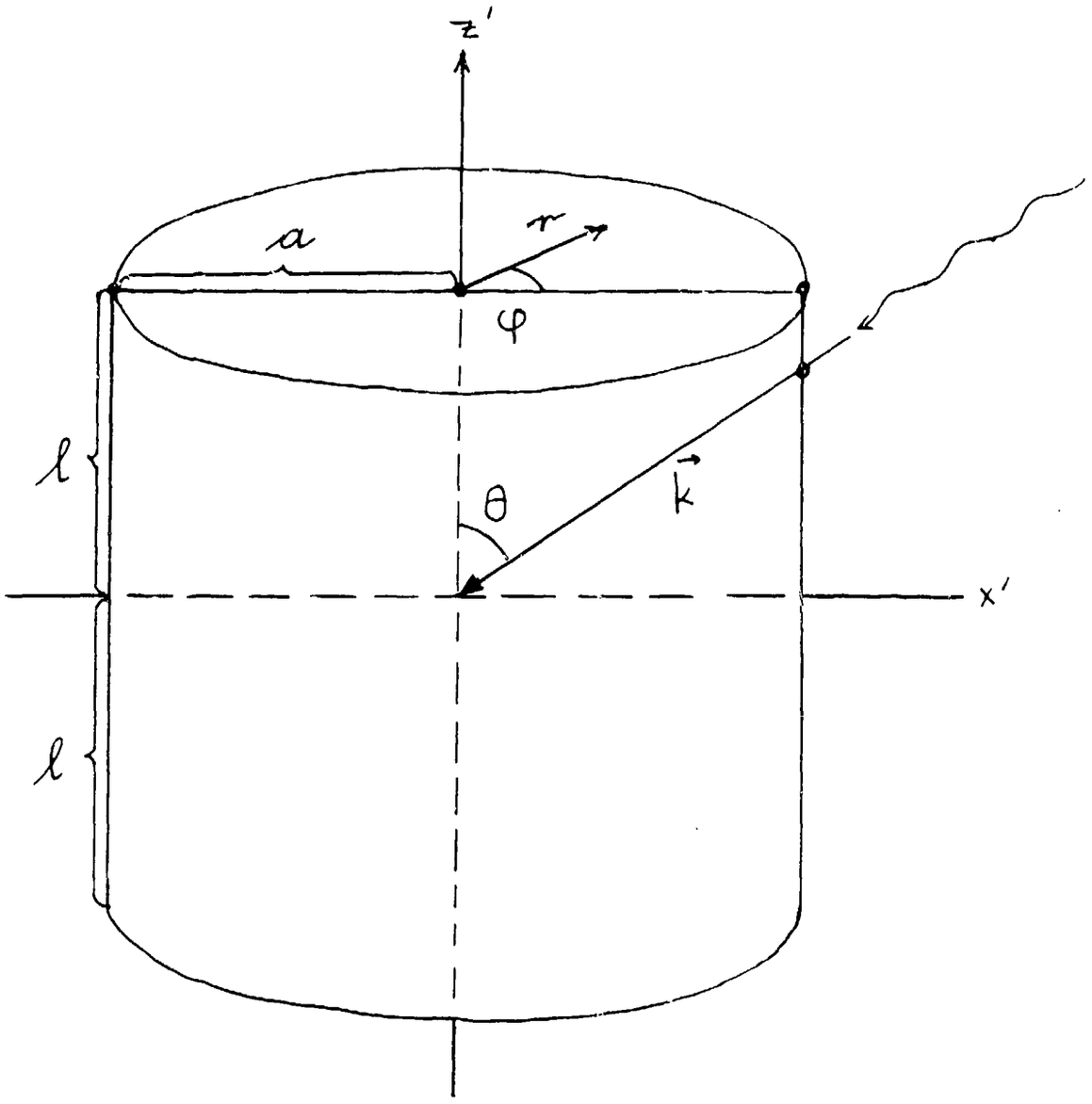

Fig. C.7

Geometry of three-dimensional sound scattering from a finite cylinder.

where r is a cylindrical radius coordinate. Using the Bessel function formulas

$$2\pi\, J_m(z) = i^m \int_0^{2\pi} \exp\{-iz\cos\varphi - im\varphi\}\, d\varphi \qquad \text{(C.4.4-109)}$$

$$\int z\, J_0(z)\, dz = z\, J_1(z) \qquad \text{(C.4.4-110)}$$

we find the amplitude

$$f_{top}(\pi) = \mp (ik/2) a^2 \cos\theta \exp\{-2ik\ell\cos\theta\} \times [J_1(2ka\sin\theta)/ka\sin\theta] \qquad \text{(C.4.4-111)}$$

which for $\ell \to 0$ also represents the backscattering amplitude for a circular flat disc. The case $\theta = 0$ may be obtained using the limit

$$\lim_{z\to 0} [J_1(z)/(z/2)] = 1 \qquad \text{(C.4.4-112)}$$

(b) Side contribution. Here

$$\vec{K}\cdot\vec{r}' = -k(a\sin\theta\cos\varphi + z\cos\theta) \qquad \text{(C.4.4-113)}$$

$$d\Lambda' = a\, d\varphi\, dz \qquad \text{(C.4.4-114)}$$

$$\hat{k}\cdot\hat{n} = -\sin\theta\cos\varphi \qquad \text{(C.4.4-115)}$$

Integration leads to the amplitude

$$f_{side}(\pi) = \mp (2i/\pi) ka\ell \sin\theta\, j_0(2k\ell\cos\theta) \times (\pi/4ka\sin\theta)^{1/2} J(2ka\sin\theta) \qquad \text{(C.4.4-116)}$$

where j_0 in the zero order spherical Bessel function, and using also the function J(z) defined in Eq. (C.4.2-94).

The total amplitude is given by

$$f(\pi) = \mp ika\{(a/2)\cos\theta \exp\{-2ik\ell\cos\theta\}$$
$$\times [J_1(2ka\sin\theta)/ka\sin\theta] + (2/\pi)\ell\sin\theta$$
$$\times j_0(2k\ell\cos\theta)(\pi/4ka\sin\theta)^{1/2} J(2ka\sin\theta)\} \quad \text{(C.4.4-117)}$$

its two contributions interfere in the sonar cross section,

$$\sigma = 4\pi(ka)^2|\{...\}|^2 \quad \text{(C.4.4-118)}$$

Limiting cases of this expression are as follows

(i) Axial aspect ($\theta=0$):

$$f_{ax}(\pi) = \mp(ik/2)a^2 \exp\{-2ik\ell\} \quad \text{(C.4.4-119)}$$
$$\sigma_{ax}/(\pi a^2) = (ka)^2 \quad \text{(C.4.4-120)}$$

(ii) Broadside aspect ($\theta=\pi/2$):

$$f_{br}(\pi) = \mp ika(2\ell/\pi)(\pi/4ka)^{1/2} J(2ka) \quad \text{(C.4.4-121)}$$
$$\sigma_{br} = ka[2\ell J(2ka)]^2 \quad \text{(C.4.4-122)}$$

In the high-frequency limit, using Eq. (C.4.2-97) this becomes

$$\lim_{ka\to\infty} \sigma_{br} = ka(2\ell)^2. \quad \text{(C.4.4-123)}$$

C.4.5 KIRCHHOFF CROSS SECTION FOR A FINITE CONE

We consider a finite cone of height h, and opening angle θ_0, with its tip at the origin, and its axis along the negative z-axis. The incident wave vector $\vec{k}$ points towards the origin (see Fig. C.8) making an angle θ with the positive z axis. We take both $\theta_0 < \pi/2$ and $\theta < \pi/2$. Note that for $\theta < \theta_0$, all of the cone is ensonified so that the azimuth in the Kirchhoff integral of Eq. (C.4.1-76) is $0 \le \varphi \le 2\pi$; but that for $\theta_0 < \theta < \pi/2$, there exists a shadow boundary $\hat{n}.\vec{k} = 0$ on the cone surface given by $\cos\varphi_s = -\tan\theta_0 \cot\theta$, so

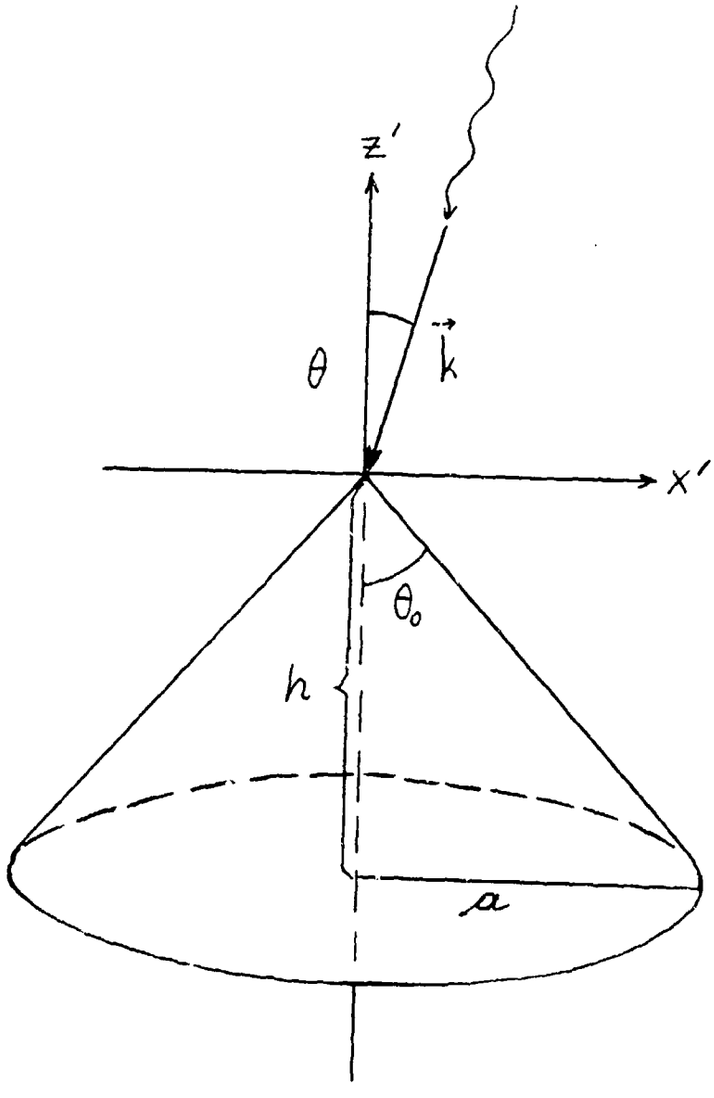

Fig. C.8

Geometry of sound scattering from a finite cone.

that the azimuthal limits are

$$0 \leq \varphi \leq \begin{cases} 2\pi & \theta < \theta_0 \\ \varphi_s & \theta < \theta_0 \end{cases} \qquad \text{(C.4.5-124)}$$

We find now

$$\vec{k}.\vec{r}' = -kr(\sin\theta \sin\theta_0 \cos\varphi - \cos\theta \cos\theta_0) \qquad \text{(C.4.5-125)}$$

$$d\Lambda' = r\, dr \sin\theta_0\, d\varphi \qquad \text{(C.4.5-126)}$$

$$\hat{k}.\hat{n} = -[\sin\theta \cos\theta_0 \cos\varphi + \cos\theta \sin\theta_0] \qquad \text{(C.4.5-127)}$$

Calling the radius of the basis circle

$$a = h \tan\theta_0 \qquad \text{(C.4.5-128)}$$

we find for the case of steep incidence ($\theta < \theta_0$) an integral expression for the amplitude using Eq. (C.4.4-109):

$$f(\pi) = \mp ik \sin\theta_0 [\cos\theta \sin\theta_0 \int_0^{a/\sin\theta_0} r dr\, J_0(2kr' \sin\theta \sin\theta_0) \times \exp\{2ikr \cos\theta \cos\theta_0\} - i \sin\theta \cos\theta_0 \int_0^{a/\sin\theta_0} r dr \times J_1(2kr \sin\theta \sin\theta_0) \exp\{2ikr \cos\theta \cos\theta_0\}]. \qquad \text{(C.4.5-129)}$$

For the case $\theta_0 \to \pi/2$, this goes over into the amplitude for scattering from a circular disc, contained in Eq. (C.4.4-111).

Specializing now to the case of axial incidence, $\theta = 0$, we can carry out the integrals and find

$$f_{ax}(\pi) = \pm(\tan^2\theta_0/4ik)[1 - (1 - 2ika \cot\theta_0) \times \exp\{2ika \cot\theta_0\}] \qquad \text{(C.4.5-130)}$$

Of the expression in square brackets, the term 1 represents the contribution from the tip, and the remaining terms the contribution from the base of the cone.

C.4.6 KIRCHHOFF CROSS SECTION FOR AN INFINITE CONE

For an infinite cone, the base radius $a \to \infty$ and the base contribution of the amplitude of Eq. (C.4.5-130) seems to diverge linearly. It may be argued, however, that in the contrary, this contribution actually vanishes, by invoking the "principle of differential absorption": due to the absorption in the medium, the propagation constant has always a small imaginary part, i.e.

$$k \to k + i\varepsilon, \qquad \varepsilon > 0 \tag{C.4.6-131}$$

The factor $\exp\{-2i\varepsilon a \cot\theta_0\}$ indeed makes then the base contribution vanish if the base recedes to infinity. The Kirchhoff amplitude for axial incidence on an infinite cone then becomes

$$f_{ax}^{\infty}(\pi) = \pm\tan^2\theta_0/(4ik), \tag{C.4.6-132}$$

and the cross section is

$$\sigma_{ax}^{\infty} = \pi \tan^4\theta_0/(4k^2). \tag{C.4.6-133}$$

This also holds for a cone that is so long that its base contribution is negligible.

We now consider the case of near-axial incidence for a long cone (so that we retain the tip contribution only). Eq. (C.4.5-129) then contains the integrals

$$\int_0^{\Lambda} x\,dx\, J_p(x) \exp\{i\beta x\}, \qquad p = 0, 1 \tag{C.4.6-134}$$

with

$$\Lambda = 2ka \sin\theta \tag{C.4.6-135}$$

and

$$\beta = \cot\theta \cot\theta_0 \qquad \text{(C.4.6-136)}$$

which may be integrated by parts to yield a series in powers of $(1/\beta)$, always neglecting the base contribution. The series converges asymptotically if $\beta << 1$, i.e. if $\tan\theta \tan\theta_0 << 1$ (note we always assume $\theta < \theta_0$). We then get the amplitude.

$$f^{\infty}(\pi) = \pm\frac{\tan^2\theta_0}{4ik\cos\theta}\{1 + \mathcal{O}(\tan\theta_0 \tan\theta)\}, \qquad \text{(C.4.6-137)}$$

which is valid either for $\theta_0 << 1$ (i.e., a cone of small opening angle) and $\theta < \theta_0$, or for $\theta << 1$ (i.e., near-axial incidence) and any θ_0 not too close to $\pi/2$. The corresponding cross section is

$$\sigma^{\infty} = \pi\tan^4\theta_0/(2k\cos\theta)^2 \qquad \text{(C.4.6-138)}$$

Considering now the case of a finite cone (i.e. retaining the base contribution) with axial incidence, we get the following cross section from Eq. (C.4.5-130):

$$\sigma_{ax} = \sigma_{ax}^{g}\tan^2\theta_0\{1 - 2j_0(2ka\cot\theta_0) - [2/(2ka\cot\theta_0)^2][\cos(2ka\cot\theta_0) - 1]\}, \qquad \text{(C.4.6-139)}$$

using the geometrical base cross section

$$\sigma_{ax}^{g} = \pi a^2. \qquad \text{(C.4.6-140)}$$

The squared tip contribution is here given by 1/2 of the term -1 in the last square bracket. In the high-frequency limit, $ka >> 1$, one obtains from Eq. (C.4.6-139):

$$\sigma_{ax} \to \sigma_{ax}^{g}\tan^2\theta_0; \qquad \text{(C.4.6-141)}$$

this result comes exclusively from the base.

A comparison between Kirchhoff and exact solutions (for axial incidence on the infinite cone) has been carried out by [SIEGEL, et al - 1955], who found that the exact cross section for the small-angle cone is four times larger than that given by the Kirchhoff method, Eq. (C.4.6-133). They also derived the corresponding cross sections for axial incidence on a cone with opening angle close to $\pi/2$, and found complete agreement between exact and Kirchhoff results in this case. It is to be noted that for the cone as a sonar target, the scattering does not originate from any specular point. The good agreement of Kirchhoff results (if any) for a target with a tip that violates the applicability of the method [eq. (C.3.2-71)] is explained by the fact that the surface within a wavelength or so of the tip contributes little to the scattering [ÜBERALL - 1964 and 1966].

C.4.7 KIRCHHOFF CROSS SECTION OF QUADRIC SURFACES

Kirchhoff cross sections for general quadric surfaces (with axial incidence) have been obtained by [RUDGERS - 1966]. For an ellipsoid with three principal axes ℓ_1, ℓ_2, ℓ_3 and incidence along ℓ_1, he finds

$$\sigma_{ax} = \pi(\ell_2\ell_3/\ell_1)^2\{1 - [(\sin 2k\ell_1)/k\ell_1] + [(\sin k\ell_1)/k\ell_1]^2\}. \qquad \text{(C.4.7-142)}$$

The oscillating terms represent, of course, the interference of the specular contribution with the spurious one from the sharp shadow boundary, typical for the Kirchhoff cross section for a smooth body.

The finite cone with elliptic cross section (principal axes ℓ_2, ℓ_3) may be treated as a degenerate quadric, with the result

for axial incidence:

$$\sigma_{ax} = (\ell_2/\ell_3)^2(\tan^4\theta_0)\pi h^2\{1 - [(\sin 2kh)/kh] + [(\sin kh)/kh]^2\}, \qquad (C.4.7\text{-}143)$$

with $h = a\cot\theta_0$. For $\ell_2 = \ell_3$, this agrees with Eq. (C.4.6-139).

C.5 POSSIBLE IMPROVEMENTS OF THE KIRCHHOFF METHOD

C.5.1 INTRODUCTION

The Kirchhoff approximation may be improved for several types of the targets discussed in the preceding section. Pioneering work in this direction is due to [UFIMTSEV - 1962], as mentioned at the end of Subsection C.4.3. For the case of targets where the sonar cross section is due to edge or tip diffraction, e.g., the known exact surface field near the edge or tip is utilized in the Kirchhoff-Rayleigh integral, Eq. (C.3.3-35). The same approach is used near the specular point of a curved-surface target, where the known exact surface field of a simple body of appropiate curvature is employed. This corresponds exactly to the "canonical problems" used by Keller in his Geometrical Theory of Diffraction (Appendix D), but while Keller had developed his method in order to improve on the geometrical acoustics approximation, Ufintsev's method is designed to improve on the Kirchhoff approximation. On the basis of some examples, [SENIOR and USLENGHI - 1971] have shown, however, that Keller's theory tends to agree more closely with the exact scattering results than Ufintsev's.

A simpler approach, for the case of smoothly curved bodies with specular points, was suggested at the end of Subsection C.4.1 for the example of the sphere. We then pointed out a way of im-

proving on the Kirchhoff approximation, which consists in an evaluation of the integral in Eqs. (C.2.4-55) to (C.2.4-58) by the stationary-phase method that automatically furnishes the specular contribution only (including higher-order corrections*), so that the spurious shadow boundary reflections are eliminated. This implies, of course, that possible creeping-wave contributions will not have been included either; but these should be important only for scatterers of simple shape such as spheres, while for targets of more complicated, irregular shapes where the creeping waves will not cause any effects of general importance, the Kirchhoff cross section as limited to the specular contributions by the use of the above-mentioned technique, may be expected to give results that are generally close to the exact cross section.

In the following, we shall discuss the method of stationary phase, and shall show how it provides solely the specular contribution to the Kirchhoff cross section for the cylinder and the sphere.

C.5.2 METHOD OF STATIONARY PHASE FOR CYLINDER AND SPHERE

The "method of stationary phase" is due to Lord Kelvin [ERDELYI - 1956, or ECKART - 1948]. It differs from the related "saddle point method" (or "method of steepest descent") which was discussed in Section 2.2.2.2 insofar as the integral in the former case remains on the real axis.

We shall study the method using the cases of an infinite cylinder and of a sphere, which may here be treated together

*There is no guarantee, of course, that in the framework of the Kirchhoff integral, these higher-order terms are quantitatively correct. However, they may be qualitatively so, as indicated by the example of Fig. C.2.

since they contain similar integrals. The backscattering cross section for the cylinder, $f_c(\pi)$, is given in Eq. (C.4.2-93), and for the sphere, $f_s(\pi)$, in Eqs. (C.4.1-76) or (C.4.1-80). The two cases may be combined as

$$f_c(\pi) = \pm 2a(k/2\pi i)^{1/2} I_c(ka) \qquad \text{(C.5.2-144)}$$

$$f_s(\pi) = \mp ika^2 I_s(ka) \qquad \text{(C.5.2-145)}$$

(upper sign for rigid, lower for soft surface), where

$$I_{c,s}(ka) = \int_0^{\pi/2} \cos\theta \, d\theta \begin{Bmatrix} 1 \\ \sin\theta \end{Bmatrix} \exp\{-2ika \cos\theta\}. \qquad \text{(C.5.2-146)}$$

The upper line in the brace refers to the cylindrical case (c), the lower line to the spherical one (s). The limit $\theta = 0$ is the vertex (specular point, or "highlight") of the target body, and $\theta = \pi/2$ is the shadow boundary. The integrands in $I_{c,s}$ will be seen to have a point of stationary phase [$d/d\theta(2ika \cos\theta) = 0$] at the vertex, and the evaluation of $I_{c,s}$ by the method of stationary phase therefore furnishes just the specular contribution to the scattering amplitude.

The stationary-phase method is applicable for values of the exponential parameter

$$ka >> 1, \qquad \text{(C.5.2-147)}$$

and the results will be obtained as an asymptotic series in inverse powers of ka, which constitutes a high-frequency expansion of the sonar cross section. Due to the generally rapid variation of the exponential in $I_{c,s}$ if Eq. (C.5.2-147) is satisfied, only regions of θ contribute significantly where the phase $-2ika \cos\theta$

becomes stationary, i.e., where its derivative vanishes:

$$2ika \sin\theta = 0. \qquad \text{(C.5.2-148)}$$

This happens at the stationary phase point $\theta = \theta_0$, with

$$\theta_0 = 0, \qquad \text{(C.5.2-149)}$$

i.e., at the point of specular reflection. We now introduce the new variable s by defining

$$-2\cos\theta - (-2\cos\theta_0) = s^2, \qquad \text{(C.5.2-150)}$$

or

$$(1/2)s^2 = 1 - \cos\theta, \qquad \text{(C.5.2-151)}$$

so that s = 0 at the vertex. The integral then becomes

$$I_{c,s}(ka) = \exp\{-2ika\}\int_0^\infty \Phi_{c,s}(s) \exp\{ikas^2\}ds \qquad \text{(C.5.2-152)}$$

where

$$\Phi_{c,s}(s) = \left\{\begin{matrix}(1 - (1/4)s^2)^{-1/2} \\ s\end{matrix}\right\} (1 - (1/2)s^2). \qquad \text{(C.5.2-153)}$$

The upper limit of integration has been extended from $\sqrt{2}$ to ∞ with little loss of accuracy. We now expand $\Phi_{c,s}(s)$ in a series of powers of s^2, and then integrate term by using the basic integrals

$$\int_0^\infty \exp\{ikas^2\}ds = (\pi/4ka)^{1/2} \exp\{i\pi/4\} \qquad \text{(C.5.2-154)}$$

and

$$\int_0^\infty s \exp\{ikas^2\}ds = i/2ka. \qquad \text{(C.5.2-155)}$$

Inserting in Eq. (C.5.2-152) and using Eqs. (2.2-65) and (2.2-72), we obtain the sonar cross sections σ_c for the cylinder, and σ_s for the sphere, in the form of an asymptotic series (high-frequency expansion):

$$\sigma_c = \pi a\left|1 - (3i/16ka) + [15/512(ka)^2] - \ldots\right|^2 \qquad \text{(C.5.2-156)}$$

$$= \pi a\{1 + [3/32(ka)^2] + \ldots\} \qquad \text{(C.5.2-157)}$$

$$\sigma_s = \pi a^2\left|1 - (i/2ka)\right|^2 \qquad \text{(C.5.2-158)}$$

$$= \pi a^2\{1 + [1/4(ka)^2]\}. \qquad \text{(C.5.2-159)}$$

These expressions do not distinguish between rigid and soft scatterers. For the case of the sphere, the series ends with the two terms given here, and it is gratifying to note that the specular expression thusly obtained, Eq. (C.5.2-159), agrees exactly with that obtained in a more intuitive fashion (as the value of the integral taken at the specular limit) in Eq. (C.4.1-88). For the cylinder, an infinite series is obtained.

It is evident that the application of the method of stationary phase to the Kirchhoff integral has provided us with the correct geometrical-acoustics expression for the sonar cross section, modified by a high-frequency asymptotic series. The higher terms in this series arise from the fact that successive Fresnel zones about the specular point are taken into account in the stationary-phase integral. In the framework of the Kirchhoff approximation, including the tangent plane assumption, these higher terms should be correct. It stands to reason, however, that the tangent plane assumption may not be physically permissible as far as obtaining the higher terms is concerned. This problem should be critically

investigated, and other approaches should be considered.

Firstly, for the cylinder, the specular contribution to σ_c can be obtained from the Watson-transform expression Eq. (2.2-103) with $f_{creep}(\pi)$ disregarded, and with $f_{geom}(\pi)$ extracted from Eq. (2.2-84) as the successive terms of a high-frequency expansion [and not just as its lowest-order term, Eq. (2.2-99)], by retaining higher-order terms in the saddle-point method used in this connection. It is not clear, however, whether the higher-order terms obtained from the Watson-transformation method may be more reliable than those obtained by the Kirchhoff method.

There are, however, two methods available that should furnish us the guaranteed exact specular contribution to the sonar cross section (in the form of a high-frequency asymptotic series if necessary), thus being superior to Ufintsev's approach to this problem. One of these is the Luneburg-Kline method, discussed in Section 2.2.2.1, which is an approach based on differential geometry. The other one, an integral approach, consists in taking the limit of $\vec{r} \to \vec{r}_{surf}$ in the Kirchhoff-Rayleigh integrals of Eqs. (C.2.2-27) or (C.2.2-28), and solving the ensuing integral equation for the surface fields; but the practicability of such a method is not clear [URETSKY - 1963, 1965]. This latter method might be combined with a stationary-phase expansion of the exact Kirchhoff-Rayleigh integrals, in which only the (exact) surface field and its successive derivatives at the specular points have to be known. Investigations along such lines might prove quite fruitful.

APPENDIX D

KELLER'S GEOMETRICAL THEORY OF DIFFRACTION

D.1 GENERAL DESCRIPTION

Keller's theory is called the Geometrical Theory of Diffraction because it is based on the geometrical concept of the ray. The fundamental assumption of this theory is to postulate the existence of diffracted rays in addition to the ordinary rays of geometrical acoustics. Thus, in contrast with all other high frequency methods, it begins with the high frequency limit (geometrical acoustics) and perturbs away from it. Since it was introduced in 1953 this theory has won widespread acceptance for electromagnetic applications. Its potential for acoustic scattering is just beginning to be explored. It should not yet be considered to be complete or even self consistent. It continues to evolve as its applications are worked out.

The main practical advantage of the theory is that it can be applied to bodies of complex geometry. This property of the theory derives from a second fundamental assumption, viz., that diffraction is a local phenomenon, which allows the scattered field from a complicated target to be treated as a sum of contributions from separate idealized parts of the body.

Diffracted rays, which originate on the target, are assumed to be continued away from the target according to the ordinary laws of geometrical acoustics. Initial conditions on these rays at their point of origin on the target are assumed to be determined by the

local geometry of the body and the incident rays. For example, locally an edge should behave like an infinite wedge, for which an exact solution of the diffraction problem is available. Comparison with this known solution determines the initial condition on rays originating from an edge. Idealized problems whose exact solutions are used in this way are called canonical problems in Keller's theory.

D.2 THEORETICAL BASIS

The total field at a point is assumed to be equal to the sum of the contributions from all rays which reach that point. These may include the incident and reflected rays of geometrical acoustics as well as diffracted rays. There are three classes of diffracted rays; they are, in decreasing order of importance: (a) edge diffracted rays, (b) tip diffracted rays, (c) creeping wave rays.

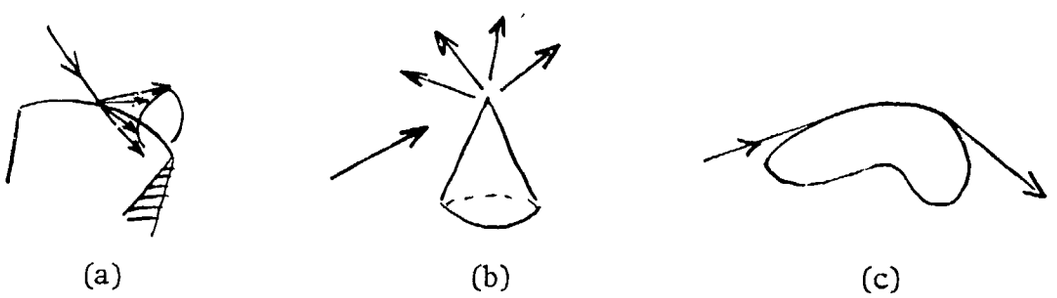

Fig. D.2-1 (a) Edge diffracted rays, (b) Tip diffracted rays, (c) Creeping wave rays

A ray incident on an edge is assumed to give rise to a cone of diffracted rays, the half angle of the cone being equal to the angle of the incident ray with the edge. A ray incident on a tip gives rise to diffracted rays in all directions. A ray tangentially

incident on a convex body launches a circumferential wave on the surface (creeping wave) which re-radiates to the observation point via another tangential ray (the path from source to observation point would coincide with a taut string connecting the two points). The magnitudes of the fields on edge diffracted and tip diffracted rays are proportional to $k^{-1/2}$ and k^{-1} respectively, while fields on creeping wave rays are exponentially damped. We shall now discuss the calculation of these fields in detail. All of the results of this appendix are for rigid bodies. This is not a limitation of the theory, which can also be applied to soft and penetrable bodies.

D.2.1 EDGE DIFFRACTION

A ray incident on an edge gives rise to a cone of diffracted rays whose half angle is equal to the angle of the incident ray with the edge (Fig. D.2-1 (a)). We express the field along such a diffracted ray by means of geometrical acoustics; from eqs. (b-8,26) we have

$$p(\ell) = p(\ell_0) \sqrt{\frac{\rho_1 \rho_2}{(\rho_1 + \ell - \ell_0)(\rho_2 + \ell - \ell_0)}}\, e^{ik(\ell - \ell_0)}$$

where in our present notation ρ_1 and ρ_2 are the distances of the reference wavefront at ℓ_0 from the two caustics of the ray bundle. The edge is a caustic since cones of diffracted rays intersect there. We therefore have a configuration such as the one shown in the figure below.

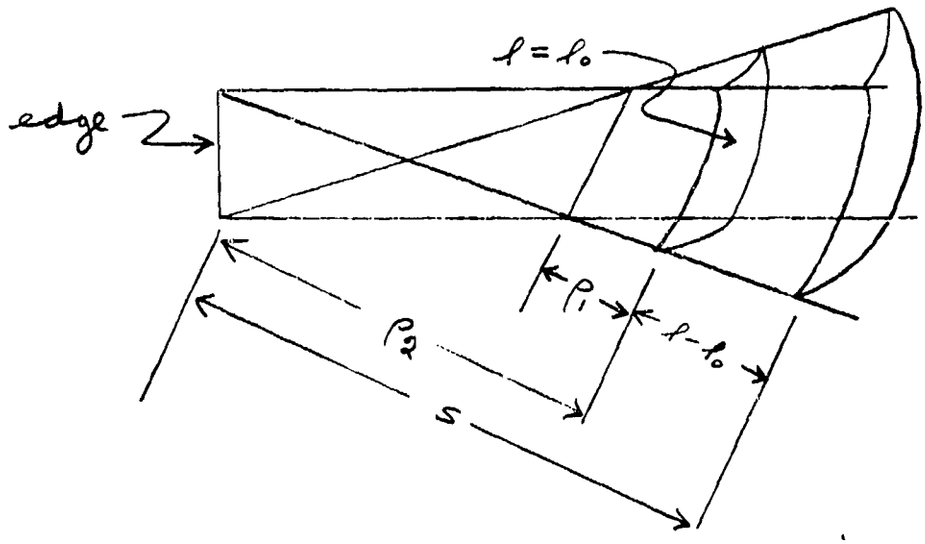

We wish to measure the distance along the ray from the edge. Therefore, we let $\ell = s$, $\ell_0 = \rho_2$. We also wish to position the reference wavefront at the edge. We know from geometrical acoustics that the field is infinite on a caustic. However, we assume that the field has the form of a cylindrical wave near the caustic so that

$$\sqrt{\rho_2}\, p(\ell_0) = \sqrt{\ell_0}\, p(\ell_0) \longrightarrow \text{constant} \quad \ell_0 \to 0$$

Therefore, we express the field along a diffracted ray by

$$p(s) = p_{inc}(0)\, D\, e^{iks} / \sqrt{s(1 + s/\rho_1)} \qquad (d-1)$$

where D is a constant called the diffraction coefficient.

The quantity ρ_1 is equal to the distance of the other caustic from the edge along the diffracted ray. This distance is negative if the caustic is between the edge and the observation point, positive otherwise. The principles of differential geometry may be used

[KELLER - 1957] to determine ρ_1 in terms of the geometry of the edge and the incident and diffracted rays, giving the result

$$\rho_1 = \frac{-\rho \sin^2\beta}{\rho \frac{d\beta}{d\ell} \sin\beta + \cos\delta} \qquad \text{(d-2)}$$

where ρ is the radius of curvature of the edge, β is the angle between the incident ray and the tangent to the edge, ℓ is arc length along the edge, and δ is the angle between the diffracted ray and the principal normal to the edge. ("Principal normal" is a term from differential geometry which indicates the normal which lies in the osculating plane of the edge and points toward the center of curvature. For a curved planar edge the osculating plane is the plane of the edge.)

For small values of s (near field) the solution expressed by eq. (d-1) has the form of an outgoing cylindrical wave, whereas for large values (far field) it has the form of an outgoing spherical wave, except in the case of a straight edge. In this case we have ρ, and hence ρ_1, infinite. The solution is a cylindrical wave at all ranges. Thus, for finite straight edges the method fails to account for physically required spherical spreading at sufficiently large distances from the edge. We conclude that the Keller method fails in the far field in the specular direction for finite straight edges. It is possible that tip contributions (see next section) from the ends of the straight line could cancel the cylindrical wave and produce a valid approximation, but this is conjectural since the required canonical solutions for tip diffraction are not available.

The diffraction coefficient D is chosen so that the solution agrees with the exact solution for an infinite wedge as the edge is approached. Comparison with the asymptotic form of the exact solution [KELLER - 1962] gives the following expression for the diffraction coefficient

$$D = \frac{e^{\frac{\pi i}{4}} \sin\frac{\pi}{n}}{n\sqrt{2\pi k}\sin\beta}\left\{\left(\cos\frac{\pi}{n} - \cos\frac{\theta-\alpha}{n}\right)^{-1} + \left(\cos\frac{\pi}{n} - \cos\frac{\theta+\alpha+\pi}{n}\right)^{-1}\right\} \qquad \text{(d-3)}$$

where $(2-n)\pi$ is the wedge angle, β is the angle of the incident ray with the edge, and angles α and θ are shown in Fig. D.2-2

$$\left(-\frac{\pi}{2} < \alpha, \theta < n\pi - \frac{\pi}{2}\right).$$

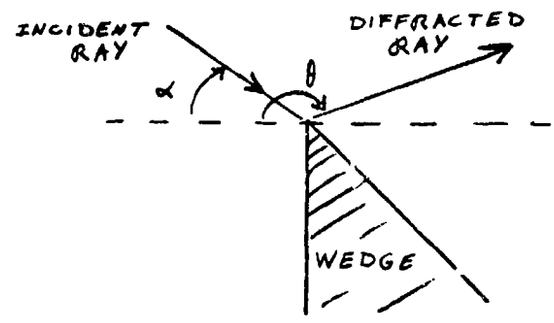

Fig. D.2-2
Projection of Incident & Diffraction Rays onto Plane Normal to Edge.

The far field expression for the field given by eq.(d-1) is

$$p \approx p_{inc} D\sqrt{\rho_1}\, e^{ikS}/s \qquad \rho_1 > 0 \qquad \text{(d-3a)}$$

If ρ_1 is negative the diffracted ray passes through a caustic. In this case we choose the sign of $\pm i$ so that our result agrees with the known phase change as given by geometrical acoustics. Thus, we have [KELLER - 1957]

$$p \approx p_{inc} D\sqrt{|\rho_1|}\, e^{ikS - \frac{\pi}{2}i}/s \qquad \rho_1 < 0 \qquad \text{(d-4)}$$

Scattering by a finite cylinder is presented in § D.3.1. as an example of edge diffraction.

D.2.2 TIP DIFFRACTION

A tip is assumed to act as a point source producing an outgoing spherical wave. Therefore, we write the scattered field from a tip in the form

$$p = p_{inc}\, D\, e^{jks}/s \qquad \text{(d-5)}$$

where p_{inc} is the value of the incident field at the tip, s is the distance of the field point from the tip, and D is a diffraction coefficient to be determined by comparison with a canonical problem. A reasonably general canonical problem for tip diffraction is scattering by a semi-infinite elliptic cone.

While this problem has been solved [KRAUS and LEVINE - 1961], a simple expression for D has been obtained only for circular cones in the thin cone angle limit. This result is [BOWMAN et al. - 1969, p. 655]:

$$D \approx \frac{2j \sin^2(\alpha/2)}{k(\cos\theta + \cos\theta_0)^3}\Big[1 + \cos\theta\cos\theta_0 \qquad \theta+\theta_0 \neq \pi$$

$$+ 2\cos(\varphi-\varphi_0)\sin\theta\sin\theta_0\Big]; \quad \theta+\theta_0 \neq \pi \qquad \text{(d-6)}$$

where α is the half-angle of the cone and θ_0, ϕ_0 and θ, ϕ are the spherical angles of the incident and diffracted rays.

It follows from dimensional arguments that D is always proportional to k^{-1} for tip diffraction. Since D is proportional to $k^{-1/2}$ for edge diffraction it follows that tip diffraction is less important than edge diffraction at high frequencies. For this reason and because of the difficult analytical expressions for tip diffraction coefficients tip diffraction has received little attention in the Keller literature.

D.2.3 CREEPING WAVE DIFFRACTION

A ray tangentially incident on a smooth body (see Fig. D.2-3) launches a surface wave at Q_1 called a creeping wave (§ 2.2.2.2)

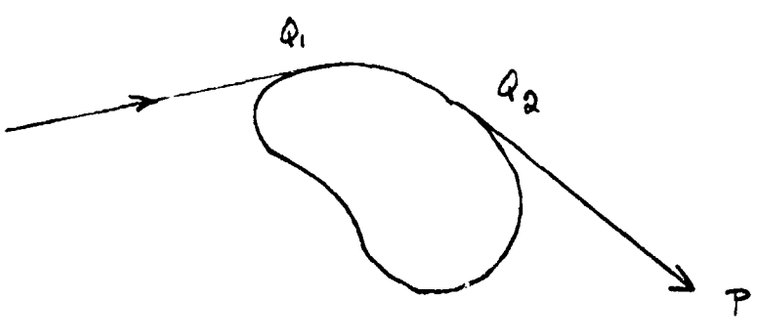

Fig. D.2-3

As the creeping wave propagates along a geodesic in the surface it continuously re-radiates along tangential rays. Suppose one such ray launched at Q_2 reaches the observation point P. The field at P is written as the product of the following factors:

(1) The value, p_{inc}, of the incident field at Q_1.

(2) Diffraction coefficients $D(Q_1)$ and $D(Q_2)$ associated with the points Q_1 and Q_2. It is assumed that only the curvature of the surface in the direction of the creeping wave affects the field. Thus, locally the surface would behave like a cylinder of radius equal to the radius of curvature in the direction of propagation. Using this as a canonical problem we obtain [LEVY and KELLER - 1959]

$$D^2 = \left(\frac{ka}{2}\right)^{\frac{1}{3}} e^{\frac{\pi i}{12}} \Big/ \sqrt{2\pi k}\, \beta_1\, A_i^2(-\beta_1) \qquad \text{(d-7)}$$

where a is the radius of curvature and β_1 (= 1.01879 ...) is the smallest root of $A_i'(-\beta) = 0$. A_i is the Airy function and $A_i(-\beta_1) =$ 0.53566...

(3) A phase and attenuation factor. We express this in the form

$$\exp\left\{ ik(t+s) - \int_0^t \alpha(\tau)\, d\tau \right\} \qquad \text{(d-8)}$$

where t is the distance from Q_1 to Q_2 in the surface, s is the distance from Q_2 to P, and $\alpha(\tau)$ is the attenuation constant, which is assumed to be a function of surface curvature in the direction of propagation. By using the circular cylinder as the canonical problem we obtain [LEVY and KELLER - 1959]

$$\alpha = \left(\frac{ka}{2}\right)^{\frac{1}{3}} \beta_1\, e^{-\pi i/6}\, a^{-1} \qquad \text{(d-9)}$$

where a is a function of τ.

(4) A factor which expresses the geometrical spreading of rays in the surface. This is derived [LEVY and KELLER - 1959] by assuming that the energy lost by an area element of a narrow bundle of surface rays is proportional to the area element. The resulting expression for this factor is

$$\sqrt{\frac{d\sigma(Q_1)}{d\sigma(Q_2)}} \tag{d-10}$$

where $d\sigma(Q)$ is the width of an infinitesimal bundle at Q.

(5) A factor which expresses the geometrical spreading of rays about the ray from Q_2 to P. The surface is a caustic of diffracted rays and by reasoning similar to that used in § D.2.1 this is the same factor which appears in eq.(d-1), viz.,

$$[\, s(1 + s/\rho_1) \,]^{-1/2} \tag{d-11}$$

where s is the distance from Q_2 to P and ρ_1 is the distance from Q_2 to the other caustic along the direction of the diffracted ray. The latter is negative if the diffracted ray passes through the caustic, positive otherwise.

Combining the above factors we express the field at P by

$$p = p_{inc}\, D(Q_1)\, D(Q_2) \sqrt{\frac{d\sigma(Q_1)}{d\sigma(Q_2)}} \sqrt{\frac{\rho_1}{s(s+\rho_1)}}$$

$$\cdot \exp\left\{ ik(t+s) - \int_0^t \alpha(\tau)\, d\tau \right\} \tag{d-12}$$

The above result is obtained by considering only the predominant mode of the canonical problem. In reality there are an infinite number of modes. Higher order terms can be included by replacing D, α, β_1 by D_m, α_m, β_m and summing over m. Voltmer [1970] has derived higher order corrections to D and α which take into account transverse surface curvature.

Scattering by a sphere is presented in § D.3.2 as an example of creeping wave diffraction.

D.2.4 THE CAUSTIC CORRECTION

Eqs. (d-1) and (d-12) fail (blow up) at a caustic. These expressions may be modified in the neighborhood of a caustic by reference to a canonical problem. The car cal problem in this case is a straight line caustic in free space (no boundaries are present). The solution of the wave equation

$$e^{in\varphi}\, e^{iKz\sin\delta}\, J_n(Kr\cos\delta) \qquad \text{(d-13)}$$

in cylindrical coordinates r, ϕ, z with δ a constant represents such a caustic, for if we replace the Bessel function J_n by its asymptotic form for large argument we obtain

$$\frac{e^{in\varphi}}{\sqrt{2\pi Kr\cos\delta}} \left\{ \exp\left[iK(r\cos\delta + z\sin\delta) - \frac{n\pi i}{2} - \frac{\pi i}{4}\right] \right.$$

$$\left. + \exp\left[iK(-r\cos\delta + z\sin\delta) + \frac{n\pi i}{2} + \frac{\pi i}{4}\right] \right\} \qquad \text{(d-14)}$$

Thus, the solution corresponds to two cylindrically symmetric families of rays which both intersect the z-axis, which is, therefore, a caustic (Fig. D.2.4)

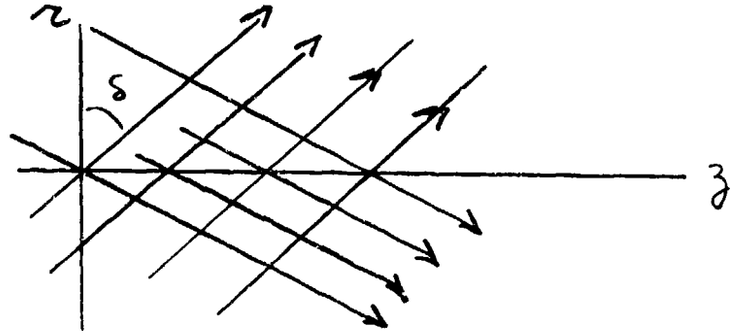

Fig. D.2.4

The method of caustic correction consists of the following procedure. We first express the field in a form which can be recognized as the asymptotic form of an expression of the type (d-13). If the argument of the Bessel function is real we simply replace the asymptotic form of the Bessel function by the Bessel function itself. The resulting expression will be well behaved in a neighborhood of the caustic and we assume it to be correct there. Examples of this procedure applied to diffraction by a finite cylinder can be found in §§ D.3.1.7-8.

If the argument of the Bessel function would be complex according to the above procedure then we need to state the principle a little more carefully. The caustic correction is performed by multiplying the expression for the field by the factor

$$\sqrt{\frac{\pi K r \cos\delta}{2}}\, \sec\left\{ K r \cos\delta - \frac{n\pi}{2} - \frac{\pi}{4} \right\} J_n(K r \cos\delta)$$

An example of the latter procedure applied to diffraction by a sphere is given in § D.3.2.6.

D.2.5 MULTIPLE DIFFRACTION

One of the advantages of the Keller method over the Kirchhoff method is that it can take account of multiple diffraction. For example, a diffracted ray from one edge may be incident on another edge giving rise to secondary diffraction. The diffracted rays from the second edge are called doubly diffracted. (An example of double diffraction is given in § D.3.1.8)

Since each scattering introduces a factor of $k^{-1/2}$ (from the diffraction coefficient) into the solution, summing the contributions from such multiply diffracted rays produces an expansion in inverse powers of k. If we were to compare this expansion with the asymptotic expansion of an exact solution we would expect them to disagree after a certain number of terms. For example, for an infinite slit failure occurs after two terms [KARP and KELLER - 1961]. There, is, unfortunately no general theorem which enables us to predict at which term failure occurs. Higher order terms which actually improve the solution extend its range of applicability to lower frequencies. Thus, even where the Kirchhoff and Keller methods agree in the high frequency limit the latter may produce better results at lower frequencies.

D.3 APPLICATIONS

D.3.1 THE FINITE CYLINDER

As an example of edge diffraction we now consider the

backscattering of a plane wave from a rigid cylinder of radius a and length 2ℓ. At a general edge point (P) the cone of diffracted rays does not contain any rays in the backscattering direction. However, assuming the aspect θ restricted to the range $0 < \theta < 90^{\circ}$, at points 1, 2, and 3 (Fig. D.3-1) this cone flattens out into the plane of the paper producing back-scattered rays. Each of these three points makes a contribution to the backscattered pressure of the form given by eq.(d-1), or, restricting to far field values, of the form given by eq.(d-3) or eq.(d-4). Combining the latter two equations, the form of the contribution to the far backscattered field from each of the three points is

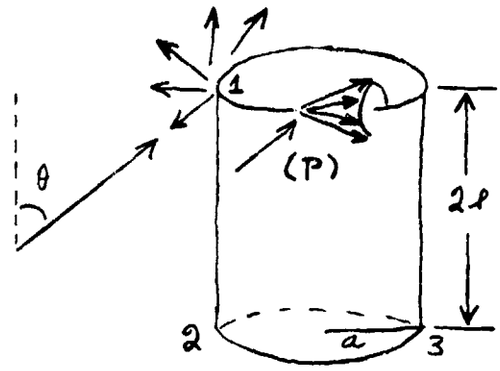

Fig. D.3-1

$$p_{inc} \to \sqrt{|\rho_1|}\ \frac{e^{ikS}}{s} \begin{cases} 1 & \rho_1 > 0 \\ e^{-i\frac{\pi}{2}} & \rho_1 < 0 \end{cases} \qquad \text{(d-15)}$$

where p_{inc} is the incident pressure at the point in question, D is the diffraction coefficient, s is the distance from the point, and the principal radius of curvature of the wavefront ρ_1 is given by eq.(d-2).

We now calculate each of these factors.

D.3.1.1 THE INCIDENT FIELD

Let the incident plane wave be given by

$$p_{inc} = \exp i \hat{k}_{inc} \cdot \vec{r} \qquad \text{(d-16)}$$

where $\hat{k}_{inc} = (0, \sin\theta, \cos\theta)$ (d-17)

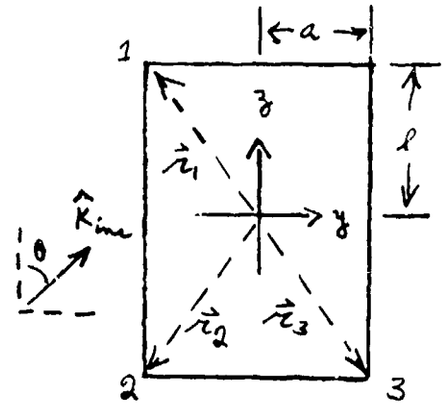

Fig. D.3-2

We evaluate this expression at points 1-3 on the cylinder. From Fig. D.3-2 we immediately obtain

$$\begin{aligned} p_{inc}(1) &= \exp ik\{-a\sin\theta + \ell\cos\theta\} \\ p_{inc}(2) &= \exp ik\{-a\sin\theta - \ell\cos\theta\} \\ p_{inc}(3) &= \exp ik\{a\sin\theta - \ell\cos\theta\} \end{aligned} \qquad \text{(d-18)}$$

D.3.1.2 THE PHASE FACTORS

We now calculate the phase factor e^{iks} associated with each point. Let s_i be the distance of the field point from the i^{th} point on the cylinder.

$$s_i = |\vec{r} - \vec{r}_i| \qquad i = 1, 2, 3 \qquad \text{(d-19)}$$

Making the far field approximation we obtain

$$\exp iks_i \approx \exp ik(r - \vec{r}\cdot\vec{r}_i/r) \qquad \text{(d-20)}$$

It follows from Fig. D.3-2 that these factors are all proportional to the incident field; specifically

$$\exp iKs_i = \rho_{inc}(\vec{r}_i)\exp iKr \qquad \text{(d-21)}$$

D.3.1.3 THE DIFFRACTION COEFFICIENTS

The diffraction coefficients are obtained from eq.(d-3). We set n = 3/2 since the wedge angle is 90° and β, the angle of the incident ray with the edge, is 90° at each point of diffraction. We obtain,

$$D_i = \frac{e^{\pi i/4}}{\sqrt{6\pi K}}\left\{-\frac{2}{3}+\left[-\frac{1}{2}-\cos\frac{2}{3}(\pi+2\alpha_i)\right]^{-1}\right\} \qquad \text{(d-22)}$$

where

$$\alpha_1 = \theta - \frac{\pi}{2}$$

$$\alpha_2 = \theta$$

$$\alpha_3 = \theta + \frac{\pi}{2}$$

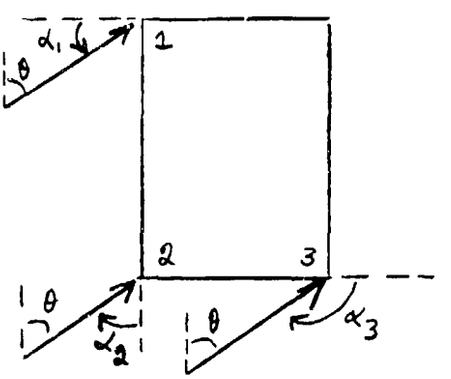

Fig. D.3-3

D.3.1.4 THE PRINCIPAL RADIUS OF CURVATURE

The principal radius ρ_1 is obtained from eq.(d-2). Referring to Fig. D.3-4 where $\ell = a\alpha$ is arch length along the edge and t is the unit tangent to the edge

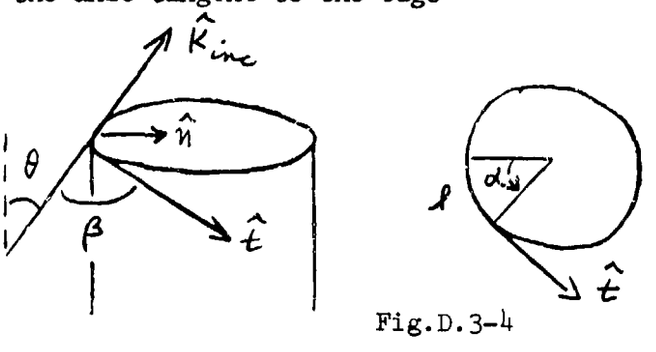

Fig.D.3-4

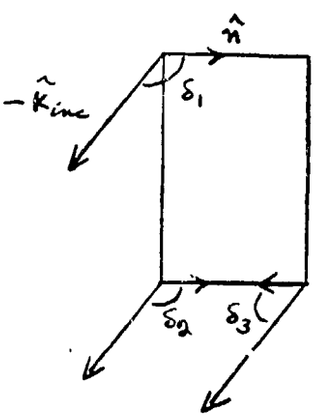

We see that since

$$\hat{K}_{inc} = (\sin\theta, 0, \cos\theta)$$
$$\hat{t} = (\sin\alpha, \cos\alpha, 0) \tag{d-23}$$

we have

$$\cos\beta = \hat{K}_{inc}\cdot\hat{t} = \sin\theta\sin\phi/a$$
$$-\frac{d\beta}{d\phi}\sin\beta = \frac{1}{a}\sin\theta\cos\phi/a \tag{d-24}$$

Substituting into eq. (d-2) we obtain

$$\rho_1 = \frac{a\sin^2\beta}{\sin\theta\cos\alpha - \cos\delta} \tag{d-25}$$

and using

$$\delta_1 = \delta_2 = \frac{\pi}{2} + \theta$$
$$\delta_3 = \frac{\pi}{2} - \theta \tag{d-26}$$

we finally obtain

$$\rho_1(\vec{r}_1) = \rho_1(\vec{r}_2) = a/2\sin\theta$$
$$\rho_1(\vec{r}_3) = -a/2\sin\theta \tag{d-27}$$

As we have seen the negative sign in the latter expression introduces a factor of exp $-i\pi/2$ which represents a phase change of

90^{o} due to the fact that the diffracted ray passes through a caustic.

D.3.1.5 CROSS SECTION (SINGLE DIFFRACTION)

In the calculation of the above factors we have considered singly diffracted rays only. Combining these factors as in eq.(d-15), summing from one to three, and using eq. (2.2-65) for the cross section, we obtain

$$\sigma_{KEL} = \frac{\pi a^2}{3\pi ka \sin\theta} \left| \sum_{i=1}^{3} E_i D_i \right|^2 \qquad \text{(d-28)}$$

where

$$E_1 = \exp\left\{ 2ik(-a\sin\theta + \ell\cos\theta) + \frac{\pi}{4} i \right\}$$

$$E_2 = \exp\left\{ 2ik(-a\sin\theta - \ell\cos\theta) + \frac{\pi}{4} i \right\} \qquad \text{(d-29)}$$

$$E_3 = \exp\left\{ 2ik(a\sin\theta - \ell\cos\theta) - \frac{\pi}{4} i \right\}$$

$$D_1 = -\frac{2}{3} + \left[-\frac{1}{2} - \cos\frac{4}{3}\theta \right]^{-1}$$

$$D_2 = -\frac{2}{3} + \left[-\frac{1}{2} - \cos\frac{2}{3}(\pi + 2\theta) \right]^{-1} \qquad \text{(d-30)}$$

$$D_3 = -\frac{2}{3} + \left[-\frac{1}{2} - \cos\frac{4}{3}(\pi + \theta) \right]^{-1}$$

D.3.1.6 BROADSIDE INCIDENCE

We note that diffraction coefficients D_1 and D_2 are singular at broadside incidence ($\theta = 90^{o}$). From eq.(d-30) we may see that they

approach $\mp \frac{\sqrt{3}}{2}\left(\frac{\pi}{2} - \theta\right)^{-1}$, respectively. However, the singular terms combine so as to cancel the singularity. Thus, neglecting the contribution from D_3, which is of higher order in k^{-1}, we have

$$\sigma_{KEL}\left(\frac{\pi}{2}\right) = \frac{\pi a^2}{3\pi k a} \lim_{\theta \to \frac{\pi}{2}} \left| E_1 D_1 + E_2 D_2 \right|^2$$

$$= \frac{a}{4k} \lim_{\theta \to \frac{\pi}{2}} \left| \frac{2i \sin 2k\rho\left(\frac{\pi}{2} - \theta\right)}{\pi/2 - \theta} \right|^2$$

$$= ka\,(2\rho)^2 \qquad \text{(d-31)}$$

which agrees with the Kirchhoff result, eq.(c-124).

At broadside incidence there are specularly reflected rays which have not been included in the present calculation. This would appear to be an exception to our principle, stated at the beginning of § D.2, that every ray which reaches a point contributes to the field there. This principle implies that the geometrical acoustics field should be included in regions of specular reflection. However, in far field calculations of this type in which one or more of the surface radii of curvature is infinite we have seen in § B.2 that the geometrical acoustics method fails. In these cases the effect of the infinite radius of curvature is felt through the singularity in the diffraction coefficient. A similar problem has been treated by Keller [1957, p. 432].

An unexpected difficulty arises when we attempt to include doubly diffracted rays at broadside incidence. Only one of the rays diffracted by an edge of the cylinder reaches the other edge. However, the calculation of the principal radius ρ_1 of the doubly diffracted rays requires a bundle of rays. Thus, the Keller postulates do not seem to cover this case, which could possibly be dealt with through the introduction of another canonical problem. Ahluwalia [1970] has dealt with the problem of scattering of a plane wave by a finite cylinder by means of a uniform asymptotic expansion. However, his result for backscattering at broadside incidence (from his eq. 6.26) differs in first order from our Keller and Kirchhoff results by a factor of 2. Apparently the discrepancy arises because he has explicitly included a reflected wave which, in the specular direction, should enter through a singularity of the diffraction coefficient as explained in the previous paragraph.

D.3.1.7 AXIAL INCIDENCE

The diffraction coefficients D_2 and D_3 are singular at axial incidence ($\theta = 0$), being proportional to $\mp \frac{\sqrt{3}}{2} \theta^{-1}$ respectively as we see from eq.(d-30). The singularity occurs because there is specular reflection in this direction. However, when D_2 and D_3 are combined, the singularity does not cancel as for broadside incidence. Instead, we obtain

$$\frac{1}{\sqrt{\sin\theta}} \left(E_2 D_2 + E_3 D_3\right) \approx i\sqrt{3}\, e^{-2ik\rho}\, \theta^{-3/2} \sin\left(2ka\theta - \frac{\pi}{4}\right) \qquad \text{(d-32)}$$

The singularity remains because the axis of the cylinder is a caustic of diffracted rays. A caustic correction as described in § D.2.4 must be applied. We recognize that the right hand side of eq.(d-32) is the asymptotic expansion of

$$(2ka)^{3/2}\sqrt{\frac{3\pi}{2}}\; i\; e^{-2ikl}\; J_1(2ka\theta)/2ka\theta \qquad \text{(d-33)}$$

Since $\lim_{x\to 0} J_1(x)/x = \frac{1}{2}$ we can set θ equal to zero in the above expression. We replace the right hand side of eq.(d-32) by the value thus obtained. Then neglecting the contribution from D_1, which is of higher order in k^{-1}, eq.(d-28) gives the following result for the cross section

$$\sigma_{KEL}(0^\circ) = \pi a^2 (ka)^2 \qquad \text{(d-34)}$$

which agrees with the Kirchhoff result, eq.(c-120).

D.3.1.8 AXIAL INCIDENCE (DOUBLE DIFFRACTION)

We now consider singly diffracted rays which cross the disc of the cylinder at axial incidence and produce other diffracted rays at the opposite side. For an observation direction slightly off-axis there are two such doubly diffracted rays, as shown in Fig. D.3-5

(a) (b)

Fig. D.3-5

Doubly diffracted rays

The singly diffracted rays are treated as the incident field for the doubly diffracted rays. They have a principal radius ρ_1 equal to -a. This follows because ρ_1 is equal to the distance from the diffraction point to the axial caustic. The quantity is negative because the ray passes through the caustic. The diffraction coefficient is obtained from eq.(d-3) by setting n = 3/2, $\beta = \pi/2$ and $\alpha = 0$, $\theta = -\pi/2$ and $\alpha = \pi/2$, $\theta = \pi$ for cases (a) and (b) respectively. In both cases we find the following value for the incident field of the doubly diffracted rays.

$$\rho_1 = -\exp\{2ika - ik\ell - \pi i/4\} / \sqrt{3\pi ka} \qquad \text{(d-35)}$$

The axis of the cylinder is also a caustic of doubly diffracted rays. Therefore, the value of ρ_1 is $\mp a/\sin\gamma$ for cases (a) and (b) respectively. To obtain the diffraction coefficients we set n = 3/2, $\beta = \pi/2$ in eq. (d-3) and replace α, θ by (a) π, $\pi/2 + \gamma$, (b) $-\pi/2$, γ. In both cases we find that

$$D \to -2 e^{\pi i/4} / \sqrt{6\pi k} \qquad \gamma \to 0 \qquad \text{(d-36)}$$

The sum of the two contributions give the following result for the doubly diffracted field.

$$\rho_2 = \frac{2}{3}\sqrt{\frac{a}{k\pi}} \exp\{-2ik\ell + 2ika - \frac{\pi i}{4}\}$$

$$\cdot \sqrt{\frac{2}{\pi}} \frac{\cos\{ka\sin\gamma - \pi/4\}}{\sqrt{ka\sin\gamma}} \frac{e^{ikr}}{r} \qquad \text{(d-37)}$$

We apply the caustic correction by recognizing that the right hand side of eq.(d-37) is the asymptotic expansion of

$$\frac{2}{3}\sqrt{\frac{a}{k\pi}}\exp\left\{-2ikl+2ika-\frac{\pi i}{4}\right\}J_0(ka\sin\gamma)\frac{e^{ikr}}{r} \qquad \text{(d-38)}$$

We now assume that this expression gives the correct limit as $\gamma\to 0$, i.e.,

$$\rho_2 \to \frac{2}{3}\sqrt{\frac{a}{k\pi}}\exp\left\{2ika-2ikl-\frac{\pi i}{4}\right\}\frac{e^{ikr}}{r} \qquad \gamma\to 0 \qquad \text{(d-39)}$$

Combining the above result with the corresponding expression for the singly diffracted field and calculating the cross section from eq.(2.2-65) we obtain

$$\sigma_{KEL}(0^\circ) = \pi a^2 (ka)^2 \left| 1+\frac{4}{3\sqrt{\pi}}\frac{e^{2ika-3\pi i/4}}{(ka)^{3/2}}\right|^2 \qquad \text{(d-40)}$$

D.3.2 THE RIGID SPHERE

We now consider the backscattering of a plane wave from a rigid sphere as an example of creeping wave diffraction. If the plane wave is incident in the North to South direction then at each point on the equator an incident ray launches a creeping wave which travels along a great circle, passes through the South pole, and returns to the

equator where it re-radiates. Thus, each point on the equator produces a diffracted ray in the backscattering direction, which is, therefore, an axial caustic.

In order to apply the caustic correction we must consider a direction of observation which is slightly off-axis and take the limit by the method explained in § D.2.4. There are two diffracted rays in such a direction as shown in Fig. D.3-6.

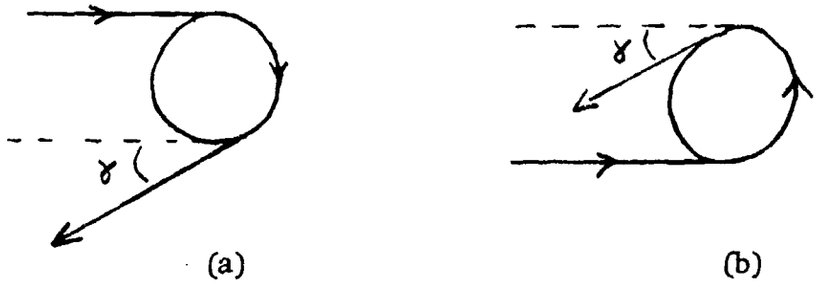

Fig. D.3-6

Each of these rays will contribute a term of the type given by eq.(d-12). We now calculate each of the factors in the latter equation.

D.3.2.1 THE INCIDENT FIELD

The field of the incident plane wave, $p_{inc} = \exp i k z$ is equal to unity at the equator, $z = 0$.

D.3.2.2 THE DIFFRACTION COEFFICIENTS

The radius of curvature of the sphere is equal to the radius, a, of the sphere. Since it has the same value at every point the

product $D(Q_1)\ D(Q_2)$ in eq.(d-12) can be replaced by D^2 where D^2 is given by eq.(d-7).

D.3.2.2 PHASE AND ATTENUATION

The attenuation constant given by eq.(d-9) is constant in the present example. We see that the phase and attenuation factor given by expression (d-8) is

$$\exp\left\{ ik(\pi \mp \gamma)a + iks - (\pi \mp \gamma)a\alpha \right\} \qquad \text{(d-41)}$$

for diffracted rays (a) and (b) respectively (Fig. D.3-6). Making the far field approximation we have

$$e^{iks} \approx e^{ikr} \qquad \text{(d-42)}$$

D.3.2.4 SPREADING OF SURFACE RAYS

The effect of geometrical spreading of surface rays is given by expression (d-10) in the form $\left[d\sigma(Q_1)/d\sigma(Q_2)\right]^{\frac{1}{2}}$ where $d\sigma(Q)$ is the width of an infinitesimal bundle of rays at Q. For a sphere this width is proportional to the radius of the latitude circle. We find

$$\left| \frac{d\sigma(Q_1)}{d\sigma(Q_2)} \right| = \cos\gamma \to 1 \qquad \gamma \to 0 \qquad \text{(d-43)}$$

From symmetry we would expect this ratio to approach unity. However, we should note that the surface rays both pass through a caustic (focal point at the South pole), which introduces a factor $\exp\left\{-\pi\ i/2\right\}$.

D.3.2.5 THE PRINCIPAL RADIUS OF CURVATURE

The principal radius ρ_1 is the distance from the launch point of the diffracted ray to the axial caustic.

$$\rho_1 = \pm \frac{a}{\tan\gamma} \approx \pm \frac{a}{\gamma} \qquad \gamma << 1 \tag{d-44}$$

for rays (a) and (b) respectively. We have a minus sign in the latter case because the ray passes through the caustic. Making the far field approximation,

$$\text{(a)} \quad \sqrt{\frac{\rho_1}{s(s+\rho_1)}} \approx \sqrt{\frac{a}{\gamma}}\,\frac{1}{r} \qquad ; \rho_1 > 0 \tag{d-45}$$

$$\text{(b)} \quad \sqrt{\frac{\rho_1}{s(s+\rho_1)}} \approx \sqrt{\frac{a}{\gamma}}\,\frac{1}{r}\,e^{-\pi i/2} \qquad ; \rho_1 < 0$$

D.3.2.6 THE CAUSTIC CORRECTION

Combining the contributions from the two diffracted rays we can express the creeping wave contribution to the field in the form

$$P_{cw} = 2\sqrt{a}\,\gamma^{-1/2} D^2 \cos\left\{(k+i\alpha)a\gamma - \frac{\pi}{4}\right\}$$

$$\cdot \exp\left\{ika\pi - \pi a\alpha - \frac{3\pi i}{4}\right\} \frac{e^{ikr}}{r} \tag{d-46}$$

Contained in the above expression is the asymptotic form of $J_0([k + i\alpha]\, a\gamma)$. Since the argument of this Bessel function is complex we perform the caustic correction according to the principle stated in § D.2.4 by multiplying by the factor

$$\sqrt{\frac{\pi k a \gamma}{2}}\, \sec\left(ka\gamma - \frac{\pi}{4}\right) J_0(ka\gamma)$$

After taking the limit $\gamma \to 0$, substituting from eq. (d-7) for D^2, and substituting from eq. (d-9) for α, the creeping wave contribution to the backscattered field can be written

$$p_{crw} = -\frac{(ka/2)^{1/3}\, a\, e^{\frac{\pi i}{3}}}{\beta_1 A_i^2(-\beta_1)} \exp\left\{ i\pi ka - \pi\beta_1 \left(\frac{ka}{2}\right)^{\frac{1}{3}} e^{-\frac{\pi i}{6}} \right\} \frac{e^{ikr}}{r} \qquad \text{(d-47)}$$

D.3.2.7 CROSS SECTION

Since there are specularly reflected rays as well as creeping wave rays in the backscattering direction, contributions from both must be included in the calculation of the total field. The specular reflection term is calculated according to the principles of geometrical acoustics (Appendix B). We obtain for the cross section

$$\sigma = 4\pi r^2 \left| p_{refl} + p_{crw} \right|^2 \qquad \text{(d-48)}$$

where

$$p_{eff} = \frac{1}{2} a\, e^{-2ika}\, e^{ikr}/r \qquad \text{(d-49)}$$

D.4 LIMITATIONS: DOMAINS OF VALIDITY: EXTENSIONS

The purpose of Keller's method is to provide a prescription for treating scattering from a complex target as a weighted sum of scatterings from its component parts, modeled as simple idealized bodies. To accomplish this it introduces a number of well founded postulates of an ad hoc nature whose application is not always straightforward. Some skill and experience are required to avoid occasional pitfalls, and, as we saw in § D.3.1.6, situations may be encountered which are not covered by the basic postulates.

However, while its difficulties may be subtle, they are seldom intractable. In the hands of an experienced analyst the theory can usually provide a solution for a complex target which is suitable for numerical computation. This is one of its main practical advantages, one which has been demonstrated in many applications, especially in electromagnetic theory.

We now list some specific limitations of the theory along with possible remedies or extensions.

1. Required solutions to canonical problems may not be available, especially for penetrable bodies. As an example, consider diffraction by a rectangular flat plate. The Keller solution includes tip diffraction terms corresponding to the corners. To evaluate the

diffraction coefficients we could use as the canonical problem the elliptic cone in the limit that it approaches an angular sector. As we saw in § D.2.2 this result is not presently known. Nevertheless, Ross [1966] has shown good agreement with experiment for a result based on the Keller solution for an infinite strip modified by a factor which allows for finite length. The latter factor is based on Kirchhoff theory with edge on aspect.

2. Keller's method fails in neighborhoods of caustics, shadow boundaries, and other transition regions. In this respect it displays a characteristic property of asymptotic expansions in general. An ad hoc method for making a caustic correction was described in § D.2.4 and illustrated in the examples. However, the mathematically rigorous way of dealing with this difficulty is to derive a uniform asymptotic expansion, which is valid throughout the transition region. Some recent progress has been made in this area, for example see [LUDWIG - 1966, LEWIS and BOERSMA - 1969, AHLUWALIA - 1970].

3. The Keller method fails in the specular direction in the far field for scattering from a finite straight edge. Thus, in cross section calculations it fails for normal incidence on a finite straight edge.

4. The diffraction and attenuation coefficients given by eqs. (d-7,9) for creeping wave diffraction involve the surface curvature in the direction of propagation. Keller and Levy [1959] have derived corrections which incorporate the rate of change of curvature in the direction of propagation and Voltmer [1970] has given corrections

which also include the effect of transverse curvature. Even with these refinements Keller's theory will break down for sufficiently large wavelength. In applying this criterion the wavelength should be compared with the smallest dimension of the body. Thus, as we have seen in the example problems, a long thin body such as a prolate spheroid may require a very high frequency in order for the Keller method to be applicable. In such problems the physical phenomena resemble traveling waves more closely than creeping waves. Thus, a more suitable approach for long thin bodies is one based on traveling waves such as that of Goodrich and Kazarinoff [1963].

5. As we saw in § D.2.5 the range of the solution may be extended to lower frequencies by the inclusion of multiple diffraction but there is no general theorem which determines the optimum number of multiple scatterings to be included in a given calculation. In view of this it is prudent to limit calculations to one such correction unless comparison with the asymptotic expansion of the exact solution can be made.

6. In regions of specular reflection the Keller solution for the scattered field consists of the geometrical acoustics solution plus the diffracted field. Thus, higher order corrections to the geometrical acoustics solution may become important in such regions. Methods for calculating these corrections are described by Keller, Lewis and Seckler [1956].

7. In the Keller method the incident field must be describable by rays (the Kirchhoff method does not have this limitation). A wide variety of fields satisfy this requirement but the theory has been worked out only for simple sources and plane waves. Recent work [FASNACHT - 1973] indicates that for more complicated sources the method may have to be modified.

8. The geometrical theory of diffraction has been formulated for inhomogeneous as well as uniform media [SECKLER and KELLER - 1959]. Except for applications in the above paper, this potentiality of the theory has been very little exploited.

BIBLIOGRAPHY

ABRAMOWITZ, M. and I. A. STEGUN [1964], Handbook of Mathematical Functions, Dover Publications, New York.

AHLUWALIA, D. S. [1970], Uniform Asymptotic Theory of Diffraction by the Edge of a Three-Dimensional Body, SIAM J. Appl. Math. 18, 287-301.

BOAS, M. L. [1966], Mathematical Methods in the Physical Sciences, Wiley, New York, 328.

BOUWKAMP, C. J. [1954], Diffraction Theory, Rep. Prog. Phys. 17, 35-100.

BOWMAN, J. J., T. B. A. SENIOR and P. L. E. USLENGHI [1969], Electromagnetic and Acoustic Scattering by Simple Shapes, Wiley Interscience, New York.

BREKHOVSKIKH, L. M. [1965], Waves in Layered Media, Academic Press, New York.

BRUNDRIT, G. B. [1965], A Solution to the Problem of Scalar Scattering from a Smooth, Bounded Obstacle Using Integral Equations, Quart. J. Mech. Appl. Math. 19, 473-489.

CRISPIN, J. W. [1963], The Resonance Region, in: Radio Waves and Circuits, ed. S. Silver, 11-37, Elsevier Publishing Company, Amsterdam.

CRISPIN, J. W. and K. M. SIEGEL [1968], (ed.) Methods of Radar Cross Section Analysis, Academic Press, New York.

DUNSIGER, A. D. [1970], High Frequency Acoustic Echoes Received from Simple Geometric Shapes with Possible Applications to Target Recognition, J. Sound Vib. 13, 323-345.

ECKART, C. [1948], Approximate Solution of One-dimensional Wave Equations, Revs. Mod. Phys. 20, 399-417.

EISENHART, L. B. [1964], An Introduction to Differential Geometry, Princeton University Press, Princeton, New Jersey.

ERDÉLYI, A. [1956], Asymptotic Expansions, Dover Publications, New York.

FASNACHT, W. E. [1973], Scattering of a Cylindrical Wave by a Cylinder, Doctoral Dissertation, The Catholic University of America, Washington, D. C.

FELSEN, L. B. [1955], Back Scattering from Wide-Angle and Narrow-Angle Cones, J. Appl. Phys. 26, 138-151.

FLAMMER, C. [1957], Spheroidal Wave Functions, Stanford University Press, Stanford, Calif.

FRANZ, W. [1954], Über die Greenschen Funktionen des Zylinders und der Kugel, Z. Naturforsch. 9a, 705-716.

FRANZ, W. [1957], Theorie der Bengung elektromagnetischer Wellen, Springer, Berlin and New York.

FREEDMAN, A. [1962], The High Frequency Echo Structure of Some Simple Body Shapes, Acustica 12, 61-70.

FRIEDLANDER, F. G. [1958], Sound Pulses, Cambridge University Press.

GOLDSTEIN, H. [1950], Classical Mechanics, Addison Wesley, Reading, Mass.

GOODRICH, R. F. and N. D. KAZARINOFF [1963], Scalar Diffraction by Prolate Spheroids whose Eccentricities are almost One, Proc. Cambridge Phil. Soc. 59, 167-183.

HART, W. L. [1957], Analytic Geometry and Calculus, D. C. Heath and Co., Boston, Mass.

HICKLING, R. [1958], Frequency Dependence of Echoes from Bodies of Different Shapes, J. Acoust. Soc. Am. 30, 137-139.

JACKSON, J. D. [1962], Classical Electrodynamics, Wiley, New York.

JAHNKE, E. and F. EMDE [1954], Tables of Functions, Dover Publications, New York.

KARP, S. N. and J. B. KELLER [1961], Multiple Diffraction by an Aperture in a Hard Screen, Optica Acta 8, 61-72.

KELLER, J. B. [1954], Geometrical Acoustics. I. The Theory of Weak Shock Waves, J. Appl. Phys. 25, 938-947.

KELLER, J. B. [1956], Diffraction by a Convex Cylinder, IRE Trans. AP-4, 312-321.

KELLER, J. B. [1957], Diffraction by an Aperture, J. Appl. Phys. 28, 426-444.

KELLER, J. B. [1960], Backscattering from a Finite Cone, IRE Trans. AP-8, 175-182.

KELLER, J. B. [1962], Geometric Theory of Diffraction, J. Opt. Soc. Am. 52, 116-130.

KELLER, J. B. and B. R. LEVY [1959], Decay Exponents and Diffraction Coefficients for Surface Waves on Surfaces of Nonconstant Curvature, IRE Trans. (Supplement) AP-7, S52-S61.

KELLER, J. B., R. M. LEWIS and B. D. SECKLER [1956], Asymptotic Solution of Some Diffraction Problems, Comm. Pure Appl. Math. 9, 207-265.

KLINE, M. [1951], An Asymptotic Solution of Maxwell's Equations, Comm. Pure Appl. Math. 4, 225-263.

KOUYOUMJIANM R.G. [1965], Asymptotic High-Frequency Methods, Proceedings IEEE, 53, 864-876.

KOUYOUMJIAN, R. G. [1972], Unpublished Lecture Notes.

KRAUS, L. and L. M. LEVINE [1961], Diffraction by an Elliptic Cone, Comm. Pure Appl. Math. 24, 49-68.

LEVY, B. R. and J. B. KELLER [1959], Diffraction by a Smooth Object, Comm. Pure Appl. Math. 12, 159-209.

LEVY, B. R. and J. B. KELLER [1960], Diffraction by a Spheroid, Can. J. Phys. 38, 128-144 (corrected by CRISPIN [1963]).

LEWIS, R. M. and J. BOERSMA [1969], Uniform Asymptotic Theory of Edge Diffraction, J. Math. Phys. 10, 2291-2305.

LUDWIG, D. [1966], Uniform Asymptotic Expansions at a Caustic, Comm. Pure Appl. Math. 19, 215-250.

LUNEBURG, R. K. [1944], The Mathematical Theory of Optics, Brown University Press, Providence, R. I. and [1966] University of California Press, Berkeley, Calif.

MAJOR, J. K. [1946], Physics of Sound in the Sea, Part III, National Defense Research Comm. Div. 6 Sum. Tech. Report 8.

MORSE, P. M. and H. FESHBACH [1953], Methods of Theoretical Physics, McGraw-Hill, New York.

NEUBAUER, W. G. [1963], Summation Formula for Use in Determining the Reflection from Irregular Bodies, J. Acoust. Soc. Am. 35, 279-285.

PRIMAKOFF, H. and J. B. KELLER [1947], Reflection and Transmission of Sound by Thin Curved Shells, J. Acoust. Soc. Am. 5, 820-832.

RUCK, G. T., D. E. BARRICK, W. D. STUART and C. K. KIRCHBAUM [1970], Radar Cross Section Handbook, Plenum Press, New York.

ROSS, R. A. [1966], Radar Cross Section of Rectangular Flat Plates as a Function of Aspect Angle, IRE Trans. AP-14, 329-335.

RUDGERS, A. J. [1965], Calculation of the Monostatically Reflected Velocity Potential in the Far Field of Certain Finite Rigid Bodies, NRL Report 6285, U. S. Naval Research Laboratory, Washington, D.C.

RUDGERS, A. J. [1966], Monostatic Reflection from Rigid Objects Defined by Quadric Surfaces, J. Acoust. Soc. Am. 39, 294-300.

SCHENSTED, C. E. [1955], Electromagnetic and Acoustical Scattering by a Semi-Infinite Body of Revolution, J. Appl. Phys. 26, 306-308.

SCHOCH, A. [1950], Schallreflexion, Schallbreihung, und Schallbeugung, Ergebnisse der exakten Naturw. 23, 127-234.

SECKLER, B. D. and J. B. KELLER [1959], Geometrical Theory of Diffraction in Inhomogeneous Media, J. Acoust. Soc. Am. 31, 192-205.

SENIOR, T. B. A. [1965], Analytical and Numerical Studies of the Backscattering Behavior of Spheres, University of Michigan Report No. 7030-1-T.

SENIOR, T. B. A. [1966], The Scattering from Acoustically Hard and Soft Prolate Spheroids for Axial Incidence, Can. J. Phys. 44, 655-667.

SENIOR, T. B. A. and P. L. E. Uslenghi [1971], Comparison Between Keller's and Ufimtsev's Theories for the Strip. IEEE Trans. AP-19, 557-558.

SIEGEL, K. M., J. W. CRISPIN and C. E. SCHENSTED [1955], Electromagnetic and Acoustic Scattering from a Semi-Infinite Cone, J. Appl. Phys. 26, 309-313.

SOMMERFELD, A. and J. RUNGE [1911], Anwendung der Vektorrechnung auf die Grundlagen der Geometrischen optik, Ann. der Phys. 35, 277-298.

SOMMERFELD, A. [1949], Partial Differential Equations in Physics, Academic Press, New York.

ÜBERALL, H. [1964], Radar Scattering from Coated Perfect Conductors; Application to the Semi-Infinite Cone and Use of Exact Eikonal, J. Res. NBS 68D, 749-766.

ÜBERALL, H. [1966], Radar Scattering from Imperfectly Conducting or Coated Perfectly Conducting Wedges and Cones, Acta Physica Austriaca 22, 67-93.

ÜBERALL, H., R. D. DOOLITTLE and J. V. McNICHOLAS [1966], Use of Sound Pulses for a Study of Circumferential Waves, J. Acoust. Soc. Am. 39, 564-578.

UFINTSEV, P. Ya. [1971], Method of Edge Waves in the Physical Theory of Diffraction, Foreign Technology Division, Wright-Patterson Air Force Base, Ohio, AD-733203.

URETSKY, J. L. [1963], Reflection of a Plane Sound Wave from a Sinusoidal Surface, J. Acoust. Soc. Am. 35, 1293-1294.

URETSKY, J. L. [1965], The Scattering of Plane Waves from Periodic Surfaces, Ann. Phys. 33, 400-427.

URICK, R. J. [1967], Principles of Underwater Sound for Engineers, McGraw-Hill, New York.

VAN BUREN, A. L. [1972], Calculations of Spheroidal Wave Functions, J. Acoust. Soc. Amer. 51, 414-416.

VOLTMER, D. R. [1970], Diffraction by Doubly Curved Convex Surfaces, Doctoral Dissertation, The Ohio State University, Columbus, Ohio.

WATSON, G. N. [1918a], The Diffraction of Electric Waves by the Earth, Proc. Roy. Soc. London A95, 83-99.

WATSON, G. N. [1918b], The Transmission of Electric Waves Round the Earth, Proc. Roy. Soc. London A95, 546-563.

WATSON, G. N. [1952], Theory of Bessel Functions, Cambridge University Press.

WIDDER, D. V. [1965], Advanced Calculus, Prentice-Hall, Englewood Cliffs, N. J.

WILSON, W. A. and J. I. TRACY [1949], Analytic Geometry, Heath and Co., New York.